UNIVERSITY OF OVIEDO

DEPARTMENT OF CHEMICAL AND ENVIRONMENTAL ENGINEERING

Salicylic acid biodegradation by *Pseudomonas putida*: Effect of particulate materials, microorganisms and other substrates

DOCTORAL THESIS

Program in Chemical, Environmental and Bio-Food Engineering

BY

Rosana González Combarros

March, 2016

No puedes cambiar el viento, pero puedes ajustar las velas para alcanzar tu destino.

Paulo Coelho

Agradecimientos

Debo agradecer al Dr Mario Díaz, por aceptarme para realizar esta Tesis doctoral bajo su dirección además del asesoramiento, apoyo, sugerencias e ideas y confianza en mí.

En segundo lugar, quiero agradecer de manera especial y sincera, a mi co-director de Tesis, el Dr. Sergio Collado por su importante aporte y participación activa en el desarrollo de esta Tesis. Debo destacar, por encima de todo, su disponibilidad y paciencia. No cabe duda que su participación ha enriquecido el trabajo realizado.

También es justo mencionar al Dr. Manuel Rendueles y a la Dra. Adriana Laca con los que he tenido la oportunidad de trabajar de una forma cercana en parte del proyecto.

Llegado a este punto tengo que agradecer a Ana Salas (Servicio de Citometría de los SCT´s, Universidad de Oviedo) y a Marta Alonso (Área de Procesos de Imágenes de los SCT´s, Universidad de Oviedo) por la amabilidad, el buen hacer, la eficiencia y por la inmensa ayuda prestada en los análisis de las muestras.

Hago extensivo el agradecimiento a todas las personas que forman parte de Departamento de Ingeniería Química y Tecnología del Medio Ambiente porque siempre han estado dispuestas a echar una mano fuese cual fuese el problema. De entre todas las personas que han contribuido a la consecución de esta Tesis se merecen una mención especial el Dr. Sergio Collado (ahora como compañero y no como co-director), por implicarse en este trabajo hasta tal punto que me debe unos ocho cachopos, por los consejos y ayuda constantes y sobre todo por su gran sentido del humor; a la Dra. Paula Oulego, con quien he compartido, durante estos años, trabajo, confidencias, risas y penas. Al Dr. Kike Antón, experto informático y mejor compañero, alguien con el que puedes tener la absoluta seguridad de saber que se puede contar con él, tanto para lo bueno como para lo malo. A Cristina García, buena compañera de fatigas y mejor persona. No me viene nadie mejor a la cabeza con quien haber trabajado mis últimos años en el Laboratorio de Biotecnología. A José Luis Urrea, Ana Álvarez y Elena Piedra, por vuestra simpatía, haciendo que el día a día en la sala fuese estupendo. Al Dr. David Blanco, persona optimista donde las hay, gracias por tus consejos. Al Dr. Saúl Alonso y a Irene Rosas, por introducirme en el mundo de la investigación e instruirme en trabajo con "bichos" de manera rigurosa, y por ayudarme con la citometría de flujo, aunque fuera en la distancia, a vosotros os debo mis inicios. Únicamente me queda añadir que, empezasteis siendo compañeros de trabajo, pero a día de hoy, sólo os puedo llamar amigos.

A Yoly, con quien empecé este viaje, son tantas cosas las que te quiero decir que sería casi una nueva Tesis. Resumiendo, estoy segura que el resultado final de este proyecto habría sido muy diferente si no hubieras estado conmigo apoyándome y ayudándome. Sólo me queda decir, gracias por estar ahí.

A vosotros, papá y mamá, gracias por el sacrificio que me permitió ir a estudiar lejos, por animarme cuando os dije que me embarcaba en este nuevo viaje, por preocuparos, por la ayuda en los momentos difíciles y las alegrías compartidas en las grandes ocasiones… en definitiva, ¡Muchas gracias por todo!. También a mis hermanos, Patri y Edu, debo agradecer el estar ahí siempre y para todo.

Por último, a ti, Alberto, en este caso las palabras sobran y sin embargo quiero que sepas que tu presencia, apoyo, ayuda, comprensión y ánimo, que los rápidos arreglos de equipos y madrugones domingueros han sido parte fundamental para que la finalización de esta Tesis fuese posible. Gracias por acompañarme en este arduo camino y seguir haciéndolo de ahora en adelante.

Índice

Resumen

La contaminación de aguas debida a compuestos de naturaleza fenólica o cianurada, adquiere una elevada importancia, no sólo por su potencial toxicidad sino también por los elevados volúmenes generados, principalmente en los sectores siderúrgico y farmacéutico.

El proceso biológico con lodos activos es el método más comúnmente utilizado en el tratamiento de aguas residuales industriales que contienen este tipo de compuestos, aunque su aplicación está limitada a bajas concentraciones de estos compuestos. Por otra parte, el estudio cada vez más habitual de microorganismos puros para el tratamiento de contaminantes específicos nos permite adquirir conocimientos sobre los mecanismos involucrados en la biodegradación además de encontrar especies que pueden eliminar altas concentraciones de los contaminantes en cuestión. Con ello se da un paso más hacia la bioaumentación de los sistemas tradicionales de tratamiento.

Las aguas residuales generalmente contienen, además del propio contaminante, otras sustancias, añadidas de forma voluntaria o no, que llegan al proceso biológico y cuyo efecto apenas están estudiados. Por ello, es importante conocer, en los sistemas de tratamiento biológico de aguas residuales, el efecto que produce sobre el bioproceso la presencia de ciertos agentes externos que aún no han sido estudiados en detalle, tales como materiales sólidos como el carbón activo, sólidos nanoparticulados como los óxidos de grafeno o el dióxido de titanio o la presencia de especies competidoras y/ o de otros contaminantes.

Como paso previo necesario para lo anterior, se ha comenzado estudiando la biodegradación mediante microorganismos puros en suspensión, *Pseudomonas putida* y *Paracoccus thiocyanatus*, de ácido salicílico (como contaminante fenólico modelo) y tiocianato (como contaminantes cianurado modelo), analizando el efecto de las condiciones de operación, de la composición del medio y de la concentración inicial. Así, se obtuvieron los modelos cinéticos, que servirán como base para cuantificar los efectos de los distintos agentes externos estudiados.

Estos agentes pueden producir respuestas sinérgicas o antagónicas sobre el proceso de biodegradación. Se comenzó estudiando el efecto de la presencia de carbón activo sobre el proceso de biodegradación de ácido salicílico por *P. putida*, para lo que se realizaron ensayos de adsorción del contaminante con carbón activo y con carbón activo más biomasa.

En el presente trabajo también se ensayó el efecto de la presencia de materiales nanoparticulados como el dióxido de titanio y el óxido de grafeno, materiales cuyo uso y

fabricación están en auge hoy en día. Los resultados obtenidos mostraron que los materiales nanoparticulados provocaron cambios en el estado fisiológico de las bacterias, afectando a su actividad metabólica.

Asimismo, se estudió la presencia de bacterias competidoras o co-sustratos en el proceso de biodegradación para finalmente llevar a cabo una biodegradación simultánea de los contaminantes fenólicos y cianurados mediante el uso de un co-cultivo de *P. putida* y *P. thiocyanatus*. En todos los casos, se analizó el efecto de la concentración del agente externo y las condiciones de operación modelizando la cinética del proceso. Los resultados obtenidos demostraron una mejora en la eficacia de biodegradación simultánea de los contaminantes en presencia del co-cultivo bacteriano.

En resumen, todos los estudios se llevaron a cabo con el fin de localizar y poner en evidencia los efectos derivados de la presencia de agentes externos sobre un proceso clásico de biodegradación mediante cultivo puro, optimizando el sistema en base a consideraciones operacionales lo más adecuadas tanto para la fisiología como para el rendimiento de *P. putida* y *P. thiocyanatus*. Para ello, la monitorización de la heterogeneidad fisiológica del sistema, a través de citometría de flujo multiparamétrica, ha proporcionado el conocimiento preciso sobre el comportamiento funcional bacteriano asociado a la exposición al correspondiente agente externo durante la biodegradación de contaminantes fenólicos.

Abstract

Water pollution caused by phenolic or cyanide compounds, acquires a high relevance not only due to its potential toxicity, but also by the high volumes generated, mainly, in the steel and pharmaceutical industries.

Activated sludge process is the most commonly method used in the treatment of industrial wastewater containing this kind of compounds, although its application is limited to low concentrations of these pollutants. Moreover, the increasingly common study of pure culture of microorganisms for the treatment of specific pollutants allows us to learn about the mechanisms involved in the biodegradation, besides finding species that can remove high concentrations of the pollutants concerned. In so doing, another step is taking towards the bioaugmentation of traditional treatment systems.

Wastewater generally contain, besides the pollutant itself, other substances, added voluntarily or not, that reach into the biological process and which effect is hardly studied. Therefore, it is important to know, in biological wastewater treatment systems, the effect on the biotreatment of the presence of certain external agents that have not yet been studied in detail, such as solid materials like activated carbon, nanoparticles as graphene oxide or titanium dioxide or the presence of competing species and / or other contaminants.

As a necessary preliminary step to the above-mentioned, it has studied the biodegradation by suspended pure cultures, *Pseudomonas putida* and *Paracoccus thiocyanatus*, of salicylic acid (as model of phenolic pollutant) and thiocyanate (as model of cyanide pollutant), analysing the effect of operating conditions, medium composition and initial concentration. Thus, the kinetic models, which could be used as reference for quantifying the effects of the different external agents studied, were obtained.

These external agents may produce synergistic or antagonistic responses on the biodegradation process. Work begun studying the effect of the presence of activated carbon on the biodegradation process of salicylic acid by *P. putida*, for which contaminant adsorption test with activated carbon and with activated carbon plus biomass were conducted.

In the present work, the effect of the presence of nanoparticles such as titanium dioxide and graphene oxide materials, whose use and manufacturing are on the rise, was also tested. The results showed that the nanoparticle materials caused changes in the bacterial physiological state, affecting their metabolic activity.

Likewise, the presence of competitive bacteria or co-substrates in the process of biodegradation were studied, to carry out the simultaneous biodegradation of phenolic

and cyanide contaminants finally, by means of a co-culture of *P. putida* and *P. thiocyanatus*. In all cases, the effect of the external agent concentration and the operating conditions were analysed, modelling the kinetics of the process. The results showed an improvement in the efficacy of simultaneous contaminants biodegradation in presence of the bacterial co-culture.

In summary, all studies were conducted in order to locate and reveal the effects of the presence of external agents on a classic biodegradation process by pure culture, optimizing the system in basis of the most appropriate operational considerations for either the physiology or the yield of *P. putida* and *P. thiocyanatus*. For this, the monitoring of system´s physiological heterogeneity, by means of multiparametric flow cytometry, has provided the precise knowledge about the bacterial functional behavior associated with the exposure to the corresponding external agent during biodegradation of phenolic contaminants.

1. Introducción

1.1. Situación actual

El agua es una de las sustancias químicas más importantes para los seres vivos. El agua cubre aproximadamente el 72% de la superficie de la Tierra. Sin embargo, de este porcentaje sólo el 0.7% es agua dulce y del total de agua dulce, sólo el 0.01% es agua superficial [1]. Además, estos porcentajes no se distribuyen de forma equitativa sobre el planeta; una gran parte de la población mundial carece de la cantidad y/ o calidad de agua necesaria para satisfacer sus necesidades personales [2].

Toda comunidad genera residuos tanto sólidos como líquidos. La fracción líquida de los mismos, aguas residuales, es esencialmente el agua de que se desprende la comunidad una vez ha sido contaminada durante los diferentes usos para los cuales ha sido empleada. Desde el punto de vista de las fuentes de generación, se puede definir el agua residual como la combinación de los residuos líquidos, o aguas portadoras de residuos, procedentes tanto de residencias como de instituciones públicas y establecimientos industriales y comerciales, a los que pueden agregarse, eventualmente, aguas subterráneas, superficiales y pluviales [3].

Todos los gobiernos del mundo intentan regular la calidad del agua con el fin de garantizar la salud pública y la protección del medio ambiente. Por ello, se han centrado en investigar diferentes técnicas de tratamiento de aguas para reducir los efectos dañinos que la contaminación ha ocasionado en este recurso [2].

El tratamiento biológico de aguas residuales se considera como una de las técnicas más prometedoras para la eliminación de contaminantes de las aguas, debido a su coste asequible y alta eficacia [4]. Sin embargo, su principal limitación es la falta de conocimiento sobre los procesos específicos de eliminación mediante esta técnica. Aunque existen otros tratamientos muy efectivos como los procesos de oxidación avanzada, técnicas con membranas o procesos de adsorción que están siendo desarrollados, desafortunadamente la aplicación de estas técnicas está restringido debido a su alto coste [4].

Las plantas de lodos activos son la solución más extendida para el tratamiento biológico de aguas residuales industriales. Sin embargo, los efluentes de las plantas industriales, tales como las industrias petroquímicas, plantas de procesamiento de coque o fábricas farmacéuticas, son difíciles de ser biodegradados debido a las propiedades tóxicas o inertes de algunos contaminantes normalmente presentes en ellos [5-7]. Además, si estas sustancias tóxicas no se degradan *in situ*, pueden afectar al rendimiento de las plantas de tratamiento de aguas residuales, que reciban los efluentes de uno o varios parques industriales [4, 8]. La biodegradación de una mezcla de contaminantes procedentes de

diferentes fuentes industriales utilizando lodos activos es muy complejo, de modo que un análisis de las interacciones que se producen entre sustratos y bacterias ayuda a conseguir un enfoque global del proceso que ocurre durante el tratamiento biológico.

La solución a este problema es conseguir un sistema lo suficientemente complejo como para simular unos lodos reales pero, a la vez, lo más sencillo posible para permitir el estudio de las interacciones entre especies [9]. Los trabajos que se basan en este enfoque se centran en el estudio de la degradación de uno o más compuestos por dos o más bacterias, obteniendo interacciones simbióticas o antagónicas entre ellas o dando lugar a fenómenos de cometabolismo de los compuestos contaminantes, inhibición de tipo competitivo o efectos tóxicos como consecuencia del co-sustrato [9-11]. Este tipo de estudios son muy atractivos como paso previo en la investigación de los posibles beneficios que se pueden obtener mediante la adición de cultivos puros a cultivos mixtos con el fin de mejorar la degradación de estos xenobióticos (bioamentación) [12-14].

Por otro lado, los tratamientos biológicos que emplean carbón activo biológico (BAC) para el tratamiento de contaminantes orgánicos en las aguas residuales, se caracterizan por exhibir frecuentemente prestaciones superiores a las obtenidas en sistemas convencionales. El rendimiento mejorado del sistema suele manifestarse en una mayor eficacia de eliminación, periodos de aclimatación de los microorganismos más cortos y una mayor estabilidad del proceso frente a picos en la carga contaminante del influente [15-20]. La función principal del carbón es servir de soporte a los microorganismos y actuar como amortiguador para las fluctuaciones de carga contaminante del efluente [21]. A pesar de que existen algunos trabajos en los que el carbón activo biológico se ha aplicado con éxito para el tratamiento de aguas residuales [16, 17, 19, 20, 22, 23], aún se necesita más investigación en este campo [15].

Asimismo, hay que tener en cuenta los posibles efectos que pueden surgir como consecuencia de la presencia de agentes externos en el proceso biológico. Por ejemplo, el empleo cada vez más habitual de materiales nanoparticulados, ha provocado que la presencia de estos materiales en las plantas de tratamiento de aguas residuales urbanas o industriales sea frecuente [24]. En consecuencia, ha surgido la preocupación de estudiar sus posibles efectos adversos e interacciones con las biomoléculas [25-28]. A pesar de que la literatura presenta un número creciente de investigaciones científicas sobre la toxicidad de los nanomateriales, su comportamiento ambiental y su ecotoxicidad, no hay muchos estudios sobre el efecto que su presencia puede producir en los tratamientos biológicos de aguas residuales [29].

1.2. Estructura de la Memoria

Esta tesis se presenta como un compendio de publicaciones que se enmarcan dentro del campo del tratamiento biológico de efluentes con elevadas concentraciones de ácido

salicílico, haciendo hincapié en el efecto de la presencia de agentes externos como materiales sólidos (carbón activo y nanopartículas), otros sustratos o bacterias. En cada una de las publicaciones se identifica claramente la estructura tradicional (introducción, materiales y métodos, resultados y discusión y conclusiones). Estas publicaciones han sido aceptadas o están siendo evaluadas por revistas incluidas en *Science Citation Index*. La estructura de la presente memoria está dividida en 8 capítulos.

En el **capítulo 1**, correspondiente a las consideraciones previas, se plantea la problemática actual derivada de la presencia de ácido salicílico (SA) en los efluentes de varias industrias así como la presencia de elementos externos, que pueden tener efectos negativos o positivos sobre el tratamiento biológico de estas aguas.

En el **capítulo 2,** se indican los objetivos generales y específicos derivados de la Tesis Doctoral.

En el **capítulo 3** se desarrollan las consideraciones teóricas. En este capítulo se incluye el problema medioambiental derivado de los efluentes que contienen SA, se describe la técnica de tratamiento biológico, y se analizan los posibles efectos que surgen de la presencia de agentes externos (sólidos particulados, otros microorganismos o sustratos adicionales) sobre el tratamiento biológico. Además, se compara el proceso de tratamiento biológico del SA con un proceso físico como es la adsorción con carbón activo y con la combinación de los dos procesos anteriores o bioadsorción. Se describe brevemente la técnica de citometría de flujo, con la que se realizó el seguimiento celular de una gran parte del trabajo aquí incluido.

La metodología general empleada en la parte experimental del trabajo se describe en el **capítulo 4**. Una descripción más detallada de las metodologías específicas utilizadas en cada estudio se puede consultar en su correspondiente sección “Materials and Methods”.

En el **capítulo 5,** se desarrolla la parte de resultados experimentales y discusión. Cada subapartado de este capítulo corresponde a uno de los artículos, bien publicado o en vista de serlo.

En el subapartado **5.1.,** se analiza el efecto de la presencia de carbón activo sobre el tratamiento biológico. Para ello, se realiza un estudio sobre el tratamiento de efluentes que contienen SA mediante un proceso biológico con un cultivo puro, *Pseudomonas putida*, mediante un proceso físico de adsorción con carbón activo y mediante el proceso combinado de los dos anteriores (bioadsorción).

El efecto de la presencia de materiales nanoparticulados sobre el proceso de biodegradación del ácido salicílico se estudia en los subapartados **5.2.** y **5.3.** En el subapartado **5.2.**, se recogen los resultados obtenidos sobre los efectos producidos por la

presencia de nanopartículas de TiO_2 sobre la activividad y viabilidad de *P. putida*, mientras que en el apartado **5.3.** se analiza el efecto del óxido de grafeno sobre la misma bacteria.

En los subapartados posteriores de resultados, se analizan los efectos de la existencia de un proceso degradativo en paralelo (biodegradación de un sustrato cianurado, tiocianato (SCN^-), por la bacteria *Paracoccus thiocyanatus*) en la biodegradación del SA por *P. putida*. Con el fin de llevar a cabo este análisis, se hizo necesario un estudio previo sobre la biodegradación del tiocianato por la bacteria *P. thiocyanatus*, así como del proceso de adsorción con carbón activo y la bioadsorción (subapartado **5.4.**). Estos resultados fueron empleados como referencia a la hora de analizar las posibles interacciones entre bacterias (*P. thiocyanatus* y *P. putida*) y sustratos (SCN^- y SA) durante su biodegradación simultánea. Los resultados obtenidos se recogen en el subapartado **5.5.**.

En el **capítulo 6 y 7,** se exponen las principales conclusiones obtenidas en la presente memoria.

En el **capítulo 8** se incluye la bibliografía común de la memoria.

Finalmente, en un último capítulo, **Capítulo 9**, se recoge información adicional que se cree de interés con el fin de reforzar algunos aspectos comentados en el apartado de Resultados.

2. Objetivos

El objetivo principal de este trabajo es analizar el efecto, de la presencia de ciertos agentes externos, poco estudiados hasta ahora, sobre cultivos puros bacterianos en la biodegradación de un efluente de la industria farmacéutica. Para ello, se selecciona el ácido salicílico como modelo, puesto que ha sido identificado como un contaminante muy habitual en aguas residuales de distintos sectores que soporta el crecimiento de la *P. putida* e induce enzimas específicas para la degradación de sustratos como el carbanzol o el 4-clorofenol, además de ser considerado como un contaminante emergente por varios autores. La bacteria *Pseudomonas putida* se ha escogido como cultivo puro por ser el género más abundante en los lodos activos. Los agentes externo seleccionados son material particulado, como carbón activo y nanopartículas de dióxido de titanio y óxido de grafeno, así como otras especies bacterianas y/ o co-sustratos presentes en el medio.

Específicamente, los objetivos desarrollados se detallan a continuación:

- Estudiar el proceso de biodegradación del ácido salicílico por *Pseudomonas putida* (DSM-4478). Modelización del proceso en base a los resultados obtenidos usando un amplio rango de condiciones de operación.

- Analizar el proceso de adsorción con carbón activo del ácido salicílico en disolución acuosa.

- Estudiar el efecto de la presencia de carbón activo sobre el proceso de biodegradación de ácido salicílico.

- Determinar las condiciones óptimas de formación de un biofilm de *P. putida* sobre carbón activo

- Analizar el efecto de la presencia de materiales sólidos nanoparticulados, dióxido de titanio y óxido de grafeno sobre el proceso de biodegradación del ácido salicílico y viabilidad bacteriana.

- Evaluación de la técnica de citometría de flujo como nuevo método de análisis de la biotoxicidad de los materiales nanoparticulados sobre *P. putida*.

- Estudiar el proceso de biodegradación de un compuesto de la familia de los cianuros, el tiocianato, mediante la bacteria *Paracoccus thiocyanatus* (LMG 24666).

- Determinar el efecto de la presencia de otros microorganismos, *P. thiocyanatus*, y otros sustratos (tiocianato), sobre la biodegradación del ácido salicílico por *P. putida*.

3. Consideraciones teóricas

3.1. Compuestos fenólicos

3.1.1. Problemática

Los compuestos fenólicos se caracterizan por ser utilizados en una gran variedad de industrias como química, petroquímica, textil, pesticidas, fabricación de papel, fabricación de resinas, plantas de coquización… entre otras [30-34]. En consecuencia, son uno de los contaminantes orgánicos más abundante en las aguas residuales industriales [30, 35, 36].

En la siguiente figura se muestra el volumen de vertido de fenoles, número de empresas y principales sectores generadores durante el año 2013, según *The European Pollutant Release and Transfer Register* (E-PRTR) [37].

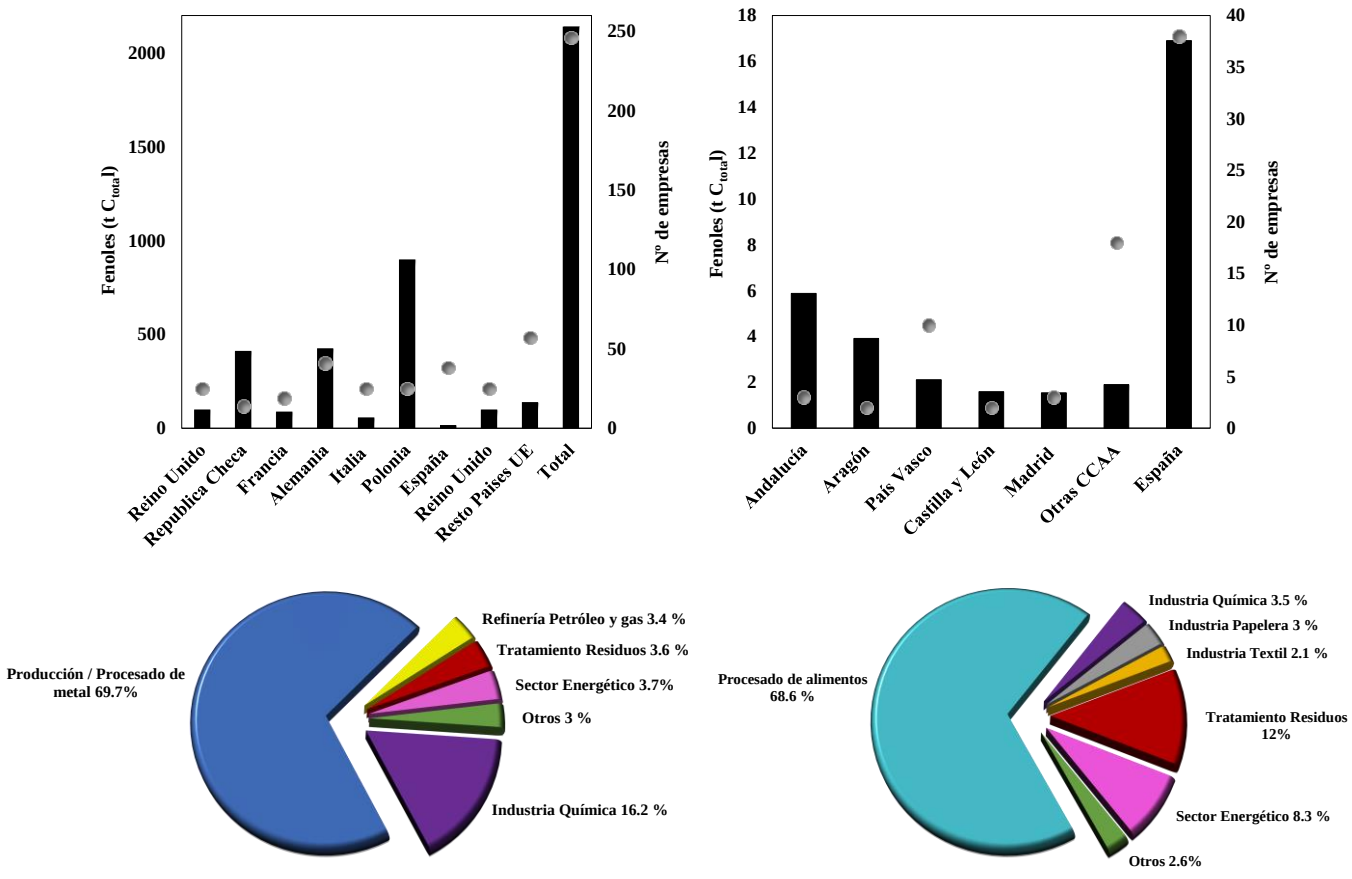

Figura 3.1: Volumen vertido de fenoles y número de empresas generadoras en la UE 28 (a) y en España (b) durante el 2013. Principales sectores generadores de fenoles en la UE 28 (c) y en España durante el 2013 [37]

La concentración típica de compuestos fenólico en aguas residuales varía entre 10-300 mgL^{-1}, pero puede elevarse hasta 4.5 g L^{-1} en aguas muy contaminadas [38]. Algunos ejemplos de aguas residuales con alto contenido en compuestos fenólicos son las aguas residuales de refinerías (6-500 mgL^{-1}), aguas de coquización (29-3900 mgL^{-1}), aguas procedentes del procesado del carbón (9-6800 mgL^{-1}), aguas residuales de la industria petroquímica (2.8-1220 mgL^{-1}) o aguas residuales de industrias farmacéutica, papeleras o de producción de plástico (0.1-1600 mgL^{-1}) [34].

Los compuestos fenólicos son considerados como uno de los contaminantes prioritarios por US EPA debido a sus efectos adversos sobre la salud humana, su toxicidad, persistencia y su bioacumulación en los animales y las plantas [30, 32-34, 36, 38-40].

La creciente preocupación de la sociedad sobre este tema y la problemática medioambiental que genera ha llevado a delimitar los niveles máximos permitidos de compuestos fenólicos en efluentes industriales. Según Real Decreto 1138/1990, de 14 de septiembre (BOE nº 226, 20-9-90), la concentración máxima admisible de fenoles en agua potable es de 9.5 μg/L [32, 34].

Los procesos biológicos de tratamiento para la eliminación de los compuestos fenólicos han demostrado ser generalmente ineficientes como consecuencia de su naturaleza refractaria, bio-resistencia y toxicidad a la población microbiana causada por el anillo de benceno estable [31, 35, 39, 40]. La mayor parte de los compuestos fenólicos que se encuentran en los ríos proceden de plantas de tratamiento de aguas residuales como consecuencia de un tratamiento biológico ineficaz [39].

3.1.1.1. El ácido salicílico

En el caso concreto de la industria farmaquímica, sus efluentes se caracterizan por presentar elevadas cargas orgánicas y tóxicas. Muchos de los compuestos existentes son nocivos, incluso a muy bajas concentraciones, para los sistemas de tratamiento biológico frecuentemente empleados en las estaciones de depuración de aguas, tanto industriales como municipales [41, 42].

El ácido salicílico (SA), también conocido como ácido 2-hidroxibenzoico ($C_7H_6O_3$), es un contaminante fenólico típico en las aguas residuales de la industria farmacéutica y cosmética [43, 44]. Es un ácido orgánico débil cuya estructura y características físicas se muestran en la Figura 3.2 y Tabla 3.1, respectivamente.

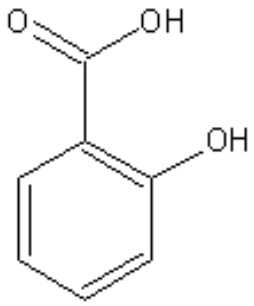

Figura 3.2: Estructura del ácido salicílico

Tabla 3.1: Características físicas del ácido salicílico [45]

Estado de agregación	Sólido
Apariencia	Polvo cristalino incoloro Cristales en forma de agujas
Solubilidad en agua, g/100 ml a 20 °C	1.8
Densidad relativa (agua =1)	1.4
Masa Molar $gmol^{-1}$	138.12
Punto de fusión K	432
Punto de ebullición K	484
Temperatura de autoignición K	813
Acidez pKa	4.19

El ácido salicílico y sus derivados se encuentran en el mercado en una amplia gama de productos. El SA tiene características analgésicas y antiinflamatorias, pero, debido a que provoca irritaciones estomacales, no se aplica como tal sino en forma de sus derivados, siendo los más conocidos el ácido acetilsalicílico y el salicilato de metilo (el éster con el alcohol metílico) [46]. Sin embargo, el ácido salicílico sí se puede aplicar directamente sobre la piel. En la actualidad, es utilizado en medicinas para la eliminación de verrugas, en el tratamiento de infecciones fúngicas, como un tópico en el tratamiento del acné y para aumentar la renovación celular como componente de cremas para la piel. Otras aplicaciones del ácido salicílico se relacionan con la protección de plantas contra insectos y patógenos [46, 47].

En su mayoría, las aguas residuales que contienen SA se originan principalmente durante la síntesis del SA y sus derivados y del aclarado de los equipos de fabricación médicos y cosméticos [46].

El ácido salicílico se caracteriza por ser un contaminante difícilmente biodegradable y contribuye a aumentar la DQO de las aguas residuales [44]. Este contaminante tiene

efectos tóxicos sobre los ecosistemas y la salud humana, por lo que debe ser eliminada de las aguas residuales para evitar su propagación en el medio ambiente [44]. El ácido salicílico presenta unas concentraciones de toxicidad crónica y aguda en *Daphnia magna* iguales a 13.3 y 1031.7 mgL^{-1}, respectivamente [48].

El SA presenta un peligro ambiental grave debido a su alta toxicidad y la tendencia a acumularse en el medioambiente. Como resultado, la eliminación eficiente del SA de disoluciones acuosas ha recibido mucha atención en los últimos años [49, 50].

3.1.2. Técnicas de tratamiento

En la bibliografía, se han encontrado una gran variedad de procesos para la eliminación de los compuestos fenólicos de las aguas residuales. Estos tratamientos pueden ser clasificados como físicos, químicos y biológicos [32, 33]. El método adecuado para la eliminación de compuestos fenólicos debe ser seleccionado basado en la disponibilidad del material, el grado de separación requerido y las propiedades de efluente fenólico [36]. Normalmente, los tratamientos de aguas residuales comerciales utilizan una combinación de tratamientos biológicos, físicos y químicos [30].

3.1.2.1. Métodos químicos

Una alternativa atractiva para el tratamiento de compuestos fenólicos en las aguas residuales son los llamados procesos de oxidación avanzada, los cuales generan radicales hidroxilo en cantidad suficiente para oxidar la mayoría de los compuestos orgánicos presentes en el agua. Se pueden nombrar, entre otros, Fenton, ozonización, oxidación fotoquímica y electroquímica, fotólisis con H_2O_2 y O_3, fotocatálisis con TiO_2 y distintas combinaciones de estos métodos [30].

En la tabla 3.2 se indican los métodos químicos más utilizados para el tratamiento de aguas contaminadas con compuestos fenólicos, así como sus condiciones de operación y valores de rendimientos.

El principal problema de los métodos químicos de tratamiento es debido a los altos costes como consecuencia de los reactivos como el ozono o el peróxido de hidrógeno, y de las fuentes de luz como por ejemplo los UV [51].

Tabla 3.2: Principales técnicas químicas para el tratamiento de aguas contaminadas con compuestos fenólicos. Modificada de Busca *et al.* [34]

Técnica	T (K)	P (atm)	pH	Aditivos	Rendimiento	Comentario
WAO	450-500	20-160	3-7	Aire	15-120 min conv. 75-90%	Comercial, requiere post-tratamiento
SWAO	670-920	250-350	NA	Aire	Conv. 99.99% TOC	Comercial, combustión completa
CWAO	370-470	3-35	NA	Aire, catalizador	Conv. 80-90% TOC t>20 min	Comercial, pérdida del catalizador (lixiviado)
Ozonización	300-330	~ 1	>8	Ozono Base (catal.)	Conv. 100% Ph 80 min	Comercial
CWPO	300-330	~ 1	<5	H_2O_2, $FeSO_4$, Ácido	Conv. > 90% Ph 5 h	Comercial, recuperación del catalizador
Electro-Fenton	300-330	~ 1	NA	H_2O_2, $FeSO_4$, Ácido	Conv. 99% DQO, <1V	Recuperación del catalizador
Oxidación Anódica	300-330	~ 1	NA	Electrodos (BDD)	Conv. > 60% TOC, 10h, 4-15 V	
Foto-oxidación (UV)	300-330	~ 1	NA	TiO_2	Conv. > 90% TOC, 5h, < 400 nm	Comercial, recuperación del catalizador
Foto-oxidación (vis)	300-330	~ 1	NA	TiO_2 dopado con N	Conv. 27 % Ph, < luz solar 2 h	Comercial, recuperación del catalizador, y estabilidad

3.1.2.2. Métodos físicos: Adsorción con carbón activo

En la tabla 3.3 se indican los métodos físicos más utilizados para el tratamiento de aguas contaminadas con compuestos fenólicos.

Estos métodos se basan en la separación del fenol de la corriente acuosa. Los tratamientos físicos presentan, en general, la ventaja de su bajo coste operacional, pero, en algunos casos, la operación se encarece como consecuencia de la necesidad de regeneración de los adsorbentes, tratamiento de las corrientes concentradas o eliminación de los regenerantes. La mayoría de ellos sólo son adecuados para efluentes con bajas concentraciones de compuestos fenólicos [33].

Tabla 3.3: Principales técnicas físicas para el tratamiento de aguas contaminadas con compuestos fenólicos. Modificada de Busca *et al.* [34]

Técnica	T (K)	P (atm)	pH	Aditivos	Rendimiento	Comentario
Destilación	370-45	~ 1	NA	No	Separación completa	Comercial, recuperación del fenol, costoso
Extracción	300-450	~ 1	NA	DIPE, MIBK	Kd=100 (MIBK/H_2O)	Comercial, recuperación del fenol, costoso
Adsorción (resinas)	300-330	~ 1	~ 7	Resina Regenerador	80-100 $mg_{Ph}g_{resina}^{-1}$	Comercial, recuperación del fenol, eliminación del regenerador
Oligom.enz./ Adsorción	300-330	~ 1	3-7	Encima Soporte Chitosan	Co_{Ph}=0.02 mgL^{-1} Conv.> 90%	Eliminación de enzima, soporte y adsorbente
Per-vaporación	300-330	20 Torr	NA	Membrana	0.3 $kg_{Ph}(m^2h)^{-1}$	Comercial, recuperación del fenol

A continuación se trata con más detalle la adsorción con carbón activo como principal técnica física de eliminación de fenoles.

La adsorción en el tratamiento de aguas implica la separación de uno o más solutos (adsorbato/s) de la disolución y su concentración en la superficie del sólido (adsorbente) hasta que se establece un equilibrio dinámico en dicha superficie, entre la concentración de soluto que permanece en la disolución y la concentración superficial de soluto sobre el adsorbente [3, 52].

En la adsorción con carbón activo, las fuerzas de atracción entre las moléculas de fluido y la superficie sólida son del tipo Van der Waals [53]. En estos casos, la molécula adsorbida no está fija en un lugar específico de la superficie, sino más bien es libre de trasladarse dentro de la interfase. Esta adsorción, en general, predomina a temperaturas bajas [53]. Información adicional sobre el proceso de adsorción con carbón activo se puede encontrar en el anexo I del presente trabajo.

La adsorción sobre carbón activo se usa ampliamente para eliminar incluso trazas de los compuestos fenólicos; esta técnica se considera como una de las mejores y de más frecuente uso, puesto que es capaz de satisfacer el alto nivel de las exigencias ambientales [34, 54]. Esto es debido a la gran superficie específica del carbón activo, su naturaleza microporosa, la alta capacidad de adsorción y la fácil disponibilidad [55]. Sin embargo, en ocasiones, la regeneración del lecho de carbón activo no es posible o conveniente, de modo que el lecho saturado debe retirarse y desecharse o incluso destruirse, lo que supone un problema ambiental y económico [34].

En la bibliografía se encuentran capacidades de adsorción de compuestos fenólicos por carbón activo con valores entre 1-550 mg g^{-1} [34, 56-59]. Por ejemplo, Otero *et al.* [47] estudió la capacidad de adsorción del carbón activo Filtrasorb F400 con soluciones acuosas de ácido salicílico, obteniendo una capacidad máxima de 351 mgg^{-1}. Dhidan [60] empleó carbones activos preparados a partir de huesos de dátiles por activación química con cloruro férrico para la adsorción de compuesto fenólicos de una disolución acuosa, alcanzando eficacias de eliminación del 98% a valores de pH de 5 y 90 minutos de contacto. Sin embargo, Atieh [61] obtuvo que la máxima eliminación de fenol por adsorción con carbón activo fue a pH 7 con un porcentaje de eliminación del 65%.

3.1.2.3. Métodos biológicos convencionales

Los métodos anteriormente descritos para la eliminación de compuestos fenólicos de efluentes acuosos son comercialmente poco prácticos, ya sea debido a su alto coste de operación o como consecuencia de la dificultad de tratamiento de los residuos generados en la operación. Debe tenerse en cuenta que la mayoría de estas técnicas no degradan los compuestos fenólicos, sino que lo mueven a otra fase (contaminación secundaria) [38, 51].

La biodegradación, sin embargo, se considera una de las técnicas disponibles más eficiente y rentable de tratamiento de aguas residuales [33, 38, 51]. En este caso, el tratamiento de las corrientes de aguas residuales se lleva a cabo mediante el uso de sistemas biológicos en los que los microorganismos proliferan a expensas de los contaminantes [51].

Es común emplear la biodegradación aerobia para eliminar compuestos aromáticos de las aguas residuales cuando se encuentran en concentraciones relativamente bajas. En concentraciones altas, los compuestos fenólicos resultan tóxicos e inhiben la velocidad de crecimiento, por lo que para tratar biológicamente una corriente contaminada por compuestos fenólicos es necesario mantener su concentración por debajo de los límites tóxicos y se requiere un periodo de aclimatación previo [34].

Se pueden encontrar en la bibliografía numerosos estudios sobre biodegradación de compuestos fenólicos empleando distintas configuraciones y tipos de microorganismos. Por ejemplo, Levén y Schnürer [62] observaron que 47 mgL^{-1} de fenol eran eliminados de un reactor semicontinuo por lodos activos a 37 ºC en 23 ± 8 días, de los cuales 12 ± 8 días correspondieron a la fase Lag del sistema, obteniendo como intermedio de reacción ácido benzoico. Vázquez *et al.* [63] y Marañón *et al.* [64] obtuvieron eficacias mayores del 97% en la eliminación de concentraciones de fenol entre 185-264 mgL^{-1} por lodos activos con un reactor aerobio y un reactor discontinuo secuencial (SBR), respectivamente. Sin embargo, cuando la concentración de fenol en el efluente se aumenta hasta 456 mgL^{-1}, la eficacia de eliminación desciende hasta un 89% en un reactor de lecho

móvil con biofilm (MBBR), independientemente de tiempo hidráulico de residencia [65]. Tziotzios *et al.* [66] encontraron que concentraciones de fenol mayores de 1200 mgL^{-1} producían un fuerte efecto inhibitorio sobre los microorganismos en un SBR. Estos resultados concuerdan con los mostrados por Yoong *et al.* [67], en cuyo trabajo se observó que concentraciones mayores de 1300 mgL^{-1} de fenol producían una inhibición total del tratamiento de los contaminantes por lodos activados.

En este punto, se hace necesario recordar que los tratamientos biológicos también se emplean para la eliminación de nitrógeno en corrientes residuales nitrogenadas como aguas residuales, lixiviados de vertederos, estiércol, efluentes industriales…[68]. Los procesos de eliminación biológica de nitrógeno consisten en procesos típicamente aerobios – anóxicos, basados en la nitrificación - desnitrificación o en la nitritación parcial - anamox [68, 69]. En los últimos años, las emisiones de óxido nitroso (N_2O) procedentes del tratamiento biológico de este tipo de aguas han ganado un considerables interés, puesto que las emisiones procedentes de estos sistemas pueden llegar a suponer hasta el 10% de las emisiones globales de N_2O antropogénico. El N_2O es considerado como uno de los gases de efecto invernadero más peligrosos, con un poder 300 veces más destructivo que el CO_2 [69-71]. La mayor generación de N_2O durante el proceso biológico de eliminación nitrógeno suele ser debida a una nitritación imperfecta causada por un desequilibrio en el metabolismo de las bacterias oxidantes del amoniaco, siendo la hidroxilamina y el nitrito los principales precursores. Durante los procesos con bajo nivel de oxígeno, la desnitrificación nitrificante y la desnitrificacion heterótrofa son los dos principales procesos responsables de la emisión de N_2O [68, 70].

En el contexto del desarrollo de la investigación de la presente Tesis, se realizó un breve estudio sobre la cuantificación de la producción de N_2O en sistemas biológicos de eliminación de nitrógeno a escala de laboratorio con lodos activos. Este trabajo fue llevado a cabo en el Departamento de Ingeniería Ambiental de la Universidad Técnica de Dinamarca (DTU), en el grupo *Urban Water Engineering* bajo la supervisión del catedrático Barth F. Smets. El objetivo del trabajo fue la obtención de un modelo biocinético a escala de laboratorio a partir de los datos obtenidos en los ensayos realizados con el propósito final de poder predecir con dicho modelo la producción de N_2O a escala industrial. Para ello, se cuantificó la producción de N_2O para la vía de nitrificación, la vía de desnitrificación autótrofa y la vía de desnitrificación heterótrofa y se estudió el efecto de los principales parámetros del proceso (oxígeno disuelto, concentración de amonio, nitrito y nitrato y la relación carbono-nitrógeno del proceso) sobre cada una de las vías.

Los resultados obtenidos están siendo preparados para su publicación como artículo científico. En el anexo III se muestran el resumen y póster presentado en International Conference on Nitrification, Edmonton (Canada), en ellos se exponen parte de los

resultados y conclusiones obtenidas durante la estancia breve realizada en la Universidad Técnica de Dinamarca (DTU).

3.2. Tratamientos biológicos no convencionales de compuestos inertes/ tóxicos

3.2.1. Procesos acoplados: Procesos de oxidación avanzada y tratamiento biológico

El uso de los procesos biológicos convencionales con aguas residuales industriales no siempre resulta satisfactorio, puesto que muchos de los contaminantes orgánicos generados en las industrias son tóxicos y resistentes al tratamiento biológico [34, 38, 72]. Una opción factible para este tipo de aguas es el uso de procesos de oxidación avanzada (PAO). Esta técnica degrada contaminantes orgánicos mediante la formación de radicales hidroxilo; además es una técnica altamente reactiva y poco selectiva. Sin embargo, el uso de estas técnicas para la mineralización completa de los contaminantes es muy caro, debido a que los intermedios de reacción formados son cada vez más resistentes a su completa degradación química, lo que provoca un consumo creciente de energía y reactivos químicos [30, 32, 34, 72].

Una alternativa más atractiva es aplicar el proceso de oxidación avanzada como tratamiento previo, convirtiendo los contaminantes orgánicos persistentes en compuestos intermedios más biodegradables, que a continuación serán tratados en un proceso biológico, dando lugar a un coste global considerablemente menor [31, 34, 35, 72, 73].

Existen en la literatura varios ejemplos de procesos combinados para el tratamiento de aguas residuales industriales contaminadas con compuestos fenólicos. Entezari y Pétrier [74] comprobaron que la combinación de un proceso de sonólisis y una biodegradación enzimática es una opción muy eficaz para el tratamiento de fenol y sus haloderivados. Lafi *et al.* [75] investigaron el tratamiento de aguas residuales del procesado de la aceituna mediante procesos de oxidación avanzada, (ozonización o fotodegradación por UV), seguidos por un proceso aerobio de biodegradación con lodos activos. Con la ozonización o con la ozonización y fotodegradación combinadas se obtuvieron valores finales de demanda química de oxígeno (DQO) demasiado altos. Sin embargo, el tratamiento biológico de las aguas pretratadas mediante la combinación de ozonización y fotodegradación permite alcanzar la mayor eliminación de DQO, alcanzando eficacias en torno al 91%.

Moussavi *et al.* [73] trataron biológicamente mediante lodos activados una corriente salina contaminada por fenol, comprobando el efecto sobre el proceso de un tratamiento previo de ozonización catalizada por MgO. Con sólo el proceso biológico, fueron necesarias 50 h para la reducción de la DQO por debajo de 100 mgL^{-1} (95% de la concentración inicial) y 20 h para reducir la concentración de fenol de 1000 a 10 mgL^{-1}. Cuando la corriente salina fue pretratada por ozonización, el tiempo necesario para

reducir la DQO de 800 a 20 mgL^{-1} fueron unas 10 h y la concentración de fenol remanente que se mantuvo en el efluente tras el proceso de ozonización (100 mg L^{-1}), fue eliminada completamente en 160 minutos. Miller *et al.* [76] demostraron que un leve tratamiento previo con UV de una corriente que contenía 2,4-diclorofenol y 2,4,5-triclorofenol facilitaba enormemente la bioeliminación de ambos contaminantes de las aguas residuales.

3.2.2. Cultivos puros

Como se ha comentado en los apartados anteriores, la aplicación práctica de sistemas biológicos convencionales a aguas fenólicas está limitada por su pobre capacidad de ajuste a las posibles fluctuaciones en la carga fenólica, la variabilidad en la composición de la corriente residual, la aclimatación de los lodos, las velocidades de reacción lentas y a las elevadas concentraciones de los contaminantes presentes en las corrientes [30, 38, 77]. La incapacidad de los procesos biológicos convencionales para eliminar efectivamente muchos de los contaminantes que provienen de los procesos industriales, ha hecho necesario la aparición de tratamientos biológicos novedosos. El uso de cultivos puros y mixtos de microorganismos se ha convertid en una propuesta prometedora en los últimos años [38, 78]. Además, el uso de cultivos puros contribuye a un mejor entendimiento de los mecanismos e interacciones surgidas durante el proceso de biodegradación, bajo unas condiciones perfectamente definidas [79, 80].

Un gran número de microorganismos, incluyendo bacterias, hongos y algas, son capaces de degradar compuestos fenólicos. De hecho, la biodegradación de fenol y sus derivados mediante el uso de cultivos puros de bacterias ha sido ampliamente estudiada, aislando un gran número de especies con capacidad para degradar compuestos fenólicos, que a su vez han sido caracterizadas genética y fisiológicamente [38, 51, 81]. Algunas de ellas se muestran en la tabla 3.4.

Tabla 3.4: Lista de microorganismos aislados para la degradación de fenol (modificada de Gami *et al.* [82])

Género	**Especie**	**Concentración fenol (mgL^{-1})**
Bacillus	*Bacillus cereus mtcc 9817 strain akg1*	< 600
	Bacillus megaterium	< 400
	Bacillus simplex	< 1600
Arthrobacter	*Arthrobacter sp.*	< 300
Acinetobacter	*Acinetobacter baumannii*	100-2790
	Acinetobacter sp. Edp3	< 1000
	Acinetobacter lowffii	<2500
Rhodococcus	*Rhodococcus phenolicus sp.*	<750
	Rhodococcus ad049	<1000

Género	Especie	Concentración fenol (mgL^{-1})
	Rhodococcus coprophilus	600-1000
Pseudomonas	*Pseudomonas sp.*	<600
	Pseudomonas aeruginosa mtcc 4996	<1300
	Pseudomonas resinovorans strain p-1	< 600
Halomonas	*Halomonas sp. Strain ph2-2*	<1100
Achromobacter	*Achromobacter sp. Strain c1*	<600
Brevibacillus	*Brevibacillus sp. Strain p-6*	<600
Sphingomonas	*Sphingomonas sp fg03*	<1000
Micrococcus	*Micrococcus sp.*	. <500

3.2.2.1. *Pseudomonas putida*

Los cultivos, tanto puros como mixtos, de bacterias del género *Pseudomonas*, suelen ser la biomasa más utilizada para la biodegradación de compuestos fenólicos. Este género se ha caracterizado por tener un buen potencial en distintas aplicaciones biotecnológicas [38, 83].

Pseudomonas son bacteria Gram negativas con forma de bacilos rectos o ligeramente curvados, móviles mediante uno o varios flagelos polares. Son aerobias, con un metabolismo respiratorio estricto, con oxígeno como aceptor final de electrones. En algunos casos utilizan el nitrato como aceptor de electrones alternativo, lo que permite un crecimiento anaerobio. El diámetro de las células es normalmente inferior a 1 μm, mientras que la longitud oscila entre 1.5 y 5 μm. En la mayoría de los casos, *Pseudomonas* no son capaces de crecer a pH menores de 4.5. Algunas especies sintetizan una capa polisacárida que facilita la adhesión celular y la formación de biopelículas, aumentando así su patogenicidad. No generan esporas [83-86].

El género *Pseudomonas* es muy heterogéneo. Estas bacterias presentan un amplio espectro nutricional que varía entre las especies, disminuyendo esta variabilidad entre cepas de la misma especie. Entre los compuestos orgánicos empleados por estas bacterias como fuente de carbono y energía, se encuentran hidrocarburos lineales y aromáticos, ácidos alifáticos, aminas, amidas, aminoácidos alcoholes y compuestos aromáticos [85, 86].

Específicamente, *Pseudomonas putida* ha sido comúnmente utilizada para la biodegradación de fenol, debido a su alta eficacia de eliminación. La respuesta de *P. putida* frente agresiones químicas indican que sus células pueden desarrollar distintos mecanismos de protección para la supervivencia en ambientes extremos [38]. Esta bacteria se caracteriza además por ser una de las bacterias predominantes en los lodos activos [79, 80]. *Pseudomonas putida* pueden colonizar distintos ambientes, ya que han sido aisladas en agua, tierra y plantas de la rizosfera, donde hay oxígeno. Crecen de

manera óptima a 25-30 ºC y se puede aislar fácilmente. En la Fig. 3.3. se puede observar su estructura mediante tinción Gram y microscopía confocal.

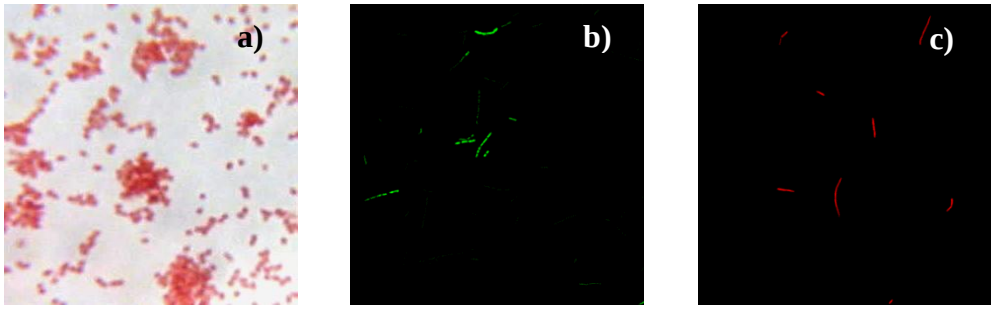

Figura 3.3: Observación de *Pseudomonas putida* DSM 4478 mediante tinción Gram (a) y mediante microscopía confocal láser con fluorocromo cFDA (b) y PI (c).

Dentro de esta especie, no se conoce ninguna cepa que sea patógena para plantas o animales. Además, son capaces de utilizar gran variedad de compuestos orgánicos como fuente de carbono y energía, gracias a que esta bacteria tiene muchos plásmidos importantes, tales como el plásmido TOL o el plásmido OCT, que juegan un papel importante en la degradación de diversos contaminantes [87, 88] . Esto hace que *P. putida* sea uno de los microbios más importantes en el campo de la biorremediación [89]. Por ello, *P. putida* se está empleando actualmente en el desarrollo de numerosas técnicas biotecnológicas como, por ejemplo, el diseño de nuevas rutas catabólicas destinadas a la degradación de compuestos orgánicos contaminantes [90].

La ubicuidad de *P. putida* refleja su elevada capacidad para adaptarse a una enorme variedad de condiciones físico-químicas presentes en los distintos hábitats donde vive. Esta habilidad representa la capacidad que tiene la cepa de integrar las señales recibidas del medio extracelular con el estado fisiológico celular, conllevando la activación de una apropiada y compleja red de regulación que controla el metabolismo celular [91].

Movahedyan *et al.* [92] investigaron la detección de bacterias capaces de degradar fenol en lodos activos mediante la técnica de reacción en cadena de polimerasa. De acuerdo con sus resultados, la bacteria que mejor degrada fenol puede eliminar completamente del medio entre 500-600 mgL^{-1} en 48 h de incubación y pertenece a la cepa *Pseudomonas putida*. Disoluciones acuosa de fenol con una concentración inicial de 1000 mgL^{-1} son tratadas con éxito por la bacteria *P. putida* ATCC17484 en suspensión en un biorreactor de tanque agitado obteniendo eficacias mayores del 95% [78], mientras que *P. putida* MTCC 1194 fue capaz de conseguir un 100 % de eficacia en 162 h trabajando en discontinuo [93]. Shourian *et al.* [94] utilizaron una cepa de *Pseudomonas sp.* SA01 para la eliminación de concentraciones de fenol comprendidas entre 300 y 1000 mgL^{-1} en un proceso en discontinuo, en todos los casos se alcanzaron eficacias del 100 % con tiempos comprendidos entre 20 y 85 h.

Los estudios del tratamiento por poblaciones mixtas de aguas contaminadas con ácido salicílico resultan prácticamente inexistentes. Sin embargo, se han investigado las bases genéticas de varios tipos de bacterias cuando este compuesto entra en su metabolismo. Existen dos vías para la degradación del ácido salicílico, la vía meta y la vía orto. La más común de estas dos vías es la meta, los enzimas que interviene se encuentran codificados en genes situados en un plásmido extracromosómico, denominado plásmido SAL. Se ha demostrado que este plásmido, inicialmente descrito en *P. putida*, puede ser fácilmente transmitido por conjugación a otras especies del género *Pseudomonas*, como *P. aeruginosa* o *P. fluorescens* [95]. La mayoría de las bacterias capaces de utilizar ácido salicílico como sustrato poseen las enzima salicilato hidroxilasa, que convierte el ácido salicílico en catecol, y la enzima catecol 2-3 oxigenasa, que degrada el catecol en acetaldehído y ácido pirúvico como productos finales (Figura 3.4.)

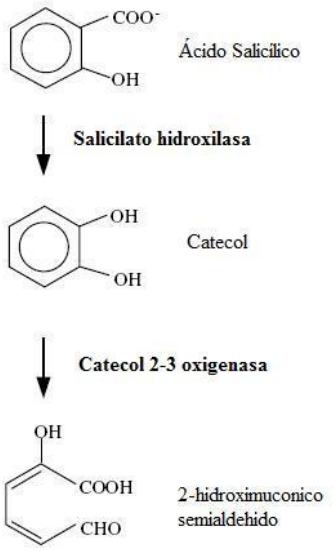

Figura 3.4: Degradación del ácido salicílico y comienzo de la vía meta (modificado de Chakrabarty [95]).

3.2.2.2. *Paracoccus thiocyanatus*

Dado que en los subapartados 5.4 y 5.5 de los resultados se estudia la biodegradación de tiocianato por *P. thiocyanatus*, como proceso de biodegradación aislado o en paralelo a la biodegradación de SA por *P. putida*, se ha considerado conveniente realizar en este punto una pequeña reseña sobre el tiocianato y las características de la bacteria *P. thiocyanatus.*

El tiocianato (SCN^-), junto con algunas otras especies cianuradas, constituye uno de los contaminantes más importantes presentes en las aguas residuales industriales. El tiocianato es tóxico para muchos organismos, incluso a bajas concentraciones (su LC50

se encuentra entre 50-100 mgL^{-1}) [96]. Una absorción crónica puede causar vértigo, mareos, erupciones cutáneas, derrames nasales, vómitos y nauseas [6, 96]. Su vertido en aguas naturales produce toxicidad en la flora y la fauna acuática y su presencia en aguas residuales dificulta el tratamiento biológico de las mismas [97]. El tratamiento biológico de tiocianato puede ser llevado a cabo mediante microorganismos autótrofos y heterótrofos: generalmente se considera que en las plantas de tratamiento biológico de aguas residuales son los microorganismos autótrofos los principales responsables de la biodegradación de este compuesto, describiéndose dos vías principales para la degradación de tiocianato: la ruta del cianato y la ruta del sulfuro de carbonilo [98].

Durante la ruta del cianato, el tiocianato es primeramente hidrolizado a cianato, que posteriormente se hidroliza a amonio y bicarbonato. De igual forma, el sulfuro producido es transformado rápidamente por oxidación a sulfato. El proceso viene representado por:

$$SCN^- + 3H_2O + 2O_2 \longrightarrow HCO_3^- + NH_4^+ + SO_4^{2-} + H^+ \quad (1)$$

La ruta del sulfuro carbonilo tiene lugar por la acción del encima tiocianato hidrolasa, producida por la bacteria quimiolitoautótrofa *Thiobacillus thioparus*, que permite la degradación del tiocianato a sulfuro de carbonilo y amoniaco, con el consiguiente aumento de pH. El sulfuro de carbonilo puede ser posteriormente asimilado por los microorganismos, dando lugar a la formación de un modo equimolar de sulfato a partir del tiocianato.

$$SCN^- + 2H_2O \longrightarrow COS + NH_3 + OH^- \quad (2)$$

A pesar de que la eliminación de tiocianato mediante procesos biológicos es una alternativa medioambientalmente muy adecuada, se ha encontrado en la bibliografía que a concentraciones superiores a 20 mgL^{-1} comienza la inhibición por sustrato, inhibiendo completamente el proceso a concentraciones superiores a 1000 mgL^{-1} [99, 100].

Al igual que en el caso de compuestos fenólicos, el estudio del proceso mediante cultivos puros puede resultar beneficioso para la comprensión del proceso. En este caso se ha seleccionado como cultivo puro la bacteria *Paracoccus thiocyanatus* anteriormente nombrada como *Thiobacillus sp.*. El origen de esta bacteria son unos lodos activos enriquecidos con tiocianato procedentes de Japón de donde se aisló el microorganismo. Son bacterias Gram-negativa con forma de varilla, de 0.5-0.7 μm de ancho y 0.8-1.3 μm de largo, que crecen solas o en parejas, no forman esporas y no son móviles. Crece de forma aerobia y anaerobia con oxígeno o nitrato como aceptor terminal de electrones, respectivamente. Son neutrófilas y mesófilas. Se caracterizan porque son capaces de utilizar el tiocianato como fuente de energía [101].

La bacteria *Thiobacillus thioparus* THI115 es capaz de degradar concentraciones de tiocianato por encima de los 3400 mgL^{-1} en 130 h cuando se suministra al sistema suficiente oxígeno y se mantiene el pH del medio en torno a 6.2 [102]. Katayama y Kuraishi [103] investigaron el comportamiento de *Thiobacillus thioparus* TK21 en un medio salino que contenía entre 300 y 1500 mgL^{-1} de tiocianato. Los resultados del trabajo mostraron que la velocidad de degradación del tiocianato por la bacteria alcanzó el máximo valor entre las 25 y 40 h, no siendo dependiente de la concentración del contaminante en el medio. Se observó que 500 mgL^{-1} de tiocianato se eliminaban completamente en 60 h, sin embargo, cuando la concentración de tiocianato estuvo entre 800 y 1500 mgL^{-1}, la bacteria *T. thioparus* TK21 sólo pudo eliminar unos 500 mgL^{-1} durante las primeras 75 h. Katayama *et al.* [104] y Bezsudnova *et al*. [105] extrajeron la enzima tiocianato hidrolasa, la cual desempeña un papel importante en el metabolismo de degradación del tiocianato por *T. thioparus* y *T. thiocyanoxidans*. *Thiobacillus sp*. THI 011^T presentó una tasa de crecimiento específico en presencia de tiocianato de 0.059 h^{-1} siendo capaz de degradar completamente 3500 mgL^{-1} de tiocianato potásico, con la consecuente producción de sulfato e iones de amonio y potasio [101].

3.3. Efecto de agentes externos en cultivos puros

Como ya se ha comentado en apartados anteriores, el tratamiento biológico es una de las técnicas de tratamiento de aguas residuales más prometedora y económica. Por ello, existen multitud de estudios en la literatura que analizan el efecto de variables como temperatura, composición del medio, concentración del contaminante, agitación, tipos de biomasa, tipos de reactores…sobre el proceso biológico [38, 51, 102, 106-108]. Sin embargo, debido a los avances científicos, surgen nuevas sustancias, como materiales nanoparticulados o carbón activo, con un uso cada vez más habitual en la sociedad, cuyo destino final, bien de forma accidental o intencionada, son las plantas de tratamiento de aguas residuales. El problema es que apenas existen estudios sobre el efecto que producen estos agentes externos sobre el tratamiento biológico ni sobre el proceso de biodegradación de contaminantes orgánicos [28, 29, 109, 110].

3.3.1. Partículas: Carbón activo

El proceso biológico de degradación de fenol puede emplear biomasa en suspensión o células inmovilizadas. Se ha demostrado que la velocidad de degradación de los compuestos fenólicos se puede mejorar mediante la inmovilización de las células atrapándolas sobre un soporte sólido como el carbón activo [38]. A este respecto, Rice y Robson fueron los primeros en proponer el término carbón activo biológico para el sistema de tratamiento de aguas residuales en el que la actividad microbiana aerobia es promovido por un carbón activo granular. Este tipo de tratamiento, basado en la adsorción y la biodegradación simultánea, es una opción técnica y económicamente factible para

tratar diferentes tipos de aguas residuales industriales, que contienen una elevada concentración de contaminantes orgánicos tóxicos [17, 18, 23].

El carbón activo biológico presenta una serie de ventajas y desventajas [17]. Entre las ventajas está que el sistema combinado de carbón activo con biomasa tiene una efectividad muy superior al de ambos sistemas convencionales de tratamiento de aguas por separado. Además, esta configuración permite adsorber materias no biodegradables y oxidar los contaminantes biodegradables en un solo reactor y el coste de capital para el sistema de reactor único es inferior que el necesario para los procesos individuales. Asimismo, la regeneración del sistema combinado es mucho menos frecuente, lo que implica menores gastos energéticos y de explotación. Adicionalmente, la presencia de carbón activo sirve como protección de las bacterias a los efectos tóxicos de altas concentraciones de contaminantes. A diferencia de la adsorción con carbón activo, en el que se debe regenerar el carbón térmicamente cuando alcanza la saturación, en la bioadsorción puede llevarse a cabo una regeneración del sistema *in situ* debido a la actuación bacteriana sobre el contaminante adherido al carbón activo [17, 111]. Las principales desventajas del carbón activo biológico son el escaso conocimiento existente sobre el sistema; de hecho, se ha aplicado en muy pocas ocasiones en el tratamiento de aguas a nivel industrial debido a la elevada caída de presión provocada por obstrucción del lecho por crecimiento microbiano. Otra limitación de esta técnica es que las bacterias unidas al carbón están protegidas frente a los efectos tóxicos de los contaminantes, pero también frente a los sistemas de desinfección, lo que puede provocar la proliferación de microorganismos patógenos. [17, 112, 113].

El proceso de bioadsorción y la regeneración del carbón activo por el biofilm bacteriano se han estudiado por varios autores, tratando de encontrar cómo ocurre el mecanismo de bioregeneración. Una de las teorías propuestas en la bibliografía sugiere que la presencia del carbón aumenta la interfase sólido-fluido, en la cual las células microbianas, enzimas, materia orgánica y oxígeno se adsorben, lo que proporciona un ambiente enriquecido para el metabolismo microbiano [23]. Por otro lado, si bien el tamaño de las bacterias es demasiado grande para colonizar los microporos del carbón, las enzimas producidas por estas pueden difundir fácilmente por lo microporos y reaccionar con el sustrato adsorbido. Los productos de reacción formados estarían más débilmente unidos con lo que se desorberían y serían un nuevo sustrato para el biofilm [17]. Otra de las teorías disponibles explica que el sistema no es más que una simple combinación de biodegradación y adsorción con carbón activo sin la existencia de bioregeneración en el sistema, la mejora de la eficacia es debido únicamente a un efecto sinérgico de los dos procesos [17, 23]. Por último, varios autores piensan que la bioregeneración se produce como consecuencia de una desorción de la especie adsorbida, que podría a continuación ser degradado por el biofilm. Esta desorción ocurriría como consecuencia de una disminución de la concentración del adsorbato en la fase líquida. Se deduce de lo anterior que la

bioregeneración sólo puede darse en compuesto que son a la vez biodegradables y fácilmente adsorbibles [17].

Pai *et al.* [114] observaron que el proceso de bioadsorción resultaba mucho más eficaz en el tratamiento de aguas contaminadas por fenol por *Rhodococcus sp.*. En su estudio, la velocidad de degradación del fenol aumentó desde 0.432 g $(Ld)^{-1}$ a 2.91 g $(Ld)^{-1}$ al usar carbón activo biológico en lugar de células en suspensión. Walker y Weatherley [17] comprobaron que la biodegradación del colorante color azul ácido (TB4R) por la bacteria *P. putida* (NICMB 9776) aumentaba en un 60% cuando las bacterias formaban un biofilm sobre el carbón activo, en lugar de encontrarse en suspensión. Orshansky y Narkis [23] también llevaron a cabo el tratamiento de fenol mediante su adsorción sobre carbón activo y biodegradación simultánea con lodos activos, obteniendo calidades de agua mejores con el proceso simultáneo que con los tratamientos llevados a cabo por separado. La presencia del carbón activo en los lodos supuso una mejora de la biooxidación del fenol y de la respiración microbiana. En otro trabajo, el uso de biopartículas de *Candida tropicalis* sobre carbón activo también supuso la eliminación eficaz de fenol, con una velocidad volumétrica superior a 60 mg fenol $(L\ h)^{-1}$ en un reactor fluidizado [108]. Además, el carbón activo biológico puede biorregenerarse y volver a utilizarse, tal y como muestran Ivancev-Tumbas *et al.* [115]. Estos autores estudiaron la eficacia de la bioadsorción del fenol antes y después del proceso de biorregeneración del carbón activo biológico, con concentraciones de fenol que variaban entre 1.9-1053 mgL^{-1}. Obtuvieron eficacias entre el 92-100%, independientemente de si se utilizaba carbón activo biológico fresco o biorregenerado.

3.3.2. Materiales sólidos nanoparticulados

Las partículas con tamaño nanométrico han estado presentes en la tierra durante millones de años, siendo utilizadas por el ser vivo desde hace miles de años [24, 109]. Un ejemplo es el hollín que procede de la combustión incompleta de los combustibles fósiles [109]. Sin embargo, las nanopartículas (NP) atraen mucha atención a día de hoy, debido a la creciente capacidad del ser humano para sintetizarlas y manipularlas [24, 116].

Las NP se definen como aquellas sustancias que poseen al menos una de sus dimensiones con un tamaño inferior a 100 nm. Estas partículas pueden ser esféricas, tubulares o de forma irregular; además, pueden existir fusionadas, agregadas o aglomeradas [24, 109, 116, 117]

Las NP pueden definirse como partículas de procedencia natural o antropogénica, haciendo una subdivisión teniendo en cuenta su composición química, como NP que contienen carbono o NP inorgánicas [24]. Dentro de las NP naturales que contienen carbono se pueden distinguir NP biogénicas, geogénicas, atmosférica y pirogénica. Algunos ejemplos son los fullerenos de origen pirogénico o los aerosoles atmosféricos.

Las NP antropogénicas son aquellas partículas que se han formado involuntariamente como subproducto o aquellas que se han generado intencionadamente debido a sus características particulares; en este último caso se denominan NP de ingeniería. Algunos ejemplos son las nanopartículas de dióxido de titanio, de plata, o materiales de la familia del grafeno [24].

Las NP tienen una infinidad de usos en diferentes áreas, como la electrónica, biomédica, farmacéutica, nutrición, cosmética, energía, medioambiente, catálisis, aplicaciones materiales… [24, 116, 118]. Los datos publicados sobre el uso y producción de las NP suelen ser escasos y, a menudo, contradictorios. La previsión de la producción de NP entre los años 2011-2020 es de unas 58.000 toneladas [24]. El enorme aumento previsto en la fabricación y uso de estos nanomateriales hace muy probable que exista una exposición del ser humano y el medioambiente a este tipo de compuestos [24]. Como resultado, las NP están siendo sometidas actualmente a estudios sobre sus potenciales efectos adversos sobre la salud y el medioambiente.[24, 118].

Para poder realizar una evaluación de los riesgos que surgen como consecuencia del uso de NP, es necesaria un estudio previo de su movilidad, biodisponibilidad y toxicidad. Para que los nanomateriales comprendan un riesgo tiene que darse un potencial de exposición y un peligro como resultado de la exposición [24, 109, 116, 117].

En la figura 3.5, se observan las diferentes formas de contacto de las NP con el entorno, así como las posibles vías de entrada de las NP en el medio ambiente. La liberación de las NP puede provenir de fuentes puntales, como las instalaciones de producción, vertederos o plantas de tratamiento de aguas residuales, de fuentes no puntuales, como el desgaste de los materiales que contienen NP. Otras vías de entrada son los vertidos accidentales durante la producción o transporte y la liberación intencionada; sería el caso de la inyección de nanopartículas de hierro con valencia cero (nZVI) en aguas subterráneas contaminadas con solventes clorados [24]. Las NP en su estado agregado o adsorbidas son menos móviles, pero la acumulación de las mismas en organismos vivos es posible [24, 117]. La presencia de NP en, por ejemplo, los suelos plantea la posibilidad de que importantes procesos que ocurren en él, como es el ciclo del carbono y nitrógeno, se vean negativamente afectados siendo esto también aplicable a otros procesos, como es el tratamiento de aguas residuales [118].

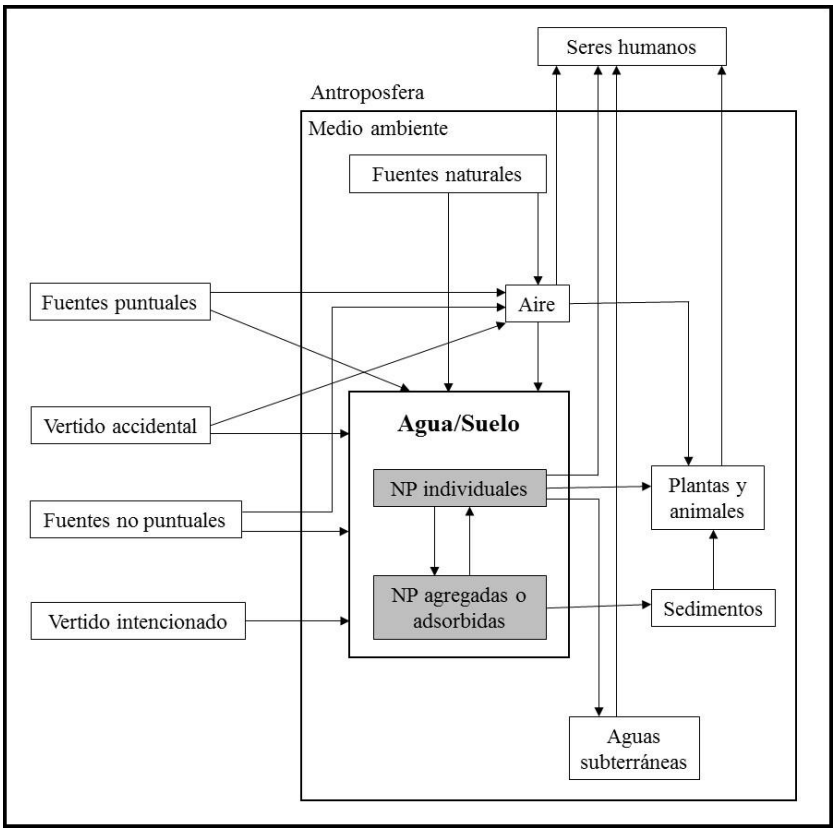

Figura 3.5: Vías de entrada de las nanopartículas de la antroposfera al Medio Ambiente, reacciones en el entorno ambiental y exposición de los seres humanos a los nanomateriales. Figura adaptada de Nowack y Bucheli [24].

Existen una serie de investigaciones que muestran que las partículas de tamaño nanométrico son adsorbidas por una amplia variedad de células procedentes de mamíferos, siendo las NP capaces de atravesar la membrana celular y ser internalizadas [24, 116]. Dentro de la célula, las NP se almacenan en ciertos lugares, como por ejemplo en las vesículas, para desde ahí emitir una respuesta toxica. Los efectos causados por la presencia de las NP son la inflamación y la fibrosis a nivel de organismo y el estrés oxidativo, la actividad antioxidante y la citotoxicidad a nivel celular [24, 118]. Estudios ecotoxicológicos han demostrado, por otro lado, que las NP también son tóxicas para organismos acuáticos tanto unicelulares como animales [24], además de para las bacterias [118]. No hay estudios concluyentes sobre el efecto de las NP sobre la plantas. En muchas ocasiones, estos resultados suelen ser bastante inconsistentes, puesto que en la bibliografía se suelen encontrar resultados contradictorios [109].

En comparación con otros contaminantes convencionales o contaminantes emergentes, las NP plantean un nuevo reto para los investigadores. Mientras que es obvio que el tamaño de estos materiales juega un papel importante con respecto a su toxicidad, no se sabe nada acerca de cómo ese tamaño afecta al comportamiento y a su toxicidad [109]. Además, es importante darse cuenta de que muchas de las NP han sido funcionalizadas,

que los factores ambientales pueden cambiar dicha funcionalización o que el recubrimiento de la superficie de las NP por compuestos de origen natural también pueden afectar al comportamiento de las NP en el medio ambiente; y todo esto sólo ha sido estudiado de manera incipiente [24, 117, 118].

3.3.2.1. Nanopartículas de óxido de grafeno

Recientemente, los materiales de la familia del grafeno han recibido mucha atención, ya que se han comenzado a introducir en distintos campos [119]. Dentro de la familia del grafeno, se encuentra el óxido de grafeno (GO), que es el precursor de los materiales de esta familia. El GO se caracteriza por sus propiedades electrónicas y mecánicas, su magnetismo específico, su alta conductividad, su elevada superficie específica y su actividad electrocatalítica [119]. Debido a sus características específicas, las aplicaciones más importantes de este tipo de materiales, son células solares, sensores, adsorbentes para la eliminación de metales pesados, baterías de litio, condensadores, catalizadores, dispositivos de almacenamiento de energía… [25, 26, 119, 120]. Hoy en día, se está investigando el uso del GO como adsorbente de enzimas o administrador de fármacos y en biosensores [119].

El gran número de aplicaciones del GO conlleva una elevada producción del mismo y, en consecuencia, una mayor probabilidad de presencia de este compuesto en el medio ambiente. Por lo tanto, es de vital importancia conocer sus efectos sobre la salud y el medio ambiente [25, 26]. En este sentido, la literatura ofrece un creciente número de estudios sobre la toxicidad, el comportamiento ambiental y ecotoxicidad de estos materiales [25, 29, 119, 121].

Las causas de la inactivación bacteriana como consecuencia de los GO son, principalmente, el estrés oxidativo como consecuencia de la formación de ROS (especies reactivas de oxígeno o “reactive oxygen species”), el corte de las rutas metabólicas intracelulares y la ruptura de la membrana [119, 122-127]. Algunas propiedades físico-químicas han demostrado tener efecto en el grado de inhibición del GO sobre la bacteria; entre ellas está la concentración del GO, el tiempo de incubación, la orientación del nanomaterial, el tipo de bacteria (Gram - o Gram +), el medio… [25, 26, 119, 120, 122, 125-130].

3.3.2.2. Nanopartículas de dióxido de titanio

Las nanopartículas de dióxido de titanio (TiO_2-NPs) son un nanomaterial que se incluyen dentro del grupo de las NP de ingeniería. Los óxidos de nanopartículas metálicas se encuentran entre los más utilizados. El TiO_2 se ha producido durante muchos años a granel; sin embargo, se está fabricando este material recientemente en tamaño

nanométrico [24, 117]. De hecho, es una de las NP con mayor volumen de producción, llegando a las 10.000 toneladas al año [116].

Las TiO_2-NPs son ampliamente empleadas en fotocatálisis y como pigmentos en papel, pinturas, tintas y plásticos. Además, se usan también como aditivo en cosméticos [24, 117, 131-133]. Este producto es utilizado en cantidades considerables para la protección UV, especialmente en protectores solares y recubrimientos. Entre un 50 y un 80% de la producción total es usado para este fin, mientras que un 10-30% de la producción se emplea como aditivo de pinturas [116].

La amplia aplicación de TiO_2-NPs en diversa industrias y en la vida cotidiana ha provocado la detección de este nanomaterial en el suelo y en aguas superficiales y residuales, [131, 134], lo que ha despertado una preocupación global con respecto a los posibles efectos adversos en los sistemas biológicos. Aunque los factores que pueden tener un posible impacto en las interacciones entre nanomateriales y las biomoléculas ha sido ampliamente estudiado, no es un tema resuelto a día de hoy [28, 110].

El mecanismo de toxicidad bacteriana como consecuencia de nanopartículas metálicas aún se está dilucidando, pero las posibilidades que se están barajando incluyen la toxicidad provocada por la presencia de iones metálicos libres y el estrés oxidativo por la formación de ROS [133, 135-137]. La inactivación celular se relaciona con la inhibición de la respiración celular, descomposición de la capa de lipopolisacáridos, daño en el ADN, genotoxicidad, la liberación de componentes tóxicos y el desarreglo estructural de la membrana citoplasmática [117, 118, 131, 133, 135]. Parámetros como la concentración de TiO_2-NPs, el tipo e intensidad de la radiación a la que se somete el proceso, el tiempo de exposición, la presencia de la NP en suspensión o como fijadas en una superficie, la funcionalización del TiO_2-NPs…. [132, 133, 136-141] se han estudiado para comprobar si afectan al grado de inhibición bacteriana.

3.3.2.3. Efecto de las nanopartículas sobre el tratamiento biológico de aguas residuales

En ambos casos, GO y TiO_2-NPs, no se han realizado apenas investigaciones sobre el efecto de ambos en el tratamiento biológico de aguas residuales, donde la presencia de estos nanomateriales es cada vez más común, ya que llega a través de aguas residuales urbanas o industriales [29]. Si se tiene en cuenta que las estaciones depuradoras de aguas residuales son la última barrera antes del vertido de las nanopartículas al medio ambiente, un buen conocimiento sobre el efecto de éstas sobre las bacterias puede ser clave [24, 116].

Entre los pocos estudios sobre el efecto que produce la presencia de NP sobre el tratamiento biológico de aguas residuales, podemos nombrar a Li *et at.* [131] quienes estudiaron el efecto de la presencia de concentraciones entre 2-200 mgL^{-1} de TiO_2-NPs

sobre el proceso de nitrificación con lodos activos en un reactor secuencial. La eficacia de nitrificación del sistema se redujo del 80 a 20.3% en presencia de la concentración de NP más elevada. Puay *et al.* [142] analizaron el efecto de la presencia de ZnO-NPs sobre el proceso biológico en un reactor secuencial, en este caso observaron que 1 mgL^{-1} de ZnO-NPs causó un impacto significativo sobre las propiedades de sedimentación de los lodos activos, redujo la diversidad bacteriana presente en el sistema y afectó negativamente a la eficacia de eliminación del nitrógeno, disminuyendo del 100 al 70% en tan sólo dos días de exposición. Estos resultados están de acuerdo con el trabajo de Zheng *et al.* [143], quienes obtuvieron un descenso de la eficacia de eliminación del nitrógeno de 81.5% a 75.6 y 70.8% y un incremento de la concentración del fósforo en el efluente de no detectable a 10.3 y 16.5 mgL^{-1} en presencia de 10 y 50 mgL^{-1} de ZnO-NPs, respectivamente. Muchas de las investigaciones hechas hasta ahora sobre la toxicidad de las nanopartículas basan sus conclusiones sobre la pérdida de viabilidad bacteriana o muerte en los resultados obtenidos de medidas con ioduro de propidio (PI) y el microscopio confocal [123, 144], el análisis de $CFUmL^{-1}$ [25, 120, 125, 129, 130, 133, 136, 137, 144-146], o análisis de ADN o ARN libres [122, 125] y medidas de densidad óptica (OD) [135, 145]. La mayoría de los estudios realizados utilizan a la bacteria *Eschericia coli* para comprobar el efecto que produce sobre ellas la presencia de los materiales nanoparticulados, no encontrando ningún estudio que utilice *P. putida*. Además en estas investigaciones no tienen en cuenta el efecto de los nanomateriales sobre la actividad metabólica de los microorganismos.

3.3.3. Otros sustratos: compuestos cianurados

La biodegradación se caracteriza por ser un proceso multifacético en el que tanto elementos abióticos como bióticos están involucrados. Hay muchos factores que pueden afectar a la capacidad de degradación o al metabolismo de los microorganismos, tanto en la prevención como en la estimulación del crecimiento de los mismos [38].

El rendimiento de la biodegradación puede verse afectado por la presencia de inhibidores metabólicos o sustratos en competencia. Hay limitaciones impuestas por la presencia de contaminantes ambientales en mezclas, como que la degradación de uno de los componentes puede ser inhibida por los otros componentes de la mezcla [5, 38]. Las corrientes de aguas residuales contaminadas por compuestos fenólicos en raras ocasiones se encuentran solos en la corriente, esto puede producir una ralentización o inhibición de la degradación del compuesto fenólico o, al contrario, puede dar lugar a fenómenos de sinergia entre ambos contaminantes [38, 98, 147-149]. Uno de los contaminantes que frecuentemente nos encontramos mezclados con los compuestos fenólicos son los compuestos cianurados, especialmente en aguas de coquería [5, 7, 65, 148, 150].

En la bibliografía pueden encontrarse numerosas investigaciones en las que se estudia el efecto que produce la presencia de compuestos cianurados o fenólicos sobre la

biodegradación de compuestos fenólicos o cianurados, respectivamente. Sharma *et al.* [149] comprobaron que la presencia de cianuro (2.5mgL^{-1}) producía un incremento en la fase Lag del proceso de la eliminación de compuestos fenólicos por lodos activos de modo aerobio, además de un aumento en los tiempos de eliminación de los compuestos fenólicos. Neufeld y Valiknac [151] también encontraron que un compuesto cianurado como el tiocianato, inhibía la oxidación de fenol por lodos activos. Banerjee [5] estudió el tratamiento de aguas residuales contaminadas por fenol y tiocianato en un reactor biológico segmentado en cuatro etapas con lodos activos. En el proceso se observó una eliminación secuencial de los contaminantes. En los dos primeros segmentos del reactor se eliminó principalmente el fenol mientras que el tiocianato se biodegradó en las dos últimas etapas del proceso, en los que las inhibición como consecuencia de la presencia de fenol era prácticamente inexistente. Este fenómeno se contrasta con los resultados obtenidos por Adjei y Ohta [152], quienes observaron que el fenol era un inhibidor de la utilización del cianuro por *Burkholderia cepacia* C-3. Los resultados de Pan *et al.* [153] también mostraron que la presencia de 738 mgL^{-1} de fenol producía un aumento en el tiempo de eliminación de 108 mgL^{-1} de tiocianato de 18.5 h en un sistema de tratamiento con lodos activos. Kwon *et al.* [148] encontraron que *Acremonium strictum* era capaz de eliminar hasta 7.4 gL^{-1} de tiocianato. Una concentración de 1.2 gL^{-1} de tiocianato fue completamente eliminada del sistema en 23 h, sin embargo, la presencia de 312 mgL^{-1} de fenol supuso un aumento en el tiempo necesario para alcanzar el 100 % de eliminación a 60 h. Una concentración mayor de fenol (625 mgL^{-1}) implicó una mayor inhibición de la biodegradación de tiocianato por *Acremonium strictum*, eliminándose tan sólo el 33% de la concentración del tiocianato inicialmente introducido en 60 h.

3.3.4. Otras bacterias

En su hábitat natural, las bacterias pueden interaccionar con bacterias de otras especies, surgiendo la competición por recursos, el consumo de metabolitos secundarios o la producción de biosurfactantes, entre otros. Dependiendo de las interacciones específicas, aparecen pues los fenómenos de comensalismo, mutualismo, parasitismo o competición [10].

De modo que, basándonos en el conocimiento de los productos y capacidades de degradación de las bacterias individuales, se puede proponer una cooperación de los diferentes organismos en la biodegradación de determinados contaminantes. La construcción de una comunidad funcional de microorganismos es necesaria para el éxito microbiano. Además, aprender cómo los distintos módulos microbianos interaccionan entre ellos es fundamental para el desarrollo de los procesos biotecnológicos, incluyendo la biorremediación [13]. El estudio de las interacciones entre especies microbianas es necesario como paso previo para investigar los beneficios que surgen al adicionar uno o

varios cultivos puros a uno mixto con el fin de mejorar la degradación de los contaminantes (bioaumentación) [12-14].

En trabajos recientes se han encontrado que el uso de un consorcio microbiano presenta un comportamiento biodegradativo mejor que el obtenido por los microorganismos de forma individual. Se obtienen mayores eficacias de biodegradación de contaminantes orgánicos con co-cultivos que combinan la actividad enzimática inherente de cada uno de los microorganismos del consorcio [6, 7, 9, 154-163].

3.4. Principios de la técnica de citometría de flujo

En la cuantificación celular, los parámetros habitualmente utilizados son el peso seco, la densidad óptica y las $CFUmL^{-1}$. Sin embargo, estas medidas no dan valores reales; en el caso del peso seco y la densidad óptica, su valor no coincide con la cantidad efectiva de biomasa, ya que incluye la biomasa endógena y materia orgánica particulada no biótica. El método de conteo en placa, se caracteriza por ser una técnica lenta y laboriosa y que subestima el número de células, además de ser muy variable debido al sesgo introducido por las condiciones de incubación seleccionadas y factores físicos que reducen la cultivabilidad de las células [164]. Además, el conteo en placa sólo revela una pequeña porción (bacterias viables y cultivables) de la población microbiana total, y no considera al resto de los microorganismos que están estresados o que han entrado en un estado en el que son incapaces de crecer en placa [165].

La citometría de flujo (FC) es una técnica sofisticada de análisis cuantitativo que permite la caracterización fisiológica de una población microbiana a nivel individual. La citometría de flujo puede llevar a cabo diferenciación de cultivos mixtos y estudiar las heterogeneidades presentes en una población en relación a sus propiedades estructurales y funcionales gracias a su capacidad de análisis multiparamétrico basado en las propiedades intrínsecas de la célula, como la dispersión de la luz y las características controladas por la fluorescencia [166-169].

La citometría de flujo multiparamétrico que es capaz de dar una cuantificación más precisa de las células libres en una suspensión en comparación con la observación microscópica convencional de suspensiones microbianas. Además, la tinción simultánea de las bacterias con diferentes fluorocromos proporciona una manera extremadamente poderosa no sólo para demostrar la heterogeneidad fisiológica de la muestra, sino también para comprender la funcionalidad microbiana [169-171].

La técnica de citometría de flujo se fundamenta en el paso de una suspensión de partículas alineadas y de forma individual a través de un haz de luz láser focalizado. De esta forma, se mide el impacto de cada célula con el rayo de luz, lo que produce señales relacionadas con distintos parámetros celulares y hace posible la medición simultánea de múltiples

características a partir de una sola célula. Si además se añaden a la muestra fluorocromos con capacidad de adherirse a ciertas estructuras celulares de manera específica, se podrán distinguir los diferentes estados metabólicos celulares según la fluorescencia emitida [169].

A pesar de que el uso de citometría de flujo ha sido restringido a ciertos campos especializados, los avances técnicos en instrumentación y metodología han permitido que su aplicación se comience a extender en el campo de la microbiología ambiental [164, 169]. En la tabla 3.5 se muestran algunos trabajos de microbiología ambiental en los que se aplica la técnica citometría de flujo.

Tabla 3.5: Aplicaciones ambientales actuales de la técnica citometría de flujo [164, 172]

Medio	Objetivo	Referencia
Agua potable	Detección en los sistemas de distribución de *Cryptosporidium, Giardia* y rotavirus humanos; Comparación de comunidades microbianas, y sus cambios como consecuencia de factores ambientales	[170, 173-175]
Agua superficial	Sondeos microbianos, mapeo de cuencas hidrográficas, evaluación microbiana durante la resuspensión de sedimentos y bacterias específicas de la zona	[176-178]
Agua subterránea	Mapeo de contaminación microbiana en cuencas dinámica. Aplicaciones de biorremediación y transporte microbiano; Incorporación escapes para la caracterización del agua subterránea en la superficie. Estudios realizados con *Legionella*, *Cryptosporidium* y bacterias totales	[179-181]
Aguas residuales	Detección y cuantificación de bacterias específica y totales; Cuantificación de concentración de virus; Cambios en la comunidad bacteriana;	[168, 182, 183]
Lodos activos	Detección y cuantificación de bacterias específica y totales; Estudios de viabilidad y biodiversidad en lodos activos.	[168, 182, 184-187]

3.4.1. Instrumentación, adquisición y tratamiento de datos

Un citómetro de flujo se describe como un microscopio automático que se caracteriza por su objetividad, velocidad de análisis, precisión y sensibilidad [166, 169]. El citómetro de flujo está formado por cinco unidades de operación: una fuente de luz (lámpara de mercurio de alta presión o láser), una celda de flujo o mezcla, un sistema de fluidos, una serie de filtros ópticos para la detección de longitudes de onda específicas sobre un rango

espectral más amplio, una serie de fotodiodos o tubos fotomultiplicadores para la detección de señales de interés, y una unidad de procesamiento de datos [166, 169]. En la figura 3.6 se muestran cada una de las partes del citómetro de flujo descritos anteriormente.

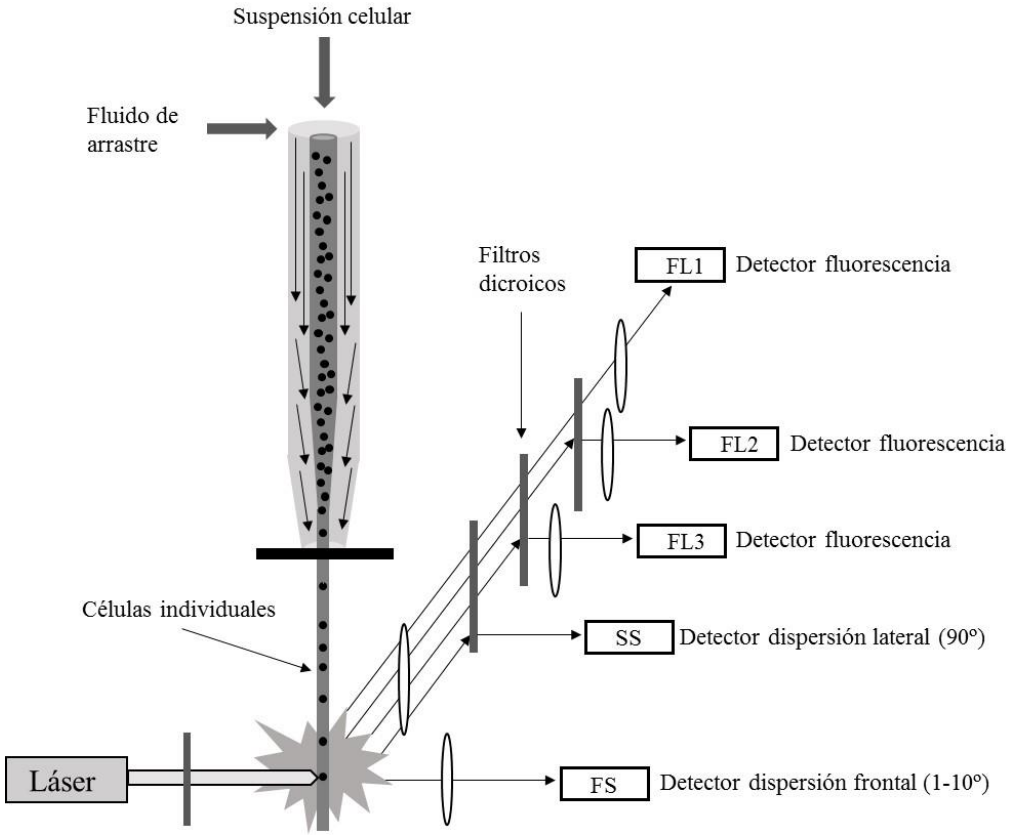

Figura 3.6: Esquema de un citómetro de flujo. La figura representa la cámara de flujo, la fuente de luz (láser), el sistema óptico con una serie de filtros y espejos y el sistema de detección formado por dos detectores de dispersión (SS y FS) y tres de fluorescencia (FL1, FL2, FL3). Modificado de Díaz *et al.* [169]

En resumen, el sistema de flujo introduce y restringe a las células para su análisis individual y el sistema óptico excita la muestra al pasar por delante de un rayo láser ortogonal al flujo y recoge las señales de luz provenientes de la misma, ya que emite luz fluorescente (en caso se utilización de fluorocromos) y dispersada. Las señales de dispersión se correlacionan con las propiedades de refracción de la célula, es decir, con las características superficiales y la estructura interna de la misma. Las características morfológicas celulares que determinan la dispersión de la luz son fundamentalmente el tamaño, la membrana, el núcleo y el material granular del interior de la célula, lo que constituye la complejidad celular [166]. La luz dispersada hacia el frente es recogida por un detector en ángulo cónico (entre 1 y 10º) sobre el punto de incidencia del láser. Esta fracción de luz dispersada que coincide prácticamente con la dirección del haz incidente, se conoce como FS (*Forward Scatter* o dispersión frontal) y es una medida relacionada

con el tamaño de la partícula que produce la dispersión, de modo que la cantidad de luz dispersada en esta dirección tiende a aumentar con el tamaño de la célula. La luz dispersada lateralmente y la fluorescencia son recogidas y separadas por una lente situada a 90º del eje de incidencia del láser. La luz dispersada en ángulo recto, llamada SS (*Side Scatter* o dispersión lateral) es proporcional a la complejidad de la estructura interna de la partícula. La fluorescencia es dividida a su vez por un espejo dicroico, distinguiendo entre diferentes longitudes de onda [169].

Finalmente, el sistema electrónico convierte la señal óptica en una señal electrónica y la digitaliza para el análisis de los datos. La adquisición celular es la visualización en tiempo real de los parámetros de dispersión y fluorescencia, pudiendo se almacenados para su posterior análisis. Los datos adquiridos de cada parámetro se denominan eventos y se refiere al número de células que presentan la característica física o el marcador de interés. La información obtenida se representa en forma de distribuciones de frecuencia o histogramas (un solo parámetro), citogramas (dos parámetros) o representaciones isométricas (3D). En la Figura 3.7 se muestran las distintas formas de representar los datos adquiridos por citometría de flujo.

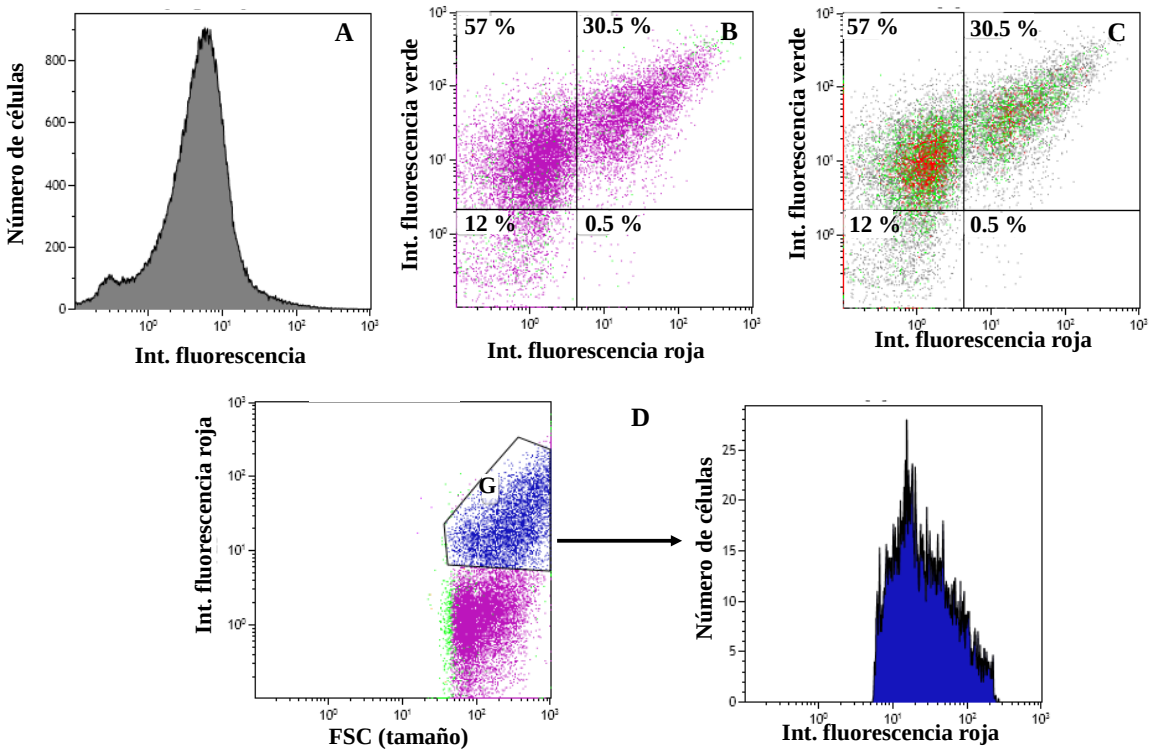

Figura 3.7: Representación de los datos adquiridos por citometría de flujo. A. Histograma. B. Gráfico de puntos. C. Gráfico de densidad. D. Análisis de la proporción de células seleccionadas. Histograma de la intensidad de fluorescencia en la población seleccionada (Gate G).

Otra característica propia del análisis de datos en citometría de flujo es la utilización de ventanas de análisis ("gates") para seleccionar de manera específica una población de células o partículas de interés. Tradicionalmente, las células se seleccionan en función de las características físicas para diferenciarlas del ruido de fondo u otras partículas de pequeño tamaño que pueden estar presentes en la suspensión. La utilización de ventanas de análisis durante la adquisición permite seleccionar, normalmente en base a los parámetros de dispersión frontal y ortogonal de la luz, poblaciones de interés.

3.4.2. Marcaje celular con fluorocromos

Los parámetros celulares detectados por citometría de flujo pueden ser intrínsecos o extrínsecos. No se requieren pretratamientos para la medida de los parámetros intrínsecos; sin embargo, el estudio de los componentes celulares específicos con colorantes de fluorescencia (extrínsecos) requiere un procedimiento de tinción previo con fluorocromos específicos. De hecho, las posibilidades analíticas de la citometría de flujo se han incrementado notablemente con el desarrollo de un amplio número de fluorocromos. El uso de fluorocromos en análisis simples o múltiples suministra información adicional sobre la estructura celular, la funcionalidad o vitalidad del organismo. En consecuencia, es posible evaluar partículas de casi cualquier naturaleza, incluso mostrando tamaños por debajo del límite de resolución de la luz visible [169, 188].

Un fluorocromo es una molécula química que absorbe la luz a una determinada longitud de onda y emite a una longitud de onda superior (menor energía). Los fluorocromos utilizados en citometría de flujo deben poseer una serie de propiedades. El fluorocromo debe ser biológicamente inerte y mostrar un alto coeficiente de extinción y rendimiento cuántico, es decir, elevadas intensidades de fluorescencia provenientes de la asociación célula con fluorocromo y bajas señales del tinte que no esté unido a las células. Además su espectro de emisión debe ser estrecho para evitar la superposición, debe ser fotoestable, con una toxicidad baja y una solubilidad en agua elevada…[169].

Algunos fluorocromos se unen específicamente a la célula o a moléculas de ésta (ácidos nucleicos, proteínas y lípidos). Otros modifican sus propiedades a través de reacciones bioquímicas específicas en respuesta a cambios en el medio ambiente tales como el pH, la polarización de la membrana o la actividad enzimática o se acumulan selectivamente en los compartimentos celulares [169]. Hay una amplia variedad de fluorocromos usados en citometría de flujo, así como numerosas clasificaciones dependiendo del criterio que se aplique. Para una revisión exhaustiva de los tipos de fluorocromos disponibles para el análisis celular por microscopía y citometría, se recomienda la lectura de los trabajos de Shapiro [166] y Haugland [189].

3.4.3. Evaluación de la viabilidad y funcionalidad celular

Desde el punto de vista clásico, el concepto de viabilidad celular se basa en la capacidad reproductiva de las células. Sin embargo, esta afirmación se considera simplista hoy en día, ya que existen muchas situaciones en las que una célula pierde la capacidad de reproducirse [190]. La ausencia de colonias en el medio sólido no implica necesariamente que la célula esté muerta; la capacidad de división se puede perder temporalmente o bien las condiciones de cultivo pueden no ser las óptimas [169]. Surge el concepto de células en estado viable pero no cultivable (VBNC), dañadas o en estado de latencia, las cuales no son capaces de crecer en medios selectivos [191-193].

Los ensayos clásicos de estudios de viabilidad son muy limitados, distinguiendo solamente dos niveles extremos de actividad, células viables o células muertas. En este sentido, la técnica de citometría de flujo permite llevar a cabo una diferenciación de los estados fisiológicos intermedios, gracias a la posibilidad de medir otras funciones y propiedades celulares, como puede ser la actividad metabólica, el potencial y la integridad de membrana o la biosíntesis de macromoléculas [167].

La detección de la actividad metabólica suele llevarse a cabo mediante análisis de su actividad enzimática [169]. Los sustratos fluorogénicos más utilizados son el diacetato de carboxi-fluoresceína (cFDA) y la familia del ChemChrome (Chemunex) para la medida de la actividad esterasa. El cFDA es un sustrato fluorogénico de las esterasas intracelulares no específicas. Debido a su carácter neutro, este sustrato entra en las células por difusión; una vez dentro, tras la acción de las enzimas intracelulares, se convierte en un producto fluorescente que es retenido en el interior de las células con la membrana íntegra. Por el contrario, el sustrato no hidrolizado y el producto fluorescente son liberados rápidamente en células muertas o con membranas comprometidas. Por tanto, la integridad de la membrana es un requisito necesario para la detección de la fluorescencia en estos casos [194].

La integridad de la membrana puede ser detectada por la retención o la exclusión de colorantes. Sin embargo, las medidas relacionadas con la retención de colorantes pueden ser imprecisas debido a una entrada limitada del sustrato o a la eliminación activa del colorante. Algunas células pueden también retener el producto en vacuolas, incluso después de la permeabilización de la membrana. Por otro lado, las células con membranas intactas son impermeables a fluorocromos como SYTOX, ioduro de propidio (PI). Si la célula pierde la integridad de la membrana, estos fluorocromos penetran en la célula, asociándose al ADN y emitiendo fluorescencia [167, 169, 194]. El fluorocromo más habitualmente utilizado en la evaluación de la integridad de la membrana es el PI [167]; éste presenta una unión de tipo intercalante, estequiométrica e inespecífica al ADN, de modo que una molécula de PI se une a 4-5 pares de bases, aumentando la fluorescencia

unas 100 veces tras la unión. Es utilizado para la tinción de células muertas y es adecuado para la tinción conjunta con sondas que emiten fluorescencia verde [169].

Para llevar a cabo una evaluación más precisa de la viabilidad celular, lo más habitual es la combinación de varios fluorocromos en un análisis multiparamétrico [194]. Muchas aplicaciones se basan en la combinación de marcadores de integridad de membrana y actividad esterasa para la distinción de células viables y muertas [169, 192, 195].

En este trabajo, la determinación de los distintos estados fisiológicos celulares se basó en la combinación de medidas de la actividad metabólica e integridad de la membrana, utilizando determinados colorantes de fluorescencia que difieren en sus características espectrales. El cFDA se empleó como indicador de la actividad enzimática celular. El PI, un fluorocromo impermeable a la membrana celular, se utilizó en la evaluación de la integridad de la membrana. Las células teñidas con PI presentan presumiblemente daños en la membrana permitiendo la entrada del fluorocromo en su interior. La tinción de cFDA requiere actividad metabólica. Las células muertas, totalmente permeabilizadas, liberan rápidamente el fluorocromo, incluso aunque retenga cierta actividad esterasa residual sintetizada en el pasado [167-169, 193].

A lo largo de esta Tesis, el término viabilidad celular hace referencia a la fracción de células capaces de crecer en placa, es decir, aquella fracción de células que muestran capacidad reproductiva en medio sólido. De este modo, la concentración de células viables se expresa como unidades formadoras de colonias por mililitro ($CFUmL^{-1}$). El término vitalidad se refiere a las células teñidas con cFDA, es decir, aquellas metabólicamente activas. La población de células metabólicamente activas comprende la fracción de células viables (cultivables en medio sólido) y la fracción de células viables no cultivables (VBNC), que no son detectadas por los métodos tradicionales de recuento pero están vivas [167]. Finalmente, la fracción de células que incorporan PI en su interior, indicativo de la ausencia de integridad de membrana, se consideró muerta. La combinación de las medidas de actividad enzimática, integridad de membrana y viabilidad celular permite la diferenciación de los diferentes estados fisiológicos que se muestran en la Figura 3.8.

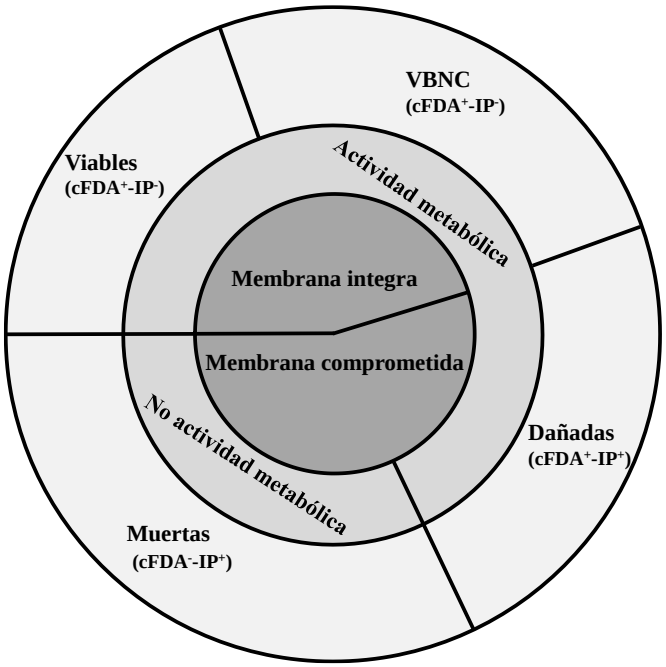

Figura 3.8: Estados fisiológicos celulares detectados mediante la combinación del análisis por citometría de flujo con tinción dual de los fluorocromos cFDA y PI y el recuento en medio sólido. Modificado de Quirós [196].

De este modo, aplicando el protocolo de tinción dual desarrollado, fue posible distinguir entre células metabólicamente activas ($cFDA^+$-PI^-) (viables y VBNC), células dañadas ($cFDA^+$-PI^+) y células muertas ($cFDA^-$-PI^+). La población dañada se encuentra en un paso transitorio entre los estados activos y aquellos otros con la membrana comprometida o irreversiblemente dañada. La tinción doble indica que las células mantienen ciertos niveles de actividad, pero además presentan pequeños poros o grietas en la membrana.

3.5. Desarrollo de modelos cinéticos: modelos no segregados y segregados

Uno de los principales objetivos en biotecnología es el desarrollo de modelos matemáticos que describan las cinéticas de crecimiento, consumo de sustratos y formación de productos para el diseño, la optimización y el control de los bioprocesos. El seguimiento de parámetros como la biomasa y la viabilidad celular proporcionan la información necesaria para el cálculo de las características de cultivo (velocidades específicas de crecimiento, rendimientos o velocidades de consumo) que permiten conocer si el sistema opera bajo condiciones de máxima eficacia [197].

La mayor parte de los modelos matemáticos desarrollados para describir las cinéticas de crecimiento de un cultivo se basan en la medida de propiedades macroscópicas, como la biomasa celular. Por ello, se emplean como métodos de análisis la medida del peso seco, del peso húmedo, de la densidad óptica (OD) o la determinación del número de células. En estas condiciones, los modelos matemáticos para un cultivo celular derivados de estas

medidas resultan muy sencillos, pero imprecisos. Estos modelos son llamados modelos no segregados y se caracterizan por considerar al microorganismo como un único componente que, de forma genérica, se denomina biomasa. Presuponen la homogeneidad de las poblaciones, obviando la heterogeneidad fisiológica existente y las propiedades de las células individuales dentro de la población [198, 199].

Puesto que el comportamiento celular promedio no es representativo de toda la población global, se recurre al desarrollo de modelos cinéticos, modelos cinéticos segregados, que tengan en cuenta la citada heterogeneidad poblacional [200]. De hecho, el rendimiento de un proceso es dependiente de la fisiología de cada célula individual, de la distribución de las células a lo largo del ciclo celular, y de los efectos de las condiciones medioambientales [201]. Obviamente, el desarrollo de estos modelos requiere de una información rigurosa y precisa acerca de la distribución de células con respecto a un parámetro concreto o bien la fracción de células en las diferentes fases del ciclo de una determinada población, una información que puede ser obtenida mediante el empleo de técnicas de citometría de flujo multiparamétrica.

4. Materiales y métodos

4.1. Microorganismos

Los organismos seleccionados para el presente trabajo fueron dos bacterias. La bacteria *Pseudomonas putida* (DSM-4478, Colección alemana de microorganismos y células cultivables) se empleó en el proceso de biodegradación del ácido salicílico. Esta bacteria se caracteriza por poseer un plásmido transmisible que codifica los enzimas necesarios para la ruta meta para la oxidación final de salicilato el cual utiliza como fuente de carbono. Por su parte, la bacteria *Paracoccus thiocyanatus* (LMG-24666T, Colección belga de microorganismos) fue utilizada para el proceso de biodegradación de tiocianato.

4.2. Medios de cultivo

Los medios de cultivos empleados en el presente trabajo se muestran las tablas 4.1, 4.2 y 4.3.

Tabla 4.1: Medios enriquecidos empleados en el proceso de biodegradación del ácido salicílico y del tiocianato para la *P. putida* y el *P. thiocyanatus*, respectivamente (capítulos 5.1, 5.4 y 5.5)

Medio enriquecido *P. putida*	Medio enriquecido *P. thiocyanatus*
5 gL^{-1} peptona	5 gL^{-1} peptona
3 gL^{-1} extracto de carne	5 gL^{-1} extracto de carne
0.422 gL^{-1} KH_2PO_4	5 gL^{-1} extracto de levadura
0.375 gL^{-1} K_2HPO_4	2.5 gL^{-1} NaCl
0.244 gL^{-1} $(NH_4)_2SO_4$	0.1 gL^{-1} K_2HPO_4
0.05 gL^{-1} $MgSO_4$ $7H_2O$	0.05 gL^{-1} $MgSO_4$ $7H_2O$
0.054 gL^{-1} $C_6H_{11}FeNO_7$	
0.015 gL^{-1} $CaCl_2$ $2H_2O$	
0.015 gL^{-1} NaCl	
100 mgL^{-1} SA	

Tabla 4.2: Medios minerales empleados en el proceso de biodegradación del ácido salicílico y del tiocianato (capítulo 5.1, 5.4 y 5.5)

PpMM	PtMM o MM	CCMM
0.422 gL^{-1} KH_2PO_4	0.5 gL^{-1} K_2HPO_4	0.5 gL^{-1} K_2HPO_4
0.375 gL^{-1} K_2HPO_4	0.3 gL^{-1} $(NH_4)_2SO_4$	0.3 gL^{-1} $(NH_4)_2SO_4$
0.244 gL^{-1} $(NH_4)_2SO_4$	0.05 gL^{-1} $MgSO_4$ $\cdot 7H_2O$	0.05 gL^{-1} $MgSO_4$ $\cdot 7H_2O$
0.05 gL^{-1} $MgSO_4$ $\cdot 7H_2O$	0.01 gL^{-1} $FeCl_3 \cdot 6H_2O$	0.01 gL^{-1} $FeCl_3 \cdot 6H_2O$
0.054 gL^{-1} $C_6H_{11}FeNO_7$	0.01 gL^{-1} $CaCl_2 \cdot 2H_2O$	0.01 gL^{-1} $CaCl_2 \cdot 2H_2O$
0.015 gL^{-1} $CaCl_2$ $2H_2O$	10 mL^{-1} de disolución traza	0.05 gL^{-1} triptona
0.015 gL^{-1}NaCl		10 mL^{-1} de disolución traza
0.05 gL^{-1} triptona		

En el estudio de biodegradación de tiocianato por *P. thiocyanatus* se utilizó también un medio libre de nitrógeno y azufre (FM); éste se preparó sustituyendo el $MgSO_4$ por $MgCl_2$ y eliminando $(NH_4)_2SO_4$ en el MM.

Tabla 4.3: Medios empleados en el estudio de toxicidad de materiales nanoparticulados sobre la *P. putida* (capítulo 5.2 y 5.3)

SUW o GM	SIW
5 gL^{-1} peptona	0.5 gL^{-1} K_2HPO_4
3 gL^{-1} extracto de carne	0.3 gL^{-1} $(NH_4)_2SO_4$
0.422 gL^{-1} KH_2PO_4	0.05 gL^{-1} $MgSO_4 \cdot 7H_2O$
0.375 gL^{-1} K_2HPO_4	0.01 gL^{-1} $FeCl_3 \cdot 6H_2O$
0.244 gL^{-1} $(NH_4)_2SO_4$	0.01 gL^{-1} $CaCl_2 \cdot 2H_2O$
0.05 gL^{-1} $MgSO_4$ $7H_2O$	0.05 gL^{-1} triptona
0.054 gL^{-1} $C_6H_{11}FeNO_7$	10 mL^{-1} de disolución traza
0.015 gL^{-1} $CaCl_2$ $2H_2O$	500 mgL^{-1} SA
0.015 gL^{-1} NaCl	
100 mgL^{-1} SA	

En todos los casos, la disolución traza está compuesta por 8 mgL^{-1} $ZnSO_4$ $7H_2O$, 4 mgL^{-1} H_3BO_3, 4 mgL^{-1} $Na_2MoO_4 \cdot 2H_2O$, 4 mgL^{-1} $CuSO_4 \cdot 5H_2O$, 4 mgL^{-1} $MnCl_2 \cdot 4H_2O$, 4 mgL^{-1} $CoCl_2 \cdot 6H_2O$ [202]. En el caso del medio libre de nitrógeno y azufre, $ZnSO_4 \cdot 7H_2O$ and $CuSO_4 \cdot 5H_2O$ fueron sustituidos por $ZnCl_2$ and $CuCl_2 \cdot 2H_2O$, respectivamente.

4.3. Preinóculo

El preinóculo se preparó previamente a partir de los cultivos congelados (a -20º C) en glicerol, mediante pases sucesivos de la bacteria en placas con su correspondiente medio de crecimiento en estado sólido.

En el caso de la *P. putida*, las placas con el medio sólido se incubaron durante 24 horas a 30º C. Una vez transcurrido ese tiempo, la bacteria se incubó en 50 mL de medio de crecimiento en un matraz de 250 mL durante 16 h a 150 rpm y 30ºC, hasta que alcanzó la fase exponencial de crecimiento [107, 203, 204].

El *P. thiocyanatus* se mantuvo en las placas con medio sólido durante 4 días a 30 ºC, momento en el cual fue inoculado en 50 mL de su medio de crecimiento en un matraz de 250 mL durante 24 h a 250 rpm y 28ºC, hasta que alcanza la fase exponencial de crecimiento [202].

En ambos casos, se tomó una alícuota que servirá como inóculo para posteriores experimentos. El inóculo se centrifugó a 10.000 x g durante 10 minutos (Kubota 6700), separando de este modo el sobrenadante de la biomasa. La biomasa se lavó dos veces con NaCl (0.7%) con el fin de eliminar los restos del medio de crecimiento.

4.4. Condiciones experimentales de cultivo

En la tabla 4.4. se recogen las condiciones experimentales de cada uno de los procesos estudiados en el presente trabajo.

Tanto los medios salinos y de crecimiento como todo el material que fuera a ser utilizado durante el proceso, se esterilizaron a 121 ºC durante 20 minutos (AES-75, Raypa Steam Sterilizer). La disolución madre de SA (empleada como stock) y los materiales nanoparticulados se esterilizaron individualmente. La bacteria o bacterias se inocularon en los medios correspondientes que contenían el agente externo (carbón activo o nanoparticulas) que se deseaba estudiar, con una concentración de 10^7 $CFUmL^{-1}$, y se mantuvieron las condiciones de cultivo con un incubador New Brunswick Scientific (Edison, New York), tomando muestras a tiempos determinados en cada caso. Las muestras recogidas fueron centrifugadas (16.000 x g 5 minutos) para separar el sobrenadante de la biomasa.

En el caso del estudio de toxicidad, se repitieron los experimentos en las mismas condiciones pero sin añadir la bacteria, de modo que, se estudiaron las posibles interacciones SA-nanopartículas.

Tabla 4.4: Condiciones experimentales de cultivo en el proceso de biodegradación de aguas contaminadas por ácido salicílico y/o tiocianato

Medio mineral	Condiciones cultivo *	Bacteria	Sustrato	Parámetros en estudio	Capítulo
PpMM	Pp	*P. putida*	50-500 mg SA L^{-1}	Biocinética; Inhibición	5.1
PpMM	Pp	*P. putida*	500 mg SA L^{-1} 500 mg SCN^- L^{-1}	Interacción co-sustato; Inhibición	5.5
PpMM	Pp	*P. putida*	500 mg SCN^- L^{-1}	Inhibición	5.5
PtMM	Pt	*P. thiocyanatus*	100-6000 mg SCN^- L^{-1}	Biocinética; Inhibicion; Condiciones cultivo	5.4
PtMM	Pt	*P. thiocyanatus*	500 mg SCN^- L^{-1} 500 mg SA L^{-1}	Interacción co-sustato; Inhibición	5.5
PtMM	Pt	*P. thiocyanatus*	500 mg SA L^{-1}	Inhibición	5.5
PpMM	Mix	*P. putida*	500 mg SA L^{-1} 500 mg SCN^- L^{-1}	Condiciones cultivo; Inhibición; Interacción co-sustato;	5.5
CCMM	Mix	*P. putida*	500 mg SA L^{-1} 500 mg SCN^- L^{-1}	Medio salino; Inhibión; Interacción co-sustato;	5.5
PtMM	Mix	*P. thiocyanatus*	500 mg SCN^- L^{-1} 500 mg SA L^{-1}	Condiciones cultivo; Inhibión; Interacción co-sustato	5.5
CCMM	Mix	*P. thiocyanatus*	500 mg SCN^- L^{-1} 500 mg SA L^{-1}	Medio salino; Inhibión; Interacción co-sustato	5.5
CCMM	Mix	*P. putida*	500 mg SA L^{-1}	Biocinética	5.5
CCMM	Mix	*P. thiocyanatus*	500 mg SCN^- L^{-1}	Biocinética	5.5
CCMM	Mix	*P. thiocyanatus* *P. putida*	500 mg SCN^- L^{-1}	Interacción co-cultivo	5.5
CCMM	Mix	*P. thiocyanatus* *P. putida*	500 mg SA L^{-1}	Interacción co-cultivo	5.5
CCMM	Mix	*P. thiocyanatus* *P. putida*	300-4000 mg SCN^- L^{-1} 300-4000 mg SA L^{-1}	Biocinética; Inhibión; Interacción co-sustato; Interacción co-cultivo; Viabilidad; Actividad	5.5
SUW	Pp	*P. putida*	500 mg SA L^{-1} 0-1 $mgmL^{-1}$ GO	Toxicidad GO; Viabilidad; Actividad; Efecto de la luz	5.3
SIW	Mix				
GM	Pp	*P. putida*	500 mg SA L^{-1} 0-2 $mgmL^{-1}$ TiO_2	Toxicidad TiO_2; Viabilidad; Actividad	5.2
SIW	Mix				

*Condiciones de cultivo: Pp: 200 rpm, 30ºC y 100 mL de medio en Erlenmeyer flasks de 250 mL; Pt: 250 rpm, 28ºC y 100 mL de medio en Erlenmeyer flasks de 500 mL; Mix: 30°C, 250 rpm y 100 mL de medio en Erlenmeyer flasks de 500 mL

4.5. Adsorción con carbón activo: Metodología experimental

Se llevaron a cabo una serie de experimentos de adsorción con dos tipos de carbón activo granular, GAC 830 (Cabot Norit Americas Inc, USA) y Filttrasorb 400 (Chemviron carbon Ltd., UK). Las características más importantes de los carbones estudiados se indican en la tabla 4.5.

Tabla 4.5: Características del carbón activo GAC 830 y Filtrasorb 400 [205, 206]

	GAC 830	**Filtrasorb 400**
Índice de yodo mg/g	920	1050
Número de abrasión, min.	75	75
Contenido de humedad, max., %w/w	2	2
Tamaño efectivo, mm.	1	0.6-0.7
Densidad aparente g/ml	0.9117	0.8611
Coeficiente de uniformidad	1.7	1.7

Antes de utilizar el carbón activo, éste se sometió a un acondicionamiento previo, que consistió en lavarlo repetidamente con agua destilada, con objeto de eliminar los finos para, a continuación, secarlo 14 horas a 100ºC. Posteriormente, se dejó enfriar hasta temperatura ambiente en un desecador, donde se mantuvo hasta su uso. De este modo se consigue una homogeneización del tamaño del grano del material, eliminando los finos del sistema, que son los que generan alteraciones hidrodinámicas en el mismo [207].

El proceso de adsorción en discontinuo se llevó a cabo a temperatura ambiente (20ºC). En un vaso de precipitados se introdujeron cantidades variables de carbón activo granular (0.12-0.5 g) en 250 de disolución sintética de SA o SCN^- (100 mgL^{-1}), de modo que se determinó la relación líquido-sólido óptima (volumen de líquido (mL)/masa de carbón activo (g)) [54]. A continuación, se realizaron nuevos ensayos de adsorción, utilizando disoluciones de adsorbato con concentraciones comprendidas entre 10 y 100 mgL^{-1} , usando la relación líquido–sólido óptima obtenida anteriormente [54].

La suspensión se mantuvo en agitación durante 90 minutos, considerando este tiempo de contacto suficiente para que se alcanzase el equilibrio [55]. Se trabajó con el pH natural de la disolución y con una velocidad de agitación de 250 rpm, que provee al sistema de una mezcla adecuada y no causa daños físicos importantes al sólido [54]. Cabe mencionar que antes de su uso, el carbón tuvo que humedecerse con agua destilada para minimizar la formación de burbujas de aire en el interior del sólido [207].

4.6. Adsorción y biodegradación combinada: Bioadsorción

El tratamiento de aguas residuales a nivel industrial con carbón activo o carbón activo biológico suele presentar una configuración de lecho fijo o fluidizado en continuo. Sin embargo, el análisis del proceso de adsorción o bioadsorción realizado de forma

discontinua pueden proporcionar datos útiles de diseño aplicables a los procesos continuos [17].

4.6.1. Formación del biofilm

La inmovilización de las bacterias *P. putida* y *P. thiocyanatus* sobre el carbón activo se produce por adsorción, para ello se pone el contacto el carbón activo granular con la bacteria en un medio nutritivo [17]. La relación líquido –sólido utilizada fue la relación optima hallada en el proceso de adsorción para cada caso.

En el caso de *P. putida*, las condiciones de cultivo fueron 30ºC, con dos volúmenes de trabajo, 100 mL y 1000 mL en Erlenmeyer de 250 mL y 2000 mL, respectivamente, aplicando dos velocidades de agitación (50 y 150 rpm) y dos tamaños de inóculo (0.05 y 0.1 unidades de DO) y con tiempo de contacto de 24 h. Para el *P. thiocyanatus*, las condiciones de cultivo fueron 28ºC, 100 mL en un Erlenmeyer de 500 mL, velocidades de agitación de 50, 75 y 250 rpm y tiempo de contacto de 0, 24, 48, 72, 96, 120, 144, 168 y192 h.

Las bacterias inoculadas en el proceso de formación de la biopelícula se encontraban en su fase de crecimiento exponencial [203], además el carbón que se utilizó para la formación de la biopelícula fue esterilizado (100ºC durante 12h) para evitar cualquier fuente de contaminación [17]

La cuantificación de la biomasa acumulada en una biopelícula se realizó mediante la determinación de unidades formadores de colonias. Para ello se separó la biopelícula del carbón activo mediante el uso de ultrasonidos (15 segundos), a continuación la muestra se sometió a un mezclado en el Vortex (unos segundos), consiguiendo la suspensión y desagregación de las bacterias. Esta muestra fue diluida y sembrada en placa para obtener el valor de $CFUmL^{-1}$ [203, 208]. Otro método de control de la cantidad de biomasa sobre el carbón activo, consistió en medidas del peso seco del carbón antes y después de haberse formado la biopelícula sobre éste. De este modo las diferencias de peso correspondieron a la cantidad de biomasa adherida. La distribución de la biomasa sobre el carbón activo se observó mediante microscopía electrónica de barrido (SEM) [203].

4.6.2. Bioadsorción

El procedimiento de bioadsorción es el mismo para las configuraciones de biomasa viva o muerta adherida sobre el carbón activo. Para obtener biomasa muerta inmovilizada, el carbón activo biológico fue introducido en un horno a 100 ºC durante 30 minutos antes del proceso de bioadsorción [19, 209]. Las bacterias inmovilizadas sobre el carbón activo se introdujeron en un Erlenmeyer que contenía 100 mL del medio mineral PpMM o PtMM (para *P. putida* y *P. thiocyanatus*, respectivamente,) con concentraciones variables

de SA (100 y 500 mgL^{-1}) o SCN^- (1000, 3000 y 7000 mgL^{-1}) y se mantuvieron las condiciones de cultivo correspondiente a cada bacteria.

4.7. Métodos analíticos

Los métodos analíticos que a continuación se indican han sido empleados para la determinación cuantitativa de los compuestos implicados en el proceso en estudio. Un resumen detallado se muestra en la tabla 4.6.

Tabla 4.6: Parámetros medidos y método analíticos empleados

	Parámetro	Método analítico
Concentración	Ácido salicílico	Espectrofotometría, método del nitrato férrico (Thermo Scientific, Heλiosγ) HPLC (Agilent 1200 Series)
	Tiocianato	Espectrofotometría, método del nitrato férrico (Thermo Scientific, Heλiosγ) HPLC (Agilent 1200 Series)
	2-hidroximuconico semialdehido	LC-MS (Agilent 6460 Triple Quad más Agilent 1290 Infinity UPLC)
	Carbono orgánico total	Analizador de TOC (TOC-V_{CSH}, Shimadzu)
	Biomasa	Densidad óptica (Shimadzu, UV-vis 1203) Unidades formadoras de colonias Citómetro de flujo Cytomics FC 500 (Beckman Coulter). SYBR Green con microesferas fluorescentes
	Estado fisiológico de las bacterias	Citómetro de flujo Cytomics FC 500 (Beckman Coulter) con microesferas fluorescentes Activas ($cFDA^+$) Dañadas ($cFDA^+$-PI^+) Muertas ($cFDA^+$-PI^+) Viables y VBNC ($cFDA^+$-PI^-)
Tinción fluorocromos		Microscopio Confocal)Ultra-Espectral Leica TCS-SP2-AOBS)
Morfología		Microscopio electrónico de barrido (JEOL JMS-6610LV).
Dispersión de partículas sólidas en medio acuoso		Microscopio óptico (Olympus BX61, Japan)
Distribución del tamaño de partícula		Malven Mastersizer S Long Bench (Malvern Instruments Ltd.) Zetasizer Nano ZS (Malvern Instruments Ltd).

4.7.1. Monitorización mediante citometría de flujo

Las muestras tomadas a lo largo de los procesos de biodegradación de los contaminantes fueron centrifugadas (16000 x g durante 5 minutos), separando la biomasa celular del sobrenadante. Previo al proceso de tinción, las células se lavaron dos veces con tampón fosfato salino (PBS, pH 7.4, filtrado por 0.22 μm y estéril) y sometidas posteriormente a

un tratamiento en ultrasonidos durante 5 segundos con el fin de evitar cualquier posible agregación celular previa al análisis multiparamétrico [193]. Ioduro de propidio (PI) y carboxifluoresceína (cFDA) se utilizaron como fluorocromos en un protocolo de tinción doble y dual, con el objeto de evaluar el status fisiológico celular. El número de células totales se midió mediante el uso conjunto de SYBR Green con microesferas fluorescentes (Perfect Count; Cytognos, Spain) como patrón interno siguiendo las recomendaciones del fabricante de pipeteo reverso para el recuento radiométrico [167].

La disolución stock de PI se preparó con una concentración de 1 $mgmL^{-1}$ en agua destilada (filtrada por .22 μm y estéril) y se almacenó a 4 ºC. Las disoluciones stock de cFDA y SYBR Green se prepararon en dimetil sulfóxido (DMSO) a una concentración de 1mM y posteriormente ambas fueron almacenadas a - 20 ºC. La disolución de tinción de PI se preparó mediante la dilución de la disolución stock hasta una concentración final de 140 μgmL^{-1} en agua destilada estéril, añadiendo esta disolución a la suspensión celular hasta una concentración final de 5 μgmL^{-1}. Esta mezcla fue incubada bajo condiciones de oscuridad a temperatura ambiente durante 30 minutos. Las soluciones de trabajo de cFDA y SYBR Green se prepararon en una concentración 10 μM en PBS conteniendo 1mM EDTA. Las células teñidas con 0.1 μM de estos fluorocromos se incubaron durante 15 minutos en oscuridad y temperatura ambiente.

La adquisición de los correspondientes datos multiparamétricos se llevó a cabo en un citómetro analizador Cytomics FC 500 (Beckman Coulter) equipado con una fuente de excitación láser de 488 nm y 633 nm procedente de un láser de argón. La fluorescencia verde de las muestras (correspondiente a las células teñidas con cFDA y SYBR Green) se recogió en el canal FL1 (530 nm), mientras que la fluorescencia del PI se registró en el canal FL3 (610 nm). Cada análisis fue realizado por duplicado con una velocidad de adquisición de 4000 eventos s^{-1}. La adquisición se llevó a cabo con el software Cytomics RXP, recogiendo 200.000 eventos en cada análisis. Los datos fueron analizados mediante Kaluza® Flow Analysis Software, Beckman Coulter.

La aplicación de la técnica de citometría de flujo al recuento y detección de los microorganismos requiere una relación señal/ruido adecuada durante el análisis, especialmente en el caso de células bacterianas en las que el tamaño es muy inferior al de las células de mamífero. Para ello resulta útil el uso de marcadores específicos de ácidos nucleicos. En este caso, utilizamos el fluorocromo SYBR Green para el recuento total de microorganismos. Este fluorocromo refleja el contenido en ADN celular [169]. Para minimizar otras posibles interferencias, todas las soluciones se filtraron por 0.22 μm.

Con el fin de validar el protocolo de análisis, fue necesario establecer una serie de controles positivos para, de esta manera, definir los patrones de tinción de ambos microorganismos con los fluorocromos seleccionados, según las distintas condiciones fisiológicas. En los experimentos previos se utilizaron los cultivos puros de *P. putida* y

P. thiocyanatus en medio sintético bajo diferentes condiciones fisiológicas inducidas. Alícuotas de estos cultivos en fase de crecimiento exponencial, en condiciones de estrés o muerte, y en estados intermedios (mezcla de cultivos frescos y tras un tratamiento de calor en la misma proporción) se analizaron por citometría de flujo y recuento en placa.

En los cultivos en fase exponencial temprana, la viabilidad celular fue prácticamente del 100%. La aplicación del tratamiento térmico condujo a la eliminación total de la fluorescencia observada del cFDA y, por tanto, a una pérdida drástica de la actividad celular, además de la capacidad de crecer en placa. Asimismo, el calentamiento de los cultivos conllevó a la rotura parcial o total de la membrana celular, lo que se tradujo en incremento de casi un 100% de la tinción con PI. En ambos casos, control de células metabólicamente activas y células muertas, se observó una única población que mostraba una señal de fluorescencia verde o roja intensa, respectivamente, obteniendo de este modo las ventanas correspondientes a su estado fisiológico, además de la compensación espectral que fue necesario aplicar para evitar el solapamiento de las señales.

4.7.2. Espectrofotometría

El análisis de la concentración de SA y SCN^- se realizó espectrofotométricamente empleando el método estándar del nitrato férrico con pH acidificado [210, 211]. Las medidas se realizaron en espectrofotómetro UV/VIS (Thermo Scientific, Helιosγ) a longitudes de onda de 530 nm para el ácido salicílico y 460 nm para tiocianato.

4.7.3. Cromatografía líquida de alta eficacia

El análisis de las muestras que contenían simultáneamente ácido salicílico y tiocianato, se llevó a cabo mediante cromatografía líquida de alta eficacia (HPLC). Se empleó un cromatógrafo Agilent (modelo serie 1200) combinado con un detector UV, utilizando una columna C18 de fase reversa, Mediterranea Sea_{18} (5 μm x 25 cm x 46 cm) (Teknokroma). La adquisición y análisis de datos fue realizada por el software Agilent ChemStation. Previo al análisis, las muestras fueron filtradas a través de filtros de PVDF de 0.45 μm. La fase móvil empleada fue un mezcla de acetonitrilo y una disolución 0.4% de ácido fosfórico en agua [212]. El método de análisis consistió en un gradiente binario con un flujo constante de 1 $mLmin^{-1}$ y unas longitudes de onda de 290 nm para el ácido salicílico y 214 nm para el tiocianato. Los tiempos de retención fueron de 3 y 6 minutos para el tiocianato y ácido salicílico, respectivamente.

Parte de los análisis de muestras que contenían un solo contaminante fueron también realizados mediante el uso de HPLC y con el método anteriormente descrito, realizando antes las comprobaciones y curvas de calibrado pertinentes.

4.7.4. Cromatografía líquida de alta eficacia con espectrómetro de masas

Los productos obtenidos como consecuencia del proceso de biodegradación del ácido salicílico por *P. putida*, fueron analizados por cromatografía líquida de alta eficacia con espectrómetro de masas (Agilent 6460 Triple Quad más Agilent 1290 Infinity UPLC), con una columna de fase reversa Zorbax Eclipse Plus C18 (2.1 x 50mm, 1.8 μm). La fuente de ionización fue un electrospray, realizando la medida en modo scan negativo. Previo al análisis, las muestras fueron filtradas a través de filtros de PVDF de 0.45 μm. Las fases móviles fueron agua y acetonitrilo, ambas conteniendo un 0.1% de ácido fórmico.

4.7.5. Análisis de carbono orgánico total

En las muestras que contenían simultáneamente el ácido salicílico y el tiocianato, se analizó el carbono orgánico total (TOC). Para ello, se utilizó un analizador de TOC (TOC-V_{CSH}, Shimadzu). Se obtuvieron medidas de carbono total (TC) y carbono inorgánico (IC); la diferencia entre los dos valores corresponde al valor del TOC.

El análisis del TC consiste en la combustión de la muestra en un reactor que contiene un catalizador de Pt soportado sobre esferas de alúmina a 953 K. El TC contenido en la muestra se oxida dando lugar a la formación de CO_2 que es transportado por un flujo de aire a un detector de infrarrojos no dispersivo (NDIR), donde se obtiene un pico cuya área es proporcional al ala cantidad de carbono contenida en la muestra.

En la medida de IC, el aire se introduce a través de la muestra en presencia de ácido ortofosfórico (25% p/v). La descomposición de los carbonatos y bicarbonatos presentes en la muestra generan también CO_2, que es de nuevo analizado por el NDIR.

Las muestras fueron previamente filtradas a través de filtros PTFE con un tamaño de poro de 0.45 μm.

4.7.6. Determinación de la absorbancia (OD_{600nm})

La evolución de la biomasa en medio líquido se determinó midiendo la densidad óptica a 600 nm en un espectrofotómetro (Shimadzu, UV-vis 1203) frente a un blanco (el mismo medio sin células). Los datos obtenidos se convirtieron en peso seco utilizando la curva de calibrado correspondiente, en caso de la *P. putida*, una unidad de OD equivale a 0.49 gL^{-1} ($3 \cdot 10^8$ $CFUmL^{-1}$), mientras que para el *P. thiocyanatus* una unidad de OD equivale a 0.52 gL^{-1} ($3.4 \cdot 10^9$ $CFUmL^{-1}$).

4.7.7. Determinación del número de células viables en medio sólido

El número de células viables se determinó mediante el método de recuento en placa. Las células se separaron del sobrenadante por centrifugación (16.000 x g, 5 minutos) y se resuspendieron en un volumen de tampón NaCl al 0.7%. Las células se sometieron a cinco segundos de tratamiento de ultrasonidos justo antes de la siembra en medio sólido para evitar la formación de agregados. Se sembraron triplicados de tres de las diluciones estadísticamente significativas (20-200 colonias) en placas con el medio sólido correspondiente para cada bacteria (2% p/v agar). El recuento de las colonias se realizó tras 1 y 4 días de incubación a 30º C, para *P. putida* y *P. thiocyanatus,* respectivamente. El número promedio de las células viables se expresó como unidades formadoras de colonias ($CFUmL^{-1}$). En estas condiciones, asumiendo que una colonia procede de una única célula, las células viables de *P. putida* se expresaron finalmente en gL^{-1} cuando procedió, según la curva de calibrado obtenida para el peso seco (gL^{-1}) vs concentración total de células ($célulasmL^{-1}$) calculada a partir de la tinción con SYBR Green ($1gL^{-1}$ corresponde a $8.2 \cdot 10^{10}$ células mL^{-1}).

4.7.8. Microscopía confocal y óptica

Para verificar la efectividad de la tinción de los diferentes colorantes (cFDA, PI, SYBR Green) sobre los microorganismos, las muestras de control se observaron en microscopio láser confocal (Microscopio Confocal Ultra-Espectral Leica TCS-SP2-AOBS) acoplado a un procesador de imágenes. Las micrografías se realizaron en los modos de transmisión, fluorescencia y ambos superpuestos.

Para estudiar la dispersión de los óxidos de grafeno en una suspensión acuosa se utilizó un microscopio óptico (Olympus BX61, Japan), obteniendo de este modo imágenes en campo claro de la muestra a distintas resoluciones.

4.7.9. Microscopía electrónica de barrido

La morfología del carbón y de los óxidos de grafeno y las interacciones producidas entre estos sólidos con la bacteria *P. putida* se estudiaron mediante el uso de un microscopio electrónico de barrido (SEM) (JEOL JMS-6610LV). El equipo cuenta con un cañón de electrones de filamento de wolframio, con posibilidad de trabajo de 0.5 a 30 kV. Previo al análisis de las muestras, éstas fueron recubiertas con un pulverizado de oro para transformarlas en eléctricamente conductoras.

4.7.10. Distribución del tamaño de partícula

Se realizó un estudio de la distribución del tamaño de partícula de los carbones activos utilizados en el proceso de adsorción mediante difracción de luz con láser. Para ello, se utilizó el equipo Malven Mastersizer S Long Bench (Malvern Instruments Ltd.) que

permite trabajar en el intervalo de tamaños comprendidos entre 4-3500 μm. Las medidas se realizaron en las tres situaciones diferentes a las que se sometió el carbón, antes de su uso en el proceso de adsorción, después de la adsorción del ácido salicílico, y tras haberlo sometido a una regeneración térmica (800 °C, 2 horas). La distribución del tamaño de partícula de los óxidos de grafeno se obtuvo en base a la dispersión de la luz dinámica utilizando el equipo Zetasizer Nano ZS (Malvern Instruments Ltd).

En ambos casos, los análisis se realizaron por triplicado y a temperatura ambiente.

5. Resultados Experimentales y Discusión

5.1. Biodegradación, adsorción con carbón activo y bioadsorción de ácido salicílico por *Pseudomonas putida*

En el presente subapartado se recogen los resultados referentes al estudio del tratamiento de una corriente residual contaminada con ácido salicílico, como modelo de compuesto fenólico, mediante tres técnicas diferentes, la biodegradación con *Pseudomonas putida*, la adsorción con carbón activo y la combinación de las dos técnicas anteriores o bioadsorción. Las eficacias de eliminación del ácido salicílico obtenidas para cada uno de los procesos en estudio se compararon, de modo que se pudo valorar el efecto que produce la presencia del biofilm sobre los procesos individuales. Se utilizó también un intervalo de concentración de ácido salicílico amplio con el fin de estudiar el efecto de la concentración sobre cada uno de los procesos en estudio.

En el caso del proceso físico de adsorción del ácido salicílico, se estudió tanto el equilibrio como la cinética del mismo. Se obtuvieron parámetros de ajuste de las isotermas de adsorción de Langmuir y SIPS a los datos experimentales y las constantes cinéticas para la difusión a través de los poros y para la transferencia de materia en la película líquida.

Además, en el presente trabajo se analizó el proceso de formación de biofilm sobre el carbón activo con el fin de obtener las condiciones óptimas de formación.

Los resultados de este trabajo se presentan a través de una publicación cuya referencia y estado se muestran a continuación.

Referencia: Combarros, R.G., Rosas, I., Lavín, A.G., Rendueles, M. Díaz, M. 2014. Influence of biofilm on activated carbon on the adsorption and biodegradation of salicylic acid in wastewater. Water Air and Soil Pollution, 225 (2), 1-12.

Estado: Publicada

Water Air Soil Pollut (2014) 225:1858
DOI 10.1007/s11270-013-1858-9

Influence of Biofilm on Activated Carbon on the Adsorption and Biodegradation of Salicylic Acid in Wastewater

R. G. Combarros · I. Rosas · A. G. Lavín · M. Rendueles · M. Díaz

Received: 4 September 2013 / Accepted: 30 December 2013 / Published online: 18 January 2014

Abstract This paper presents a study of the combined process of adsorption and biodegradation in solid biologically activated carbon (AC) for the removal of salicylic acid aimed at determining the influence of the presence of biofilm on the process. Adsorption on AC and biodegradation of free cell cultures were studied separately so as to compare their performance with that of the combined biosorption system. The formation of bacterial biofilm on the surface of the carbon was investigated. The study was carried out using a range of synthetic solutions containing between 15 and 500 mg/L salicylic acid simulating an industrial effluent from the pharmaceutical industry. An individual bacterium, *Pseudomonas putida* (DSM 4478), was used to study the differentiated effects. Filtrasorb 400 and GAC 830 ACs were used in the adsorption processes and Filtrasorb 400 in the biofilm formation and combined biosorption processes. As regards, combined adsorption/biodegradation results indicated that the bioactivated carbon system outperformed the combination of conventional AC and biological water treatment processes when working with high pollutant concentrations.

Keywords Biofilm · Salicylic acid · Activated carbon · Biodegradation · *Pseudomonas putida*

R. G. Combarros · I. Rosas · A. G. Lavín · M. Rendueles · M. Díaz (✉)
Department of Chemical Engineering and Environmental Technology, University of Oviedo, Oviedo, Spain
e-mail: mariodiaz@uniovi.es

1 Introduction

Salicylic acid (o-hydroxylbenzoic acid) is a typical pollutant in industrial wastewater (Khenniche and Aissani 2010). Salicylic acid (SA) is a common derivative of phenol. It presents a serious environmental hazard due to its high toxicity and tendency to accumulate in the environment. As a result, efficient removal and recycling of SA from aqueous solutions have received a great deal of attention in recent years (Wang et al. 2012a, b).

Different methods designed to remove phenol compounds have been put forward, including the application of biodegradation processes using pure cultures of microorganisms specially adapted to metabolize pollutants (González et al. 2001). Besides, the use of pure cultures contributes to our understanding of biodegradation processes under well-defined conditions. The use of *Pseudomonas putida* cultures appears to be an interesting alternative for this purpose, not only due to its importance as a bacterium capable of carrying out the degradation of phenolic compounds but also because it is commonly found in the mixed cultures present in activated sludge, where it plays an important role in removing toxic compounds for the environment (Loh and Bin 2008).

The treatment of wastes using activated carbon (AC) is considered an effective method for the removal of phenol compounds from waste solutions due to its large surface area, microporous nature, high adsorption capacity, high purity, and easy availability (Qadeer and Rehan 2002; Özkaya 2006).

AC adsorption systems may therefore be applied to produce a high quality effluent from sewage treatment

plants which can be reused for various purposes. However, despite its high adsorption capacity, AC can only maintain this adsorption capacity for a short time once its available adsorption sites become exhausted by adsorbed organic pollutants. It is well known that AC is also a good support media for microbial growth. Thus, biologically AC with an attached biomass can effectively remove organic pollutants both by adsorption and biodegradation (Xing et al. 2008).

In wastewater treatment, a reactor with immobilized microbial cells may offer several advantages over processes with a suspended biomass. These advantages include (1) retention of a high concentration of microorganisms in the reactor, (2) protection of cells from toxic substances, (3) prevention of suspended particles from the effluent, and (4) lower capital costs for single reactor systems than that for individual processes and to the fact that less frequent regeneration of the carbon will result in lower energy requirements and operating costs (Walker and Weatherley 1999; Olmstead and Weber 1991). Although the aforementioned reports highlight obvious advantages of bioactivated carbon (BAC) columns over conventional granular activated carbon (GAC) systems in laboratory and pilot plant tests, it should be noted that few specifically designed BAC systems have been employed for industrial wastewater treatment. This may be due to physical disadvantages such as the increased pressure drop due to clogging by microbial growth (Characklis 1981). This problem may be alleviated, however, by frequent backwashing and air scouring to remove excess biomass (Ying and Weber 1979). The advantage provided by BAC systems of shielding bacteria from toxic effects could also serve as a drawback should pathogenic bacteria attached to the carbon be shielded from disinfection (LeChevalier et al. 1984).

There are numerous studies on the advantages of BAC processes over conventional biodegradation systems using free cells to remove organic matter. Some authors have reported an apparent synergism in the combined BAC process (Orshansky and Narkis 1996). However, there are reports that organic matter removal in these systems is a simple addition of effects from carbon adsorption and biological removal (Tsuneda et al. 2002), (2003). These contradictory findings indicate that the mechanisms involved in the combined BAC process have not been fully elucidated. In order to evaluate the degree of synergism of the BAC process to remove a given hazardous/toxic compound, many researchers have often studied its removal using biodegradation alone, then the efficiency of AC to remove such a compound, and finally the performance of the combined BAC process (Ferro Orozco et al. 2010).

The aim of the present study was to investigate SA removal efficiency using a combined process of adsorption and biodegradation, testing the influence of the presence of biofilm on the individual processes, i.e., AC adsorption and biodegradation by *P. putida*. The efficiency of this system was compared with AC adsorption and biological treatment via *P. putida* biodegradation. Biofilm formation on AC by *P. putida* was analyzed in order to obtain the optimal conditions.

2 Materials and Methods

2.1 Solutions

A pharmaceutical wastewater was simulated for the initial tests. Synthetic solutions with concentrations between 15 and 500 mg/L SA were prepared with SA (Panreac Qca. S.A.) and NaOH to increase pH to a suitable value for use in the mineral medium of *P. putida*. The solutions were used to test adsorption with AC, biodegradation with *P. putida*, the formation of attached biomass, and finally biosorption. The pH of these solutions was approximately 11–12.

The following chemical reagents were used in this study: meat extract, peptone, and agar, manufactured by Cultimed, KH_2PO_4, K_2HPO_4, $(NH_4)_2SO_4$, $MgSO_4$ 7 H_2O, and $C_6H_{11}NO_7Fe$ manufactured by Panreac Qca S.A., NaCl, NaOH, CaC_{l2} 12·H_2O, and $Fe(NO_3)_3$ 9·H_2O manufactured by Sigma-Aldrich and tryptone manufactured by Biokar Diagnostics.

2.2 Activated Carbon

Filtrasorb 400 (Chemviron carbon Ltd., UK) and GAC 830 (Cabot Norit Americas Inc, USA) carbons were used in this study. The former, F400, has a surface area of 1,050 m^2/g, an iodine number of 1,050 mg/(g min), density of 861 g/L, and an effective size and moisture content of 0.6–0.7 mm and 2 %, respectively. GAC 830 has a surface area of 950–1,050 m^2/g, an iodine number of 920 mg/(g min), density of 907 g/L, and an effective size and moisture content of 1 mm and 2 %, respectively.

2.3 Bacteria

A specific bacterium, *P. putida* [Leibniz Institute DSMZ-German Collection of Microorganism and Cells Cultures, Germany (DSM 4478)], was chosen to degrade SA. This bacterium was selected because it is one of the main microorganisms present in sludges, is harmless, and metabolizes under aerobic conditions, at 30 °C and neutral pH, making it suitable for use in the treatment of industrial effluents.

2.4 Experimental Methods

2.4.1 Batch Adsorption Experiments

Prior to use in experiments, both ACs were rinse with distilled water to remove fines and dried at 105 °C in an oven. The carbon was then cooled in desiccators, where it remained until use.

Batch adsorption experiments were conducted at room temperature (20 °C) using synthetic solutions, varying the AC dosage from 0.12 to 0.5 g in the SA solution (250 mL) in order to determine a suitable L/S ratio [volume of liquid (mL)/mass of AC (g)] for subsequent experiments. 250 mL of each SA solution (15–115 mg/L) was respectively placed in different 500 mL stirred tanks adding a specific amount of AC to each tank. The solution was equilibrated for 90 min in a mechanical shaker at 250 rpm monitoring the SA concentration over time. This time was considered sufficient to reach operative equilibrium. The volume of the samples extracted from the tank each time was 2 mL, which did not substantially change the solution volume.

The adsorbed amount (q) from equilibrium experimental data was calculated via the following equation (Xing et al. 2008):

$$q = \frac{V(C_i - C_e)}{M} \quad (1)$$

where q is the adsorbed amount (mg/g), V is the volume (L) of solution, C_i is the initial SA concentration in the wastewater (mg/L), C_e is the equilibrium SA concentration (mg/L), and M is the amount of adsorbent (g).

2.4.2 Salicylic Acid Biodegradation

Nutrient medium was prepared by dissolving the following reagents in 1 L of distilled water: peptone (5 g), meat extract (3 g), KH_2PO_4 (0.422 g), K_2HPO_4 (0.375 g), $(NH_4)_2SO_4$ (0.244 g), $MgSO_4$ $7{\cdot}H_2O$ (0.05 g), $C_6H_{11}NO_7Fe$ (0.054 g), $CaCl_2$ $12{\cdot}H_2O$ (0.015 g), and NaCl (0.015 g) (Juang and Tsai 200
The mineral salt medium was composed of the follo
ing reagents (g/L): KH_2PO_4 0.422, K_2HPO_4 0.375, $(NH_4)_2SO_4$ 0.244, $MgSO_4$ 7 H_2O 0.05, $C_6H_{11}NO_7Fe$ 0.054, $CaCl_2$ 12 H_2O 0.015, NaCl 0.015, and tryptone 0.05 (Juang and Tsai 2006). SA was added after sterilization by filtration through a Millipore filter of 0.22 μm. The final pH of these solutions should be 7 since this is the optimum value for *P. putida*; NaOH may be added, if necessary, to control the pH. The SA concentrations used ranged between 50 and 500 mg/L.

A biokinetic test of SA biodegradation was performed in a batch system to evaluate the biokinetic parameters. These experiments employed 100 mL of mineral medium in 250 mL Erlenmeyer flasks (Monteiro et al. 2000), 30 °C, 200 rpm, in which SA plus mineral salt medium was seeded with the acclimated suspended biomass (Juang and Tsai 2006; Silva et al. 2007). The biomass was previously introduced into the nutrient medium for 16 h at 150 rpm (Loh and Yu 2000; Silva et al. 2007) and 30 °C (Ploux et al. 2007), the time the bacterium takes to reach the exponential growth phase.

Samples were extracted at the onset of the batch kinetic test and subsequently at regular intervals to measure SA and the concentration of suspended biomass. The batch kinetic test provided data on the variation in SA and the concentration of suspended biomass over time.

2.4.3 Biofilm Formation

Live cells of a salicylic-degrading bacterium, *P. putida* DSM 4478, were immobilized on granular AC by adsorption. The AC was sterilized before use in the biofilm formation process.

The formation of biofilm on AC was carried out in a batch experiment by contacting carbon with *P. putida* bacteria for 24 h in a nutrient medium (Walker and Weatherley 1999). The L/S ratio [volume of liquid (mL)/mass of AC (g)] used in these series of experiments was 1,000. The experimental conditions were 30 °C, two different volumes, 100 mL in 250 mL Erlenmeyer and 1,000 mL in 2,000 mL Erlenmeyer, were used, and an initial concentration of SA of 100 mg/L. Experiments were performed employing different agitation speeds, 50

and 150 rpm, and inoculums sizes, 0.05 and 0.1 optical density units (OD, 600 nm).

The number of adsorbed cells was estimated by the difference in dry weight before and after the adsorption process and colony count determination.

In order to test whether the presence of SA influences the formation of biofilm on AC and subsequent SA biosorption, the same procedure was performed for biofilm formation as explained in the previous paragraph. In this case, however, 100 mg/L of SA was not added, the biological AC being subsequently subjected to a process of biosorption.

2.4.4 Combined Adsorption–Biodegradation

In almost all wastewater applications, AC and BAC have been used in continuous processes. However, analysis of batch processes can provide useful design data that enable continuous processes to be developed (Walker and Weatherley 1999). In this study, three batch systems were studied using the aerated stirred tank setup (Ong et al. 2008; Orshansky and Narkis 1996; Walker and Weatherley 1999).

1. Bacteria immobilized on F400 AC (Living biofilm-GAC).
2. Dead bacteria immobilized on F400 (Dead biofilm-GAC).
3. F400 granular AC with no biological activity (GAC).

The AC was sterilized prior to contact to minimize bacterial growth by heat, submitting it to 100 °C for 12 h in a sterile container (Walker and Weatherley 1999).

For the immobilized cell systems, the bacterial culture was contacted with 0.1 g F400 carbon in nutrient broth for 24 h before addition to the reaction vessel. To achieve a dead immobilized cells system, 0.1 g of F400 with biofilm was introduced in an oven at 100 °C for 30 min before the biosorption process (Ong et al. 2008). Finally, adsorption using the granular carbon system meant the addition of 0.1 g F400 to the reactor. Each of these systems was contacted with 100 mL of an autoclaved synthetic mineral salt medium in 250 mL Erlenmeyer flasks. These operated at a pH of 7, a temperature of 30 °C, and 200 rpm agitation speed, the conditions being controlled by a New Brunswick Scientific incubator.

Samples were taken from the Erlenmeyer flasks every 2 h and centrifuged (5 min at 13,200 rpm) to separate the biomass from the supernatant, thus enabling analysis of cell density and the concentration of SA.

2.5 Analytical Methods

The standard iron complex (Fe^{3+}) method (Snell and Snell 1953) was used to determine the concentration of SA in water. SA reacts with ferric ions to form a violet-colored complex, which was determined by colorimetric analysis at 530 nm on a UV/Vis (Thermo Scientific) spectrophotometer.

OD was measured at 600 nm on a UV/Vis (Shimadzu) spectrophotometer to monitor outgrowth of microorganisms during fermentation.

All experiments were performed in duplicate, and the process was repeated on subsequent days under identical conditions. Furthermore, the samples were analyzed in triplicate; the reproducibility of the concentration measurements was mostly within 5 %.

3 Results and Discussion

In the first stage of this research study, each process (adsorption and biodegradation) was studied separately.

3.1 Batch Equilibrium

As previous results show that the minimum L/S ratio which yields the highest capacity in both cases is equal to 1,000, this ratio was selected as the value for all the tests.

Several runs were carried out to obtain the capacities of the F400 and GAC 830 ACs. These were contacted with different SA solution concentrations (15–115 mg/L) with an L/S ratio=1,000 mL/g. The results show that equilibrium is reached in less than 90 min in all cases.

Two different models, the Langmuir and Separation Factor isotherms (CFS), were used to define the relationship between the loading capacity and the solution concentration. The equations of the isotherms are

$$\text{Langmuir}: q_i = \frac{K_{eq} \cdot q_t \cdot C_i}{1 + K_{eq} \cdot C_i} \tag{2}$$

where K_{eq} is the equilibrium constant, q_t is the maximum capacity of the AC, and C_i is the solution concentration of species i.

$$\text{Separation Factor}: q_i = \frac{K_{eq} \cdot q_t \cdot C_i}{C_T + (K_{eq} - 1) \cdot C_i} \quad (3)$$

where C_T is the minimum salicylic equilibrium concentration in the solution with a saturated AC.

The equilibrium constants and the maximum adsorption capacity were obtained. Experimental results were fitted to the Langmuir and CFS isotherms and are shown in Fig. 1a, b. The different isotherm parameters obtained are summarized in Table 1.

In view of the results, the SA adsorption capacity of Filtrasorb F400 is higher than that of GAC 830. Accordingly, F400 was used in subsequent experiments. Adsorption equilibrium experimental data showed a better fit to the Langmuir isotherm model. Otero et al. (2004) obtained a maximum capacity of 351 mg/g from fitting equilibrium data on the adsorption of SA (pH around 5) with F400. Significant differences between the values obtained in the present study and those reported by Otero et al. (2004) can be explained by the pH of the solutions. In our case, the solutions of SA are dissolutions with a basic pH (11.5), which produces a decrease in the adsorption of the pollutant by AC (Karimi-Jashni and Narbaitz 1997).

3.2 Batch Kinetics

The process was monitored until equilibrium was reached with all solutions. After 45 min, the solution concentration of SA does not change substantially, so operational equilibrium may be assumed. This value was taken from the loading experiments conducted in stirred tanks using synthetic solutions with initial concentrations of between 15 and 115 mg/L SA. The concentration profiles can be studied using the film mass transfer and pore diffusion kinetics models to determine the mass transfer mechanisms.

- Film mass transfer model

In this model, the retention of SA is assumed to be limited by the external surface of the particle. The behavior of this model can be described by the following equation (Torre et al. 2006):

$$q_i(t) = C_0 (V_L/V_S)\left(1 - \frac{C^*}{C_0}\right)\left(1 - \exp\left(\frac{-K \cdot t}{V_L/V_S}\right)\right) \quad (4)$$

where q_i is the concentration of species i in the AC at time t, K is the apparent constant of mass transfer, C^* is the equilibrium concentration of SA in the solution, V_L is the volume of liquid, V_s is the volume of AC, and C_0 is the initial SA concentration in solution.

The apparent constant of mass transfer, K, can be determined by linear regression using the experimental data, fitting these to Eq. (4). The AC beads are of constant size and have a spherical geometry; therefore, $K_f = K/a_p$. Hence, a comparison of the experimental results for SA concentration and the theoretical values obtained with Eq. (3) will give the goodness of the obtained value for all the experiments. Experimental kinetic results were fitted to the film mass transfer model and are shown in Fig. 2a.

- Pore diffusion model

This model considers carbon to be a porous matrix. In this study, we used the system described for Torre

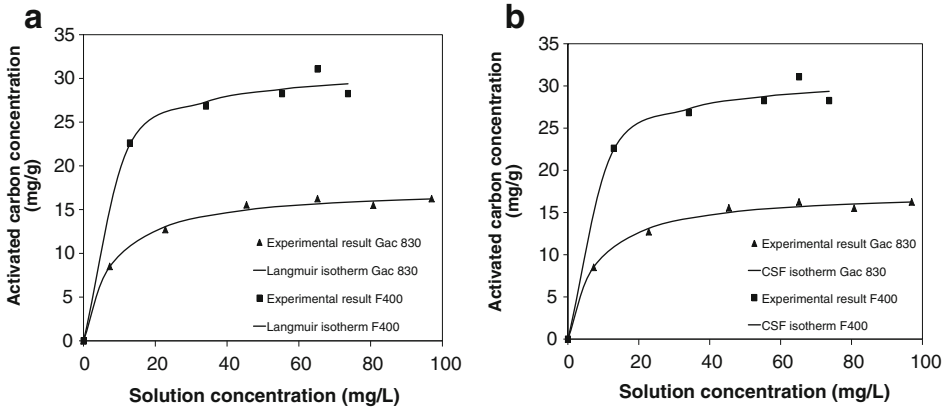

Fig. 1 Fitting of experimental data to the Langmuir isotherm (**a**) and to the FSC isotherm (**b**), employing a synthetic solution of salicylic acid (15–115 mg/L), 20 °C, 250 rpm, L/S: 1,000, pH:11.5

Table 1 Isotherms parameters obtained for both activated carbons

	Filtrasorb 400		GAC 830	
	Langmuir isotherm	CFS isotherm	Langmuir isotherm	CFS isotherm
K_{eq}	0.194 (L/mg carbon)	46.99	0.128 (L/mg carbon)	21.9
q_t (mg SA/g carbon)	31.4	30.7	17.5	16.7
C_T (mg SA/L solution)	–	240	–	160

et al. (2006) and a FORTRAN subroutine, PDECOL, to solve these equations. The subroutine uses the method of orthogonal collocation on finite elements to solve the system of nonlinear differential equations.

Figure 2b shows the fit of the experimental results to this model. The good agreement between experimental data and the theoretical prediction shows the goodness of the model.

The apparent constants of mass transfer and diffusion coefficient values were obtained from the fit of the experimental data shown in Table 2 for the ACs used in this study.

The results suggest that the kinetics is slightly faster for the GAC 830 carbon than for F400. However, as the adsorption of SA by Filtrasorb 400 is 40 % higher compared to GAC 830, F400 was chosen for subsequent biofilm formation and biosorption tests.

Other examples of values for the pore diffusion coefficient would be 1.85×10^{-10} m^2/s for the F400 carbon with SA (Otero et al. 2004), 7×10^{-12} m^2/s for orthochlorophenol and an AC particle diameter equal to 1.015 mm (Chourio et al. 1997), and 9.5×10^{-12} m^2/s for F400, 2-nitrophenol and pH 13 (Karimi-Jashni and Narbaitz 1997). The apparent constant of mass transfer values of around $(0.4–2)\times10^{-4}$ m/s was obtained for phenolic compounds (Navia et al. 2003), 8.02×10^{-4} m/s for F400, 2-nitrophenol and pH 13 (Karimi-Jashni and Narbaitz 1997), and 1.36×10^{-8} m/s for F400, SA and pH 5 (Otero et al. 2004).

3.3 Salicylic Acid Biodegradation

The suspended biomass data show a typical growth curve with a well-defined growth phase followed by a constant growth phase (Fig. 3a). The SA concentration and suspended biomass data provide an a priori estimation of the biokinetic parameters for evaluating the growth rate of the suspended biomass and the utilization rate of SA.

Batch cultures of SA-utilizing bacteria were conducted in media containing initial SA concentrations ranging between 50 and 500 mg/L. Cellular growth of *P. putida* at different initial concentrations of SA and the consumption of SA depending on the initial concentration are shown in Fig. 3a, b, respectively.

Figure 3a shows a steady increase in biomass over time for all initial concentrations of SA. Employing

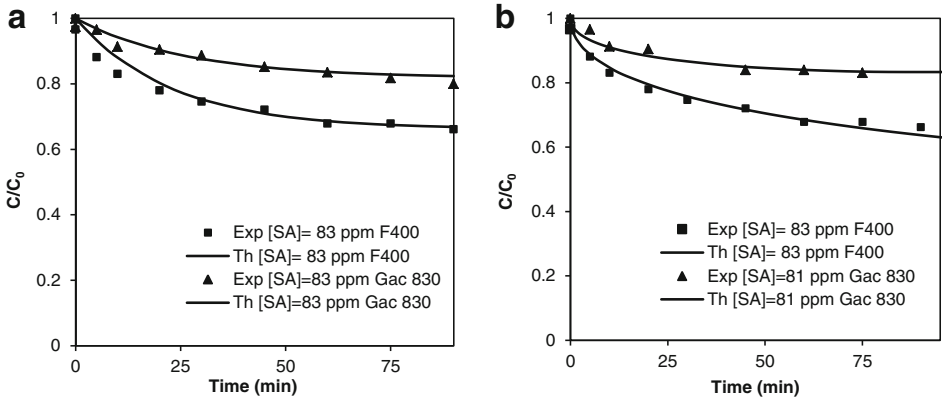

Fig. 2 Fitting of experimental theoretical kinetic data to the film mass transfer model (**a**) and to the pore diffusion model (**b**), employing a synthetic solution of salicylic acid (15–115 mg/L), 20 °C, 250 rpm, L/S: 1,000, pH:11.5

Table 2 Mass transfer constant and pore diffusivities calculated by film mass transfer and pore diffusion model respectively for activated carbon F400 and GAC 830

Experiments (F400)	D_p(m^2/s)	K_f(m/s)	Experiments (GAC 830)	D_p(m^2/s)	K_f(m/s)
Synthetic solution, $C_{0\ AS}$=35 mg/L	8.6×10^{-11}	7.7×10^{-5}	Synthetic solution, $C_{0\ AS}$=35 mg/L	6.95×10^{-11}	$9.95\times1($
Synthetic solution, $C_{0\ AS}$=60 mg/L	2.4×10^{-11}	5.1×10^{-5}	Synthetic solution, $C_{0\ AS}$=60 mg/L	6.95×10^{-11}	1.00×10^{-4}
Synthetic solution, $C_{0\ AS}$=85 mg/L	2.8×10^{-11}	7.3×10^{-5}	Synthetic solution, $C_{0\ AS}$=80 mg/L	6.95×10^{-11}	9.90×10^{-5}
Synthetic solution, $C_{0\ AS}$=95 mg/L	2.8×10^{-11}	8.8×10^{-5}	Synthetic solution, $C_{0\ AS}$=95 mg/L	6.95×10^{-11}	1.1×10^{-4}
Synthetic solution, $C_{0\ AS}$=100 mg/L	2.8×10^{-11}	8.3×10^{-5}	Synthetic solution, $C_{0\ AS}$=115 mg/L	6.95×10^{-11}	2.7×10^{-4}

initial SA concentrations of 423 and 529 mg/L, the biomass remains constant from 10 h until 24 h.

Figure 3b shows that 100 % degradation was obtained in 6 h for initial concentrations of 60 and 110 mg/L and in 10 h for 225 mg/L SA. When the initial SA concentrations were 423 and 529 mg/L, however, only 81 and 72 % of the initial concentration were degraded in 10 h, respectively, obtaining 100 % removal in both cases after 24 h.

Exact comparisons of degradation efficiency with literature results are not direct because there are differences in the cell density and medium compositions. Without considering these factors, it has been reported by Juang and Tsai (2006) that the range between 138 and 587 mg/L of SA was degraded within 15–63 h, respectively. In the researches of Loh and Yu (2000), SA concentrations between 20 and 600 mg/L were biodegraded with times removal of the contaminant between 9 and 23 h, respectively.

The specific growth rate was calculated by means of the following equation (Juang and Tsai 2006):

$$r_X = \frac{dX}{dt} = \mu\ X \tag{5}$$

where r_x is the rate of biomass growth, X is the cell number or mean cell concentration, μ is the specific biomass growth rate, and t is time. The variation in specific growth rate (μ) versus SA concentration (S) obtained from batch tests is shown in Fig. 4. The Haldane equation for substrate-inhibited growth was fitted to the specific biomass growth rate data (μ) versus SA concentration (S) (Juang and Tsai 2006). The following parameter values were obtained: μ_{max}=0.25 h^{-1}; substrate-affinity constant, K_s=61.25 mg SA/L; substrate-inhibition constant, K_i=704.93 mg SA/L; and a correlation coefficient, r^2, of 0.991.

Literature survey on salicylic degradation shows that the K_i, μ_{max}, and K_s values ranges from 719.6 mg/L, 0.137 h^{-1}, and 15.33 mg/L using *P. putida* CCRC 14365 (Juang and Tsai 2006) to 1,201.7 mg/L, 0.52 h^{-1}, and 36.2 mg/L using *P. putida* ATCC 17484 (Loh and Yu 2000). The K_i and μ_{max} values obtained in the present work were (704.93 mg/L and 0.25 h^{-1}) which fall within the literature ranges. On the other hand, the K_s value (61.26 mg/L) determined in this work is

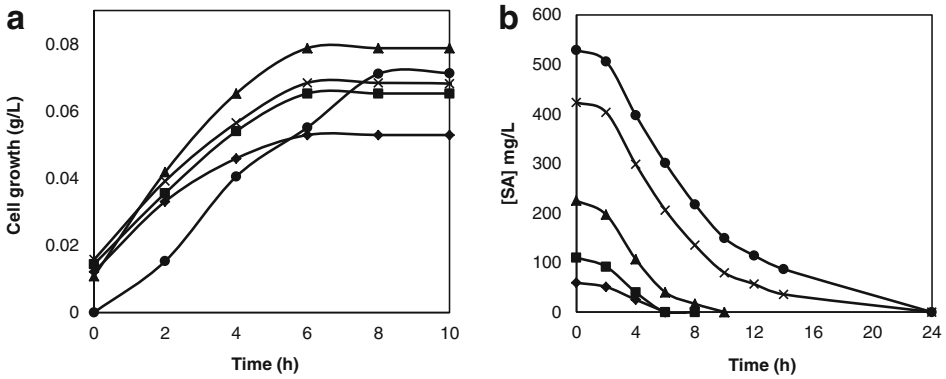

Fig. 3 Growth and salicylic acid degradation of *Pseudomonas putida* in a mineral salt medium containing 50–500 mg SA/L, 30 °C, 200 rpm, pH:7 (*black diamond* 59 mg/L, *black square* 110 mg/L, *black up-pointing triangle* 225 mg/L, × 423 mg/L, and *black circle* 529 mg/L) **a** Growth of *Pseudomonas putida* and **b** salicylic acid degradation

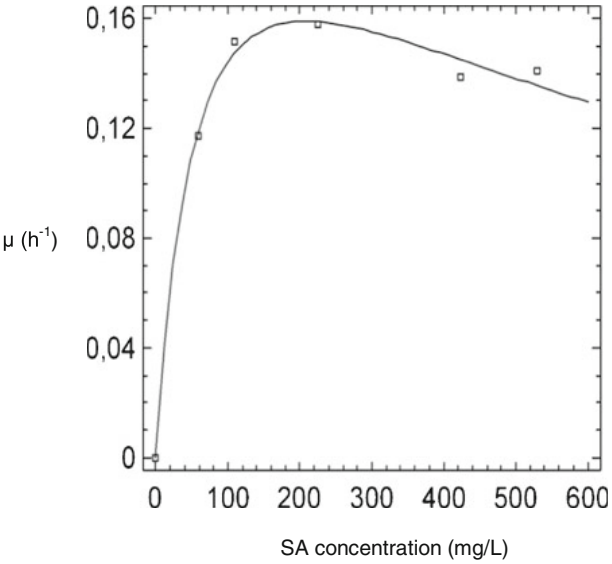

Fig. 4 Specific growth rate of suspended biomass in a salicylic acid solution (50–500 mg/L), 30 °C, 200 rpm pH: 7 (*white square* experimental data – model)

slightly higher than that found in other works indicating that *P. putida* (DSM 4478) cells have a higher SA affinity.

3.4 Biofilm Formation

Biofilm formation on AC was analyzed by varying the inoculated concentration of initial biomass and the agitation speed of the medium. The agitation speeds and inoculum sizes used in these experiments were 50 and 150 rpm and 0.05 and 0.1 OD units, respectively. Experiments were performed employing two different volumes of medium: 100 and 1,000 mL.

Table 3 shows the results obtained in the experiments. No significant differences were found in terms of biomass formation for the different process operating conditions. However, the results show that the number of colony forming units (cfu) is slightly higher at 50 rpm and 0.05 OD units than that obtained under other conditions.

Table 3 Results of the dry weight of biomass and colony forming units for the formation of biofilm on activated carbon

Inoculum size	*N* (rpm)	V_m (mL)	mg bio/g AC	cfu/mL	cfu/g AC
0.05	150	100	256.9	3.6×10^{8}	3.6×10^{10}
0.05	150	1,000	320.5	5.9×10^{8}	5.9×10^{10}
0.05	50	100	335.7	7.5×10^{8}	7.5×10^{10}
0.1	150	100	243.8	2.9×10^{8}	2.8×10^{10}
0.1	150	1,000	309.2	5.1×10^{8}	5.1×10^{10}

For the combined adsorption–biodegradation process, biofilm attachment on AC occurred under operating conditions of 50 rpm and 0.05 OD units.

In this work, the value of attached biomass on AC in optimal conditions found was 2.9×10^{5} cfu/cm^2. Data of attached biomass on AC in batch biofilm formation processes have not been found in the literature; however, some data are available in several works regarding column biofilm formation. For example, Gibert et al. (2013) estimate the amount of attached biomass on active carbon in column experiments, being 1×10^{6} cfu/cm^2 in the top of the column. In other work about biofilm formation on surfaces exposed to treated water, Van der Kooij et al. (1995) indicate biomass values adhered between 8.7×10^{3} and 2.5×10^{4} cfu/cm^2 on glass and values between 1.1×10^{4} and 2.9×10^{4} cfu/cm^2 on Teflon. In batch operations, Ploux et al. (2007) determined the amount of biomass attached on two different surface areas. These surfaces were constituted by terminated self-assembled monolayers (SAMs) on silicon wafers. For CH_3- and NH_2-surfaces, values around $(3–3.5)\times10^{7}$ cfu/cm^2, respectively, were reached in 24 h. So the values of attached biomass found in this work are in the same range that the values obtained in other systems for other authors.

Furthermore, the absence or presence of SA in the process of biofilm formation did not produce significant differences in the performance of the subsequent biosorption in either the pollutant removal rate or the rate of biomass formation in the medium.

3.5 Biofilm Influence on Adsorption and Biodegradation

Simultaneous adsorption and biodegradation of SA were studied in a series of batch experiments.

Figure 5a, b shows the SA uptake over time using two different systems, AC and dead biofilm. Duplicates biosorption process with dead biomass are shown in the figure (indicated as Dead biofilm-Gac 1 and Dead biofilm-Gac 2). This process was carried out at initial salicylic concentrations of 100 and 500 mg/L.

AC can reduce the concentration of SA from 85 to 38 and from 458 to 374 mg/L in 25 h, so it presents an adsorption capacity of 40.5 and 72.3 g/L, respectively. In this case, the AC adsorption capacity was higher than that obtained in Section 3.1. This is explained by the

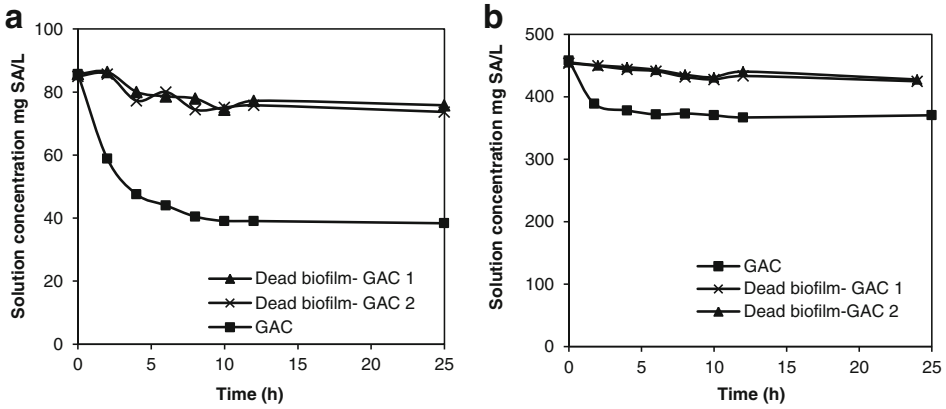

Fig. 5 Variation in the concentration of salicylic acid over time using dead biofilm and activated carbon systems. Initial concentration of acid: 100 mg/L (**a**) and 500 mg/L (**b**), 30 °C, L/S:1,000 and 200 rpm, pH:7

difference in pH between the experiments: in Section 3.1, the solution had a basic pH (11.5), while in this case, the pH of the solution was neutral, around 7. Karimi-Jashni and Narbaitz (1997) reported that increasing the pH of the solution hinders pollutant adsorption by the AC. In view of the results, the adsorption of the pollutant by the AC was adversely affected by the basicity of the medium.

In the case of the dead bacteria immobilized on AC system, only 12 and 6 % of SA was removed. The AC of the system is not able to adsorb SA because the biomass plugs its active sites or the AC is saturated during the process of biofilm formation with the acid and other components present in the medium (Ong et al. 2008; Walker and Weatherley 1999).

Figure 6a, b compares SA removal over time in the case of the biodegradation with free cells system and for biosorption with biofilm attached on the AC. Duplicates biosorption process with Living biofilm are shown in the figure (referred as Living biofilm-Gac 1 and Living biofilm-Gac 2).

Bioadsorption performed significantly better than AC adsorption. The results indicate that the same amount of AC achieves almost 100 % pollutant removal in the biosorption process, whereas the removal of SA in the case of adsorption is equal to 55 and 20 % for initial SA concentrations of 100 and 500 mg/L, respectively.

Comparing the biofilm system versus the free cells system, a difference in performance is observed depending on the initial concentration of SA. When the initial concentration is low (100 mg/L), the free cells system is more effective, as it removes the pollutant in a shorter period of time. When the initial concentration of acid is higher (500 mg/L), however, the immobilized biomass system is more effective even though biosorption is slightly lower in the first hours of the experiment and the system has a greater lag period.

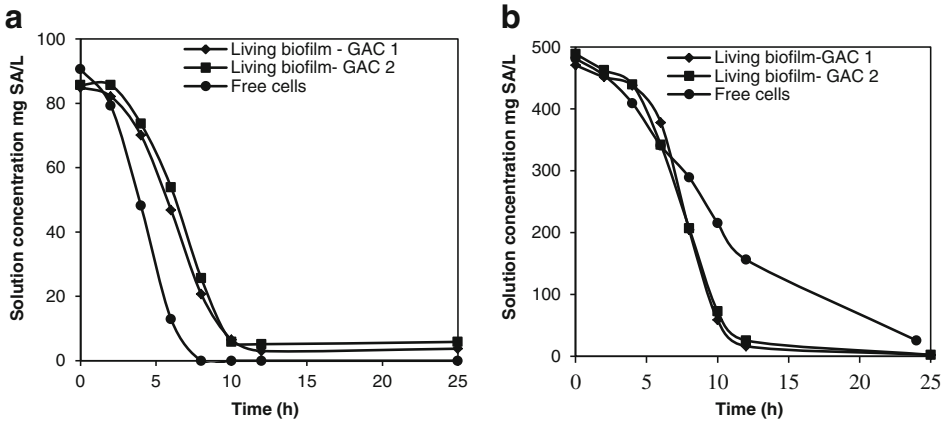

Fig. 6 Variation in the concentration of salicylic acid over time using biofilm and free cells systems. Initial concentration of acid: 100 mg/L (**a**) and 500 mg/L (**b**) 30 °C, L/S:1,000 and 200 rpm, pH:7

Table 4 Kinetics parameters for the system with biomass immobilized and free cells system

		$Y_{X/S}$	μ (h^{-1})	r_{max} (mg/L h)	Bioadsorption time (h)	Maximum concentration of biomass (mg/L)
500 mg/L	Bacteria immobilized	0.364	0.301	77.2	12	169
	Free cells	0.142	0.033	36.7	26	42.8
100 mg/L	Bacteria immobilized	0.746	0.293	13.1	25	58.9
	Free cells	0.691	0.276	17.7	8	42.2

In this case, AC bioadsorption using synthetic wastewater was found to require a longer time to reach equilibrium. Dissolved organic matter was removed from the wastewater quickly within the first 45 min, after which the removal rates increased gradually over the next 12 h. The explanation for this is that the adsorption of AC was more predominant at the beginning, while after the available sites were occupied, the organic matter was biodegraded by the activity of microorganisms which colonized the external surface and macropores of the carbon (Xing et al. 2008).

These conclusions are confirmed by the specific growth rate, maximum speed of degradation, cell yield, degradation time, and maximum concentration of biomass values shown in Table 4.

The consumption associated with the growth substrate, cell yield, and their relationship is represented as follows:

$$(X - X_0) = Y_{X/S}(S_0 - S) \quad (6)$$

where $Y_{X/S}$ is the cell yield coefficient, which is a measure of the amount of biomass produced per unit of substrate consumed, and the subscript 0 represents the initial conditions.

The observed difference in performance between the free cells and immobilized biomass systems is due to the fact that the biomass is much more protected from the toxicity of the medium in the biofilm attached to AC setup. In addition, Prober et al. (1975) showed that AC is able to enrich dissolved oxygen. This oxygen is probably also utilized by the microorganisms adsorbed on the AC.

Pai et al. (1994), Orshansky and Narkis (1996), Xing et al. (2008), and Walker and Weatherley (1999) investigated biosorption processes with different contaminants. Although different contaminants and bacteria were used, these authors found an improved contaminant removal due to the use of the biofilms. For example, Pai et al. (1994) observed that the presence of biofilm improved the rate of degradation of phenol by *Rhodococcus sp.*, increasing the value of the degradation rate from 0.432 g/Ld when operating with free cells to 2.91 g/Ld when biological AC was used. Moreover, Walker and Weatherley (1999) found that the removal of Acid Blue Color (TB4R) with *P. putida* (NICMB 9776) increased from 30 % using free cells to 90 % using biofilm on AC after 24 h.

4 Conclusions

In this paper, the influence of biofilm on individual processes of adsorption of SA on AC and its biodegradation by *P. putida* were studied. First, the individual processes were tested separately, finding that Filtrasorb 400 AC had a higher capacity than the other carbon studied. The equilibrium constant and the maximum capacity of F400 were 46.99 and 26.6 g/L AC (30.74 mg/g), respectively. The biodegradation of SA by *P. putida* follows a substrate-inhibition kinetics that can be fitted to the Haldane equation, with the following parameters: μ_{max}=0.25 h^{-1}, K_s=61.25 mg SA/L, *K*i=704.93 mg SA/L, and a correlation coefficient, r^2, of 0.991. Furthermore, the system of dead biomass attached to the AC did not show biosorption capacity. Thus, the presence of biofilm on AC has a negative effect on the adsorption process.

The free cells system employing an initial concentration of SA of 100 mg/L achieved a pollutant removal efficiency of 85.7 and 100 % at 6 and 8 h, respectively. However, when the initial concentration was 500 mg/L SA, the respective removal efficiencies were 67.5 and 94.7 % at 12 and 24 h. The bioadsorption system employing an initial concentration of 100 mg/L needed 10 h to obtain a removal efficiency of 93.16 % SA. When employing an initial pollutant concentration of

500 mg/L, however, the removal efficiency was 94.7 % at 12 h. As regards the combined adsorption/biodegradation process, the results showed that the biofilm outperformed the combination of conventional AC and biological water treatment processes in the case of working with high pollutant concentrations, as it is able to remove SA in a shorter period of time. This effect occurs in this case because the biological system is protected from adverse environmental conditions.

Acknowledgments R. G. Combarros wished to thank a research grant from the Government of the Principality of Asturias (Severo Ochoa Programme).

References

Characklis, W. G. (1981). Fouling biofilm development: a process analysis. *Biotechnology and Bioengineering, 23*, 1923–1960.

Chourio, E., Ferrer, X., Arrieta, I., Fernández, N., Sarmiento, C., & García, C. (1997). Diffusion models under the solid phase control for adsorption and ion-exchange. *Revista Técnica de la Facultad de Ingeniería Universidad del Zulia, 20*(3), 245–255.

Ferro Orozco, A. M., Contreras, E. M., & Zaritzkya, N. E. (2010). Dynamic response of combined activated sludge-powdered activated carbon batch systems. *Chemical Engineering Journal, 157*, 331–338.

Gibert, O., Lefèvre, B., Fernández, M., Bernat, X., Paraira, M., Calderer, M., Martínez-Lladó, X. (2013). Characterising biofilm development on granular activated carbon used for drinking water production. *Water Research*, 4 7, 1 1 0 1–1 1 1 0.

González, G., Herrera, M. G., García, M. T., & Peña, M. M. (2001). Biodegradation of phenol in a continuous process: comparative study of stirred tank and fluidized-bed reactor. *Bioresources Technology, 76*, 245–251.

Juang, R. S., & Tsai, S. Y. (2006). Growth kinetics of *Pseudomonas putida* in the biodegradation of single and mixed phenol and sodium salicylate. *Biochemical Engineering Journal, 3*, 133–140.

Karimi-Jashni, A., & Narbaitz, R. M. (1997). Impact of pH on the adsorption and desorption kinetics of 2-nitrophenol on activated carbons. *Water Research, 31*(12), 3039–3044.

Khenniche, L., & Aissani, F. (2010). Preparation and characterization of carbons from coffee residue: adsorption of salicylic acid on the prepared carbons. *Chemical Engineering Journal, 55*, 728–734.

LeChevalier, M. W., Hassenauer, T. S., Champer, A. K., & McFeters, G. A. (1984). Disinfection of bacteria attached to granular activated carbon. *Applied and Environmental Microbiology, 48*(5), 918–923.

Loh, K. C., & Bin, C. (2008). Paradigm in biodegradation using *Pseudomonas putida*-a review of proteomics studies. *Enzyme and Microbial Technology, 43*, 1–12.

Loh, K. C., & Yu, Y.-G. (2000). Kinetics of carbazole degradation by *Pseudomonas putida* in presence of sodium salicylate. *Water Research, 34*(17), 4131–4138.

Monteiro, A. A. M. G., Boaventura, R. A. R., & Rodrigues, A. E. (2000). Phenol biodegradation by *Pseudomonas putida* DS 548 in a batch reactor. *Biochemical Engineering Journal,* 45–49.

Navia, R., Inostroza, X., & Diez, M.C. (2003). Modelación matemática de la adsorción de contaminantes de efluentes de celulosa en el suelo de origen volcánico. *XV Congreso de ingeniería sanitaria y ambiental AIDIS-Chile*. Oct 1-3, Concepción, Chile.

Olmstead, K. P., & Weber, W. J. (1991). Interactions between microorganisms and activated carbon in water and waste treatment operations. *Chemical Engineering Communications, 108*, 113–125.

Ong, S. A., Toorisaka, E., Hirata, M., & Hano, T. (2008). Granular activated carbon-biofilm configured sequencing batch reactor treatment of C.I. Acid Orange 7. *Dyes and Pigments, 76*, 142–146.

Orshansky, F., & Narkis, N. (1996). Characteristics of organics removal by pact simultaneous adsorption and biodegradation. *Water Research, 31*(3), 391–398.

Otero, M., Grande, C. A., & Rodrigues, A. E. (2004). Adsorption of salicylic acid onto polymeric adsorbents and activated charcoal. *Reactive and Functional Polymers, 60*, 203–213.

Özkaya, B. (2006). Adsorption and desorption of phenol on activated carbon and a comparison of isotherm models. *Journal of Hazardous Materials B, 129*, 158–163.

Pai, S. L., Hsu, Y. L., Chong, N. M., Sheu, C. S., & Chen, C. H. (1994). Continuous degradation of phenol by *Rhodococcus sp*. immobilized on granular activated carbon and in calcium alginate. *Bioresource Technology, 51*, 37–42.

Ploux, L., Beckendorff, S., Nardin, M., & Neunlist, S. (2007). Quantitative and morphological analysis of biofilm formation on self-assembled monolayers. *Colloids and Surfaces, B: Biointerfaces, 57*, 174–181.

Prober, R., Pycha, J. J., & Kindon, W. E. (1975). Interaction of activated carbon with dissolved oxygen. *American Institute of Chemical Engineers Journal, 6*, 1200–1204.

Qadeer, R., & Rehan, A. H. (2002). Study of the adsorption of phenol by activated carbon from aqueous solutions. *Turkish Journal of Chemistry, 26*, 357–361.

Silva, T., Valdman, E., Valdman, B., & Leite, S. G. F. (2007). Salicylic acid degradation from aqueous solutions using Pseudomonas fluorescens HK44: parameters studies and applications tools. *Brazilian Journal of Microbiology, 38*, 39–44.

Snell F.D., & Snell C.T. (1953). *Colorimetric methods of analysis. Including some turbidimetric and nephelometric methods*. Volume III, Organic-I, New York, D. Van Nostrand Company, Inc.

Torre, M., Bachiller, D., Rendueles, M., Menéndez, C. O., & Díaz, M. (2006). Cyanide recovery from gold extraction process waste effluents by ion exchange I. equilibrium and kinetics. *Solvent Extraction and Ion Exchange, 24*, 99–117.

Tsuneda, S., Auresenia, J., Inoue, Y., Hashimoto, Y., & Hirata, A. (2002). Kinetic model for dynamic response of three-phase fluidized bed biofilm reactor for wastewater treatment. *Biochemical Engineering Journal, 10*, 31–37.

Tsuneda, S., Inoue, Y., Auresenia, J., & Hirata, A. (2003). Adsorption effect on the dynamic response of a biochemical reaction in a biofilm reactor for wastewater treatment. *Engineering in Life Sciences, 3*(9), 371–375.

Van der Kooij, D., Veenendaal, H. R., Baars-Lorist, C., Van der Klift, D. W., & Drost, Y. C. (1995). Biofilm formation on surfaces of glass and teflon exposed to treated water. *Water research, 29*(7), 1655–1662.

Walker, G. M., & Weatherley, L. R. (1999). Biological activated carbon treatment of industrial wastewater in stirred tank reactors. *Chemical Engineering Journal, 75*, 201–206.

Wang, X., Deng, R., Jin, X., & Huang, J. (2012a). Gallic acid modified hyper-cross-linked resin and its adsorption equilibria and kinetics toward salicylic acid from aqueous solution. *Chemical Engineering Journal, 191*, 195–201.

Wang, X., Wang, Y., Feng, L., Liu, P., & Zhang, X. (2012b). A novel adsorbent based on functionalized three-dimensionally ordered macroporous cross-linked polystyrene for removal of salicylic acid from aqueous solution. *Chemical Engineering Journal, 203*, 251–258.

Xing, W., Ngo, H. H., Kim, S. H., Guo, W. S., & Hagare, P. (2008). Adsorption and bioadsorption of granular activated carbon (GAC) for dissolved organic carbon (DOC) removal in wastewater. *Bioresource Technology, 99*, 8674–8678.

Ying, W.-C., & Weber, W. J. (1979). Bio-physicochemical adsorption model systems wastewater treatment. *Journal Water Pollution Control Federation, 51*(11), 2661–2677.

5.2. Toxicidad por dióxido de titanio nanopartículado sobre el estado metabólico de *Pseudomonas putida* y la biodegradación del ácido salicílico

El efecto de las nanopartículas de dióxido de titanio sobre el proceso biológico en las plantas de tratamiento de aguas residuales no ha sido estudiado en profundidad. Por ello, en el presente trabajo, se han llevado a cabo análisis de toxicidad de las nanopartículas de dióxido de titanio sobre la viabilidad y la actividad metabólica de la bacteria *Pseudomonas putida*. El cultivo puro de *P. putida* se ha considerado como un modelo sencillo de lodos activos, consiguiendo de este modo amplificar la respuesta del efecto tóxico.

La citometría de flujo multiparamétrica aplicando una tinción dual de los fluorocromos PI y cFDA se ha utilizado como herramienta en la monitorización y control de la respuesta del estado fisiológico de la bacteria causada por la presencia de las nanopartículas. Esta técnica no había sido empleada hasta el momento con el fin de estudiar la toxicidad de nanopartículas sobre el estado fisiológico de las bacterias.

En este artículo se analiza cómo la presencia de distintas concentraciones de nanopartículas de dióxido de titanio afecta a la respuesta fisiológica y metabólica de la bacteria *Pseudomonas putida* bajo dos condiciones de cultivo diferentes: en un medio con fuente adicional de carbono y nitrógeno fácilmente asimilables o en un medio mineral mínimo con ácido salicílico como única fuente de carbono, a fin de simular un agua residual industrial farmacéutica. Un modelo segregado en el que se tiene en cuenta las diferentes subpoblaciones bacterianas ha sido propuesto y ajustado a los datos experimentales obtenidos en la biodegradación del ácido salicílico en presencia de nanopartículas de dióxido de titanio.

Los resultados de este trabajo se presentan a través de una publicación cuya referencia y estado se muestran a continuación.

Referencia: Combarros, R.G, Collado, S., Díaz, M. 2016. Toxicity of titanium dioxide nanoparticles on *Pseudomonas putida*. Water Research, 90, 378-386.

Estado: Publicada

Water Research 90 (2016) 378–386

Contents lists available at ScienceDirect

Water Research

journal homepage: www.elsevier.com/locate/watres

Toxicity of titanium dioxide nanoparticles on *Pseudomonas putida*

R.G. Combarros, S. Collado, M. Díaz*

Department of Chemical and Environmental Technology, University of Oviedo, Spain

ARTICLE INFO

Article history:
Received 28 October 2015
Received in revised form
22 December 2015
Accepted 23 December 2015
Available online 29 December 2015

Keywords:
Antimicrobial activity
Flow cytometry
Metabolic activity
Pseudomonas putida
TiO_2 nanoparticles
Wastewater treatment

ABSTRACT

The increasing use of engineered nanoparticles (NPs) in industrial and household applications will very likely lead to the release of such materials into the environment. As wastewater treatment plants (WWTPs) are usually the last barrier before the water is discharged into the environment, it is important to understand the effects of these materials in the biotreatment processes, since the results in the literature are usually contradictory. We proposed the use of flow cytometry (FC) technology to obtain conclusive results. Aqueous solutions of TiO_2 nanoparticles (0–2 mg mL^{-1}) were used to check its toxicity effect using *Pseudomonas putida* as simplified model of real sludge over room light. Physiological changes in *P. putida* from viable to viable but non-culturable cells were observed by flow cytometry in presence of TiO_2. The damaged and dead cell concentrations were below 5% in all cases under study. Both FSC and SSC parameter increased with TiO_2 dose dependent manner, indicating nanoparticles uptake by the bacteria. The biological removal of salicylic acid (SA) was also significantly impacted by the presence of TiO_2 in the medium reducing the efficiency. The use of FC allows also to develop and fit segregated kinetic models, giving the impact of TiO_2 nanoparticles in the physiological subpopulations growth and implications for SA removal.

1. Introduction

TiO_2 nanoparticles (TiO_2-NPs) are effective opacifiers profusely used as pigments in paints, paper, inks, and plastics (Li et al., 2014). TiO_2-NPs have chemical stability, high photocatalytic efficiency and low cost (Erdural et al., 2014). Apart from this, TiO_2-NPs have recently become very important as catalyst in photodegradation processes aimed at removing biorecalcitrant and/or toxic pollutants from wastewaters or the inactivation of pathogens in water (Erdural et al., 2014; Ju-Nam and Lead, 2008; Rawat et al., 2007).

Due to this wide application in industries and human daily life, TiO_2-NPs have been detected in soil, surface water, wastewater and sewage sludge samples, which raises concerns about their potential environmental impacts and their possible adverse effects on biological systems (Li et al., 2015, 2014). For instance, TiO_2-NPs were found to adsorb onto activated sludge in conventional biological nutrient removal systems of WWTPs (Li et al., 2015). Nevertheless, the bibliography reports that the factors which might have an impact on interactions between the different types of nanomaterials and biomolecules have remarkably increased, but the knowledge about them is not yet deep (Ghosh et al., 2012; Kumar et al., 2011).

There have been many contradictory reports about the biocompatibility and antimicrobial activity of TiO_2-NPs. Recently, Kapri et al. (2009) and Anil and Zaidi (2010) showed that a bacteria consortium grew faster and to a higher optical density when nanoparticles of nanobarium titanate were added to a bacterial consortium at 0.1 mg mL^{-1}. On the other hand, several researchers indicated a strong antibacterial activity of TiO_2-film on *Escherichia coli* either with irradiate light or sunlight (Bonnefond et al., 2015; Cho et al., 2004; Erdural et al., 2014; Gelover et al., 2006). Erdural et al. (2014) demonstrated that the survival rate of suspended *E. coli* decreased from 100% to 30% in just 60 min, when the bacteria were in contact with TiO_2-film in an irradiated light process; nevertheless, no antibacterial activity was found in the dark process under the same conditions.

The precise mechanism for bacterial toxicity of TiO_2-NP is still being elucidated, but the possibilities include free metal ion toxicity and oxidative stress via generation of reactive oxygen species (ROS) (Besinis et al., 2014; Bonnefond et al., 2015; Cho et al., 2004; Erdural et al., 2014). The cell inactivation has frequently been related to inhibition of cell respiration, decomposition of the lipopolysaccharide layer, DNA damage, genotoxicity, release of toxic constituents and structural disarrangement of the cytoplasmic membrane

* Corresponding author.
E-mail address: mariodiaz@uniovi.es (M. Díaz).

http://dx.doi.org/10.1016/j.watres.2015.12.040
0043-1354/

due to lipid per oxidation (Besinis et al., 2014; Erdural et al., 2014; Ju-Nam and Lead, 2008; Li et al., 2014; Neal, 2008).

Many of these works about effects of TiO_2-NPs on microbial activity almost always based their conclusions on microorganism death, which is usually measured by means of propidium iodide (PI) staining and confocal microscopy (Le et al., 2014), drop-test based on measuring the colony formig unit (CFU mL^{-1}) (Anil and Zaidi, 2010; Bonnefond et al., 2015; Cho et al., 2004; Erdural et al., 2014; Le et al., 2014), or optical density (OD) (Anil and Zaidi, 2010; Besinis et al., 2014). However, after an in-depth bibliographic review, new techniques, such as flow cytometry, which can not only measure the bacterial death but also the reduction in the activity, have not been implemented for this purpose yet. The use of FC provides additional information to the studied so far, where only growth suppression and loss of bacterial viability as CFU mL^{-1} and OD were described (Bonnefond et al., 2015; Cho et al., 2004; Erdural et al., 2014; Fu et al., 2005; Kapri et al., 2009). In addition, most of these researches has been conducted with well-known model organisms, such as *E. coli* (Bonnefond et al., 2015; Cho et al., 2004; Erdural et al., 2014; Fu et al., 2005; Kumar et al., 2011; Rincón and Pulgarin, 2007), with TiO_2-NPs usually forming part of thin film deposit over different surfaces (Bonnefond et al., 2015; Erdural et al., 2014; Gelover et al., 2006).

However, information about their impact on wastewater biological treatments is very scarce (Li et al., 2015, 2014). In fact, as far is known, there are not previous studies dealing with the effect of TiO_2-NPs on *Pseudomonas putida*, even when these bacteria are the predominant ones in activated sludge (Collado et al., 2014) and the results obtained can be employed as a reference during the comparison with those from other works using mixed cultures. Moreover, the use of a pure culture instead of a mixed sludge accelerates and amplifies the response of the system to perturbations (Collado et al., 2014).

Taking into account the aforementioned considerations, the aim of the present work is to evaluate, for first time, the effects of TiO_2-NPs on the viability and activity of *P. putida*. For this purpose, the evolution of the physiological status of *P. putida* when is exposed to different suspended TiO_2-NPs concentrations was studied by means of flow cytometry, distinguishing three metabolic states: viable, damaged and dead cells.

2. Materials and methods

2.1. Preparation of TiO_2 nanoparticle suspension

The TiO_2-NPs used in this study were purchased from Sigma–Aldrich (St. Louis, MO, USA). According manufacturer data, mean nanoparticle size is less than 25 nm, and the purity is 99.5%. Stock solution (50 g L^{-1}) was prepared in sterile Milli-Q water and sonicated (35 kHz frequency, Fisherbrand FB 11010, Germany) for 1 h to disperse the materials (Besinis et al., 2014; Li et al., 2015, 2014; Zucker et al., 2010).

2.2. Cell preparation

P. putida (Leibniz Institute DSMZ-German Collection of Microorganism and Cells Cultures, Germany (DSM 4478)) was chosen. A detailed description of cell preparation procedure can be found in a previous work (Combarros et al., 2014). Stated briefly, *P. putida* colonies were inoculated in a growth medium and incubated at 30 °C and 150 rpm for 16 h. Afterwards, an aliquot was centrifuged and washed at 10,160 × g for 10 min, being then used as an inoculum for subsequent experiments.

2.3. Cell viability test

The effects of TiO_2-NP on the activity and viability of *P. putida* were studied using a synthetic industrial wastewater, composed by a minimum mineral medium which was supplemented by 500 mg L^{-1} of SA, in order to simulate an moderately biodegradable pharmaceutical wastewater. Additionally, some experiments were carried out in the growth medium recommended for *P. putida* by the supplier, with the aim of having a preliminary knowledge about TiO_2-NPs toxicity on *P. putida* under optimal medium conditions. The detailed composition of synthetic industrial wastewater and growth medium can be consulted in Table S1 (see Supplementary data).

For both media, TiO_2-NPs concentrations selected were 0, 0.1, 0.5, 1 and 2 mg mL^{-1}. The stock dispersion diluted with the growth or the simulated industrial medium above at neutral pH, dispersions were sonicated for 1 h prior to assay to ensure dispersion of the particles (Besinis et al., 2014). Typical TiO_2-NPs concentrations reported in bibliography for other toxicity studies usually range from several mg L^{-1} to 1 g L^{-1} (Cho et al., 2004; Le et al., 2014; Li et al., 2015; Rincón and Pulgarin, 2007).

For the growth medium recommended by the supplier (GM), the culture conditions were 200 rpm and 30 °C in 250 mL Erlenmeyer flasks containing 100 mL of simulated medium (Combarros et al., 2014). While, for the simulated industrial wastewater (SIW), the culture conditions were 250 rpm and 30 °C and 100 mL of simulated medium in 500 mL Erlenmeyer flasks (Combarros et al., 2015a). The higher volume and stirring speed selected in the case of SIW were chosen in order to improve the adaptation and growth of bacteria in this medium. In all cases, initial *P. putida* concentration was around 10^7 CFU mL^{-1}. Once *P. putida* was inoculated in the medium, contact TiO_2-NP-bacteria was maintained for 24 h in an incubator New Brunswick Scientific (Edison, New York) that kept constant the culture conditions, taking samples at different times. For each one of them, OD, CFU mL^{-1}, pH, SA concentration and metabolic viability and activity were analysed.

Additionally, experiments with different TiO_2-NP concentrations (0, 0.1, 0.5, 1 and 2 mg mL^{-1}) but without bacteria were also carried out with the aim of discarding possible interactions between TiO_2-NPs and SA.

All material was autoclaved at 121 °C for 20 min in order to maintain the sterility of the system. The TiO_2-NPs and SA stock solutions were sterilized separately.

2.4. Flow cytometry analysis

2.4.1. Staining procedures

The stock solutions preparation and staining procedures have been described in Combarros et al. (2015b). The samples were stained using SYBRgreen (SYBRgreen; Invitrogen) and Fluorescent microspheres (Perfect Count; Cytognos, Spain) to obtain the total count of cells. Additionally, a dual-staining procedure (carboxyfluorescein diacetate/propidium iodide) (cFDA/PI) was used to evaluate the bacterial physiological status: cFDA and PI are indicators of esterase activity and membrane integrity, respectively (Amor et al., 2002; Díaz et al., 2010; Quirós et al., 2007, 2009).

2.4.2. Multi-parameter flow cytometry

Flow cytometry measurements were performed using a Cytomics FC 500 flow cytometer (Beckman Coulter) equipped with a 488 and 633 nm excitation light source from an argon ion laser. Green fluorescence from samples (corresponding to cFDA or SYBRgreen-stained cells) was collected on the FL1 channel (530 nm), whereas PI fluorescence was registered on the FL3

channel (610 nm). Each analysis was performed in duplicate at a low flow rate setting (4000 events s^{-1}). Data acquisition was carried out using Cytomics RXP software (Beckman Coulter). Gates and quadrants were established according to staining controls. For cFDA/PI dual-parameter, data collected from 200,000 events, were analysed using Kaluza® Flow Analysis Software, Beckman Coulter. The fluorescent microspheres presented two types, A microspheres, excitable at 506 nm and B microspheres, excitable between 365 and 650 nm.

2.5. Analytical methods

Concentration of SA in the samples were measured by HPLC (Agilent 1200) using a Mediterranea Sea18 column (5 μm × 25 cm × 46 cm, plus a reverse-phase column from Waters) combined with a UV detector. The wavelength used for detection of SA was 290 nm. The mobile phase consisted in a mixture of two solutions: acetonitrile and 0.4% phosphoric acid in water (Hsu et al., 2004), employing a binary gradient at a constant flow rate of 1 mL min^{-1}.

Number of culturable bacteria (expressed as CFU mL^{-1}) was determined by the standard counting method by plating, obtaining viable counts. The evolution of total biomass was determined by means of two techniques: by optical density measurement at 660 nm (Shimadzu, UV–vis 1203) and by SYBR staining-flow cytometry. In the first case, TiO_2-NPs absorbance was corrected using control samples containing only NPs (Kuang et al., 2013). Viable and total cells were finally expressed in g L^{-1} taking into account the calibration curves previously obtained for viable or total cells stained by SYBRgreen (cell mL^{-1}) versus dry weight (g L^{-1}), respectively.

Physiological status of bacteria were established by means of a multiparameter flow cytometry using a previous dual PI/cFDA staining differentiating metabolically active cells as cFDA stained, dead cells as PI stained and damage cells as PI-cFDA stained. Finally, the cell size and cell complexity were monitored by measuring parameters FSC and SSC respectively by FC.

All experiments were carried out at least in duplicate and each sample was analysed in triplicate. Standard deviations (SD) obtained are shown as vertical lines in figures.

3. Results and discussions

3.1. Antibacterial activity of TiO_2-NPs

Before starting the experiments, it was observed that SA concentration did not change after 24 h in contact with TiO_2-NPs and in absence of *P. putida*, thus precluding any side reactions between TiO_2-NPs and SA (data not shown). Antibacterial test were performed in room light with either growth medium or synthetic wastewater (Fu et al., 2005). Bacterial viability experiments in dark were not carried out since previous studies demonstrate that TiO_2-NPs have no antibacterial effect in dark (Erdural et al., 2014; Fu et al., 2005; Rincón and Pulgarin, 2007). Moreover, Li et al. (2014) discovered that the levels of TiO_2-dependent inhibition of biological nitrogen removal were similar under both dark and light conditions.

3.1.1. Growth medium (GM)

Firstly, in order to get a preliminary estimation of the effect of TiO_2-NPs on the growth and physiological status of *P. putida*, this bacterium has been exposed to different concentrations of nanoparticles in the growth medium recommended by the supplier. Before inoculation, the system TiO_2-NPs-GM was sonicated to ensure de dispersion of nanoparticles. The prepared TiO_2-NPs suspension (0, 0.1, 0.5, 1 or 2 mg mL^{-1}) in GM were inoculated with around 10^7 CFU mL^{-1} of *P. putida* and incubated for 24 h at 200 rpm and 30 °C. In all cases, the initial pH of the media was adjusted to a value of 7.

Fig. 1a shows the evolution of *P. putida* in presence of different concentrations of TiO_2-NPs obtained by means flow cyton

The results of total cells obtained by flow cytometry reveal a clear negative effect of TiO_2-NPs on the *P. putida* growth for concentrations higher than 0.5 mg mL^{-1}. Therefore, for TiO_2-NPs lower than 0.5 mg mL^{-1}, *P. putida* showed a fast growth during the first five hours, until forty times the initial bacterial concentration, and then gradually decreases, probably due to the depletion of the GM. However, *P. putida* did not followed this trend for TiO_2-NPs concentrations higher than 0.5 mg mL^{-1}. In such cases, the higher the TiO_2-NPs concentration, the lower the initial *P. putida* growth. Moreover, the final gradual decrease in bacterial population observed for low TiO_2-NPs concentrations after the 5th hour of cultivation is hardly noticeable. Obviously, the lower the bacterial population, the higher the time required for the complete depletion of medium is.

Specific growth rates (μ) for *P. putida* were calculated for every TiO_2-NPs concentrations, getting a value of 0.67 ± 0.01 h^{-1} for TiO_2-NPs concentration equal to or lower than 0.5 mg mL^{-1}, whereas values of 0.501 ± 0.001 and 0.45 ± 0.01 h^{-1} were calculated for 1 and 2 mg mL^{-1} of TiO_2-NPs, respectively. When comparing these results with those reported for *E. coli*, it can be concluded that *P. putida* shows a higher tolerance to TiO_2-NPs than *E. Coli*. Thus, Fu et al. (2005) demonstrated that a 0.40 mg mL^{-1} TiO_2-NPs suspension inhibits effectively the *E. coli* growth.

Fig. 1b shows the FSC and SSC parameters depending on TiO_2-NPs concentration present in the medium. The intensities of FSC and SSC are proportional to the size of cells and the intracellular density, respectively. Although both parameters increased with the TiO_2-NPs concentration, this increase was more marked for SSC than for FSC. So the FSC or SSC signals for the culture with the TiO_2-NPs highest concentration (2 mg mL^{-1}) were around 2 or 13 times higher than those values obtained for cultures without nanoparticles, respectively. Moreover, both parameters are dose-dependent but not time dependent, that is, the increases in their values occur during the first minutes of reaction, then remaining constant (see Fig. S2). Others researches such as Kumar et al. (2011) and Zucker et al. (2010) have observed the SSC increased sequentially while the FSC decreased in response to TiO_2-NPs concentration with *E. Coli* and ARPE-19 cells, respectively, presumably due to substantial light reflection by the TiO_2 particles (Toduka et al., 2012; Zucker et al., 2010).

Several authors reported that the changes in intensity of SSC signal are related to the internationalization of NPs by the bacterium (Ghosh et al., 2012; Kumar et al., 2011). Thus, it seems reasonable to conclude that *P. putida* shows a fast uptake of TiO_2-NPs. Regarding the increase in FSC signal observed, it could be due to the agglomeration of NPs (Ghosh et al., 2012).

3.1.2. Simulated industrial wastewater (SIW)

The effects of different TiO_2-NPs concentrations on the growth and activity of a *P. putida* population are also evaluated, but using in this case a SIW. This wastewater consists of a minimum mineral medium to which 500 mg L^{-1} of SA was added, in order to simulate a moderately biodegradable pharmaceutical wastewater. Fig. 2 shows the evolution on the main parameters under these conditions, such as the bacterial growth or the specific SA removal rates.

Although several studies have been focused on the toxicity of NPs on bacteria, the effect of NPs on their pollutant-degrading activity has hardly been studied. As can be seen in Fig. 2a, the presence of TiO_2-NPs in the SIW involves a reduction in the SA removal

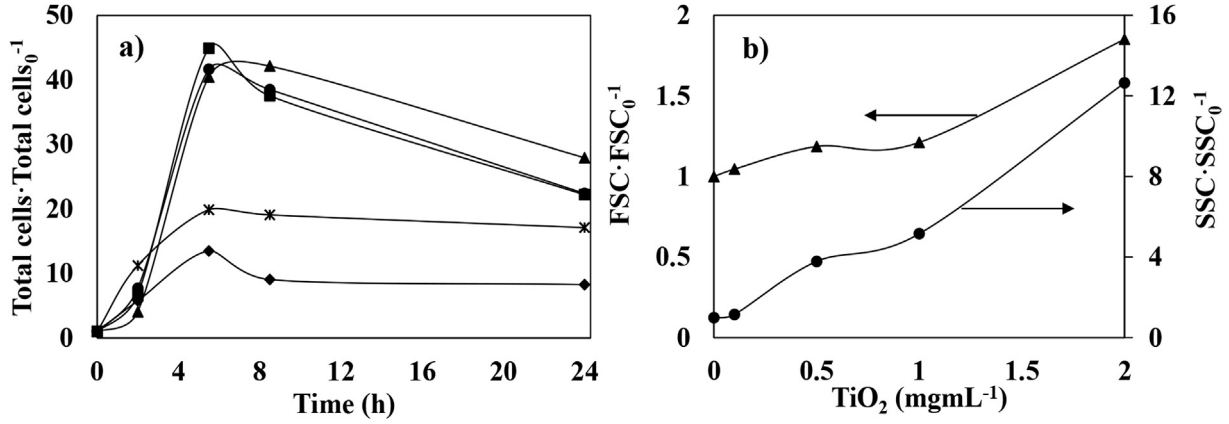

Fig. 1. a) Evolution of total *P. putida* bacteria in GM in presence of different concentrations of suspended TiO_2-NPs: 0 mg mL^{-1} (▲), 0.1 mg mL^{-1} (■), 0.5 mg mL^{-1} (●), 1 mg mL^{-1} (∗), 2 mg mL^{-1} (◆). b) Effect of suspended TiO_2-NPs concentrations on the FSC (▲) and SSC (●) signals after 8 h of *P. putida* cultivation in GM. In all cases: initial SA concentration of 100 mg L^{-1}, 200 rpm, 30 °C, *P. putida* inoculum of 10^7 CFU mL^{-1}, 100 mL in 250 mL Erlenmeyer flasks.

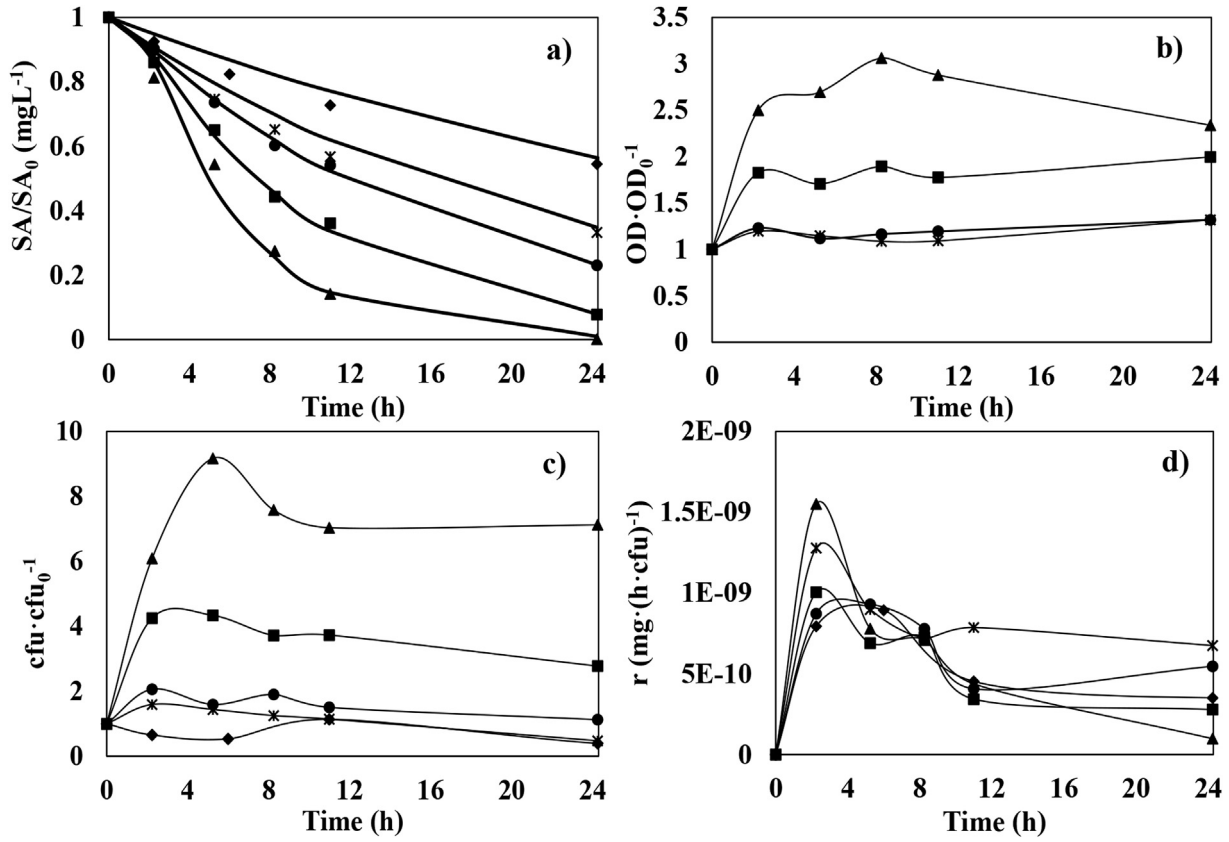

Fig. 2. Evolution of salicylic acid concentration (a), growth of *Pseudomonas putida* as OD (b) or colony forming unit (c) and specific degradation rate of salicylic acid (d) under different TiO_2-NPs concentrations in SIW (▲ 0 mg mL^{-1}, ■ 0.1 mg mL^{-1}, ● 0.5 mg mL^{-1}, ∗ 1 mg mL^{-1}, ◆ 2 mg mL^{-1}). In all cases: Initial SA concentration of 500 mgL^{-1}, 250 rpm, 30 °C, *P. putida* inoculum of 10^7 CFU mL^{-1}, 100 mL in 500 mL Erlenmeyer flasks. Solid lines in Figure a. denote fitting of salicylic acid biodegradation to a pseudo first-order kinetic models.

rate of *P. putida*. For instance, reductions in SA concentration of 86%, 64%, 46%, 43% and 27% were observed after 11 h of cultivation in presence of 0, 0.1, 0.5 1 and 2 mg mL^{-1} of TiO_2-NPs, respectively.

The evolutions of SA concentrations were successfully fitted to a pseudo first reaction order model ($C=C_0\cdot e^{(-k\cdot t)}$), obtaining the pseudo first order kinetic constant (k) for each TiO_2-NPs concentration. The relation between the k value and TiO_2-NPs concentration in the medium is represented by the following equation:

$$k\left(h^{-1}\right) = 0.20 + 0.040\cdot TiO_2^{-0.49}\left(mg\ mL^{-1}\right)\left(r^2 = 0.95\right)$$

Fig. 2b and c shows the bacterial growth measured as optical density or as colony forming units, respectively. Both parameters followed the same trend, that is, a fast increase in their value during the first hours of cultivation, then remaining approximately constant. It can also been clearly seen in these figures that the presence

of TiO_2-NPs in the SIW reduced the *P. putida* growth, this effect being significant even for low concentrations of nanoparticles. So, the bacterial growth dropped by half with only 0.1 mg mL^{-1} and the growth of the bacteria was almost completely inhibited for TiO_2-NPs concentrations in SIW higher than 0.5 mg mL^{-1}. This trend is better observed when the specific growth rates (μ) are calculated for each concentration of nanoparticles. The μ values obtained from CFU data were 0.41 ($r^2 = 0.82$), 0.26 ($r^2 = 0.70$), 0.08 ($r^2 = 0.99$), 0.07 ($r^2 = 0.85$), and 0.01 ($r^2 = 0.93$) for 0, 0.05, 0.1, 0.25, 0.5 and 1 mg mL^{-1} of TiO_2-NPs, respectively. The relation between the μ value and TiO_2-NPs concentration in the medium can be represented by the following equation:

$$\mu\left(h^{-1}\right) = 0.037 \cdot TiO_2^{-0.93}\left(mg\ mL^{-1}\right)\left(r^2 = 0.87\right)$$

Comparing these results with those previously obtained in GM, it can also be pointed out that, as expected, the inhibitory effect of TiO_2-NPs on the *P. putida* growth is more marked when the availability of carbon or nitrogen is limited. Finally, the specific degradation rates are shown in Fig. 2d; presented a maximum value at around 3 h, this trend was similar with all TiO_2-NPs concentrations.

In regards to flow cytometry measurements in presence of different concentrations of TiO_2-NPs, Fig. 3 plots the evolution of *P. putida* subpopulations, that are, total ($SYBR^+$), viable (as CFU), viable but not culturable (VBNC) ($cFDA^+$ less CFU), active ($cFDA^+$), damaged (PI^+ $cFDA^+$) and dead (PI^+ $cFDA^-$) bacteria. A more detailed description about the gates selected for each subpopulation can be found in SI, Fig. S3. At this point, it is important to point out that a study about the fluorescence emitted by the TiO_2-NPs itself or by its interactions with the dyes used (SYBRgreen, PI, cFDA) was previously carried out (data no shown). Results indicated that the fluorescence emitted by TiO_2-NPs either alone or in presence of fluorochromes, was always lower than 5%, so that, this fluorescence was not considered as significant. Therefore, interferences of TiO_2-NPs with the flow cytometry procedure were discarded.

Results of total cell concentration by flow cytometry are in accordance with those obtained by means of OD and plate counting. So, the presence of small amounts of TiO_2-NPs in the SIW involves a significant reduction in the *P. putida* growth. So, flow cytometry measurements indicated maximum total bacterial populations of $(1.7 \pm 0.4)\cdot 10^8$, $(1.4 \pm 0.1)\cdot 10^8$, $(9.2 \pm 2.8)\cdot 10^7$, $(6.8 \pm 0.2)\cdot 10^7$ and $(3.3 \pm 0.5)\cdot 10^7$ cells mL^{-1} after 3 h of cultivation with 0, 0.1, 0.5, 1 and 2 mg mL^{-1} of TiO_2-NPs, respectively (Fig. 3a). Total bacteria concentrations at zero time for all experiments were around 10^7 cell mL^{-1}. Concentration of *P. putida* subpopulation in percentage and cells mL^{-1} are shown in Fig. 3b–f for 0, 0.1, 0.5, 1 and 2 mg mL^{-1} TiO_2 concentration, respectively. In order to observe better the trends of the subpopulations, the Figs. S4 and S5 show each subpopulation (non-damaged, damaged and dead cells (S4) and actives, viable and VBNC cells (S5)) with time under different TiO_2-NPs concentrations.

The decrease in total cell concentrations observed in Fig. 3a for high times indicates that dead bacteria are rapidly lysed. This trend can be also observed in the evolution of non-damaged subpopulation (PI^-) (see Fig. S4a). So, the higher the TiO_2-NPs concentration, the lower the number of bacteria that have not lost their membrane integrity. However, when non-damaged cells are expressed as a proportion of total cells (see Fig. S4b), it is noteworthy that the higher percentages were obtained for the higher TiO_2-NPs concentrations. These results suggest that a high TiO_2-NPs concentration decreases the number of total *P. putida*, but the surviving bacteria show a better physiological status. In other words, the presence of TiO_2-NPs in the SIW reduces the number of total bacteria but also has an effect of screening, allowing obtaining a final population composed almost entirely for non-damaged bacteria (99% for 2 mg mL^{-1} of TiO_2-NPs in front of 95% in absence of nanoparticles). These results are in accordance with the evolution of damaged and dead subpopulations (Figs. S4c–d and S4e–f, respectively). As can be seen in both figures, either the percentages of dead or damaged cells are lower when the highest concentrations of nanoparticles were used. It can be also out that both subpopulations never exceeded the 5% of t population, which corroborates the fast lysis of the dead cells observed in Fig. 3a. It is also remarkable that for TiO_2-NPs concentrations lower than 0.1 mg mL^{-1}, the presence of nanoparticles increases the percentage of damaged bacteria, whereas concentrations higher than this value has the opposite effect, that is, the percentage of cells that have lost their membrane integrity decreased. In fact, the proportion of damaged cells in the SIW with 2 mg mL^{-1} of TiO_2-NPs was one order of magnitude lower than in absence of nanoparticles. In the light of these results, it seems reasonable to propose that *P. putida* in presence of TiO_2-NPs concentrations higher than 0.1 mg mL^{-1} are transformed into dead cells, which are rapidly lysed, with a small population of non-damaged bacteria remaining at the end of the experiment. PI cells stained discrimination in *E. coli* exposed to TiO_2 NPs using FC was carried out by Kumar et al. (2011), obtaining values of dead cells between 3.5 and 10% with TiO_2-NPs concentrations of 10–80 $\mu g mL^{-1}$. However, Zucker et al. (2010) observed that TiO_2-NPs showed a minimal decrease in cell viability (2%) in human-derived retinal pigment epithelial cells, at the highest concentration tested (30 $\mu g\ mL^{-1}$), this being measured as PI membrane permeability.

The impact of TiO_2-NPs in activity and culturability of *P. putida* can be seen in Fig. S5a-d. At this point, it is important to emphasize that active *P. putida* were defined as those stained by cFDA, whereas viable cells were measured by plate counting (Quirós et al., 2007, 2009). Again, the higher concentration of nanoparticles, the lower the active or culturable subpopulations. Nevertheless, when the viability results are expressed as percentage of total cells, it should be noted that the lower proportion of viable bacteria were obtained not with 2 mg mL^{-1}, but with concentrations between 0.1 and 0.5 mg mL^{-1}, as in the case of the percentage of damaged cells. This behaviour is not unexpected because both parameters are related to one another: damaged bacteria have lost their membrane integrity and are supposed to be uncapable of showing reproductive growth (Ziglio et al., 2002). The evolution of viable but non-culturable subpopulation, calculated as the active minus the viable subpopulations, also corroborates this assertion (Fig. S5e–f). It should be also noted that nearly all the total population is active but only around one third is culturable when high concentrations of TiO_2-NPs are used. It is well known that plate-culturing techniques only reveal a small proportion of the total microbial population (Giraffa, 2004) For instance, several authors have reported that it was only possible to recover 5–15% of the total bacteria in sludge, regardless the optimization of the cultural medium (Hammes et al., 2008; Ziglio et al., 2002). Finally, it was also observed that the addition of increasing amounts of TiO_2-NPs did not really correspond to an increased in cell death rate but accelerated the transition to VBNC states. SA was consumed in all assays, showing the metabolic activity associated with the VBNC state. As it was previously observed (Quirós et al., 2007, 2009), VBNC maintain the transport and biosynthesis systems, and are able to metabolize substrates. In our experiments, the cFDA fluorescence intensity was maintained during overall bacterial growth, so it can be considered that bacterial VBNC cells were able to preserve the whole enzymatic activity (Quirós et al., 2007). This can be clearer observed in Supplementary material, Fig. S6, where the SA removal rate per cell is represented. Therefore, the similar specific rates observed for all the TiO_2-NPs concentrations confirms that each non-dead

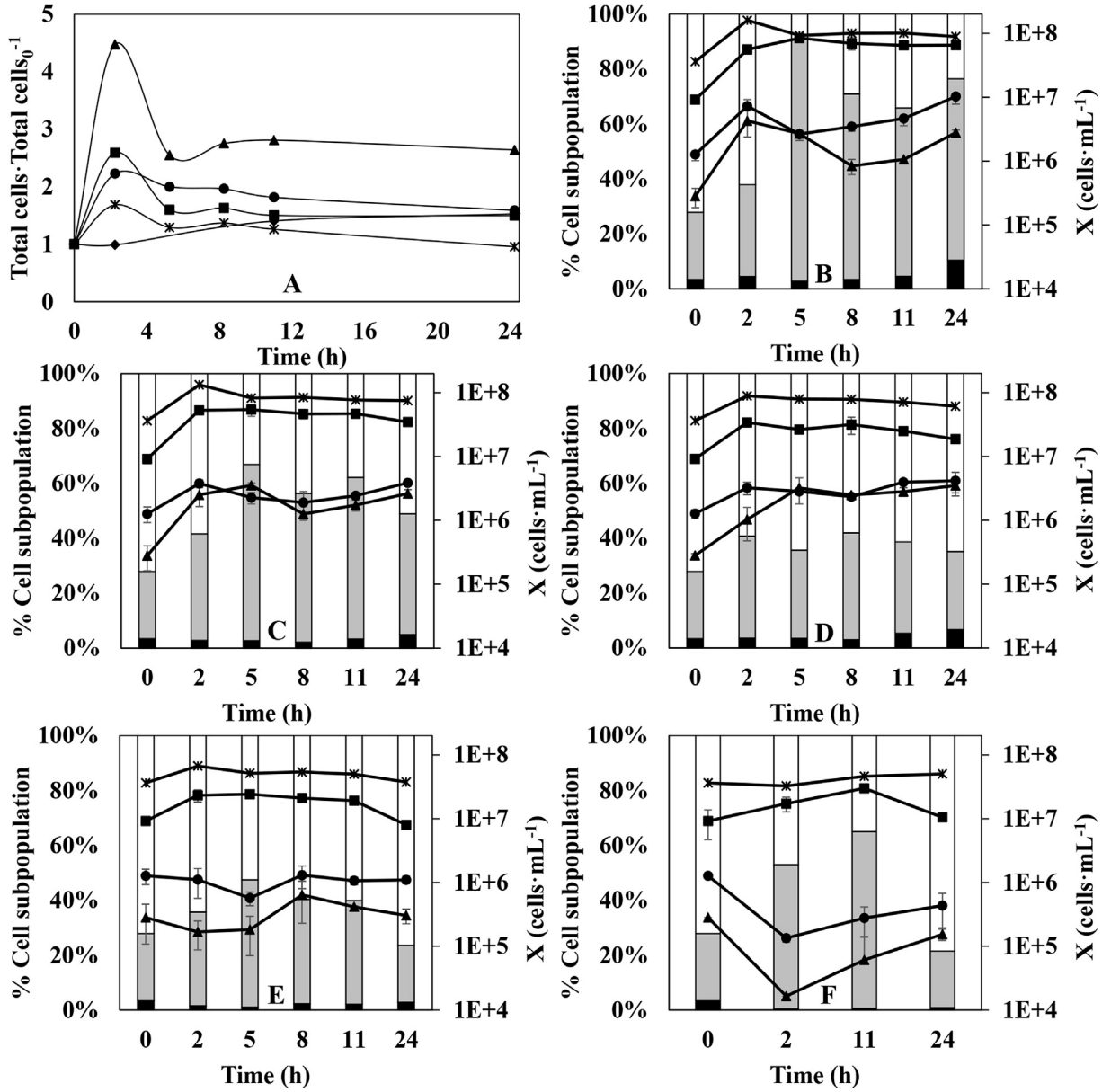

Fig. 3. Total cells concentration (A) (▲ 0 mg mL^{-1}, ■ 0.1 mg mL^{-1}, ● 0.5 mg mL^{-1}, ∗ 1 mg mL^{-1}, ◆ 2 mg mL^{-1}) and evolution of different *P. putida* subpopulation during SA removal with TiO_2-NPs concentration of 0 mg mL^{-1} (B) 0.1 mg mL^{-1} (C), 0.5 mg mL^{-1} (D), 1 mg mL^{-1} (E) and 2 mg mL^{-1} (F). Subpopulation of VBNC cells, ▭ viable cells ▭ and dead cells ■ are plotted as percentage of the total cells counts on the principal y-axis. Metabolically active (∗), viable cells (■), dead cells (●) and damaged cells (▲) are expressed as cells mL^{-1} on the secondary y-axis. In all cases: Initial SA concentration of 500 mg L^{-1}, 250 rpm, 30 °C, *P. putida* inoculum of 10^7 CFU mL^{-1}, 100 mL in 500 mL Erlenmeyer flasks.

bacterium maintained its level of activity.

FSC and SSC were monitored during all SA removal time; both parameters increased with TiO_2 concentration and remained constant with time as in the case of GM (data no shown).

3.2. Segregated kinetic model: proposal and discussion

In order to quantify the SA removal of VBNC cells, experimental data for cell subpopulations and SA uptake were fitted to a segregated kinetic model (Quirós et al., 2007, 2009). For this model, the following assumptions were made:

- The total biomass, formed by viable (C_V), viable but non-culturable plus damaged cells (C_N) and dead cells (C_D), were expressed as bacterial concentrations (g L^{-1}), using the corresponding calibration curves determined previously (dry weight (g L^{-1}) = $8.17 \cdot 10^{-10}$ cells concentration (cells mL^{-1}).
- Viable cells are the cell subpopulation which shows the ability to grow on plates.
- Both viable and non-culturable fractions can lose their integrity, which results in the cellular death. VBNC cells are either not able to recover their "culturability".
- The SA removal was conducted by C_V and C_N

Taking into account the following considerations, the segregated model showed in Fig. 4a can be proposed. Based on this scheme, Equations (1)–(6) can easily be obtained, where r_1 and r_5 are the cell growth rates of viable and VBNC cells, r_2 is the transformation rate from viable to VBNC state, r_3 and r_4 are cell death rates of viable and VBNC cells, τ' and τ'' are the inverses of viable

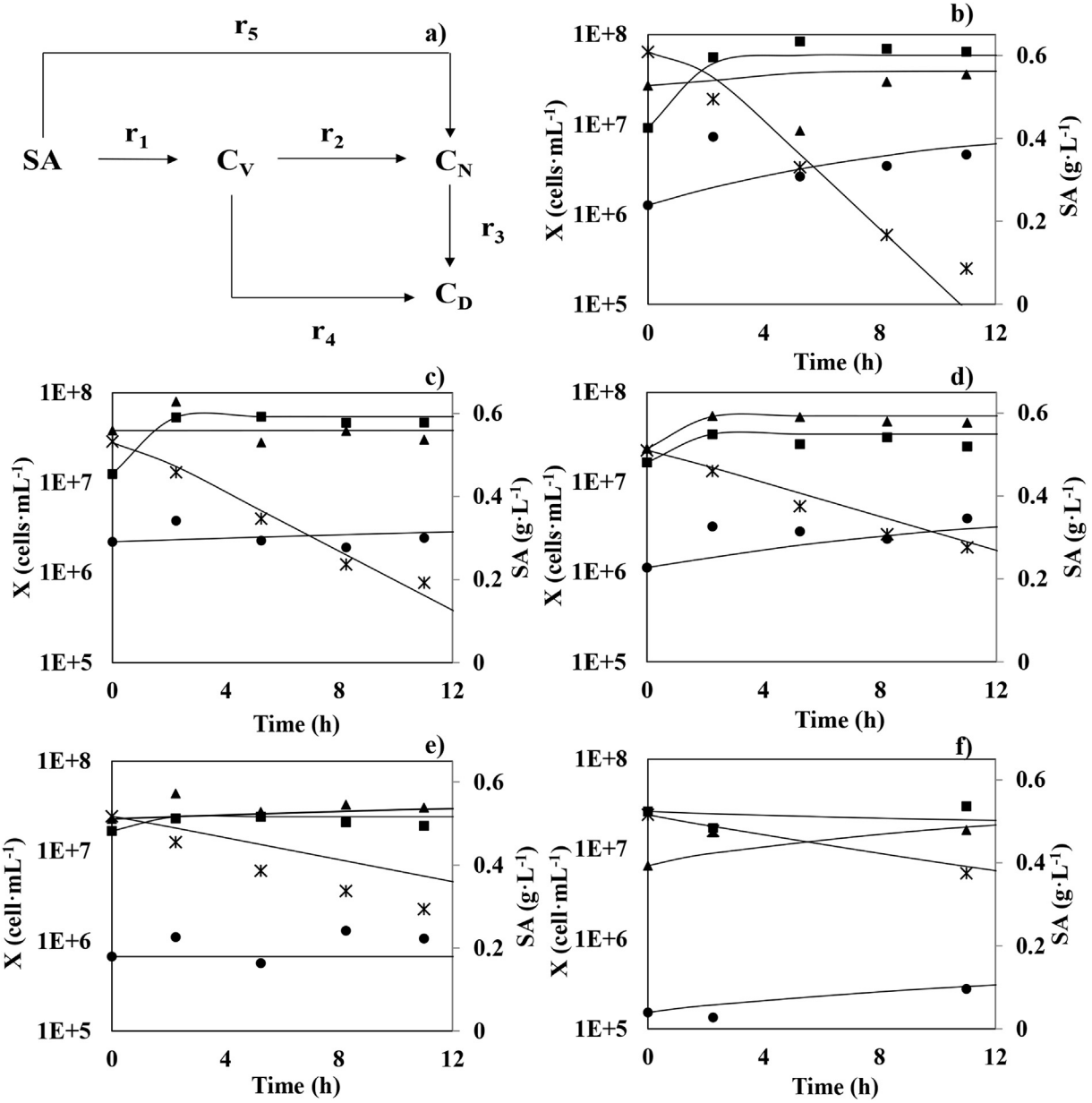

Fig. 4. Segregated kinetic model proposed (a) and evolution of VBNC (▲), viable (■) and dead cells (●) and SA concentration (✳) during the growth of *P. putida* in a SIW and in presence of different concentrations of TiO_2-NPs 0 mg mL^{-1} (b) 0.1 mg mL^{-1} (c), 0.5 mg mL^{-1} (d), 1 mg mL^{-1} (e) and 2 mg mL^{-1} (f). In all the cases: Initial SA concentration of 500 mg L^{-1}, 250 rpm, 30 °C, *P. putida* inoculum of 10^7 CFU mL^{-1}, 100 mL in 500 mL Erlenmeyer flask.

and VBNC cell concentrations in stationary phase, and q_V and q_N are the specific SA uptake rates for viable and VBNC subpopulations, respectively.

$$r_1 = k_1 \cdot C_V \cdot (1 - \tau' \cdot C_V) \quad (1)$$

$$r_2 = k_2 \cdot C_V \quad (2)$$

$$r_3 = k_3 \cdot C_N \quad (3)$$

$$r_4 = k_4 \cdot C_V \quad (4)$$

$$r_5 = k_5 \cdot C_N \cdot \left(1 - \tau'' \cdot C_N\right) \quad (5)$$

$$-\frac{dSA}{dt} = q_V \cdot C_V + q_N \cdot C_N \quad (6)$$

Equations (1)–(6) were fitted to experimental data from cell counting by flow cytometry and plate counting using *MicroMath Scientist® version 2.0*. Fig. 4 shows experimental and predicted data for *P. putida* growth curves and SA uptake with different concentrations of TiO_2-NPs. The value of the different kinetic parameters calculated for the proposed segregated kinetic model are collected in Table 1.

The model considering the growth of both viable and VBNC subpopulations provided a proper description of bacterial

Table 1
Kinetics parameters obtained for the segregated kinetic model proposed for *P. putida* growth and salicylic acid consumption in presence of TiO_2-NPs concentrations ranging from 0 to 2 mg mL^{-1}.

TiO_2 (mg mL^{-1})	k_1 (h^{-1})	k_2 (h^{-1})	k_3 (h^{-1})	k_4 (h^{-1})	k_5 (h^{-1})	q_V gSA (h gC_V)$^{-1}$	q_N gSA (h gC_N)$^{-1}$	τ' (L g^{-1})	τ'' (L g^{-1})
0	0.047	0.009	$1.2\cdot10^{-6}$	$3.0\cdot10^{-7}$	0.027	0.95	0.070	14.5	11.8
0.1	0.045	0.035	$1.4\cdot10^{-6}$	$1.9\cdot10^{-7}$	0.049	0.8	0.065	22.5	15.3
0.5	0.037	0.043	$3.3\cdot10^{-6}$	$3.3\cdot10^{-7}$	0.052	0.73	0.061	35.7	22.4
1	0.031	0.054	$3.7\cdot10^{-6}$	$1.4\cdot10^{-7}$	0.069	0.67	0.054	50.6	28.0
2	0.041	0.032	$1.5\cdot10^{-6}$	$1.6\cdot10^{-7}$	0.025	0.6	0.045	40.9	25.7

populations, as well as carbon source uptake (Quirós et al., 2007).

As can be seen in Table 1, the growth kinetic constant for viable bacteria is higher than their transformation kinetic constant into non-culturable cells ($k_1 > k_2$) for the experiment without nanoparticles. In addition, these non-culturable bacteria are mainly generated from division of others non-culturable bacteria, instead of from the viable cells which has loosen their capacity to growth in plate ($k_5 > k_2$). The increase in the TiO_2-NPs concentration leads to higher values of k_5 and k_2 and lower values of k_1. These findings indicate that nanoparticles had a negative effect on the viable subpopulation growth (k_1) but a positive effect on the viable but non-culturable cells formation rate, increasing their generation beginning from either the own multiplication (k_5) or the culturability loss of viable cells (k_2). In addition, when are compared with the others constants, the values of k_3 and k_4 were no significant, indicating that death reactions were a lot slower than the rest of the proposed ones.

Finally, q_V and q_N values can be used to discuss the effects of TiO_2-NPs on the *P. putida* capacity to degrade SA. In absence of nanoparticles, the specific degradative capacity for the viable subpopulation was far higher than for the viable but non-culturable subpopulation. This suggests that the entrance of viable cells into the VBNC state can be also accompanied by a reduction in substrate transport and metabolic activity levels in order to minimize cellular energetic requirements (Bogosian and Bourneuf, 2001; Quirós et al., 2007, 2009). A similar behaviour has been observed for non-culturable *Lactobacillus higardii* in response to SO_2 presence (Quirós et al., 2009). The presence of TiO_2-NPs reduced appreciably specific SA uptake rates for viable and VBNC subpopulations. So, qv in the SIW ranged from 0.9 gSA (h gCV)$^{-1}$ in absence of nanoparticles to 0.6 gSA (h gCV)$^{-1}$ when the concentration was 2 mg mL^{-1}. Interestingly, the q_V/q_N ratio kept approximately constant, at a value close to 12.7, suggesting that the inhibitory effect of the nanoparticles is similar for both subpopulations.

4. Conclusions

In this work, FC technique allows the study of the TiO_2-NPs effect on the physiological state of the *P. putida*. The increase of TiO_2-NPs concentrations meant a decrease of the total cell concentrations in the medium, a change in the physiological state of the bacteria was also observed since viable cells (CFU mL^{-1}) became VBNC cells. However, significant increases in the damaged or dead cells concentration were not produced. Using FC technique, FSC and SSC parameters were also measured, obtaining, in this case, an increase of both parameters with higher TiO_2-NPs concentration, which is due to NPs uptake in bacteria.

The viable cells transformation into VBNC cells affects the SA biodegradation since the metabolic capacity of VBNC cells is generally lower than that of viable cells. Finally, a segregated model including viable, VBNC and dead bacteria was fitted to the experimental data obtaining the growth and removal constants for each subpopulation.

Acknowledgements

R.G. Combarros wishes to express gratitude for a research grant from the Government of the Principality of Asturias (Severo Ochoa Programme).

Appendix A. Supplementary data

Supplementary data related to this article can be found at http://dx.doi.org/10.1016/j.watres.2015.12.040.

References

Amor, K.B., Breeuwer, P., Verbaarschot, P., Rombouts, F.M., Akkermans, A.D.L., De Vos, W.M., Abee, T., 2002. Multiparametric flow cytometry and cell sorting for the assessment of viable, injured, and dead bifidobacterium cells during bile salt stress. Appl. Environ. Microbiol. 68, 5209–5216. http://dx.doi.org/10.1128/aem.68.11.5209-5216.2002.

Anil, K., Zaidi, M.G.H., 2010. Implications of SPION and NBT nanoparticles upon in vitro and in situ biodegradation of LDPE film. J. Microbiol. Biotechnol. 20 http://dx.doi.org/10.4014/jmb.0912.12026.

Besinis, A., De Peralta, T., Handy, R.D., 2014. The antibacterial effects of silver, titanium dioxide and silica dioxide nanoparticles compared to the dental disinfectant chlorhexidine on *Streptococcus mutans* using a suite of bioassays. Nanotoxicology 8, 1–16. http://dx.doi.org/10.3109/17435390.2012.742935.

Bogosian, G., Bourneuf, E.V., 2001. A matter of bacterial life and death EMBO. Reports 2, 770–774. http://dx.doi.org/10.1093/embo-reports/kve182.

Bonnefond, A., González, E., Asua, J.M., Leiza, J.R., Kiwi, J., Pulgarin, C., Rtimi, S., 2015. New evidence for hybrid acrylic/TiO_2 films inducing bacterial inactivation under low intensity simulated sunlight. Colloids Surfaces B Biointerfaces 135, 1–7. http://dx.doi.org/10.1016/j.colsurfb.2015.07.034.

Collado, S., Rosas, I., González, E., Gutierrez-Lavin, A., Diaz, M., 2014. *Pseudomonas putida* response in membrane bioreactors under salicylic acid-induced stress conditions. J. Hazard. Mater. 267, 9–16. http://dx.doi.org/10.1016/j.jhazmat.2013.12.034.

Combarros, R.G., Collado, S., Laca, A., Díaz, M., 2015a. Conditions and mechanisms in thiocyanate biodegradation. J. Residuals Sci. Technol. 12.

Combarros, R.G., Collado, S., Laca, A., Díaz, M., 2015b. Understanding the simultaneous biodegradation of thiocyanate and salicylic acid by *Paracoccus thiocyanatus* and *Pseudomonas putida*. Int. J. Environ. Sci. Technol. http://dx.doi.org/10.1007/s13762-13015-10906-y (in press), ISSN: 1735-1472.

Combarros, R.G., Rosas, I., Lavín, A.G., Rendueles, M., Díaz, M., 2014. Influence of biofilm on activated carbon on the adsorption and biodegradation of salicylic acid in wastewater. Water Air Soil Pollut. 225, 1–12. http://dx.doi.org/10.1007/s11270-013-1858-9.

Cho, M., Chung, H., Choi, W., Yoon, J., 2004. Linear correlation between inactivation of *E. coli* and OH radical concentration in TiO_2 photocatalytic disinfection. Water Res. 38, 1069–1077. http://dx.doi.org/10.1016/j.watres.2003.10.029.

Díaz, M., Herrero, M., García, L.A., Quirós, C., 2010. Application of flow cytometry to industrial microbial bioprocesses. Biochem. Eng. J. 48, 385–407. http://dx.doi.org/10.1016/j.bej.2009.07.013.

Erdural, B., Bolukbasi, U., Karakas, G., 2014. Photocatalytic antibacterial activity of TiO_2–SiO_2 thin films: the effect of composition on cell adhesion and antibacterial activity. J. Photochem. Photobiol. A Chem. 283, 29–37. http://dx.doi.org/10.1016/j.jphotochem.2014.03.016.

Fu, G., Vary, P.S., Lin, C.-T., 2005. Anatase TiO_2 nanocomposites for antimicrobial coatings. J. Phys. Chem. B 109, 8889–8898. http://dx.doi.org/10.1021/jp0502196.

Gelover, S., Gómez, L.A., Reyes, K., Teresa Leal, M., 2006. A practical demonstration of water disinfection using TiO_2 films and sunlight. Water Res. 40, 3274–3280. http://dx.doi.org/10.1016/j.watres.2006.07.006.

Ghosh, M., J, M., Sinha, S., Chakraborty, A., Mallick, S.K., Bandyopadhyay, M., Mukherjee, A., 2012. In vitro and in vivo genotoxicity of silver nanoparticles. Mutat. Research/Genetic Toxicol. Environ. Mutagen. 749, 60–69. http://dx.doi.org/10.1016/j.mrgentox.2012.08.007.

Giraffa, G., 2004. Studying the dynamics of microbial populations during food fermentation. FEMS Microbiol. Rev. 28, 251–260. http://dx.doi.org/10.1016/

j.femsre.2003.10.005.
Hammes, F., Berney, M., Wang, Y., Vital, M., Köster, O., Egli, T., 2008. Flow-cytometric total bacterial cell counts as a descriptive microbiological parameter for drinking water treatment processes. Water Res. 42, 269–277. http://dx.doi.org/10.1016/j.watres.2007.07.009.
Hsu, Y.-C., Yang, H.-C., Chen, J.-H., 2004. The enhancement of the biodegradability of phenolic solution using preozonation based on high ozone utilization. Chemosphere 56, 149–158. http://dx.doi.org/10.1016/j.chemosphere.2004.02.011.
Ju-Nam, Y., Lead, J.R., 2008. Manufactured nanoparticles: an overview of their chemistry, interactions and potential environmental implications. Sci. Total Environ. 400, 396–414. http://dx.doi.org/10.1016/j.scitotenv.2008.06.042.
Kapri, A., Zaidi, M.G.H., Goel, R., 2009. Nanobarium titanate as supplement to accelerate plastic waste biodegradation by indigenous bacterial consortia. AIP Conf. Proc. 1147, 469–474. http://dx.doi.org/10.1063/1.3183475.
Kuang, Y., Zhou, Y., Chen, Z., Megharaj, M., Naidu, R., 2013. Impact of Fe and Ni/Fe nanoparticles on biodegradation of phenol by the strain Bacillus fusiformis (BFN) at various pH values. Bioresour. Technol. 136, 588–594. http://dx.doi.org/10.1016/j.biortech.2013.03.018.
Kumar, A., Pandey, A.K., Singh, S.S., Shanker, R., Dhawan, A., 2011. A flow cytometric method to assess nanoparticle uptake in bacteria. Cytom. Part A 79A, 707–712. http://dx.doi.org/10.1002/cyto.a.21085.
Le, T., Murugesan, K., Kim, E.-J., Chang, Y.-S., 2014. Effects of inorganic nanoparticles on viability and catabolic activities of Agrobacterium sp. PH-08 during biodegradation of dibenzofuran. Biodegradation 25, 655–668. http://dx.doi.org/10.1007/s10532-014-9689-y.
Li, B., Huang, W., Zhang, C., Feng, S., Zhang, Z., Lei, Z., Sugiura, N., 2015. Effect of TiO_2 nanoparticles on aerobic granulation of algal–bacterial symbiosis system and nutrients removal from synthetic wastewater. Bioresour. Technol. 187, 214–220. http://dx.doi.org/10.1016/j.biortech.2015.03.118.
Li, D., Cui, F., Zhao, Z., Liu, D., Xu, Y., Li, H., Yang, X., 2014. The impact of titanium dioxide nanoparticles on biological nitrogen removal from wastewater and bacterial community shifts in activated sludge. Biodegradation 25, 167–177. http://dx.doi.org/10.1007/s10532-013-9648-z.
Neal, A., 2008. What can be inferred from bacterium–nanoparticle interactions about the potential consequences of environmental exposure to nanoparticles? Ecotoxicology 17, 362–371. http://dx.doi.org/10.1007/s10646-008-0217-x.
Quirós, C., Herrero, M., García, L.A., Díaz, M., 2007. Application of flow cytometry to segregated kinetic modeling based on the physiological states of m isms. Appl. Environ. Microbiol. 73, 3993–4000. http://dx.doi.or AEM.00171-07.
Quirós, C., Herrero, M., García, L.A., Díaz, M., 2009. Quantitative approach to determining the contribution of viable-but-nonculturable subpopulations to malolactic fermentation processes. Appl. Environ. Microbiol. 75, 2977–2981. http://dx.doi.org/10.1128/AEM.01707-08.
Rawat, J., Rana, S., Srivastava, R., Misra, R.D.K., 2007. Antimicrobial activity of composite nanoparticles consisting of titania photocatalytic shell and nickel ferrite magnetic core. Mater. Sci. Eng. C 27, 540–545. http://dx.doi.org/10.1016/j.msec.2006.05.021.
Rincón, A.-G., Pulgarin, C., 2007. Absence of *E. coli* regrowth after Fe3+ and TiO_2 solar photoassisted disinfection of water in CPC solar photoreactor. Catal. Today 124, 204–214. http://dx.doi.org/10.1016/j.cattod.2007.03.039.
Toduka, Y., Toyooka, T., Ibuki, Y., 2012. Flow cytometric evaluation of nanoparticles using side-scattered light and reactive oxygen species-mediated fluorescence–correlation with genotoxicity. Environ. Sci. Technol. 46, 7629–7636. http://dx.doi.org/10.1021/es300433x.
Ziglio, G., Andreottola, G., Barbesti, S., Boschetti, G., Bruni, L., Foladori, P., Villa, R., 2002. Assessment of activated sludge viability with flow cytometry. Water Res. 36, 460–468. http://dx.doi.org/10.1016/S0043-1354(01)00228-7.
Zucker, R.M., Massaro, E.J., Sanders, K.M., Degn, L.L., Boyes, W.K., 2010. Detection of TiO_2 nanoparticles in cells by flow cytometry. Cytom. Part A 77A, 677–685. http://dx.doi.org/10.1002/cyto.a.20927.

Supplementary material to

'Toxicity of titanium dioxide nanoparticles on *Pseudomonas putida*

Combarros, R.G., Collado, S., Díaz, M*

Department of Chemical Engineering and Environmental Technology,

University of Oviedo, C/Julián Clavería s/n, E-33071, Oviedo, Spain

(7 Pages, 5 Figures, 1 Table)

Table of contents

*Corresponding author's e-mail: mariodiaz@uniovi.es
Phone: +34 985 10 34 39; Fax: +34 985 10 34 34

Table S 1: Composition of growth medium and simulated industrial medium using in cell viability test

GM	SIW
5 gL^{-1} peptone	0.5 gL^{-1} K_2HPO_4
3 gL^{-1} beef	0.3 gL^{-1} $(NH_4)_2SO_4$
0.422 gL^{-1} KH_2PO_4	0.05 gL^{-1} $MgSO_4 \cdot 7H_2O$
0.375 gL^{-1} K_2HPO_4	0.01 gL^{-1} $FeCl_3 \cdot 6H_2O$
0.244 gL^{-1} $(NH_4)_2SO_4$	0.01 gL^{-1} $CaCl_2 \cdot 2H_2O$
0.05 gL^{-1} $MgSO_4 \cdot 7H_2O$	0.05 gL^{-1} triptone
0.054 gL^{-1} $C_6H_{11}FeNO_7$	10 mL^{-1} of trace solution
0.015 gL^{-1} $CaCl_2 \cdot 2H_2O$	500 mgL^{-1} salicylic acid (SA)
0.015 gL^{-1} NaCl	

The trace solution was composed of 8 mgL^{-1} $ZnSO_4 \cdot 7H_2O$, 4 mgL^{-1} H_3BO_3, 4 mgL^{-1} Na_2MoO_4 $2H_2O$, 4 mgL^{-1} $CuSO_4 \cdot 5H_2O$, 4 mgL^{-1} $MnCl_2 \cdot 4H_2O$, 4 mgL^{-1} $CoCl_2$ $6H_2O$ [202]

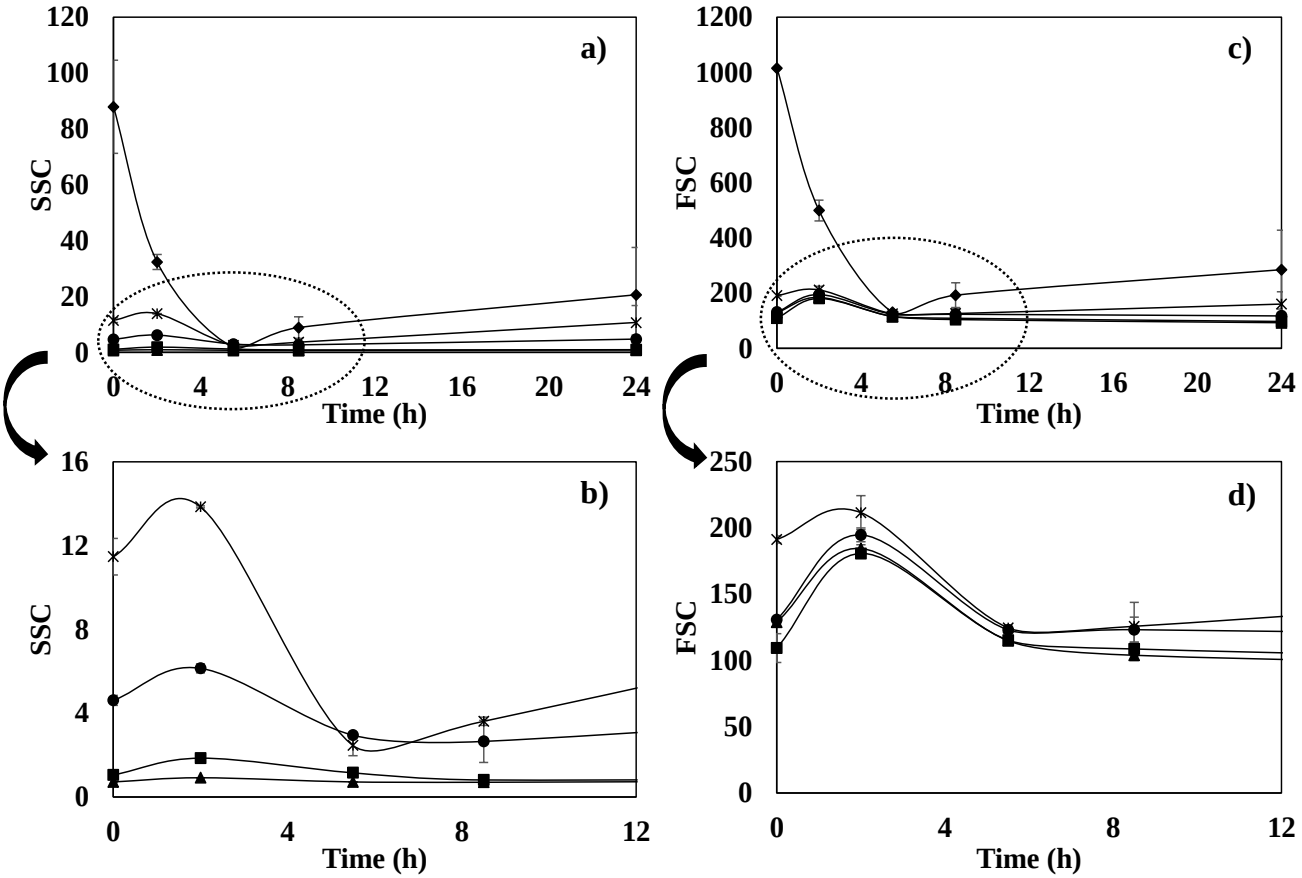

Figure S 1: Evolution of SSC (a-b) and FSC (c-d) signals for *P. putida* cultivation in GM in presence of different concentrations of suspended TiO2- NPs: 0 $mgmL^{-1}$ (▲), 0.1 $mgmL^{-1}$ (■), 0.5 $mgmL^{-1}$ (•), 1 $mgmL^{-1}$ (✳), 2 $mgmL^{-1}$ (◆). The circles indicate the area magnified in image 2b and 2d. In all cases: initial SA concentration of 100 mgL^{-1}, 200 rpm, 30ºC, *P. putida* inoculum of 10^7 $CFUmL^{-1}$, 100 mL in 250 mL Erlenmeyer flasks.

The gates for each physiological state selected in the antibacterial study are shown in fig. S3. The multiparametric analysis permitted the distinction between different population with dual parameter dot plots: cFDA-stained cells (metabolically active), PI-stained cells (dead cells), and cFDA-PI stained cells (dual-stained, intermediate populations considered damage)

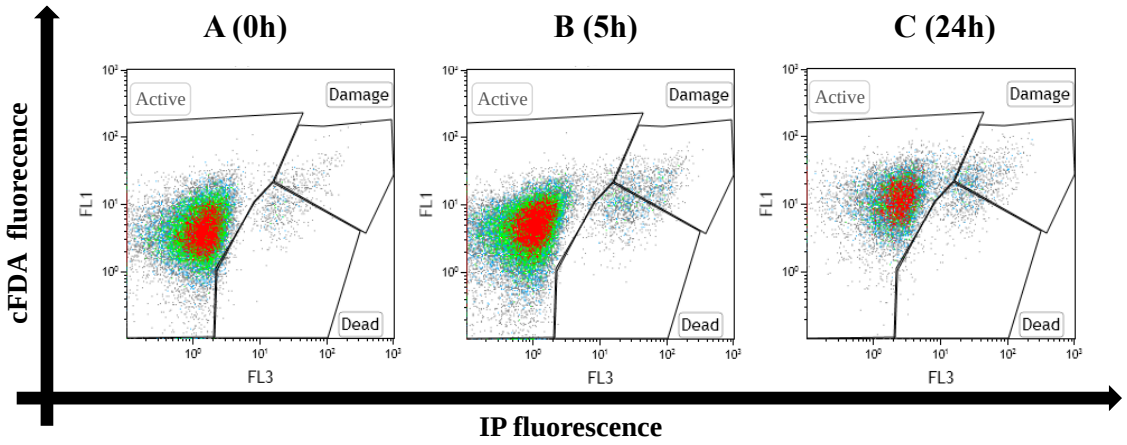

Figure S 2: Dot plots representing cFDA fluorescence versus PI fluorescence for *P. putida* during shake-flask cultivation in SIW with 0.5 $mgmL^{-1}$ of TiO_2. A, B and C plots correspond to 0, 5 and 24 hours respectively. In all cases, initial SA concentration of 500 mg L^{-1} 250 rpm, 30ºC, *P. putida* inoculum of 10^7 $CFUmL^{-1}$, 100 mL in 500 mL Erlenmeyer flasks.

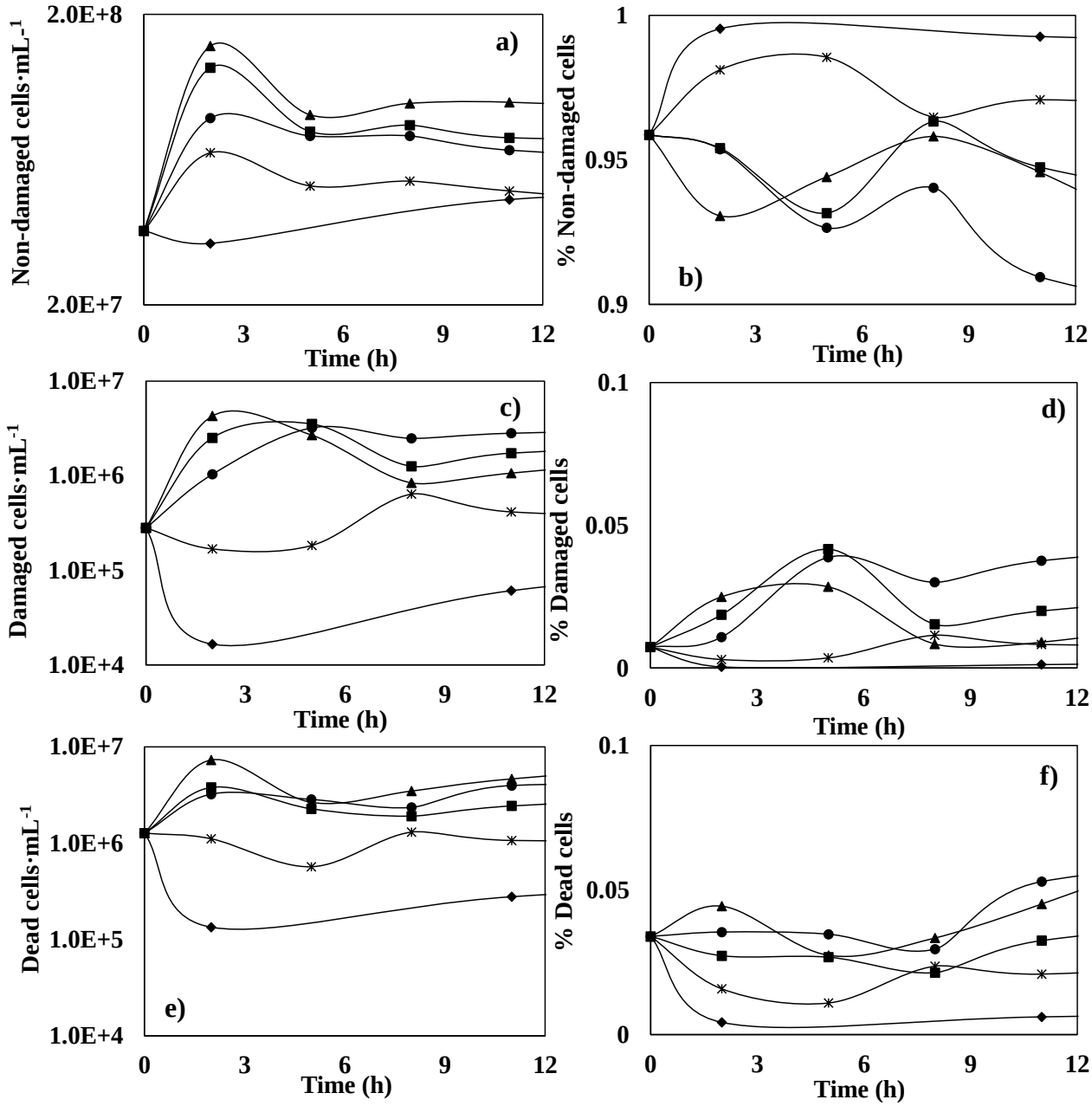

Figure S 3: Evolution of different *P. putida* subpopulation during SA removal under TiO_2-NPs concentrations of 0 $mgmL^{-1}$ (▲), 0.1 $mgmL^{-1}$ (■), 0.5 mgmL-1 (•), 1 $mgmL^{-1}$ (✳), 2 $mgmL^{-1}$ (◆). Total non-damaged cells·mL^{-1} (a) and percentage of non-damaged cells (b), total damaged cells·mL^{-1} (c) and percentage of damaged cells (d) and total dead cells·mL^{-1} (e) and percentage of dead cells (f). In all cases, initial SA concentration of 500 mgL^{-1}, 250 rpm, 30ºC, *P. putida* inoculum of 10^7 $CFUmL^{-1}$, 100 mL in 500 mL Erlenmeyer flasks.

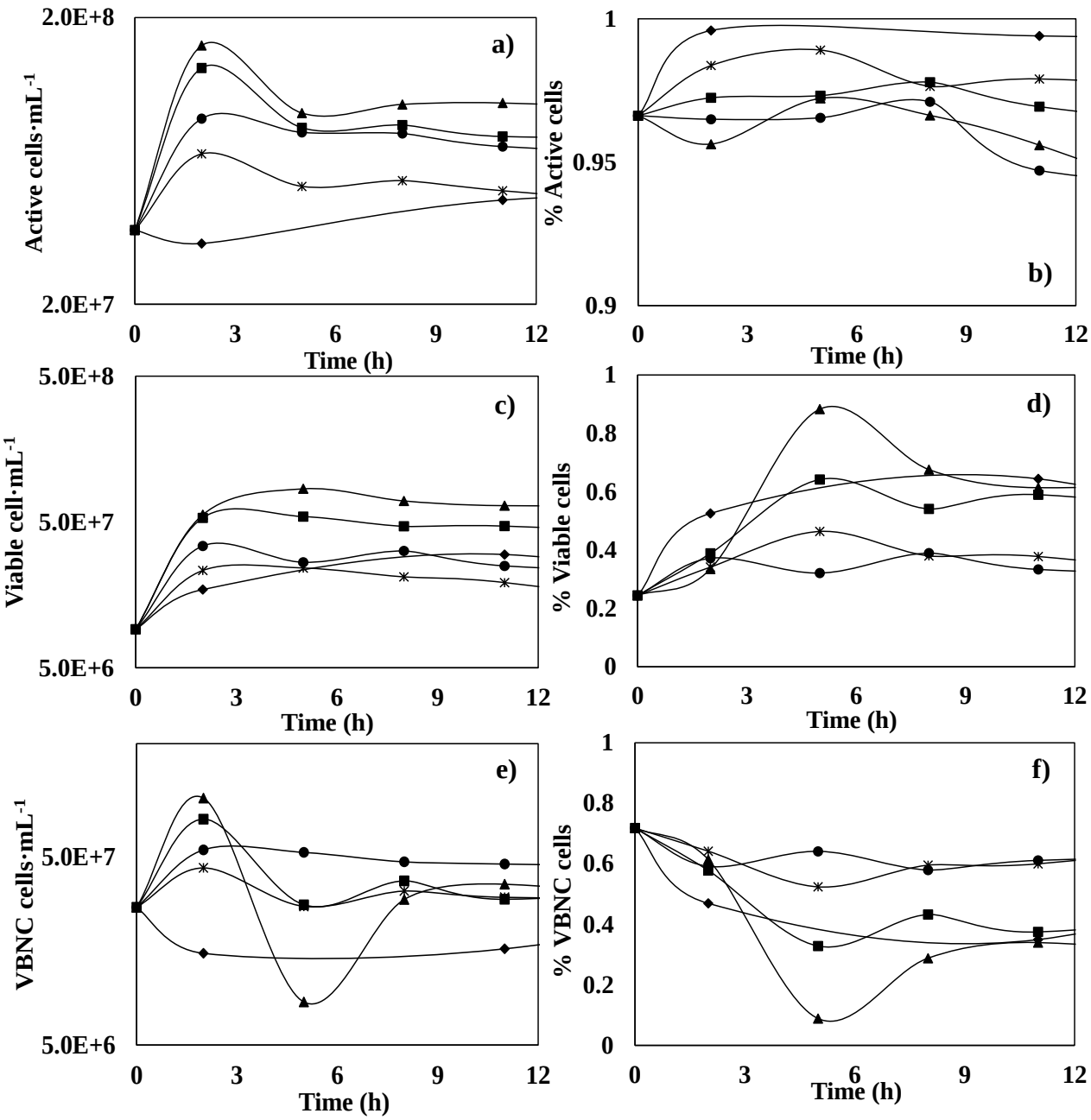

Figure S 4: Evolution of different *P. putida* subpopulation during SA removal under TiO_2-NPs concentrations of 0 $mgmL^{-1}$ (▲), 0.1 $mgmL^{-1}$ (■), 0.5 $mgmL^{-1}$ (•), 1 $mgmL^{-1}$ (✳), 2 $mgmL^{-1}$ (◆). Total active cells·mL^{-1} (a) and percentage of active cells (b), total viable cells·mL^{-1} (c) and percentage of viable cells (d) and total VBNC cells·mL^{-1} (e) and percentage of VBNC cells (f). In all cases, initial SA concentration of 500 mgL^{-1}, 250 rpm, 30ºC, *P. putida* inoculum of 107 $CFUmL^{-1}$, 100 mL in 500 mL Erlenmeyer flasks.

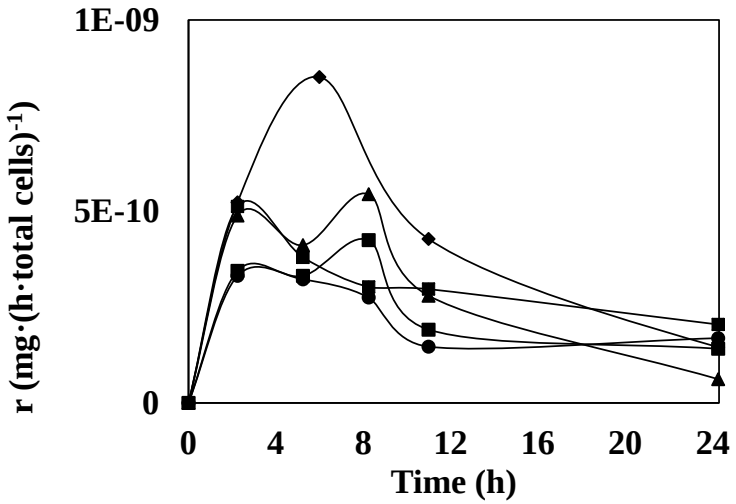

Figure S 5: Specific biodegradation rates observed during the *P. putida* biodegradation of 500 mgL^{-1} SA as sole carbon source in a SIW at different TiO_2-NPs concentrations: 0 $mgmL^{-1}$ (▲), 0.1 $mgmL^{-1}$ (■), 0.5 $mgmL^{-1}$ (●), 1 $mgmL^{-1}$ (✳), 2 $mgmL^{-1}$ (◆). In all cases: 250 rpm, 30ºC, *P. putida* inoculum of 10^7 $CFUmL^{-1}$, 100 mL in 500 mL Erlenmeyer flasks

5.3. Toxicidad por nanopartículas de óxido de grafeno sobre el estado metabólico de *Pseudomonas putida* y la biodegradación del ácido salicílico

En el presente apartado se ha llevado a cabo un análisis de toxicidad de nanopartículas de óxido de grafeno sobre la viabilidad y la actividad metabólica de la bacteria *Pseudomonas putida*. Se ha seleccionado el óxido de grafeno debido a su cada vez mayor consumo y producción en varios ámbitos industriales. Además, se ha considerado nuevamente el cultivo puro de *P. putida* como un modelo sencillo de lodos activos.

La técnica citometría de flujo multiparamétrica ha sido utilizada en la monitorización y control de la respuesta del estado fisiológico de la bacteria en presencia de diferentes concentraciones de óxido de grafeno. Se ha empleado una tinción dual PI-cFDA para la distinción de los diferentes estados fisiológicos de la bacteria.

En el artículo que se presenta a continuación, se estudia cómo la presencia de distintas concentraciones de nanopartículas de óxido de grafeno afectan a la respuesta fisiológica y metabólica de la bacteria *Pseudomonas putida* bajo dos condiciones de cultivo diferentes. La primera corresponde a un agua con fuente adicional de carbono y nitrógeno fácilmente asimilables, representando un agua residual urbana; la segunda, se trata de un medio mineral mínimo que simula un agua residual industrial contaminado por ácido salicílico. En este caso, se ha comprobado además la interacción bacteria-óxido de grafeno mediante el uso de imágenes obtenidas con el microscopio electrónico de barrido.

Los resultados de este trabajo se presentan a través de una publicación cuya referencia y status se muestran a continuación.

Referencia: Combarros, R.G, Collado, S., Díaz, M. Toxicity of graphene oxide on growth and metabolism of *Pseudomonas putida*.

Estado: Enviado en Octubre del 2015, bajo revisión.

Toxicity of graphene oxide on growth and metabolism of *Pseudomonas putida*

Combarros, R.G. [a], Collado, S. [a], Díaz, M* [a].
[a] Department of Chemical and Environmental Technology.
University of Oviedo, Spain.
* Tel: 985 10 34 39. Fax: 985103434. E-mail: mariodiaz@uniovi.es

Abstract

The increasing consumption of graphene derivatives drives to the higher occurrence of these materials on wastewater treatment plants and ecological systems. The toxicity effect of graphene oxide (GO) on the microbial functions related to t biological wastewater treatment process is studied, using *Pseudomonas putida* and salicylic acid (SA) as bacterial and pollutant models,. A multiparametric flow cytometry method (PI/cFDA) has been developed to measure the metabolic activity and viability of *P. putida* in contact with GO. A continuous reduction in the percentages of viable cells and a slight increase, lower than 5%, in the percentages of damaged and dead cells, suggest that *P. putida* in contact with GO loses the membrane integrity but preserves the metabolic activity. The growth of *P. putida* was strongly inhibited by GO, so 0.05 $mgmL^{-1}$ of GO reduced by a third the maximum growth, becoming critical for GO concentrations higher than 0.1 $mgmL^{-1}$. The specific SA removal rate decreased with GO concentration up to 0.1 $mgmL^{-1}$ indicating that while GO always reduces the *P. putida* growth, for concentrations higher than 0.1 $mgmL^{-1}$, it also reduces its activity. Similar behaviors are observed using simulated urban and industrial wastewaters, giving more acute effects on the industrial one.

Keywords: Antimicrobial activity; Flow cytometry; Graphene oxide; Metabolic activity; *Pseudomonas putida*.

1. Introduction

Graphene oxide (GO) is a promising precursor to produce graphene-family nanomaterials for various applications like field effect transistors, solar cells, sensors, lithium ion batteries, solar cells, and electrochemical super capacitors and a strong adsorbent for heavy metal removal [25, 26, 120]. However, the current mass production of GO supposes higher probabilities of presence of these compounds in the environment, so their potential health effect and environmental impacts need a good understanding [25, 26].

In this sense, the literature provides an increasing number of studies about the toxicities, environmental behaviors and ecotoxicities of these materials [25, 29, 119, 121]. Nevertheless, not much research has been conducted on their effect on biological wastewater treatments, even when the occurrence of these materials is becoming increasingly common in either urban or industrial wastewaters [29]. Taking into account

that wastewater treatment plants are usually the last barrier before a wastewater is discharged into the environment, it is obviously important to understand the effects of these nanomaterials on the biotreatment process.

In most of the works in which the interaction of the GO with bacteria are studied, the GO are in paper form [26, 122, 128, 130, 213]. Despite the dissimilar degrees of inhibition reported in these papers, one can concluded two facts. The first of them is that bacterial inactivation caused by OG is mainly due to oxidative stress, cutting of intracellular metabolic routes and/ or rupture of cell membrane, [119, 122-127]. The second one is the high effect of some physicochemical characteristics, such as GO concentration, incubation time, orientation of nanomaterial, type of bacteria (Gram - or Gram +), medium, light sources … on the degrees of inhibition [25, 26, 119, 120, 122, 125-130].

Due to the high number of variables involved, pure cultures instead of sludge are usually selected for studies dealing with GO-bacterium interactions, in order to accelerate and amplify the response of the system to perturbations. The species most widely used in this kind of publications is *Escherichia coli* [25, 26, 120, 122]. To the best of our knowledge, there are not studies dealing with the effects of graphene oxide on *Pseudomonas putida*, even when this species is the predominant one in activated sludge.

Another characteristic observed after the bibliographic review is that the degrees of inhibition are calculated on the basis of microorganism death measurements, which are usually obtained by means of PI staining showing and confocal microscopy [123], drop-test based on measuring of $CFUmL^{-1}$ [25, 120, 125, 129, 130, 146], or free RNA or DNA analysis [122, 125]. Nevertheless, these methods do not take into account those bacteria whose activity decreases in presence of graphene oxide, but not their viability. In this regard, the application of simultaneous staining of the bacteria with different fluorochromes combined with flow cytometry has increased its presence in recent years as an extremely powerful way to demonstrate the physiological heterogeneity. As far as is known, this technique has not been previously employed for monitoring the effects of GO on the activity and viability of any bacteria.

Taking into account all these considerations, the aim of the present work is to study, for the first time, the effect of different concentrations of GO on the viability and activity of *P. putida*, considering this species as a simplified model of an activated sludge biotreatment. For this purpose, a multiparametric cytometric method based on a dual PI/ cFDA staining has been developed and used to establish the evolution of the physiological states of *P. putida* (viable, damage and dead cell subpopulations).

2. Materials and methods

2.1. GO characteristics

The GO was supplied by INCAR-CSIC, from Oviedo, Spain. The GO physicochemical characteristics and the method of preparation appear in [214-216] (Fig. S6).

2.2. Cell preparation

A previously isolated *Pseudomonas putida* (Leibniz Institute DSMZ-German Collection of Microorganism and Cells Cultures, Germany (DSM 4478)), was chosen. Initially, *P. putida* colonies, were grown in growth medium agar for 1 day at 30 ºC, and then inoculated into 250 ml Erlenmeyer flasks containing 100 mL of growth medium [217]. After incubation (30 ºC, 150 rpm, 16 h), aliquots were centrifuged at 10160 x g for 10 minutes, removing the supernatants. So, only bacterial cells were added as inoculum to the corresponding simulated wastewaters, avoiding the introduction of compounds from the growth medium to the simulated wastewaters.

2.3. Cell viability test

The effects of GO on the activity and viability of *P. putida* were studied using two different media, simulating two possible wastewaters during the biological treatment. The first one is a rich culture medium, with a carbon and a nitrogen source easily assimilable, as model of an easily biodegradable urban wastewater. The composition of the second one, a minimum mineral medium only supplemented with 500 mgL^{-1} of salicylic acid, was selected in order to simulate a moderately biodegradable industrial wastewater. The detailed composition of both media can be consulted in table S2 (see supplementary data).

For both simulated wastewaters, the different initial GO concentrations selected were 0, 0.05, 0.1, 0.25, 0.5 and 1 $mgmL^{-1}$, these values being similar to those found in other previous studies [121]. In the simulated municipal wastewater the culture conditions were 200 rpm and 30 ºC in 250 mL Erlenmeyer flasks containing 100 mL of simulated medium [217]. While, for the simulated industrial wastewater, the culture conditions were 250 rpm and 30 ºC and 100 mL of simulated medium in 500 mL Erlenmeyer flasks [202]. The higher volume and stirring speed selected in the case of SIW were chosen in order to improve the adaptation and growth of bacteria in this medium. All material and media were autoclaved at 121ºC for 20 min in order to maintain the sterility of the system. Either GO or SA were sterilized separately. In all cases, initial *P. putida* concentration were of around 10^7 $CFUmL^{-1}$. The system GO-growth medium without bacteria was sonicated for 3 min to detach the aggregated graphene sheets. Once *P. putida* was inoculated in the media, contact GO-bacteria was maintained for 24 h in an incubator New Brunswick Scientific (Edison, New York) that kept constant the culture conditions, taking samples

at different times (0,3,6,8,11 and 24 h). For each one of them, optical density (DO), $CFUmL^{-1}$, pH, SA concentration and metabolic viability and activity were analysed.

The initial pH values for SUW media were adjusted in the range of 6.90±0.045 reaching a final pH of 8.60±0.22 in all cases. For SIW media, the initial pH of the system was 7.4 ± 0.09 and the final one was 7.9 ± 0.35.

In order to check a possible effect of the light on the biodegradation process, experiments with 0, 0.1 and 0.5 $mgmL^{-1}$ of GO in the medium were repeated, covering the Erlenmeyer flask with aluminium paper to keep out light [218]. Additionally, experiments with different GO concentrations (0, 0.05, 0.1, 0.25, 0.5, 1 $mgmL^{-1}$) but without bacteria were also carried out with the aim of discarding possible interactions between GO and SA.

2.4. Flow cytometry analysis

2.4.1. Staining procedures

The staining procedures and stock solutions preparation have been described in supplementary data. The samples, in this case, were also stained using SYBRgreen (SYBRgreen; Invitrogen) and Fluorescent microspheres (Perfect Count; Cytognos, Spain) to obtain the total count of cells, with PI to differentiate cells and GO, and using a dual-staining procedure (cFDA/PI) in order to evaluate cell physiological status. GO without bacteria dyeing with different fluorophores using in viability cells test were analysed by flow cytometry (FC) to check the fluorescence from the GO.

A study of the fluorescence emitted by the GO itself and by GO as a result of interaction with the fluorescent dyes used in the study was also carried out. GO only interacted with cFDA, giving fluorescence in FL1 channel, so that, to measure the effect of GO-cFDA fluorescence in the antibacterial study, two different stains were used: PI and dual staining PI-cFDA. The results obtained with each staining were similar to each other.

2.4.2. Multi-parameter flow cytometry

Flow cytometry measurements were performed using a Cytomics FC 500 flow cytometer (Beckman Coulter) equipped with a 488 and 633 nm excitation light source from an argon ion laser. Green fluorescence from samples (corresponding to cFDA or SYBRgreen-stained cells) was collected on the FL1 channel (530 nm), whereas PI fluorescence was registered on the FL3 channel (610 nm). Each analysis was performed in duplicate at a low flow rate setting (4000 events s^{-1}). Data acquisition was carried out using Cytomics RXP software (Beckman Coulter). Gates and quadrants were established according to staining controls. For cFDA/PI dual-parameter and PI staining flow cytometric analysis, data collected from 200000 events, were analysed using Kaluza® Flow Analysis Software, Beckman Coulter. The fluorescent microspheres presented two types, A

microspheres, excitable at 506 nm and B microspheres, excitable between 365 and 650 nm.

2.5. Analytical methods

Determinations of SA in the samples were performed by HPLC (Agilent 1200) using a Mediterranea sea18 column (5 μm x 25 cm x 46 cm, plus a reverse-phase column from Waters) combined with a UV detector. The wavelengths used for detection of SA was 290 nm. The mobile phase consisted in a mixture of two solutions: acetonitrile and 0.4 % phosphoric acid in water [212]. The method employed comprised a binary gradient at a constant flow rate of 1 $mLmin^{-1}$.

The products obtained of the SA biodegradation were analyzed by liquid chromatography-mass spectrometry (Agilent 6460 Triple Quad plus Agilent 1290 Infinity UPLC), with a column Zorbax Eclipse Plus C18 (2.1x50mm, 1.8 um), the ionization source is an electrospray and measurement was performed in scan negative mode. The mobile phases were water and acetonitrile both containing 0.1% formic acid.

Cell concentrations in the medium were measured by two techniques: spread plate counting on growth medium agar and optical density measurement at 660 nm (Shimadzu, UV-vis 1203). Cell concentrations were also obtained by FC.

To observe the interaction of microorganisms with GO, SEM was conducted [121, 219, 220]. Briefly, at the end of 24 h incubation, 2 ml of sample were taken and fixed with 3% gluteraldehyde [121, 220, 221]. Fixed samples were serially dehydrated with increasing concentrations of acetone (20, 40, 60, 80 and 100 %) [222]. All samples were gold-coated before imaging to reduce charging of the sample. SEM images were acquired at 10 Kev accelerated voltage with JEOL 6100 (Jeol, USA).

All experiments were carried out at least in duplicate and each sample was analysed in triplicate. Standard deviations (SD) obtained are shown as vertical lines in figures.

3. Results and discussions

3.1. Antibacterial activity of GO

Before starting the experiments, it was confirmed that natural light has not effects on SA process biodegradation, carrying out biodegradation experiments with different GO in which the Erlenmeyer was covered with aluminium paper. Additionally, it was observed that SA concentration did not change after 24 hours in contact with OG and in absence of *P. putida*, thus precluding any side reactions between GO and SA (data not shown).

The effect of GO-cFDA fluorescence in the antibacterial study was measured. With this purpose, two different stainining procedures were used and their results were compared: PI staining and dual PI-cFDA staining. The results obtained with each staining were similar to each other, therefore the GO-cFDA fluorescence was negligible on the bacteria fluorescence (see supplementary data S7).The gates for each physiological state selected in the antibacterial study are shown in S8 (supplementary data).

3.1.1. Simulated urban wastewater (SUW)

The growth and viability of cells were measured over time by OD and colony counting method and by flow cytometry, respectively.

Figure 5.1 shows the growth of *P putida* in the SUW, followed by means of optical density or flow cytometry, and the evolution of its physiological status in presence of different GO concentrations, which range from 0 to 1 mgmL^{-1}.

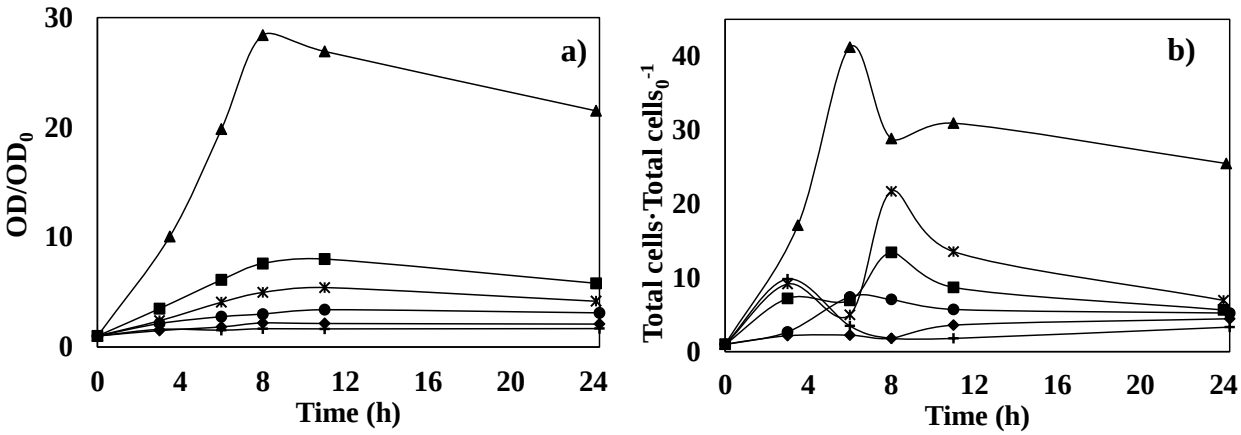

Figure 5.1: Evolution of *P. putida* growth measured as OD (a) or by means flow cytometry (b) in SUW using different GO concentrations: 0 mgmL^{-1}(▲), 0.05 mgmL^{-1} (■), 0.1 mgmL^{-1} (✳), 0.25 mgmL^{-1} (●), 0.5 mgmL^{-1} (◆), 1mgmL^{-1} (+). In all cases: 200 rpm, 30ºC, *P. putida* inoculum of 10^7 CFUmL^{-1} and 100 mL in 250 mL Erlenmeyer flasks.

As can been concluded from figure 1a, the presence of GO clearly had a negative effect on the *P. putida* growth. Therefore, the higher the GO concentration, the lower the optical densities were, with the OD variation being almost negligible for GO concentrations higher than 0.5 mg mL^{-1}. In this regard, it can be also noted that the inhibitory effect of the GO on the *P. putida* growth is much more marked at low concentrations of this compound. The presence of only 0.05 mg mL^{-1} GO reduces by a third the maximum OD achieved by the culture in absence of GO. However, when this GO concentration is doubled, the OD is only reduced approximately by a half and so on. The results of growth obtained using flow cytometry also corroborated these findings (See figure 5.1b).

The specific growth rate (μ) was calculated for each system with different GO concentration, obtaining a relationship between μ and GO represented by the following equation: $\mu(h^{-1}) = 0.058 \cdot GO^{-0.62}(mgmL^{-1})$ with r^2=0.92

The presence of GO has effect not only on the *P. putida* growth but also on its physiological status, as can be seen in table 5.1. In this contest, it is important to point out that the terms "viable" bacteria and "active" bacteria are employed in this work to indicate cells showing intact membranes (PI negative cells) and metabolic activity (cFDA positive cells), respectively [185]. In this sense, damaged cells will be active but non-viable cells (PI and cFDA positive cells).

Table 5.1: Percentage of metabolic states of *P. putida* (viable, dead and damaged cells) in contact with different GO concentration (0, 0.05, 0.1, 0.25, 0.5, 1 mgmL^{-1}) in SUW

	% Viable cells				**% Dead cells**				**% Damaged cells**			
	0 h	**6 h**	**11 h**	**24 h**	**0 h**	**6 h**	**11 h**	**24 h**	**0 h**	**6 h**	**11 h**	**24 h**
0 mgmL^{-1}	66.7 ±18.0	89.0 ±2.6	88.0 ±0.2	77.40 ±0.03	3.9 ±0.8	1.3 ±0.2	0.9 ±0.2	1.71 ±0.03	29.4 ±18.0	9.7 ±2.6	11.1 ±0.2	20.90 ±0.03
0.05 mgmL^{-1}	66.7 ±18.0	87.1 ±3.4	84.5 ±2.6	52.0 ±3.7	3.9 ±0.8	1.60 ±0.08	1.20 ±0.09	4.5 ±1.7	29.4 ±18.0	11.3 ±3.4	14.3 ±2.6	43.5 ±3.7
0.1 mgmL^{-1}	66.7 ±18.0	77.7 ±5.4	79.3 ±9.8	25.7 ±7.1	3.9 ±0.8	1.30 ±0.01	0.90 ±0.06	3.42 ±0.05	29.4 ±18.0	22.3 ±5.8	18.3 ±3.2	70.8 ±6.1
0.25 mgmL^{-1}	66.7 ±18.0	77.7 ±2.3	70.3 ±4.6	49.1 ±1.6	3.9 ±0.8	0.10 ±0.03	0.04 ±0.03	0.33 ±0.04	29.4 ±18.0	22.3 ±7.9	29.6 ±5.6	50.5 ±1.3
0.5 mgmL^{-1}	66.7 ±18.0	50.8 ±5.8	38.6 ±2.6	57.9 ±4.9	3.9 ±0.8	0.20 ±0.01	0.03 ±0.01	0.08 ±0.05	29.4 ±18.0	49.0 ±5.9	61.2 ±10.8	42.0 ±4.7
1 mgmL^{-1}	66.7 ±18.0	47.9 ±12.1	37.4 ±8.6	58.1 ±6.5	3.9 ±0.8	3.6 ±0.5	22.9 ±3.4	10.6 ±2.7	29.4 ±18.0	47.5 ±6.1	39.8 ±4.5	28.6 ±4.7

Cytometric measurements reveal that the viable subpopulation is the predominant one in the inoculum, with a percentage of 67%, although it is also remarkable that one third of the total population is damaged, probably due to the stress generated caused by the previous centrifugation and isolation. Anyway, the inoculum showed a high degree of activity (cFDA positive cells), with only a 4% of dead bacteria. In absence of GO, the viable subpopulation rises sharply, particularly during the first 11 h of cultivation, reaching a maximum and then gradually decreasing. This final reduction can probably be attributed to the bacterial ageing and to the depletion of the SUW nutrients.

As can be also observed in table 5.1, the presence of GO in the SUW, even at low concentrations, modifies the evolution of the physiological status of the *P. putida*, reducing the viable subpopulations. For GO concentrations lower than 0.5 mg mL^{-1}, initial increases in the viability percentages are still observed, although this is less marked as the GO is increased. In fact, a gradual reduction of the viability can be observed since the first minutes of experimentation when GO concentrations higher than 0.5 mgmL^{-1}

were used. It is noteworthy that the final percentage of dead cells barely increased for the different GO concentrations, indicating that viable cells are preferably transformed into a damaged status. These results suggest that the main impact of the GO on the *P. putida* was the loss of the membrane integrity, while the bacteria preserved their metabolic activity. In addition, it seems reasonable to consider the rupture of the cell membrane as the main inactivation mechanism caused by GO, instead of the other two proposed in the bibliography for graphene and its derivates: oxidative stress and cutting of intracellular metabolic routes. In this regard, it must be note these last two should be accompanied by a loss of activity, which has not been experimental observed.

3.1.2. Simulated industrial wastewater (SIW)

In this section, antibacterial activity of GO on *P. putida* cells was evaluated during the degradation of a simulated industrial wastewater containing 500 mgL^{-1} of SA as sole source of carbon. Figure 5.2 shows the evolution of SA concentration (a) and the growth curves of *P. putida* in SIW obtained by means of optical density (b) or colony counting method (c).

Figure 5.2 a revealed that presence of GO in the SIW has a slight effect on the capacity of *P. putida* to remove SA, except for very high GO concentrations, of around 1 $mgmL^{-1}$. Thus, for instance, the SA removals after 11 h of biodegradation in presence of 0, 0.25 and 1 $mgmL^{-1}$ of GO were 86.2, 75.9 and 51.1%, respectively. The evolution of the SA concentrations were successfully fitted to a zero reaction order model ($\frac{dC_{SA}}{dt} = -k$). Table 5.2 summarizes the relevant kinetic data obtained. Using the pseudo-zero order kinetic constant, the following relationship between degradation rates and GO can be obtained for GO concentrations up to 0.5 mg/ml:

$$k(mg(Lh)^{-1} = 35.5 \cdot GO^{-0.086}(mgmL^{-1})\ ;\ r^2 = 0.99$$

Table 5.2: Kinetics data obtained using pseudo-zero order kinetic model in SIW with different GO concentration

GO ($mgmL^{-1}$)	0	0.05	0.1	0.25	0.5	1
k ($mg\cdot(Lh)^{-1}$)	49.0	45.3	43.4	39.7	37.6	26.0
r^2	0.99	0.98	0.98	0.99	0.98	0.99

Although the presence of high GO concentrations in the SIW has effect on the SA removal rate, the reaction pathway was not modified. This fact was corroborated analysing samples by liquid chromatography-mass spectrometry. Regardless the GO concentration used, 2-hidroxymuconic semialdehyde was detected as a reaction product in all cases by

HPLC-MS, suggesting that the meta degradation pathway is followed, either in absence or presence of GO [95].

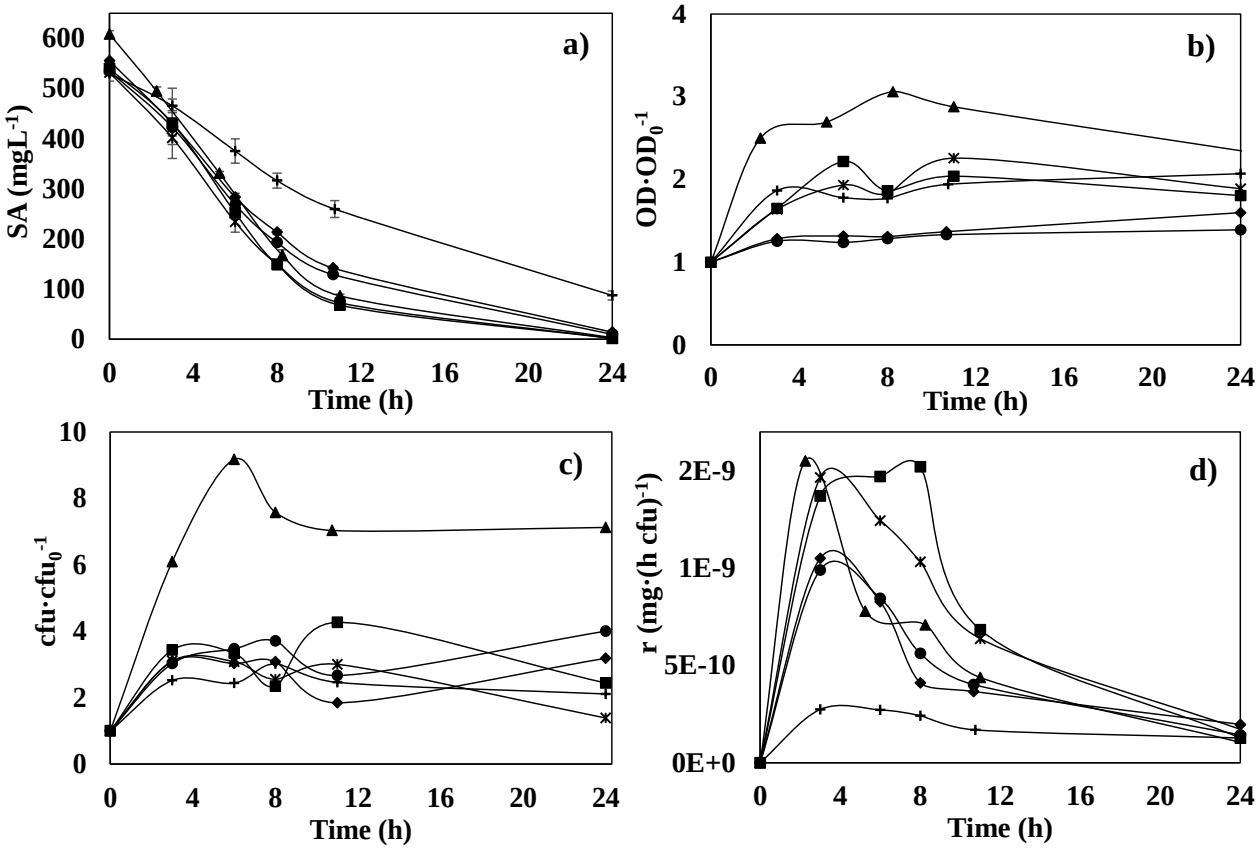

Figure 5.2: Evolution of the salicylic acid concentration (a), growth curves measured as optical densities (b) or plate counting method (c) and specific biodegradation rates (d) observed during the *P. putida* biodegradation of a SIW containing 500 mgL^{-1} SA as sole carbon source and different GO concentrations: 0 $mgmL^{-1}$(▲),0.05 $mgmL^{-1}$ (■),0.1 $mgmL^{-1}$ (✳),0.25 $mgmL^{-1}$ (●), 0.5 $mgmL^{-1}$ (◆), 1$mgmL^{-1}$ (+). In all cases: 250 rpm, 30ºC, *P. putida* inoculum of 10^7 $CFUmL^{-1}$, 100 mL in 500 mL Erlenmeyer flasks.

In regards to *P. putida* growth in SIW, the OD and cell concentration by plate counting, are shown in Fig. 5.2b and Fig. 5.2c. As can be seen, the *P. putida* growth in absence of GO either in SUW or SIW exhibited a similar behaviour: an initial increase in the OD and number of colony forming units, reaching a maximum and then decreasing gradually. Obviously, the growth is more intense in SUW than in SIW, due to the higher availability of carbon and nitrogen sources in the first medium. As in the case of SUW, the addition of GO to SIW also reduces the growth of the bacteria, with the inhibitory effect decreasing with the increase of the GO. So, a 66.2% bacterial concentration reduction in SIW was caused by the lowest GO concentration used. This impact can be best understood by calculating the specific growth rate (μ) getting values of 0.41, 0.20, 0.19, 0.16, 0.19 and 0.12 h^{-1} for 0, 0.05, 0.1, 0.25, 0.5 and 1 $mgmL^{-1}$ of GO, respectively. These results reveals that the specific growth rate is reduced by half when GO is present in the medium, even

at very low concentrations (0.05 $mgmL^{-1}$). Additionally, the cell size and cell complexity were monitored by measuring forward side scatter (FSC) and side scatter (SSC) parameters, respectively, by means of flow cytometry. Results indicated that changes in the size and complexity of the cells were negligible respect to time and GO concentrations. Results reported in the bibliography about the antimicrobial activity and biocompatibility of GO demonstrated the importance of the concentrations and bacterial species selected [125]. Recently, Ruiz *et al.* [128] showed that bacteria *E. coli* grew faster and to a higher optical density when GO was added to a bacterial culture at 25 μgmL^{-1} than cultures without GO. However, opposite results were found in other research like a strong antibacterial activity of *E. coli* of four types of graphene-based materials (400 μgmL^{-1}) (graphite (Gt), graphite oxide (GtO), GO, and reduced graphene oxide (rGO)) [223] or almost completely suppressed the growth of *E. coli* by GO (85 μgmL^{-1}), leading to a significant loss of viability but with a minimal cytotoxicity [130]. The growth of *P. aeruginosa* decreased after treatment with GO and rGO and there was no colony observed over concentrations of 175 μgmL^{-1} [125].

Figure 5.2d shows the evolution of specific SA biodegradation rates SIW, which can be easily calculated from the SA and biomass concentrations. In absence of GO, *P. putida* was able to achieved a maximum specific degradation rate in SIW of around $1.6 \cdot 10^{-9}$ $mgSA\ h^{-1}\ CFU^{-1}$, very similar to those observed with 0.05 or 0.1 $mgmL^{-1}$, that is, $1.6 \cdot 10^{-9}$ and $1.2\ 10^{-9}$ $mgSA\ h^{-1}\ CFU^{-1}$, respectively. However, these maximum specific rates decreased when higher GO concentrations were added, particularly in the experiment with 1 $mgmL^{-1}$, whose value was one sixth of the one observed in absence of GO. These results suggest that the presence of GO always reduces the *P. putida* growth but, for concentrations higher than 0.1 $mgmL^{-1}$, it also reduces the activity of the bacterium.

As in the case of SUW, the multiparametric flow cytometric method using a double cFDA/PI staining was also applied to cultures in SIW in order to evaluate percentages of viability and activity in the population (see figure 5.3).

For all the GO concentrations, the physiological status of the inoculum is 66.7 % viable cells, 29.4% damaged cells and 3.9 % dead cells. Results revealed that there was not a significant difference between the physiological status observed without or with 0.05 $mgmL^{-1}$ GO. In both cases, the percentage of viable cells increased during the first 4 h and reaches a constant value of 92 % until the eleventh hour. The final decrease in viability after 24 h is probably due to the complete depletion of the SA. The negative effect of GO on the viability becomes important for GO concentrations higher than 0.1 $mgmL^{-1}$. For this concentration, viability percentages decreased from the initial 66.7 % to a final value of 55% after 11 h. For the experiments with higher GO concentrations, the viability percentages rapidly decreased during the first 3 h, achieving final viability percentages around of 20 % independently of the GO concentration selected. For all the

experiments, these reductions in the percentages of viable cells were accompanied by the corresponding increase in the percentages of damaged cells, whereas the percentages of dead cells remained approximately constant, with values lower than 5%. The results implied that the damage occurs with the first contact bacteria-GO.

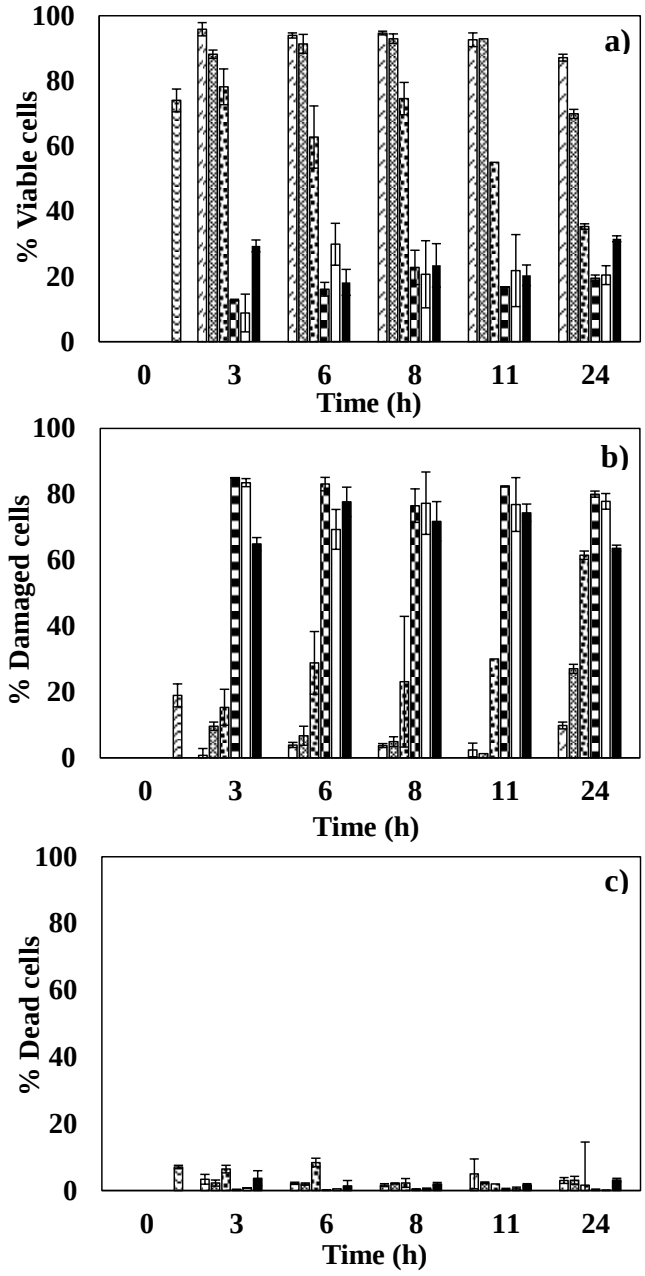

Figure 5.3: Percentages of viable cells (a), damaged cells (b) and dead cells (c) of *Pseudomonas putida* in SIW and under different GO concentration in MM. (▨ time 0h all GO concentration, ▨ 0 $mgmL^{-1}$, ▨ 0.05 $mgmL^{-1}$, ▨ 0.1 $mgmL^{-1}$, ▨ 0.25 $mgmL^{-1}$, □ 0.5 $mgmL^{-1}$, ■ 1$mgmL^{-1}$). In all cases: Initial SA concentration of 500 mgL^{-1}, 250 rpm, 30ºC, *P. putida* inoculum of 10^7 $CFUmL^{-1}$, 100 mL in 500 mL Erlenmeyer flasks.

These results reveal that the viable cells in contact with GO suffered a change in its viability becoming damaged cells. This statement provides additional information to the studied so far, where only growth suppression and loss of bacterial viability as $CFUmL^{-1}$ were described [25, 125, 130, 223], however, in this case, the bacteria were damaged by GO but remained metabolically active. However, SA removal was reduced but not completely stopped, what would happen if instead of becoming damaged were dead cells, since damaged cells reduce their metabolic capacity compared to viable cells but not completely [190, 191].

As in the case of SUW, these results suggest that the main impact of the GO on *P. putida* was the loss of the membrane integrity (PI positive cells), while the bacteria preserved largely their metabolic activity (cFDA positive cells). This assertion is also consistent with results obtained by means of Scanning Electron Micrography (SEM) (Figure 5.4). One hand, figures 5.4a and 5.4b showed micrographics of *P. putida* in absence of GO and of an aqueous suspension of GO, respectively. On the other hand, the mixture of GO and bacteria are shown in Figures 5.4c and 5.4d, with Fig. 5.4d being a magnification of the area surrounded by the circle in Fig. 5.4c. these last two SEM images show the adsorption of bacteria to the GO nanosheets because of the generation of van der Waals forces [224]. The same effect was observed by Ahmed y Rodrigues [121], Luongo y Zhang [220], Jastrzębska *et al.* [119] and Krishnamoorthy *et al.* [219]. It is also remarkable that bacteria in figure 5.4a had an outer smooth and flawless membrane. Nevertheless, most of these same bacteria, after being in contact with GO, showed a rough surface, which probably is partially permeabilisided, allowing the cell staininig by PI, but whose integrity is high enough to maintain the enzymatic activity, also being stained by cFDA, which will be in accordance with the low percentages of dead cells reported in figure 5.3c. These damages in cell membrane are usually attributed to the sharp edges of GO sheets (see figure 5.4a), which probably act as “blades” into the agitated Erlenmeyer. [119, 122, 127, 225]. In figure 5.4d, it can be also observed the presence of a few bacteria with their cell membrane partially lised (see white square in figure 5.4d), which leads to the cell death [121, 219, 220].

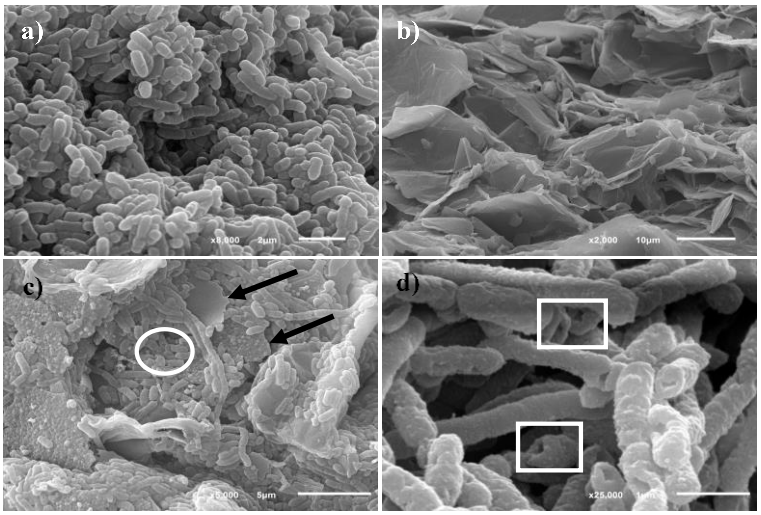

Figure 5.4: Scanning Electron micrographs of a) a *Pseudomonas putida* culture in absence of GO (a); an aqueous suspension of GO (b); c and d) *P. putida* culture in SIW in presence of 0.1 $mgmL^{-1}$ GO after 11 hours. Scale bar and magnification indicated in each image. Marked arrows showed in (c) denotes the location of graphene oxide nanosheets and the white circle indicates the area magnified in image 4d

4. Conclusions

This study reveals that the presence of GO on simulated urban and industrial wastewaters (SUW and SIW, respectively) has a negative effect on bacterial growth and viability of *Pseudomonas putida*. The growth of *P. putida* is inhibited by the presence of GO concentrations higher than 0.05 $mgmL^{-1}$, this effect being noticeable on both simulated media. In turn, the negative effect of GO on the viability becomes important for GO concentrations higher than 0.5 $mgmL^{-1}$ and 0.1 $mgmL^{-1}$ for SUW and SIW, respectively. These results suggest that the main impact of the GO on the *P. putida* was the loss of the membrane integrity, as a result to the sharp edges of GO sheets, which probably act as "blades" into the agitated Erlenmeyer. This assertion is also consistent with results obtained by means SEM.

5. Acknowledgements

R. G. Combarros wishes to express gratitude for a research grant from the Government of the Principality of Asturias (Severo Ochoa Programme). R. G. Combarros would also acknowledge the assistance provided by A. Sampedro.

6. References

References are listed in the Chapter 8.

Supporting Information

Table of contents

GO characterization

Mean (Z-Average) size of GO were determined via Dynamic Light Scattering (DSL) using a Zetasizer Nano ZS (Malvern Instruments Ltd, UK). Independent samples were taken and measurements were carried out three times at room temperature obtaining a value around 800 nm. (The supplier of the OG got a particle size of 0.5×500 nm). The GO morphology was determined using an Olympus BX61 optical microscope (Olympus, Japan) an image was shown in supplementary information (S1). The rheological characteristics of GO solution (10 $mgmL^{-1}$) were also analyzed using a rheometer MARS (Haake, Germany). The GO solution behaviour is similar that a Newtonian fluid. Rheological analysis was done with Herschel-Bulkley model obtaining values of n=1 and τ_0=1. Once a force was applied on the sample, allowing the elongated structure of GO is placed in the flow direction, the flow rate is directly proportional to the effort. Furthermore, the temperature effect on solution of GO was studied, a change of 20°C (10-30 ºC) in solution involves a change of in the slope of $2.1 \cdot 10^3$ Pa·s representing a greater fluidity of the dissolution of GO with the temperature.

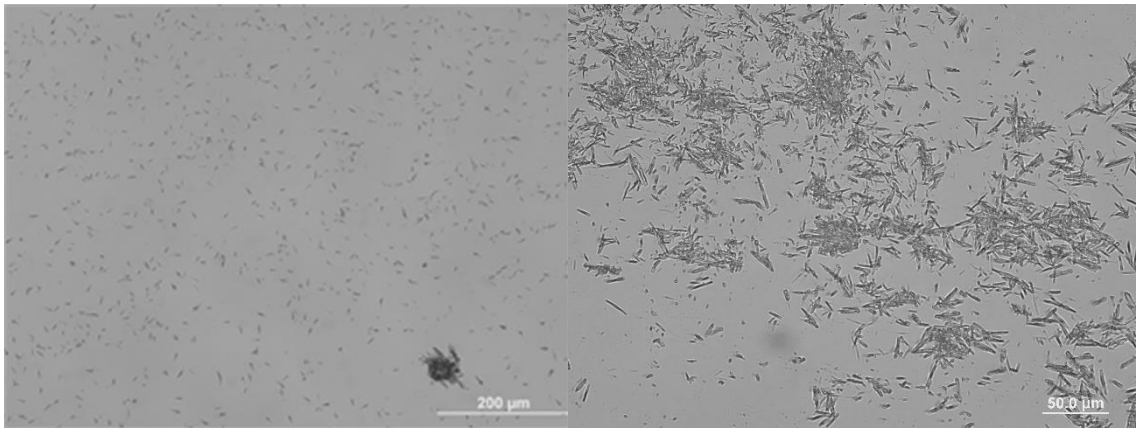

Figure S 6: Bright field image of aqueous suspension of GO with a concentration of 1 $mgmL^{-1}$

Flow cytometry staining procedures

Samples from cultures were harvested by centrifugation at 16000 × g for 5 min. Before staining, cells were washed twice in phosphate-buffered saline (PBS; pH 7.4, sterile and filtered at 0.22 μm) and were then held in the "hot spot" of a sonication bath for 2 s to prevent bacterial aggregation before flow cytometric analysis [193]. Propidum iodide (PI; Invitrogen), and carboxyfluorescein diacetate (cFDA; Invitrogen) were used as fluorescent dyes in a dual-staining procedure (cFDA/PI) in order to evaluate cell physiological status. Staining procedures were performed as previously reported Alonso *et al*. [226]. Total counts of cells were determined by staining with SYBRgreen

(SYBRgreen; Invitrogen), a green fluorescent cell-permeable DNA probe [168, 227], to differentiate the microorganisms from other particles in samples (background). Fluorescent microspheres (Perfect Count; Cytognos, Spain) were used as internal standards in each sample, following the supplier's recommendations for ratiometric counting [191]. In order to obtain a significant number of cells to ensure the efficiency of the test, 2000 microspheres were acquired in each analysis. Analyses were performed in triplicate for each dye, including an un-stained sample as a control.

Stock solutions were prepared as follows: PI was made up to 1 $mgmL^{-1}$ in distilled water (0.22 μm filtered) and maintained at 4 °C, whereas cFDA and SYBRgreen were prepared in dimethyl sulfoxide (Sigma-Aldrich) at a concentration of 1 mM and stored at −20 °C. PI staining was prepared by diluting the stock solution in sterile distilled water and adding this work solution to the cell suspension at a final concentration of 5 μgmL^{-1}. This mixture was then incubated for 30 min in the dark at room temperature. Working solutions of cFDA were made up to 10 μM in PBS containing 1 mM EDTA. PI-stained samples were subsequently incubated with 0.1 μM cFDA for 15 min in dark at room temperature [226]. SYBRgreen work solution was prepared by diluting the stock solution in PBS containing 1mM EDTA at final concentration of 0.01 mM. The SYBRgreen work solution was added to the cell suspension at a final concentration of 0.1 μM and the mixture was incubated for 15 min in dark at room temperature [168].

Table S 2: Composition of rich culture medium and minimum mineral medium using in cell viability test

SUW	**SIW**
5 gL^{-1} peptone	0.5 gL^{-1} K_2HPO_4
3 gL^{-1} beef	0.3 gL^{-1} $(NH_4)_2SO_4$
0.422 gL^{-1} KH_2PO_4	0.05 gL^{-1} $MgSO_4 \cdot 7H_2O$
0.375 gL^{-1} K_2HPO_4	0.01 gL^{-1} $FeCl_3 \cdot 6H_2O$
0.244 gL^{-1} $(NH_4)_2SO_4$	0.01 gL^{-1} $CaCl_2 \cdot 2H_2O$
0.05 gL^{-1} $MgSO_4 \cdot 7H_2O$	0.05 gL^{-1} triptone
0.054 gL^{-1} $C_6H_{11}FeNO_7$	10 mL^{-1} of trace solution
0.015 gL^{-1} $CaCl_2 \cdot 2H_2O$	500 mgL^{-1} salicylic acid (SA)
0.015 gL^{-1} NaCl	

The trace solution was composed of 8 mgL^{-1} $ZnSO_4 \cdot 7H_2O$, 4 mgL^{-1} H_3BO_3, 4 mgL^{-1} $Na_2MoO_4 \cdot 2H_2O$, 4 mgL^{-1} $CuSO_4 \cdot 5H_2O$, 4 mgL^{-1} $MnCl_2 \cdot 4H_2O$, 4 mgL^{-1} $CoCl_2 \cdot 6H_2O$ [202]

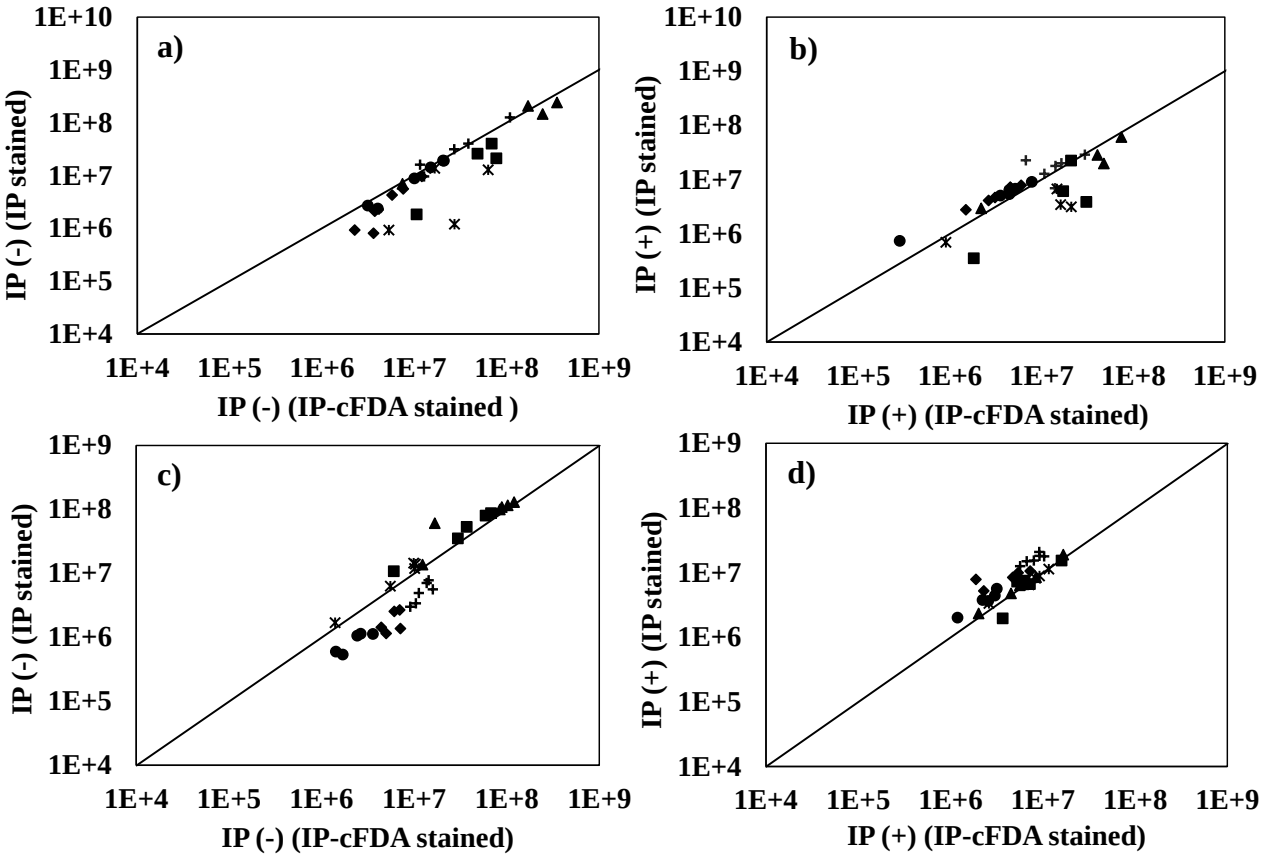

Figure S 7: Comparison of viable cells (PI (-)) obtained from simple PI staining and dual PI-cFDA staining in SUW (a) and SIW (c) and damaged and dead cells (PI (+)) obtained from simple PI staining and dual PI-cFDA staining in SUW (b) and SIW (d)

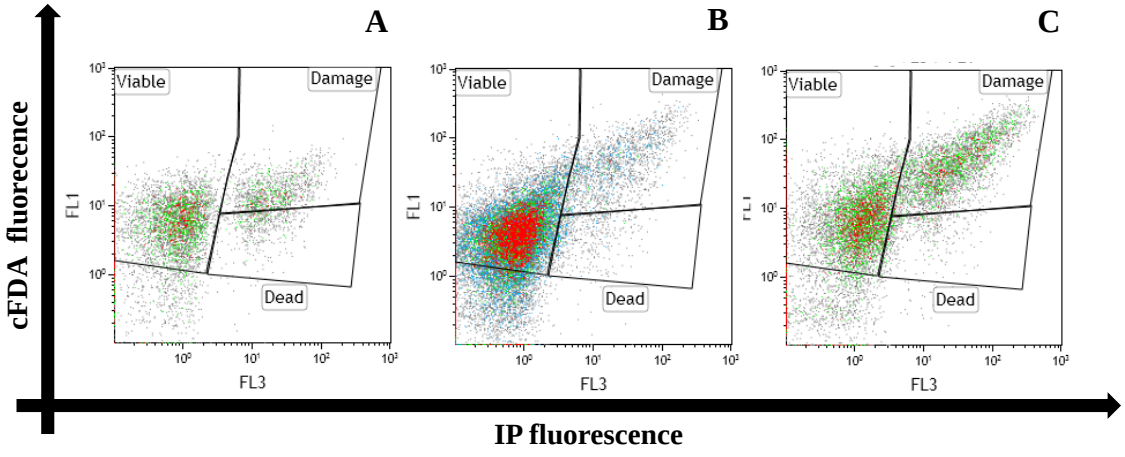

Figure S 8: Dot plots representing cFDA fluorescence versus PI fluorescence of *Pseudomonas putida* cells during shake-flask fermentation with 0.05 mgmL^{-1} of GO. A, B and C plots correspond to an initial SA of 500 mg L^{-1} at 0, 11 and 24 hours respectively.

5.4. Tratamiento de corrientes contaminadas por tiocianato mediante biodegradación con *Paracoccus thiocyanatus*

Otros contaminantes difícilmente biodegradables por lodos activos son los compuestos cianurados, dentro de los cuales se encuentra el tiocianato. Los compuestos fenólicos y cianurados se encuentran frecuentemente presentes de forma simultánea en las mismas aguas residuales industriales.

En este caso se ha tomado el tiocianato como modelo de compuesto cianurado y se ha analizado el proceso de biodegradación del mismo mediante la bacteria *Paracoccus thiocyanatus.* Se ha estudiado la influencia sobre el proceso de parámetros como la concentración del tiocianato, las condiciones de cultivo y la composición del medio.

Se ha obtenido de este modo, un profundo conocimiento sobre las condiciones y medios óptimos necesarios para la degradación del tiocianato por la bacteria *Paracoccus thiocyanatus;* estos resultados han servido de base para el posterior estudio en la sección 5.5. de las interacciones surgidas en el proceso de biodegradación como consecuencia de la presencia de un co-sustrato o de otra bacteria.

Por otro lado, y de manera paralela a la sección 5.1, se ensayó el efecto que produce la presencia de un biofilm bacteriano sobre el proceso de adsorción con carbón activo y degradación biológica del tiocianato. Los resultados de estos análisis no fueron incluidos en el artículo publicado, por ello se muestran en el anexo II.

Los resultados de este trabajo se presentan a través de una publicación cuya referencia y estado se muestran a continuación.

Referencia: Combarros, R.G., Collado, S., Laca, A., Díaz, M. 2015. Conditions and mechanisms in thiocyanate biodegradation. Journal of Residuals Science & Technology, 12(3), 113-124.

Estado: Aceptada

Conditions and Mechanisms in Thiocyanate Biodegradation

R.G. COMBARROS, S. COLLADO, A. LACA and M. DÍAZ*
Department of Chemical Engineering and Environmental Technology, University of Oviedo, Spain

ABSTRACT: Presence of thiocyanate (SCN^-) is a problem of considerable interest in many industrial wastewaters, where this contaminant often appears accompanied by secondary sources of carbon, nitrogen and/or sulphur. In order to understand the effect of these compounds on the biodegradability of SCN^-, this work investigates how the bacterium *Pararacoccus thiocyanatus* utilises the three elements that form the molecule of thiocyanate and compare this behaviour with those obtained in presence of other sources of N, S and C. Result showed that the bacterium was capable of utilizing thiocyanate as the sole substrate, achieving specific biodegradation rates of approximate 1.20 mg SCN^- (mg cell·h)$^{-1}$ and eliminating initial thiocyanate concentrations up to 5,000 mg L^{-1}. Experimental data were successfully fitted to a Teisser model, assuming the existence of substrate inhibition obtaining values of μ_{max} of 0.059 h^{-1}, K_s of 790 mg L^{-1} and K_i of 6,520 mg L^{-1} for free mineral medium. Presence of additional carbon and nitrogen sources implied catabolic repression of the biodegradation of thiocyanate. In this case, only concentrations lower than 3,500 mg L^{-1} could be treated, obtaining specific degradation rates of around 0.70 mg SCN^-·(h·mg cell)$^{-1}$. Tessier model values showed a higher maximum specific growth rate (0.344 h^{-1}), changing also the values for affinity and inhibition constants (1,150 mg L^{-1} and 1,730 mg L^{-1}, respectively).

INTRODUCTION

THIOCYANATE is an inorganic compound generated from a diverse range of natural and industrial sources. Due to some of its rather unique properties, thiocyanate is used in a variety of industrial processes such as photofinishing, plastics, organic chemicals, pharmaceuticals, fertilizer, herbicide and insecticide production, dyeing, acrylic fibre production, manufacturing of thiourea, metal separation and electroplating. Additional uses of thiocyanate include soil sterilization and corrosion inhibition [6,7,13]. Because of such wide use, thiocyanate is found in many industrial wastewaters.

Thiocyanate is stable, non-hydrolysable and non-volatile and it persists in the environment even in acid media [6]. Due to a strong protein-binding tendency and competitive characteristics, thiocyanate is toxic to many higher organisms even at low concentrations (LC50 between 50–100 mg L^{-1}) [1]. It affects the human central nervous system provoking irritability, nervousness, hallucination, psychosis, mania, delirium and convulsions. Besides, it inhibits halide transport to the thyroid glands and affects the stomach enzyme system, cornea and gills [1,6]. Therefore, thiocyanate removal from industrial wastewater and other contaminated sites is of great importance and more effective treatment systems are urgently required.

Several chemical methods, such as electrochemical oxidation, hydrogen peroxide oxidation or ozonation have been proposed for thiocyanate removal and/or detoxification [2,10,28]. However, most of these chemical techniques are either too costly, ineffective or produce a toxic residue, for example, cyanide, and thus are not widely used [10].

Biological processes are an alternative method of treatment without creating or adding new chemicals to the environment [28]. However, it has been reported that substrate inhibition begins to appear at thiocyanate concentrations higher than 20 ppm and complete inhibition occurs at concentrations higher than 1,000 ppm [14]. A number of chemolithotrophic and chemoheterotrophic bacteria isolated from a variety of sources can utilize thiocyanate as a source of energy and nutrients [6,10]. These include *Paracoccus* species which are able to oxidize not only thiocyanate, but also thiosulphate, tetrathionate, sulphide and elemental sulphur [9]. Thiobacilli can also utilize thiocyanate as both a nitrogen and sulphur source. *Arthrobacter* utilizes thiocyanate as a nitrogen source, even in the presence of other nitrogen sources (ammonia or nitrate). *Pseudomonas stutzeri* uses thiocyanate as both a sulphur and

*Author to whom correspondence should be addressed. Tel: 985 10 34 39. Fax: 985103434. E-mail: mariodiaz@uniovi.es

1544-8053/15/03 113-05

doi:10.12783/issn.1544-8053/12/3/1

nitrogen source in absence of ammonium ion [10]. Grigor'eva *et al.* [11] used a co-culture of *Pseudomonas putida* and *Pseudomonas stutzeri* to degrade both cyanide and thiocyanate. Paruchuri *et al.* [20] used a bacterial consortium containing *Pseudomonas* and *Bacillus* species to degrade thiocyanate. None of their single isolates were able to degrade thiocyanate.

In all cases, thiocyanate degradation pathways are sensitive to the thiocyanate concentration, the physicochemical conditions, and the presence of interfering and inhibitory compounds [6]. Thus, in addition to nutrients and carbon and nitrogen sources, other essential conditions for successful biological degradation of cyanide compounds must be taken into account: pH, temperature, oxygen availability, microbial population and nutrient availability being the most important [22].

Paracoccus thiocyanatus is a facultative chemolithotrophic thiocyanate-degrading bacterium which was isolated from activated sludge enriched with thiocyanate. This bacterium has been reported as capable of utilizing thiocyanate as sole energy source [17]. However, the literature describes no investigation into the effect that the presence of other carbon and nitrogen sources have on the degradation process of thiocyanate by this microorganism. Several authors have proposed the following process for the utilization of thiocyanate by *Thiobacillus thiocyanooxidans*. First, thiocyanate is hydrolysed to cyanate (OCN^-) and sulphide, followed by hydrolysis of cyanate to ammonia and bicarbonate, and oxidation of sulphide to sulphate [10,15]. In addition, Kim and Katayama [18] described the hydrolyzation of thiocyanate by *T. thioparus* THI115 to ammonia and carbonyl sulphide, which is subsequently oxidized to sulphate. Although the biological degradation of thiocyanate has been extensively studied, only a limited number of investigations have focused on the effect of the operating conditions and medium composition on the thiocyanate biodegradation kinetics, especially for *Paracoccus thiocyanatus*. In the present work, the effects of medium composition, different stirring speeds and initial inoculum size and growth stage on the degradation potential of the bacterial culture were investigated in order to determine the best conditions for the biodegradation of thiocyanate by *Paracoccus thiocyanatus*.

MATERIALS AND METHODS

Media Composition

Growth Medium (GM): 5 g peptone L^{-1}, 5 g beef extract L^{-1}, 5 g yeast extract L^{-1}, 2.5 g NaCl L^{-1}, 0.1 g K_2HPO_4 L^{-1}, 0.05 g $MgSO_4 \cdot 7H_2O$ L^{-1} [16]. GM-agar medium is composed of GM and 20% of agar.

Mineral Medium (MM): 0.5 g K_2HPO_4 L^{-1}, 0.3 g $(NH_4)_2SO_4$ L^{-1}, 0.05 g $MgSO_4 \cdot 7H_2O$ L^{-1}, 0.01 g $FeCl_3 \cdot 6H_2O$ L^{-1}, 0.01 g $CaCl_2 \cdot 2H_2O$ L^{-1} and 10 mL of trace element solution L^{-1}. The trace element solution was composed of 8 mg $ZnSO_4 \cdot 7H_2O$ L^{-1}, 4 mg H_3BO_3 L^{-1}, 4 mg $Na_2MoO_4 \cdot 2H_2O$ L^{-1}, 4 mg $CuSO_4 \cdot 5H_2O$ L^{-1}, 4 mg $MnCl_2 \cdot 4H_2O$ L^{-1}, 4 mg $CoCl_2 \cdot 6H_2O$ L^{-1} [16]. For the experiments carried out with additional carbon source, glucose (0.1, 0.5, 1, and 3%) and yeast extract (0.5 and 1%) were added to the MM. Sulphur and nitrogen-free medium (FM) was prepared using $MgCl_2$ instead of $MgSO_4$ and without $(NH_4)_2SO_4$. In the trace element solution, $ZnSO_4 \cdot 7H_2O$ and $CuSO_4 \cdot 5H_2O$ were replaced by $ZnCl_2$ and $CuCl_2 \cdot 2H_2O$, respectively. Thiocyanate degradation tests were started by inoculating bacteria into a flask containing MM or FM and 100–10000 mg L^{-1} of thiocyanate. In all cases, KSCN (Panreac, 98% purity) was the source of SCN^- in the medium.

Microbial Strain and Culture Conditions

Paracoccus thiocyanatus (BCCM, Belgian Coordinated Collections of Microorganisms (LMG 24666T)) capable of degrading thiocyanate was used. Bacterial colonies, which had been grown in the GM-agar medium for 4 days at 30°C, were inoculated into 250 ml Erlenmeyer flasks containing 50 mL of GM. After incubation at 28ºC and 250 rpm, an aliquot was taken and used as an inoculum for subsequent experiments. This inoculum was centrifuged at 10,000 g for 10 min and the supernatant was eliminated so that only bacterial cells were added to the MM to avoid introducing compounds from the GM. Inocula were taken at different times of cell growth (12–45 hrs), and different inoculum sizes (5×10^7–3×10^8 cfu mL^{-1}) were also tested.

In order to check the effect of acclimatization to SCN^- before biodegradation, some tests were carried out by supplementing GM with SCN^- (range between 100–300 mg L^{-1}). Moreover, an intermediate medium was used to provide a less abrupt transition in composition between GM and MM, trying to reduce the lag time. The intermediate medium consisted of either a 10% dilution GM or MM with 0.5% glucose or yeast extract with thiocyanate. However, no positive effects were observed, so this acclimatization step was rejected. Additionally, MM was also tried as the growth

medium, but the growth rate was too low to obtain a suitable inoculum for the following experiments.

Biodegradation Experiments

All thiocyanate biodegradation experiments were performed in an incubator (New Brunswick Scientific, Classic Series), with controlled temperature and stirring speed. No attempt was made to maintain a constant pH value. The experiments were performed at bench scale, in 500 mL Erlenmeyer flasks containing 100 ml of medium. Temperature of all experiments was maintained at 28°C and different stirring speeds (150–250 rpm) were tested. Although this temperature can be considered as scarcely high for WWTP, wastewaters containing SCN^- are frequently produced in industrial processes at medium-high temperature such as production of coke, so this temperature, after cooling the stream, appears reasonable in an industrial wastewater treatment. Samples were taken at different times and immediately analysed.

Analytical Methods

The concentration of thiocyanate was determined by a colorimetric process and according to the standard methods. Thiocyanate was estimated using ferric nitrate at acidic pH at 460 nm. This method has a detection limit of 0.1 mg L^{-1} [3]. The equipment employed for the spectrophotometric determinations was a UV/Vis spectrophotometer (Thermo Scientific, Heλiosγ).

Cell concentration in the medium was measured by spread plate counting on GM-agar medium (4 days of incubation time at 30°C) or by measuring the optical density at 660 nm (Shimazdu, UV 1203). Data were converted to cell dry weight (g L^{-1}) using the corresponding calibration curves previously obtained.

All experiments were carried out at least by duplicate and samples were analyzed in triplicate. Standard deviations, SD, obtained in each case are shown in the figures as vertical lines.

RESULTS AND DISCUSSION

Selection of Inoculum Size and Stirring Speed

The inoculum employed for the thiocyanate biodegradation test was taken from a *Paracoccus thiocyanatus* culture grown in GM. The growth curve obtained in this medium showed that the length of lag-phase was around 12 hrs, the stationary phase was reached after 36 hrs with final concentrations of around 8.3×10^9 cfu mL^{-1}, with the endogenous phase beginning after 66 hrs. The inoculum was taken at the end of the exponential phase of growth, after 36 hrs.

Firstly, the influence of the size of the inoculum introduced into the MM containing thiocyanate studied. With inoculum sizes of 3×10^8, 9×10 5×10^7 cfu L^{-1}, the thiocyanate was completely removed in 124 hrs, 65 hrs and 60 hrs respectively [Figure 1(a)]. Thus, the higher the inoculum size, the lower was the biodegradation rate. This was due in part to the increase in the induction time (t_i) required for the acclimation of the bacteria. A linear relationship between the induction time and the inoculum size (IS) of the process was obtained ($t_i = 2 \times 10^{-7} \cdot$IS (cfu mL^{-1}), $r^2 = 0.985$).

The inoculum size has been previously described as an important factor in degradative processes, higher inoculum sizes usually leading to an increase in the rate of degradation [12]. However, in this work the behaviour observed was the opposite, and as seen in Figure 1(b), the smallest inoculum size gave the highest specific degradation rates, with a maximum value of 0.29 g SCN^- (g cell·h)$^{-1}$. Zohar *et al.* [29] have already found similar behaviour. These authors reported that different inoculum sizes of *Arthrobacter 4Hβ* produced positive or negative effects on the degradation rate of p-nitrophenol (PNP), depending on the initial concentrations of PNP. So, at concentrations of 50 mg PNP L^{-1}, the increase in inoculum size did not enhance the degradation rate but with 100 mg PNP L^{-1}, a larger inoculum size led to an improvement in the degradation rates. This phenomenon was attributed to substrate limitation at 50 mg PNP L^{-1}. More recently, Salam and Lakshmi [21] investigated the biodegradation of lindane using *Rhodotorula* sp. and checked the effect of the initial inoculum size (10–90 mg dry cell weight L^{-1}) on the contaminant degradation. The yeast showed a maximum biomass production and degradation efficiency with an inoculum of 70 mg dry cell weight L^{-1}. For an inoculum size of 90 mg L^{-1}, these authors did not observe change in the rate of degradation.

Different stirring speeds have been used in previous studies that have focused on the biodegradation of contaminants by *Paracoccus* species. These values range from 120 to 250 rpm [5,25]. In this work, two values of stirring speed were tested to check the effect of agitation on the degradation rate of thiocyanate. The chosen values were 150 and 250 rpm, at the opposite extremes of the usual range. The biodegradation rate of the system was positively influenced by the stirring speed,

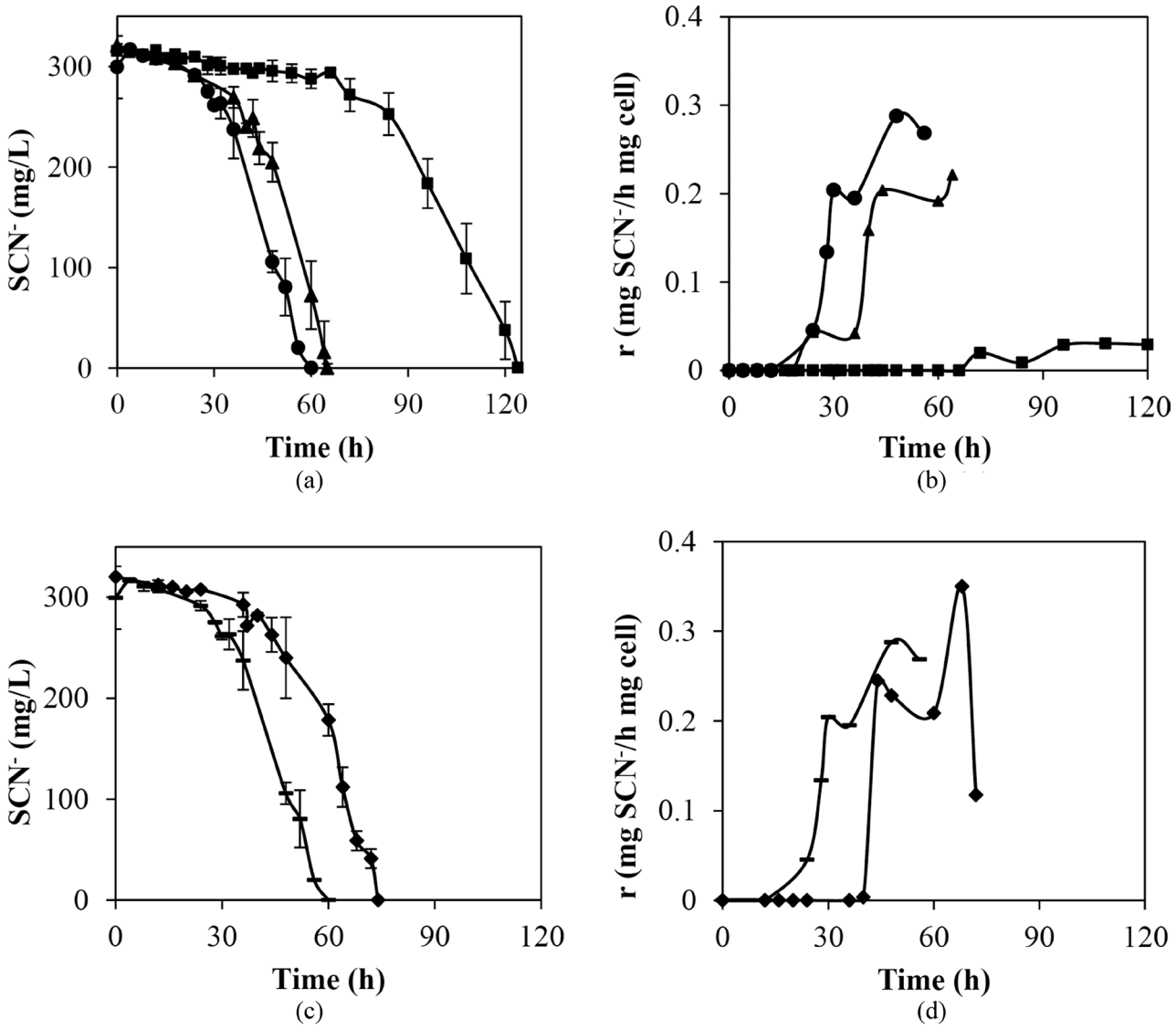

Figure 1. *Thiocyanate degradation (300 mg SCN^- L^{-1}) by Paracoccus thiocyanatus in mineral medium. (a) and (b) Effect of inoculum size at 250 rpm (● 5×10^7 cfu mL^{-1}, ▲ 9×10^7 cfu mL^{-1}, ■ 3×10^8 cfu mL^{-1}) on (a) thiocyanate degradation; and (b) specific degradation rate. (c) and (d) Effect of stirring speed (inoculum size 5×10^7 cfu mL^{-1}) (♦150 rpm, – 250 rpm) on (c) thiocyanate degaradation; and (d) specific degradation rates. In all cases, 28°C and inoculum taken at 36 hours.*

since complete removal of thiocyanate was achieved in 74 hrs at 150 rpm, this being reduced to 60 hrs at 250 rpm [Figure 1(c)]. Higher stirring speed implies higher dissolved oxygen concentration, which benefits the biodegradation of SCN^- by *P. thiocyanatus*, mainly reducing the induction time of the process and not the rate of degradation, as is shown in Figure 1(d).

Consequently, 250 rpm and an initial inoculum size of 5×10^7 cfu mL^{-1} were chosen as optimum conditions for the subsequent experiments. Twenty four hrs of growth in GM culture was selected as the inoculum age, which is a commonly used value reported by several authors because it corresponds to the middle of the exponential phase.

Utilization of Carbon, Nitrogen, and Sulphur

In this section, the way carbon, nitrogen and sulphur from thiocyanate utilized by the bacterial metabolism was studied.

Utilization of Carbon from Thiocyanate

Initially, thiocyanate biodegradation was studied in a MM that contained both nitrogen and sulphur molecules, but not carbon in its composition. The incorporation of carbon into the bacterial metabolism from the thiocyanate molecule was investigated for different thiocyanate concentrations (between 100 and

10,000 mg L^{-1}). Figures 2(a) and 2(b) show the biodegradation of thiocyanate and cell growth. Thiocyanate degradation occurred in two stages, the first where thiocyanate concentration remained almost constant due to the acclimatization of *P. thiocyanatus* to the new conditions and a second stage where the thiocyanate concentration decreased at a constant rate. Complete thiocyanate degradation was achieved after 48, 52, 79, and 107 hrs with initial concentrations of 500, 1,000, 2,500 and 3,500 mg L^{-1} respectively. With initial thiocyanate concentrations of 5,000 and 6,000 mg L^{-1} had not been completely removed at the end of the experiments, 85.5% of the initial amount having been eliminated after 315 hrs and 31% after 336 hrs, respectively. When the initial concentration was 5,000 mg L^{-1}, a constant concentration was observed at the end of the reaction period. This suggests the possibility of a product inhibition mechanism. Considering the pH (6.5) and the possible mechanisms of thiocyanate degradation found in the bibliography, it seems likely that the inhibitory product was NH_4^+. Thus, when the amount of NH_4^+ formed from the degradation of SCN^- is high enough to cause inhibition [4,27], the biodegradation rate decreases and the thiocyanate concentration remains invariable with time. If all the nitrogen metabolized was transformed into NH_4^+, the final concentration of NH_4^+ would be higher than 1,000 mg L^{-1} for an initial thiocyanate concentration of 3,600 mg L^{-1}. According to Vázquez *et al.* [27], the kinetics of SCN^- biodegradation were affected by the presence of ammonium when the concentration of NH_4^+-N increased from 49 mg L^{-1} to 135 mg NH_4^+-N L^{-1}. However, in this work inhibition by product was not observed for initial thiocyanate concentrations of 3,500 mg L^{-1} or lower.

Finally, for initial concentrations of thiocyanate higher than 7,000 mg L^{-1}, removal of thiocyanate was not observed, indicating a mechanism of substra hibition.

Figure 2(b) shows the evolution of the cell concentration (X) cfu mL^{-1} in relation to the initial cell concentration (X_0) cfu mL^{-1} for each of the initial thiocyanate concentrations. A continuous increase in biomass concentration was observed during the whole time of the experiment for initial thiocyanate concentrations lower than 2,500 mg SCN^- L^{-1}. With concentrations of 3,500 mg SCN^- L^{-1}, bacterial growth finished after 60 hrs and remained constant at a value of around 3.5×10^8 cfu mL^{-1}. For initial concentrations of 5,000 and 6,000 mg SCN^- L^{-1} the maximum concentration of biomass was 4.7×10^8 and 1.4×10^8 cfu mL^{-1} respectively, which then decreased, achieving values below the initial bacterial concentration.

The effect of the initial concentration of thiocyanate on the induction time and kinetics of the process is discussed in more detail in Section 3.2.2.

Utilization of Nitrogen and Sulphur from Thiocyanate

In MM, nitrogen was present in $(NH_4)_2SO_4$ and sulphur in $(NH_4)_2SO_4$, $MgSO_4 \cdot 7H_2O$ and in trace solutions as $ZnSO_4 \cdot 7H_2O$, $CuSO_4 \cdot 5H_2O$. In order to

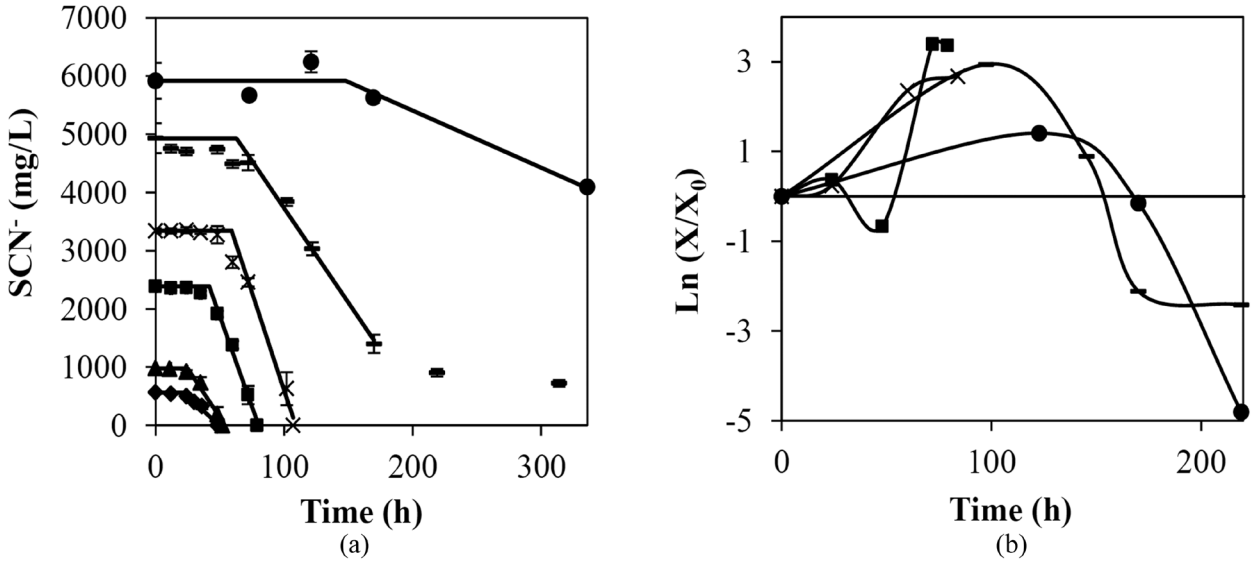

Figure 2. (a) *Thiocyanate biodegradation and (b) growth of Paracoccus thiocyanatus under different initial SCN^- concentrations (♦ 500 mg L^{-1}, ▲1000 mg L^{-1}, ■ 2500 mg L^{-1}, × 3500 mg L^{-1}, – 5000 mg L^{-1}, ● 6000 mg L^{-1}). In all cases: MM, 28ºC, 250 rpm and inoculum size of (2.06 ± 1.26) × 10^7 cfu mL^{-1}. Solid lines in (a) denote fitting of thiocyanate biodegradation to a pseudo zero-order kinetics model.*

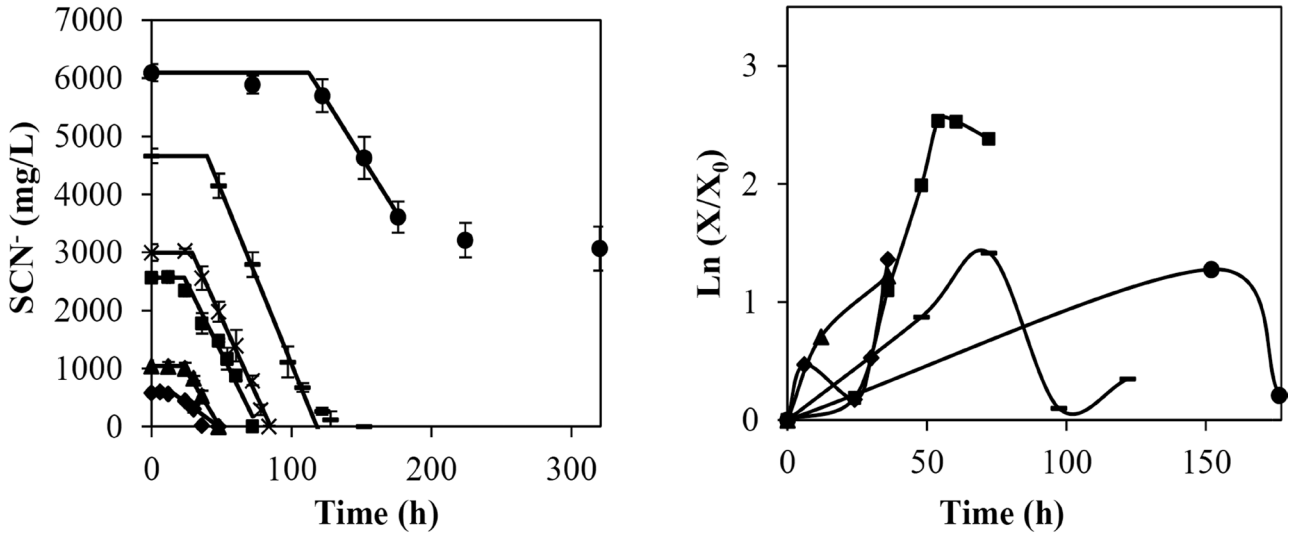

Figure 3. *(a) Thiocyanate biodegradation and (b) growth of Paracoccus thiocyanatus under different initial SCN^- concentrations (♦ 500 mg L^{-1}, ▲1000 mg L^{-1}, ■ 2500 mg L^{-1}, × 3500 mg L^{-1}, – 5000 mg L^{-1}, ● 6000 mg L^{-1}). In all cases: free medium, 28ºC, 250 rpm, inoculum age of 24 hours and inoculum size of (3.74 ± 0.47) × 10^7 cfu mL^{-1}. Solid lines in Figure a denote fitting of thiocyanate biodegradation to a pseudo zero-order kinetics model.*

discover whether the bacterium was capable of using thiocyanate as the sole N and S source, experiments were carried out using a free-mineral medium (FM) that contained these elements only in the thiocyanate molecules.

Again, different initial thiocyanate concentrations between 500 and 6,000 mg L^{-1} were tested (Figure 3). Complete degradation of thiocyanate was achieved after 40, 48, 72, 84, and 132 hrs for initial concentrations of thiocyanate of 500, 1,000, 2,500, 3,500 and 5,000 mg L^{-1}. Comparing these data with the results obtained in MM, the times for complete removal of thiocyanate were reduced when the medium had no additional sources of S and N, at all the thiocyanate concentrations used. Complete biodegradation of thiocyanate was achieved after 132 hrs in FM with an initial thiocyanate concentration of 5,000 mg L^{-1}, whereas after this time only 53% of initial thiocyanate was eliminated in MM. Of the thiocyanate initially present, 47% was removed in FM after 224 hrs when the initial concentration was 6,000 mg L^{-1}, whereas only 18% of the thiocyanate was eliminated during this time when secondary sources of S and N were added.

According to studies that focused on thiocyanate biodegradation, 2,500 mg L^{-1} of thiocyanate were biodegraded in 120 hrs with the co-culture *Klebsiella pneumoniae* and *Ralstonia* sp [6], 3,395 mg SCN^- L^{-1} were removed after 7 days by *Thiobacillus thioparus* THI115 [18] and 970 mg SCN^- L^{-1} were eliminated by *Thioalkalivibrio thiocyanodenitrificans* [24] after 30–40 days. Considering these results, our system is more efficient in terms of the thiocyanate biodegradation rate, especially when the medium is free of C, N and S sources. Kwon *et al.* [19] achieved higher removal rates by employing *Acremonium strictum*: up to 7,400 mg L^{-1} of thiocyanate was degraded in just 85 hrs.

In Figure 3(b), the bacterial growth observed during the biodegradation of thiocyanate in FM is shown. In all cases, bacterial growth exhibited the same behaviour as was observed with MM, since growth tendency and orders of magnitude were similar in both cases. Substrate inhibition of cell growth occurred for initial concentrations of thiocyanate higher than 3,500 mg L^{-1}.

Solid lines in Figures 2(a) and 3(a) denote the theoretical evolution of thiocyanate concentration according to the proposed kinetic model. In all cases, the data were successfully fitted to a zero reaction order model with induction time ($C_{SCN^-} = C_{SCN,0^-} - k(t - t_i)$). The obtained values of induction time (t_i) and the kinetic constant (k) during the fitting of each of the runs are summarized in Figure 4. Figure 4(a) shows the induction period obtained for each initial concentration of thiocyanate (SCN_0^-) and medium (MM or FM). In view of the results, the induction times in FM were always shorter than when biodegradation occurred in MM. It seems that the absence of other sources of N and S accelerate the metabolism of the bacteria in order to utilize thiocyanate as substrate. Figure 4(b) shows the kinetic constants obtained in each case. When us-

ing MM, the kinetic constant was at a maximum when the initial concentration of thiocyanate was 3,500 mg L^{-1} (67 mg $(Lh)^{-1}$). However, the maximum was obtained for an initial concentration of 5,000 mg L^{-1} (59 mg $(Lh)^{-1}$) when the biodegradation occurred in FM. Kinetic constants were higher in MM for the lowest initial concentrations of thiocyanate, whereas the opposite behaviour was observed for concentrations higher than 4,000 mg L^{-1}. Degradation rates between 1 and 87 mg $(Lh)^{-1}$ were reported for the biodegradation of thiocyanate by specific microorganisms [6,18,19,24] similar to the degradation rates obtained in this work. In fact, only *Acremonium strictum* showed higher removal rates [19].

In Figure 5, the comparison of the specific thiocyanate degradation rates in FM and MM for different initial SCN^- concentrations (500–6,000 mg L^{-1}) is shown. It is observed that the specific degradation rates are higher when no secondary sources of S and N are present in the medium. This behaviour is observed in all cases, with the exception of the final hours of the experiments with initial concentrations of thiocyanate higher than 3,500 mg L^{-1}. With initial thiocyanate concentrations of 500 and 1,000 mg L^{-1}, a rising trend of the specific degradation rate was observed. Maximum values of 0.91 and 1.17 mg $SCN^-\cdot(h\cdot mg\ cell)^{-1}$ were obtained with FM, whereas 0.32 and 0.55 mg $SCN^-\cdot(h\cdot mg\ cell)^{-1}$ were obtained with MM. For higher concentrations of thiocyanate, the specific degradation rates reached a maximum and then decreased. In all cases, the maximum value of the specific degradation rates was higher and was reached sooner with FM.

The specific growth rate (μ) was calculated by means of the following equation:

$$r_x = \frac{dX}{dt} = \mu X \tag{1}$$

where r_x is the rate of biomass growth; X is th concentration; μ is the specific biomass growth rate and t is time.

The specific growth rates (μ) *versus* thiocyanate initial concentrations obtained from batch tests are shown in Figure 6. As can be seen, μ values achieved a maximum, suggesting that there was inhibition by substrate. A non-competitive model [Equation (2)], a Teisser model [Equation (3)] and an Aiba-Edwards model [Equation (4)] were used for the fitting of substrate-inhibited growth [26].

$$\mu = \frac{\mu_{\max} \cdot S}{(K_S + S) \cdot \left(1 + \frac{S}{K_i}\right)} \tag{2}$$

$$\mu = \mu_{\max} \cdot (e^{-S/K_i} - e^{-S/K_s}) \tag{3}$$

$$\mu = \mu_{\max} \cdot S \cdot e^{\frac{-S/K_i}{(K_s+S)}} \tag{4}$$

where μ_{max} is the maximum specific growth rate; K_s is the substrate-affinity constant; and K_i is the substrate-inhibition constant.

The fitting parameters: maximum specific growth

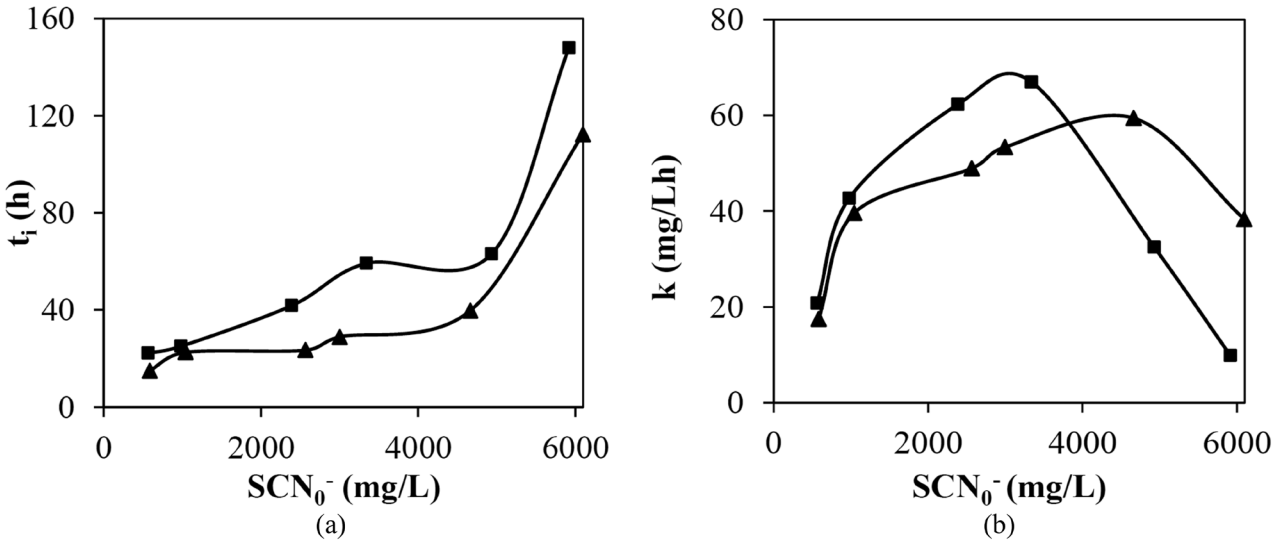

Figure 4. *(a) Induction periods (t_i) and (b) kinetic constants (k) obtained during the fitting of thiocyanate biodegradation data obtained using different initial concentrations in mineral or free media (▲ FM, ■ MM).*

rate (h^{-1}) μ_{max}, substrate-affinity constant, K_s (mg L^{-1}) and substrate-inhibition constant, K_i (mg L^{-1}) were obtained and summarized in Table 1. Experimental results and theoretical data obtained using each of the models are also compared in Figure 6.

These three models were fitted to the μ values obtained in this work and in view of the results (Figure 6) the best fits were obtained using the Teisser and Aiba-Edwards models. These models have generally been used to describe substrate inhibition of the growth of pure mi-

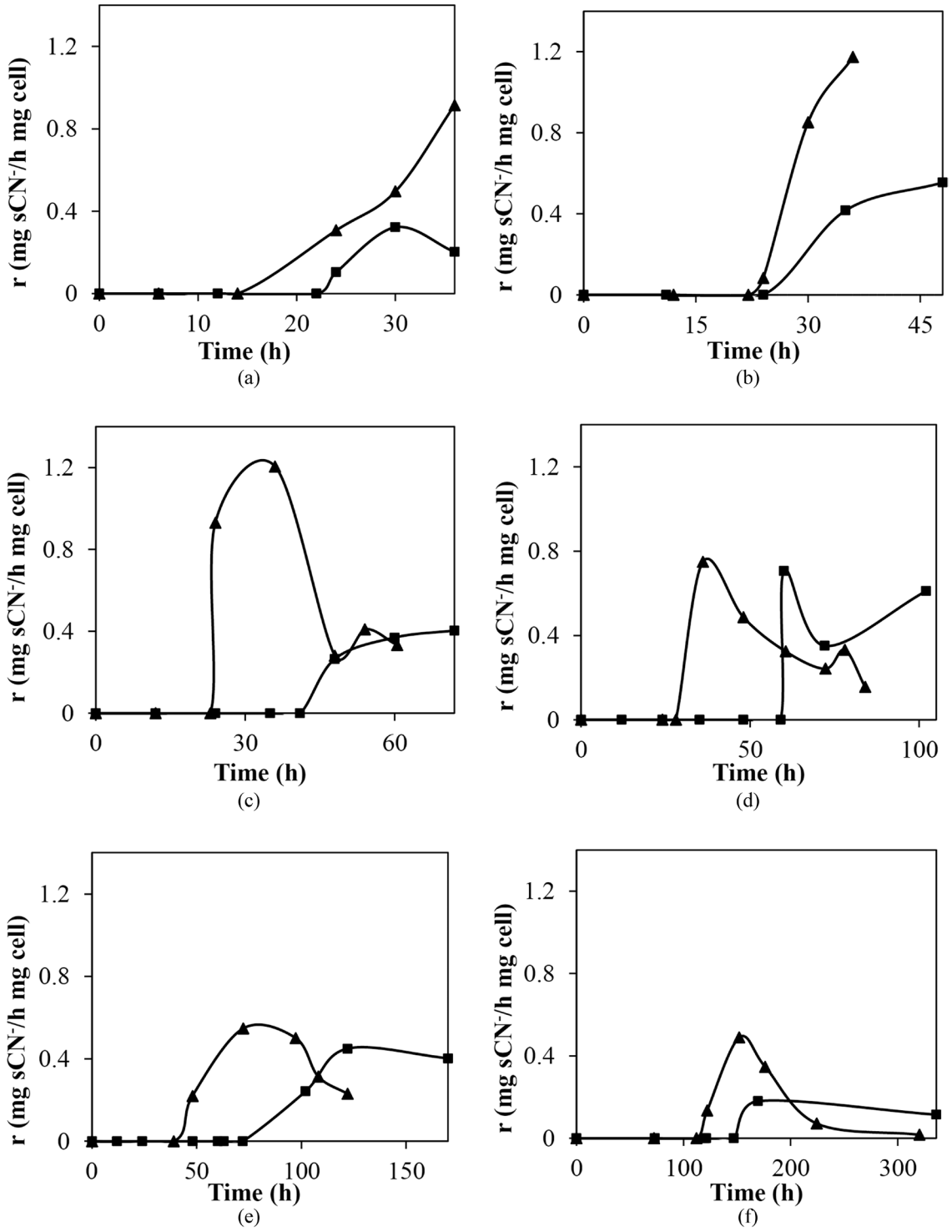

Figure 5. *Specific degradation rate for thiocyanate biodegradation in MM or FM: (a) 500 mg L^{-1}; (b) 1000 mg L^{-1}; (c) 2500 mg L^{-1}; (d) 3500 mg L^{-1}; (e) 5000 mg L^{-1}; (f) 6000 mg L^{-1} (▲FM, ■ MM). In all cases: 28°C, 250 rpm, FM inoculum size of (3.74 ± 0.47) × 10^7 cfu mL^{-1} and MM inoculum size of (2.06 ± 1.26) × 10^7 cfu mL^{-1}.*

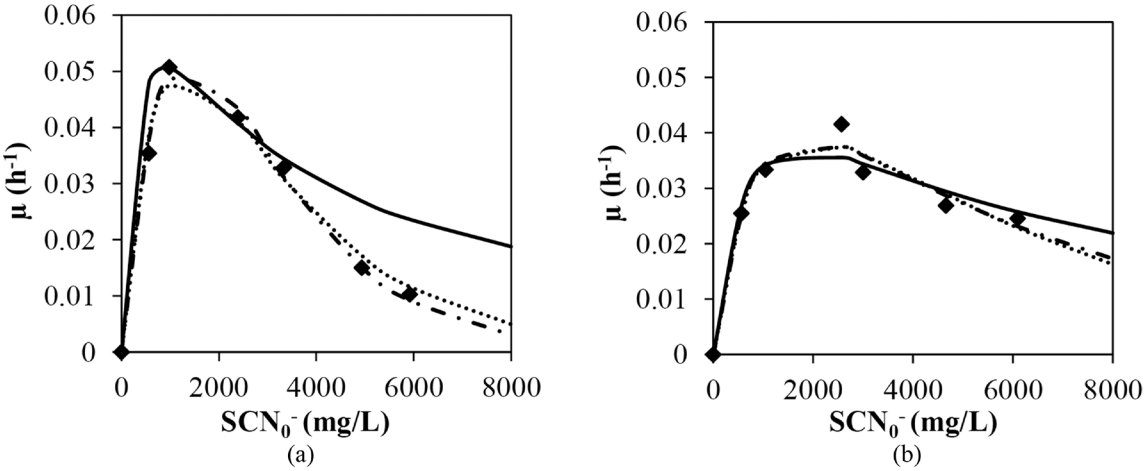

Figure 6. *Specific growth rate of suspended biomass in a thiocyanate solution (500–6000 mg L^{-1}). (♦ Experimental data, — Noncompetitive model, – · – · – · Teisser model, · · · · · Aiba-Edwards model): (a) In MM; (b) In FM. In all cases: 28ºC, 250 rpm, FM inoculum size of (3.74 ± 0.47) × 10^7 cfu mL^{-1} and MM inoculum size of (2.06 ± 1.26) × 10^7 cfu mL^{-1}.*

crobial cultures. The magnitude of K_s values indicates the affinity between substrate and microorganism [26]. For the Teisser and Aiba-Edwards models, K_s in the case of FM was slightly lower than that obtained with MM, indicating that the biomass has a higher affinity for the substrate in the case of mineral medium with no additional sources of N or S. The inhibition constant K_i is the substrate concentration at which μ is reduced to 50% of μ_{max} due to substrate inhibition. The magnitude of this parameter indicates the inhibition tendency and the degree of toxicity of the substrate towards the microorganisms [26]. Comparing the K_i values obtained in MM and FM for the Teisser and Aiba-Edwards models, it can be concluded that the presence of additional sources of N and S increases the inhibitory effect of SCN^- concentration on *Paracoccus thiocyanatus*.

The following data allow comparison with the kinetic parameters obtained for the degradation of thiocyanate with other bacteria such as *Klebsiella* sp [1]. These included μ_{max}, s, Y, K_i, which were evaluated as 0.62 ± 0.05 day^{-1}, 85 ± 8 mg SCN^- L^{-1}, 0.076 ± 0.011 mg dry cell mg^{-1} SCN^-, 131 ± 22 mg SCN^- L^{-1}, respectively, with the fourth order Runge-Kutta approximation. Chaudhari and Kodam [6] obtained values with the Haldane kinetic model of μ_{max} = 0.123 h^{-1}, K_s = 484 mg L^{-1}, K_i = 1.876 mg L^{-1} for degradation of thiocyanate with a co-culture of *Klebsiella pneumoniae* and *Ralstonia* sp. This suggested that the bacterial growth is lower for *Paracoccus thiocyanatus* than for the other species, whereas the substrate affinity was higher. At the same time, *Paracoccus thiocyanatus* shown a higher tolerance to elevated concentrations of thiocyanate than the aforementioned microorganisms.

The yield coefficient Y was estimated as $\Delta SCN^-/\Delta X$ using the experimental data of the exponential growth phase. The yield coefficients for experimental degradation data in MM and FM are listed in Table 2. In all cases, the yield coefficient in FM was lower than in MM. According to Filonov *et al.* [8], preference must be given to microorganisms that produce a lower yield of biomass per unit of the pollutant degraded. A minimum value of Y of 0.060 mg cell mg^{-1} SCN^- in MM for an initial concentration of thiocyanate of 5,920 mg L^{-1} and of 0.45 mg cell mg^{-1} SCN^- with an initial concentration of 6,090 mg L^{-1} in FM was achieved.

Presence of Carbon and Nitrogen that is Easily Assimilable by Bacterium

Influence of additional carbon and nitrogen sources

Table 1. Estimated Values of Parameters for Various Kinetic Models Employed for the Fitting of Experimental Data Obtained during Thiocyanate Biodegradation by Paracoccus Thiocyanatus.

	MM				FM			
	μ_{max} (h^{-1})	K_s (mg L^{-1})	K_i (mg L^{-1})	R^2	μ_{max} (h^{-1})	K_s (mg L^{-1})	K_i (mg L^{-1})	R^2
Noncompetitive	0.178	800	1050	92.9	0.146	1780	1790	99.2
Aiba-Edwards	0.203	1750	2280	99.3	0.094	1300	4980	99.4
Teisser	0.344	1150	1730	99.6	0.059	790	6520	99.4

Table 2. Yield Coefficients for Thiocyanate Biodegradation in MM and FM

MM		FM	
SCN_0^- (mg L^{-1})	*Y* (mg cell mg^{-1} SCN^-)	SCN_0^- (mg L^{-1})	*Y* (mg cell mg^{-1} SCN^-)
560	0.141	580	0.077
980	0.103	1040	0.064
2400	0.122	2560	0.064
3340	0.110	3000	0.108
4930	0.071	4660	0.059
5920	0.060	6090	0.045

in the wastewater during the biodegradation of thiocyanate by *Paracoccus thiocyanatus* was also checked by adding glucose (0.1 and 3%) or yeast extract (0.5 and 1%) to the MM containing thiocyanate. Figure 7 shows the evolution of thiocyanate concentration and specific degradation rate in MM with additional nitrogen and carbon sources. In view of the results (Figure 7a), thiocyanate biodegradation only occurred for the lowest glucose concentrations, 0.1 and 0.5% (61 and 72 hrs). Therefore, the system was adversely affected by the presence of glucose, since the higher the glucose concentrations, the lower was the bacterial growth obtained and the longer the time required for complete degradation of thiocyanate (data not shown). Furthermore, for glucose concentrations above 1%, there was neither bacterial growth nor thiocyanate degradation. It can be concluded that the presence of this substrate has an adverse effect on the biodegradation of thiocyanate by *P. thiocyanatus*. In Figure 7(b) the specific degradation rates of thiocyanate produced in MM containing 0.1 and 0.5% glucose is shown. It can be observed that the lower the proportion of glucose, the higher the degradation rates was.

Yeast extract was also tested as an additional carbon and nitrogen source during the biodegradation of SCN^- by *P. thiocyanatus* [Figure 7(a)]. Using this carbon and nitrogen source, high biomass concentrations were achieved, reaching values higher than 10^9 cfu mL^{-1}. These results suggest that the additional nitrogen source was utilized for biomass metabolism instead of the SCN^-. Similar behaviour was observed by Chaudhari and Kodam [6] with co-culture of *Klebsiella pneumoniae* and *Ralstonia* sp. On the other hand, according to Filonov *et al.* [8], addition of a carbon source as nutrient during naphthalene degradation by *Pseudomonas putida* G7 increases cellular activity, stimulating the growth of microorganisms capable of degrading the target compound. However, this same carbon source can inhibit degradation of some compounds, resulting in diauxic growth. Hence, it is important to add the optimal quantity of nutrients. It is a well-known fact that the addition of nutrients below or above the optimal quantity result in the reduction or cessation of the degradation. In this case, the best results were obtained when SCN^- was the only source of C, S and N.

Physiological State of Bacteria

The influence of physiological stage of the inoculum in the biodegradation process was also analysed.

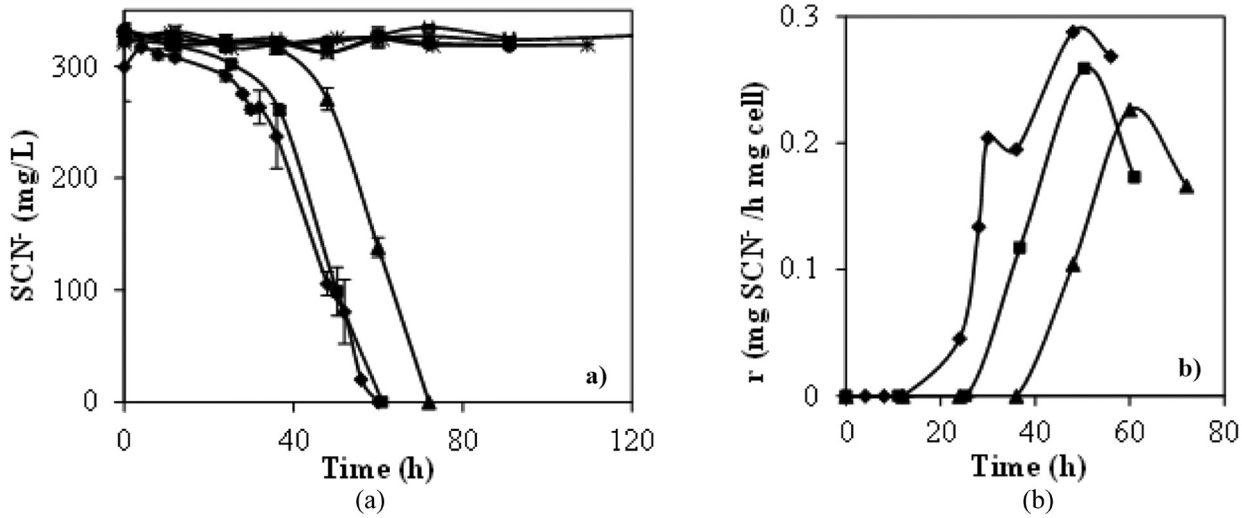

Figure 7. *Effect of addition of glucose or yeast extract in thiocyanate degradation by Paracoccus thiocyanatus. (a) Thiocyanate concentration; and (b) Specific degradation rate. In all cases: mineral medium (300 mg SCN^- L^{-1}), 28ºC, 250 rpm, inoculum size 5×10^7 cfu mL^{-1} and inoculum stage of 36 hours (♦MM, ■ 0.10% glucose, ▲0.5% glucose, ● 1% glucose, ✶ 3% glucose, × 0.5% yeast extract, – 1% yeast extract).*

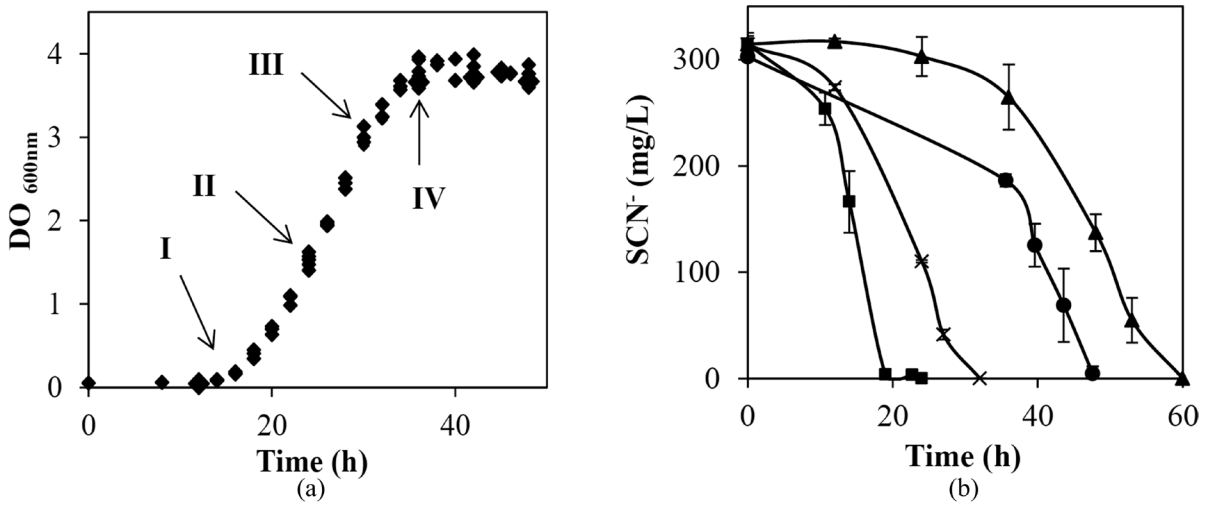

Figure 8. *(a) Growth of Paracoccus thiocyanatus in GM over 2 days. Arrows indicate the time when the inoculum was taken (b) Effect of inoculum stage on thiocyanate degradation by Paracoccus thiocyanatus. Inocula (■ I, × II, ● III and ▲ IV). In all cases: MM (300 mg SCN^- L^{-1}), 28ºC, 250 rpm and inoculum size of 5 × 10^7 cfu mL^{-1}.*

With this aim, bacterial cells taken at different growth times in GM [Figure 8(a)] were used to inoculate MM containing SCN^-, using in all cases the same inoculum size [Figure 8(b)]. When the inoculum was taken earlier, the thiocyanate degradation rate was faster. Therefore, with the inoculum obtained after 16 hrs of growth in GM (beginning of the exponential phase) complete thiocyanate degradation was achieved in just 19 hrs. However, 32 hrs where necessary if the inoculum was taken at 24 hrs of growth (middle of the exponential phase) and 60 hrs if inoculum was taken after the stationary phase of growth was reached. Silva *et al.* [23], tested the effect of the different physiological states of the bacterium *Pseudomonas fluorescens* HK44 in salicylic acid biodegradation. The percentage of salicylic acid degraded was higher (97%) when cells in the exponential phase were used, than when the inoculum corresponded to the stationary state (69%). This can be explained by the fact that cells in the exponential phase are already pre-activated and are capable of degrading their substrates faster than cells in the stationary state. In this work, it seems that cells are more active in the beginning hours of the exponential phase of growth.

CONCLUSIONS

The thiocyanate degradation process was influenced by inoculum size, so that the higher the inoculum size, the lower was the biodegradation rate. In part, this was due to the increase in the induction time required for the acclimation of the bacteria. The degradation time was reduced from 124 to 60 hrs by reducing the inoculum size from 3 × 10^8 to 5 × 10^7 cfu L^{-1}. The physiological stage of the inoculum also influenced the degradation process. In this case, it was found that when the inoculum was taken earlier, the thiocyanate degradation rate was faster. Likewise, the biodegradation rate of the system was positively influenced by the stirring speed, since higher stirring speed implies higher dissolved oxygen concentration that benefits the biodegradation of SCN^- by *P. thiocyanatus*, mainly by reducing the induction time of the process.

The degradation process of thiocyanate was different depending on the composition of the mineral medium. In the complete mineral medium (MM), *P. thiocyanatus* degraded 3,500 mg SCN^- L^{-1} in 107 hrs, whereas at concentrations greater than 5,000 mg L^{-1}, the SCN^- was not completely eliminated. When all sources of N and S were removed from the mineral medium (FM) 3,500 mg SCN^- L^{-1} was eliminated in 84 hrs and 5,000 mg SCN^- L^{-1} was completely degraded in 132 h. There were also significant differences in the specific thiocyanate degradation rates. Thus, the maximum specific degradation rate in FM was 1.21 mg SCN^-·(h·mg cell)$^{-1}$ with an initial thiocyanate concentration of 2,500 mg L^{-1}, whereas in MM the maximum specific degradation rate was 0.71 mg SCN^-·(h·mg cell)$^{-1}$ with an initial thiocyanate concentration of 3,500 mg L^{-1}. The induction time when biodegradation occurred in FM was always smaller in comparison with the induction time in MM. To improve the degradation process of thiocyanate in real wastewaters, the presence of the other sources of C, N and S that are easily assimilated by the bacteria should be avoided. It was also investigated whether the presence of organic sources of carbon and nitrogen had an adverse effect

on the biodegradation of thiocyanate by *P. thiocyanatus* and it was found that their presence led to a reduction in the degradation rates of the process.

Substrate-inhibited growth models were used for the fitting of the thiocyanate degradation by *P. thiocyanatus* and the best fits were obtained using the Teisser and Aiba-Edwards models. K_s was higher with FM than with MM, indicating that the biomass has a higher affinity for the substrate in the case of mineral medium with no additional sources of N or S. Comparing the K_i values obtained in MM and FM, it can be concluded that the presence of additional sources of N and S increases the inhibitory effect of SCN^- concentration on *Paracoccus thiocyanatus*.

ACKNOWLEGEMENTS

R. G. Combarros wishes to express gratitude for a research grant from the Government of the Principality of Asturias (Severo Ochoa Programme).

REFERENCES

1. Ahn JH, Lee S, Hwang S (2005) Growth kinetic parameter estimation of Klebsiella sp. utilizing thiocyanate. *Process Biochem 40*(3–4). http://dx.doi.org/10.1016/j.procbio.2004.06.004
2. Akcil A, Mudder T (2003) Microbial destruction of cyanide wastes in gold mining: process review. *Biotechnol Lett 25*:445–450. http://dx.doi.org/10.1023/A:1022608213814
3. American Public Health Association APHA (1999) *Standard Methods for the Examination of Water and Wastewater.* 20 th. Ed. Washington.
4. Bryant CW, Cawein CC, King PH (1988) Biological treatability of in situ coal gasification wastewater. *J Environ Eng-ASCE 114*:400–414. http://dx.doi.org/10.1061/(ASCE)0733-9372(1988)114:2(400)
5. Cai S, Li X, Cai T, He J (2013) Degradation of piperazine by Paracoccus sp. TOH isolated from activated sludge. *Bioresource Technol 130*:536–542. http://dx.doi.org/10.1016/j.biortech.2012.12.095
6. Chaudhari AU, Kodam MK (2010) Biodegradation of thiocyanate using co-culture of *Klebsiella pneumoniae* and *Ralstonia* sp. *Appl Microbiol Biotech 85*:1167–1174. http://dx.doi.org/10.1007/s00253-009-2299-7
7. Ebbs S, (2004) Biological degradation of cyanide compounds. *Curr Opin in Biotech 15*:231–236. http://dx.doi.org/10.1016/j.copbio.2004.03.006
8. Filonov AE, Karpov AV, Kosheleva IA, Puntus IF, Balashova NV, Boronin AM (2000) The efficiency of salicylate utilization by *Pseudomonas putida* strains catabolizing naphthalene via different biochemical pathways. *Process Biochem C*: 983–987. http://dx.doi.org/10.1016/S0032-9592(00)00130-8
9. Ghosh W, Roy P (2007) Chemolithoautotrophic oxidation of thiosulphate, tetrathionate and thiocyanate by a novel rhizobacterium belonging to the genus *Paracoccus*. *FEMS Microbiol Lett 270*:124–131. http://dx.doi.org/10.1111/j.1574-6968.2007.00670.x
10. Gould WG, King M, Mohapatra BR, Cameron RA, Kapoor A, Koren DW (2012) A critical review on destruction of thiocyanate in mining effluents. *Miner Eng 34*:38–47. http://dx.doi.org/10.1016/j.mineng.2012.04.009
11. Grigoréva NV, Kondratéva TF, Krasilńikova EN, Karavaiko GI (2006) Mechanism of cyanide and thiocyanate decomposition by an association of *Pseudomonas putida* and *Pseudomonas stutzeri* strains. *Microbiology 75*:266–273. http://dx.doi.org/10.1134/S0026261706030040
12. Guillén-Jiméneza F, Cristiani-Urbinab E, Cancino-Díaz JC, Flores-Morenod JL, Barragán-Huertaa BE (2012) Lindane biodegradation by the *Fusarium verticillioides* AT-100 strain, isolated from *Agave tequilana* leaves: kinetic study and identification of metabolites. *Int Biodeter Biodegr 74*:36–47. http://dx.doi.org/10.1016/j.ibiod.2012.04.020
13. Hong L. Y., Banks M. K., Schwab A. P. (2008). Removal of cyanide contaminants from rhizosphere soil. *Bioremediation Journal, 12*(4):210–215. http://dx.doi.org/10.1080/10889860802491052
14. Hung CH, Pavlostathis SG (1997) Aerobic biodegradation of thiocyanate. *Water Res 31*:2761–2770. http://dx.doi.org/10.1016/S0043-1354(97)00141-3
15. Hung CH, Pavlostathis SG (1999) Kinetics and modeling of autotrophic thiocyanate biodegradation. *Biotechnol Bioeng 62*:1–11. http://dx.doi.org/10.1002/(SICI)1097-0290(19990105)62:1<1::AID-BIT1>3.0.CO;2-Q
16. Katayama Fujimura Y, Kuraishi H (1980) Characterization of thiobacillus novellus and its thiosulfate oxidation. *J. Gen. Appl. Microbiol. 26*:357–367. http://dx.doi.org/10.2323/jgam.26.357
17. Katayama Y, Hiraishi A, Kuraishi H (1995) *Paracoccus thiocyanatus sp*. nov., a new species of thiocyanate-utilizing facultative chemolithotroph, and transfer of *Thiobacillus versutus* to the genus *Paracoccus* as *Paracoccus versutus* comb. nov. with emendation of the genus. *Microbiology 141*:1469–1477. http://dx.doi.org/10.1099/13500872-141-6-1469
18. Kim SJ, Katayama Y (2000) Effect of growth conditions on thiocyanate degradation and emission of carbonyl sulfide by *Thiobacillus thioparus* THI115. *Water Research 34*:2887–2894. http://dx.doi.org/10.1016/S0043-1354(00)00046-4
19. Kwon HK, Woo SH, Park JM (2002) Thiocyanate degradation by Acremonium strictum and inhibition by secondary toxicants. *Biotechnol Lett 24*:1347–1351. http://dx.doi.org/10.1023/A:1019825404825
20. Paruchuri YL, Shivaraman N, Kumaran P (1990) Microbial transformation of thiocyanate. *Environ Pollut 68*:15–28. http://dx.doi.org/10.1016/0269-7491(90)90011-Z
21. Salam JA, Lakshmi V, Das D, Das N (2013) Biodegradation of lindane using a novel yeast strain, *Rhodotorula* sp. VITJzN03 isolated from agricultural soil. *World J Microb Biot 29*(3):475-487. http://dx.doi.org/10.1007/s11274-012-1201-4
22. Sengupta M (1997) *Bioremediation Engineering of Mining & Mineral Processing Wastes*. Northwest Academic Pub, ISBN-10 0965302504.
23. Silva TR, Valdman E, Valdman B, Leite SGF (2007) Salicylic acid degradation from aqueous solutions using *Pseudomonas fluorescens* HK44: Parameters studies and application tools. *Braz J Microbio 38*:39–44. http://dx.doi.org/10.1590/S1517-83822007000100009
24. Sorokin DY, Tourova TP, Antipov A N, Muyzer G, Kuenen JG (2004) Anaerobic growth of the haloalkaliphilic denitrifying sulfuroxidizing bacterium *Thialkalivibrio thiocyanodenitrificans sp*. nov. with thiocyanate. Microbiology 150:2435–2442. http://dx.doi.org/10.1099/mic.0.27015-0
25. Swaroop S, Sughosh P, Ramanathanc G (2009) Biomineralization of N,N-dimethylformamide by *Paracoccus sp*. strain DMF. J Hazard Mater 171:268–272. http://dx.doi.org/10.1016/j.jhazmat.2009.05.138
26. Tazdaït D, Abdi N, Grib H, Lounici H, Pauss A, Mameri N (2013) Comparison of different models of substrate inhibition in aerobic batch biodegradation of malathion. *Turk J Engin Environ Sciences* doi:10.3906/muh-1211-7. http://dx.doi.org/10.3906/muh-1211-7
27. Vázquez I., Rodríguez J., Mara-ón E., Castrillón L., Fernández Y. (2006) Simultaneous removal of phenol, ammonium and thiocyanate from coke wastewater by aerobic biodegradation. *J of Hazard Mater B 137*:1773–1780. http://dx.doi.org/10.1016/j.jhazmat.2006.05.018
28. Vedula R. K., Dalal S., Majumder C. B. (2013). Bioremoval of cyanide and phenol from industrial wastewater: An update. *Bioremediation Journal, 17*(4):278–293. http://dx.doi.org/10.1080/10889868.2013.827615
29. Zohar S, Kviatkovski I, Masaphy S (2013) Increasing tolerance to and degradation of high p-nitrophenol concentrations by inoculum size manipulations of Arthrobacter 4Hβ isolated from agricultural soil. *Int Biodeter Biodegr 84*:80–85. http://dx.doi.org/10.1016/j.ibiod.2012.05.041

5.5. Interacciones en la biodegradación de ácido salicílico por *Pseudomonas putida* por presencia de co-sustratos (tiocianato) y otras bacterias (*Paracoccus thiocyanatus*)

La presencia de otros contaminantes o de otras bacterias supone, en el proceso de biodegradación, la aparición de interacciones cuyos efectos pueden resultar positivos o negativos en el proceso.

El objetivo principal de esta sección es el estudio de las interacciones surgidas durante la biodegradación simultánea del ácido salicílico y del tiocianato por un co-cultivo formado por las bacterias *Pseudomonas putida* y *Paracoccus thiocyanatus*. Para ello se ha analizado previamente las interacciones producidas en el proceso de biodegradación de cada uno de los compuestos individuales. En la biodegradación del ácido salicílico por *P. putida* se estudió el efecto que causaba sobre el proceso la presencia de tiocianato, de la bacteria *P. thiocyanatus* y de ambos parámetros a la vez. En el caso de la biodegradación del tiocianato por *P. thiocyanatus* la presencia del ácido salicílico, de la bacteria *P. putida* o de ambos parámetros a la vez fueron las opciones analizadas.

Un amplio intervalo de concentraciones del ácido salicílico y de tiocianato, diferentes condiciones de cultivo y de composición del medio salino fueron empleados para obtener las condiciones óptimas de trabajo. En base a los resultados obtenidos, se han determinado la aparición de efectos sinérgicos e inhibitorios entre las especies y se ha definido un modelo cinético para el proceso.

El estado fisiológico de la población bacteriana del co-cultivo se ha monitorizado mediante el uso de la técnica citometría de flujo determinando la evolución del mismo con el tiempo y en función de los parámetros considerados en el estudio.

Los resultados de este trabajo se presentan a través de una publicación cuya referencia y estado se muestran a continuación.

Referencia: Combarros, R.G, Collado, S., Laca, A., Díaz, M. Understanding the Simultaneous Biodegradation of Thiocyanate and Salicylic Acid by *Paracoccus thiocyanatus* and *Pseudomonas putida*. International Journal of Environmental Science and Technology. DOI 10.1007/s13762-015-0906-y.

Estado: Aceptada

Int. J. Environ. Sci. Technol.
DOI 10.1007/s13762-015-0906-y

ORIGINAL PAPER

Understanding the simultaneous biodegradation of thiocyanate and salicylic acid by *Paracoccus thiocyanatus* and *Pseudomonas putida*

R. G. Combarros[1] · S. Collado[1] · A. Laca[1] · M. Díaz[1]

Received: 9 June 2015 / Accepted: 7 October 2015

Abstract Phenolic and cyanide compounds, which frequently appear mixed in several industrial effluents, are difficult to be biodegraded under certain conditions. In this work, salicylic acid (SA) and thiocyanate (SCN^-) were selected as model pollutants of these two families and experiments of biodegradation with specific microorganisms were developed. It was found that the best well-known bacteria able to biodegrade each one of these pollutants, *Pseudomonas putida* for SA and *Paracoccus thiocyanatus* for SCN^-, do not biodegrade the other one. Therefore, the co-culture was required, producing interesting interaction phenomena. When both pollutants were simultaneously biodegraded, a commensalism effect was observed improving SCN^- removal. Experimental data for SCN^- and SA removals were successfully fitted to zero reaction kinetic orders, with induction time in the case of SCN^-, and substrate dependences were fitted to Tessier models. A flow cytometry method was developed and employed to obtain the evolution of the viable, damaged and dead cells for different substrate concentration and the degree of agglomeration in the co-culture experiments.

Keywords Biodegradation · Co-culture · Flow cytometry · Salicylic acid · Substrate inhibition · Thiocyanate

Electronic supplementary material The online version of this article (doi:10.1007/s13762-015-0906-y) contains supplementary material, which is available to authorized users.

✉ M. Díaz
mariodiaz@uniovi.es

[1] Department of Chemical and Environmental Technology, University of Oviedo, c/Julián Clavería s/n, 33071 Oviedo, Asturias, Spain

Introduction

Activated sludge plants are the most widespread solution for the treatment of industrial wastewaters. Nevertheless, effluents from industrial plants such as petrochemical industries, coke-processing plants, metal finishing units or pharmaceutical factories, are difficult to be biodegraded, due to the toxic properties of some pollutants usually present in them (Banerjee 1996; Chaudhari and Kodam 2010; Huang et al. 2013). Besides, if these toxics are not degraded in situ, they can affect the performance of centralized industrial wastewater treatment plants, which receive the effluents from various industrial parks (Fall et al. 2012; Lei et al. 2010). The biodegradation of a mixture of pollutants from different industrial sources by means of an activated sludge system is very complex and analysis of the interactions that occur between substrates and bacteria helps to get a general comprehensive approach of the entangled relations occurring during the activated sludge treatment.

The physical, chemical or biological degradation of the most of toxic compounds usually present in industrial wastewaters is well documented (Collado et al. 2009, 2010; Kim et al. 2008; Li et al. 2011; Marañón et al. 2008). Particular importance has been devoted to the biological removal of phenolic and cyanide compounds by activated sludge systems, either together or separately (Banerjee 1996; Huang et al. 2013; Juang and Tsai 2006; Kwon et al. 2002; Sharma et al. 2012). These two families of compounds, which frequently appear simultaneously in wastewaters from different industrial sectors, such as the pharmaceutical or iron and steel industries, are strictly regulated worldwide because of their extreme toxicity (Li et al. 2011). This has caused the development of several researching works investigating the biodegradation of these kinds of compounds. In some of these works, a real

Published online: 29 October 2015

wastewater and a bioaugmented or native mixed culture are used (Kim et al. 2008; Li et al. 2011; Marañón et al. 2008; Staib and Lant 2007), focusing on the global yields and rates obtained during the treatment or on possible changes in reactor configuration or operational conditions. Due to the high variability in the activated sludge biocenosis and even in the wastewater composition, the extrapolation of conclusions is very complicated and the interactions between bacteria and pollutants are complex and frequently not studied. So, the biological reactors in these studies were frequently considered as "black boxes" difficult to predict and control (Herrero and Stuckey). Others woks use model pollutants or synthetic wastewaters and pure cultures (Agarry et al. 2009; Agarry and Solomon 2008; Arutchelvan et al. 2005; Combarros et al. 2014, 2015; Juang and Tsai 2006; Kim and Katayama 2000; Kwon et al. 2002). The aim of these studies is usually to define the capacity of the bacterium to degrade a specific compound, the biodegradation pathway and the effect of the culture conditions on the bacterial activity. Pure cultures usually show lower resistance to stress conditions than mixed ones, amplifying the response of the system to perturbations. The removal of phenol or cyanide compounds in biological wastewaters processes using pure cultures of *Pseudomonas*, *Klebsiella*, *Ralstonia*, *Thibacillus* or *Paracoccus* has been analyzed (Agarry et al. 2009; Agarry and Solomon 2008; Combarros et al. 2014, 2015; Juang and Tsai 2006; Kim and Katayama 2000; Kwon et al. 2002). The main limitation of these studies is that they provide too simple scenarios, which usually do not reflect the complexity of the interactions.

Finally, a third group of papers employ co-culture, mixed culture or bioaugmentation. It is very common that the target contaminant can only be degraded by a very specific mixture of microorganisms that cooperate in a synergistic way. Therefore, a simplified model of the activated sludge can be built for the treatment of specific pollutant, including only the strains involved in their degradation (Chaudhari and Kodam 2010; Fuentes et al. 2014; Huang et al. 2013; Ibáñez et al. 2014; McGenity et al. 2012; Mikesková et al. 2012). The aim is to obtain a system sufficiently complex to simulate a real sludge but, at the same time, simple enough to allow the study of the interactions between species (Mikesková et al. 2012). Works using this approach are focused on the study of the degradation of a single or more compounds by two or more bacteria. In these works, persistent symbiotic interactions between bacteria or co-metabolism phenomena between compounds are frequently reported (Mikesková et al. 2012).

The bacteria species most commonly used for the biodegradation of phenolic and cyanide compounds are *Pseudomonas* and *Paracoccus*. Surprisingly, as far as we know, there are no studies dealing with the simultaneous biodegradation of cyanide and phenolic compounds using a co-culture of both species. This information would be very useful to determine synergetic effects between species comparing with results obtained using mixed cultures (Herrero and Stuckey; McLaughlin et al. 2006; Shivaraman et al. 1985). Besides, this kind of studies is also necessary as previous step for investigating the potential benefits that may be obtained by adding selected pure cultures to a mixed one in order to improve the degradation of these xenobiotics (*bioaugmentation*) (Herrero and Stuckey; McGenity et al. 2012; McLaughlin et al. 2006).

Taking into account these considerations, the aim of the present work has been to evaluate the simultaneous biodegradation of thiocyanate (as model of cyanide pollutant) and salicylic acid (as model of phenolic pollutant) by a co-culture of *P. thiocyanatus* and *P. putida*. For this purpose, the individual and simultaneous biodegradations of different concentration of thiocyanate and salicylic acid by a co-culture of both bacteria have been monitored. In basis of experimental results, the synergy/inhibitory phenomena between species are determined and a kinetic model defined. Additionally, a flow cytometry procedure by using double staining (cFDA/PI) has been developed and tested with the aim of determining the evolution of the physiological status of the co-culture bacteria and the influence of parameters considered.

Materials and methods

Media composition

Initial biodegradability tests of each pollutant by each bacterial species were carried out using the mineral medium recommended by Combarros et al. (2014, 2015) (PpMM for *Pseudomonas putida* and PtMM for *Paracoccus thiocyanatus*). For co-culture experiments, a combination of both mineral media was selected (CCMM), its final composition being: 0.5 g L^{-1} K_2HPO_4, 0.3 g L^{-1} $(NH_4)_2SO_4$, 0.05 g L^{-1} $MgSO_4{\cdot}7H_2O$, 0.01 g L^{-1} $FeCl_3{\cdot}6H_2O$, 0.01 g L^{-1} $CaCl_2{\cdot}2H_2O$, and 0.05 g L^{-1} tryptone and 10 mL L^{-1} of trace solution. The trace solution was composed of 8 mg L^{-1} $ZnSO_4{\cdot}7H_2O$, 4 mg L^{-1} H_3BO_3, 4 mg L^{-1} $Na_2MoO_4{\cdot}2H_2O$, 4 mg L^{-1} $CuSO_4{\cdot}5H_2O$, 4 mg L^{-1} $MnCl_2{\cdot}4H_2O$, 4 mg L^{-1} $CoCl_2{\cdot}6H_2O$. As can be observed, CCMM medium contained all components of individual media, selecting the higher concentration when a compound was present in both media.

Microbial strain and culture conditions

A previously isolated *Paracoccus thiocyanatus* [BCCM, Belgian Coordinated Collections of Microorganisms (LMG 24666)] and *Pseudomonas putida* [Leibniz Institute DSMZ-German Collection of Microorganism and Cells Cultures, Germany (DSM 4478)] were chosen for degrading thiocyanate and salicylic acid, respectively.

P. thiocyanatus colonies, which had been grown in growth medium (PtGM) agar for 4 days at 30 °C, were inoculated into 250-mL Erlenmeyer flasks containing 50 mL of PtGM. PtGM composition was 5 g L^{-1} peptone, 5 g L^{-1} beef extract, 5 g L^{-1} yeast extract, 2.5 g L^{-1} NaCl, 0.1 g L^{-1} K_2HPO_4 and 0.05 g L^{-1} $MgSO_4{\cdot}7H_2O$ (Combarros et al. 2015). After incubation at 28 °C and 250 rpm for 24 h, an aliquot was taken and used as an inoculum for subsequent experiments. In the same manner, *P. putida* colonies, which had been grown in growth medium (PpGM) agar for 1 day at 30 °C, were inoculated into 250-mL Erlenmeyer flasks containing 50 mL of PpGM. PpGM composition was peptone 5 g L^{-1}, meat extract 3 g L^{-1}, KH_2PO_4 0.422 g L^{-1}, K_2HPO_4 0.375 g L^{-1}, $(NH_4)_2SO_4$, 0.244 g L^{-1}, $MgSO_4{\cdot}7H_2O$ 0.05 g L^{-1}, $C_6H_{11}NO_7Fe$ 0.054 g L^{-1}, $CaCl_2{\cdot}12H_2O$ 0.015 g L^{-1} and NaCl 0.015 g L^{-1} (Combarros et al. 2014). After incubation at 30 °C and 150 rpm for 16 h, an aliquot was also taken and used as an inoculum for subsequent experiments. In both cases, the inocula were centrifuged at 10,160×*g* for 10 min and the supernatants were eliminated so that only bacterial cells were added to the corresponding mineral medium to avoid introducing compounds from the growth medium.

For the biodegradations using an only bacterium, the culture conditions for each bacteria were chosen as recommended for an optimum growth, i.e., 200 rpm and 30 °C in 250-mL Erlenmeyer flasks containing 100 mL of PpMM for *P. putida* and 250 rpm and 28 °C in 500-mL Erlenmeyer flaks containing 100 mL of PtMM for *P. thiocyanatus* (Combarros et al. 2014, 2015). The biodegradation conditions selected for the co-culture were 30 °C, 250 rpm and 100 mL of CCMM in 500-mL Erlenmeyer flasks. In all cases, initial cells concentrations were 10^7 cfu mL^{-1} of each bacterium.

Biodegradation experiments

Table S1 shows the experiments carried out in this work in order to determine the biodegradation potential and the effects of the pollutants on the pure cultures (rows 1–6), the effect of composition medium (rows 8 and 10), and the culture conditions (rows 7 and 9) on SCN^- or SA biodegradations using pure cultures and the interactions between species during the simultaneous biodegradation of SA and SCN^- (rows 11–15).

Flow cytometry analysis

Staining procedures

Samples from cultures were harvested by centrifugati
16,000×*g* for 5 min. Before staining, cells were wa
twice in phosphate-buffered saline (PBS; pH 7.4, sterile and filtered at 0.22 μm) and were then held in the "hot spot" of a sonication bath for 2 s to prevent bacterial aggregation before flow cytometric analysis (Hewitt and Nebe-von-Caron 2004). Propidium iodide (PI; Invitrogen), and carboxyfluorescein diacetate (cFDA; Invitrogen) were used as fluorescent dyes in a dual-staining procedure (cFDA/PI) in order to evaluate cell physiological status. Staining procedures were performed as previously reported Alonso et al. (Alonso et al. 2012). Total counts of cells were determined by staining with SYBRgreen (SYBRgreen; Invitrogen), a green fluorescent cell-permeable DNA probe (Foladori et al. 2010; Nielsen et al. 2009), to differentiate the microorganisms from other particles in samples (background). Fluorescent microspheres (Perfect Count; Cytognos, Spain) were used as internal standards in each sample, following the supplier's recommendations for ratiometric counting (Quirós et al. 2007). In order to obtain a significant number of cells to ensure the efficiency of the test, 2000 microspheres were acquired in each analysis. Analyses were performed in triplicate for each dye, including an un-stained sample as a control.

Stock solutions were prepared as follows: PI was made up to 1 mg mL^{-1} in distilled water (0.22 μm filtered) and maintained at 4 °C, whereas cFDA and SYBRgreen were prepared in dimethyl sulfoxide (Sigma-Aldrich) at a concentration of 1 mM and stored at −20 °C. PI staining was prepared by diluting the stock solution in sterile distilled water and adding this work solution to the cell suspension at a final concentration of 5 μg mL^{-1}. This mixture was then incubated for 30 min in the dark at room temperature. Working solutions of cFDA were made up to 10 μM in PBS containing 1 mM EDTA. PI-stained samples were subsequently incubated with 0.1 μM cFDA for 15 min in dark at room temperature (Alonso et al. 2012). SYBRgreen work solution was prepared by diluting the stock solution in PBS containing 1 mM EDTA at final concentration of 0.01 mM. The SYBRgreen work solution was added to the cell suspension at a final concentration of 0.1 μM, and the mixture was incubated for 15 min in dark at room temperature (Foladori et al. 2010).

Multi-parameter flow cytometry

Flow cytometry measurements were performed using a Cytomics FC 500 flow cytometer (Beckman Coulter) equipped with a 488 and 633 nm excitation light source

from an argon ion laser. Green fluorescence from samples (corresponding to cFDA or SYBRgreen-stained cells) was collected on the FL1 channel (530 nm), whereas PI fluorescence was registered on the FL3 channel (610 nm). Each analysis was performed in duplicate at a low flow rate setting (4000 events s^{-1}). Data acquisition was carried out using Cytomics RXP software (Beckman Coulter). Gates and quadrants were established according to staining controls. For cFDA/PI dual-parameter flow cytometric analysis, data collected from 200,000 events were analyzed using Kaluza® Flow Analysis Software, Beckman Coulter. The fluorescent microspheres presented two types: A microspheres, excitable at 506 nm, and B microspheres, excitable between 365 and 650 nm.

Fluorescence and confocal microscopy

Stained samples were examined under a Leica TCSSP2-AOBS confocal laser scanning microscope (Leica Microsystems Inc., Heidelberg, Germany) at excitation wavelengths of 488 and 568 nm with an emission wavelength of 530 (green fluorescence) or 630 nm (red fluorescence) (Alonso et al. 2012), to check that the staining procedure was suitable for both bacteria (images not shown).

Analytical methods

Determinations of SA and SCN^- in the samples were performed by HPLC (Agilent 1200) using a Mediterranean sea18 column (5 µm × 25 cm × 46 cm, plus a reverse-phase column from Waters) combined with a UV detector. The limit of detection is up to 5 mg L^{-1}, so the calibration curves of both compounds were performed from 5 to 1000 mg L^{-1}, obtaining a correlation coefficient of 0.999 in both cases. The wavelengths used for detection of SA and SCN^- were 214 and 280 nm, respectively. Prior to HPLC analysis, all the samples were filtered through 0.45-µm PVDF filters. The mobile phase consisted in a mixture of two solutions: acetonitrile (solution A) and 0.4 % phosphoric acid in water (solution B) (Hsu et al. 2004). The method employed comprised a binary gradient from 30 % solution A to 95 % solution B at a constant flow rate of 0.7 mL min^{-1}. The column was maintained stable at a temperature of 40 °C during all the analyses. Retention times observed for SA and SCN^- were 5.5 and 9.4 min, respectively.

In the case of pure cultures, cell concentrations in the medium were measured by two techniques: spread plate counting on GM-agar and optical density measurement at 660 nm (Shimadzu, UV 1203). Data were converted into cell dry weight (g L^{-1}) using the corresponding calibration curves. Cell concentrations of co-culture experiments were measured by optical density at 660 nm and by flow cytometry, thus also obtaining the physiological status of the co-culture.

All experiments were carried out at least in duplicate, and each sample was analyzed in triplicate. Standard deviations (SD) obtained are shown as vertical lines in figures.

Results and discussion

Salicylic acid and thiocyanate biodegradation using pure cultures

First of all, the ability of each bacterium to remove both contaminants together or individually was studied.

Effect of SCN^- on the degradation of SA by P. putida

The biodegradation of SA acid by *P. putida* in absence or presence of SCN^- was studied in order to determine possible inhibitory effects between pollutants. So, an inoculum of *P. putida* was added into three PpMM containing 500 mg L^{-1} of SA, 500 mg L^{-1} of SA and 500 mg L^{-1} of SCN^- or 500 mg L^{-1} of SCN^-, the biodegradation conditions being maintained at 200 rpm, 30 °C and 100 mL of PpMM in 250-mL Erlenmeyer flasks. Figure 1 shows the evolution of salicylic acid and thiocyanate concentrations (Fig. 1a, b, respectively) and cell concentration (g L^{-1}) of *P. putida* (Fig. 1c) for the individual or simultaneous biodegradation runs of both pollutants.

Figure 1a shows that in absence of thiocyanate, 500 mg L^{-1} of SA was removed from the medium in just 22 h, reaching a specific and volumetric degradation rates of 2.5 mg SA (h mg cell)$^{-1}$ and 31 mg SA (Lh)$^{-1}$, respectively. The cellular growth (Fig. 1c) achieved a μ value of 0.2459 h^{-1}. However, when 500 mg SCN^- L^{-1} was added to the mineral medium, only 73 % of the initial SA concentration was removed. In addition, the removal of the SA occurred only during the first hour, remaining constant for higher times. In presence of thiocyanate, the maximum specific degradation rate, which was reached in the early hours of the process, was 0.92 mg SA (h mg cell)$^{-1}$ and then decreased. Nevertheless, the average volumetric degradation rate has a value of around 6.25 mg SA (Lh)$^{-1}$. Moreover, *P. putida* growth was not observed under these conditions (Fig. 1c). So, the presence of SCN^- in the medium negatively affects the SA removal by *P. putida*, since it completely inhibited the growth of the bacterium, reducing by half the specific SA biodegradation rate.

A similar behavior was described by Arutchelvan et al. (2005) for the biodegradation of phenol by the strains *P.*

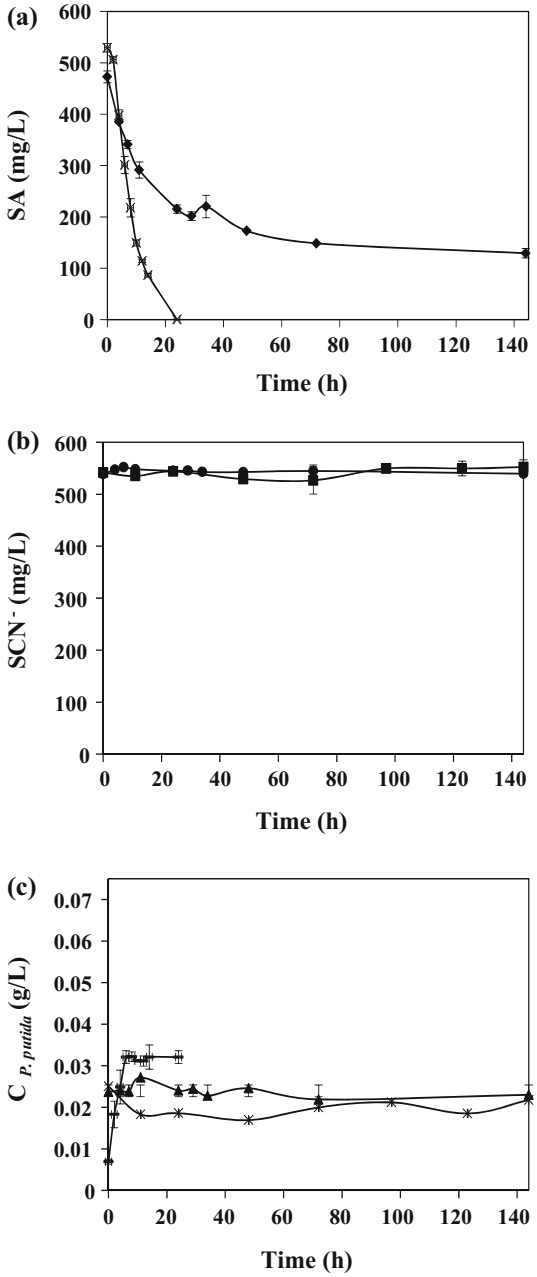

Fig. 1 Evolution of salicylic acid and thiocyanate concentrations and growth curves of *Pseudomonas putida* in PpMM. **a** Evolution of SA concentration in absence (*cross*) or presence (*diamond*) of SCN^-. **b** Evolution of SCN^- concentration in absence (*square*) or presence of SA (*circle*). **c** Growth curves for *Pseudomonas putida* in PpMM with SCN^- (*asterisk*), SA (*line*) or both (*triangle*). In all cases: initial SA concentration: 500 mg L^{-1}, initial SCN^- concentration: 500 mg L^{-1}, 200 rpm, 30 °C, 100 mL in 250-mL Erlenmeyer flasks

cepacia and *B. brevis* in presence of thiocyanate in Erlenmeyer flasks. These authors pointed out that thiocyanate concentrations up to 1000 mg L^{-1} did not inhibit the phenol degradation by *P. cepacia* and *B. brevis*, whereas, for concentrations of thiocyanate higher than 1500 mg L^{-1}, the rate of degradation was reduced considerably for *P. cepacia*. In the case of *B. brevis,* this inhibitory effect of the thiocyanate on the phenol biodegradation was more marked.

Furthermore, SCN^- biodegradations by *P. putida* in presence and absence of SA are compared in Fig Findings revealed that the removal capacity of SCN^- b *putida* (Fig. 1b) of mineral medium was negligible; after 150 h, there were no changes in SCN^- concentration in either presence or absence of SA in the mineral medium. Regarding the bacterial growth, a decrease in the biomass concentration was observed at the beginning of the biodegradation when only SCN^- was in the mineral medium, while the biomass was remaining relatively constant when SA was also present in the process (Fig. 1c).

Effect of SA on the degradation of SCN^- by P. thiocyanatus

In a similar way, the influence of SA presence in SCN^- biodegradation by *P. thiocyanatus* was also studied. For this purpose, an inoculum of *P. thiocyanatus* was added into PtMM containing 500 mg L^{-1} of SCN^-, or 500 mg L^{-1} of SCN^- and 500 mg L^{-1} of SA or 500 mg L^{-1} of SA, with the biodegradation conditions being always maintained at 250 rpm, 28 °C and 100 mL of PtMM in 500-mL Erlenmeyer flaks. Figure 2 shows the evolution of the concentrations of SCN^-, SA and *P. thiocyanatus* obtained during the biodegradation by *P. thiocyanatus* for the three experiments.

As shown in Fig. 2a, when SA was not present in the medium, 500 mg L^{-1} of SCN^- was completely removed in just 48 h, reaching a maximum specific degradation rate of 0.32 mg SCN^- (h mg cell)$^{-1}$ and a volumetric degradation rate of 20.70 mg SCN^-(h L)$^{-1}$ (not considering the initial induction time). The cellular growth (Fig. 2c) achieved a maximum μ value of 0.0314 h^{-1}. The presence of an initial stage of around 20 h where the SCN^- concentration did not change, corresponding probably to the acclimation of *P. thiocyanatus* to the new conditions, is remarkable.

However, when the SA was added to the mineral medium, *P. thiocyanatus* needed 144 h to completely remove the SCN^-. In the same manner, the acclimation of the bacteria required 48 h, twice the time needed in absence of SA. In this case, the maximum specific degradation rate was 0.35 mg SCN^- (h mg cell)$^{-1}$ [the volumetric degradation rate was 6.7 mg (SCN^-(h L^{-1}))], this value being very similar to that obtained in absence of SA. Therefore, it can be concluded that the SA had a negative impact on the initial acclimation of the *P. thiocyanatus*, but not on its final SCN^- assimilation rate. With regard to *P. thiocyanatus* growth curves, the presence of SA also had an adverse effect, considerably decreasing the growth rate of the bacterium. So, a slight cellular bacterial growth

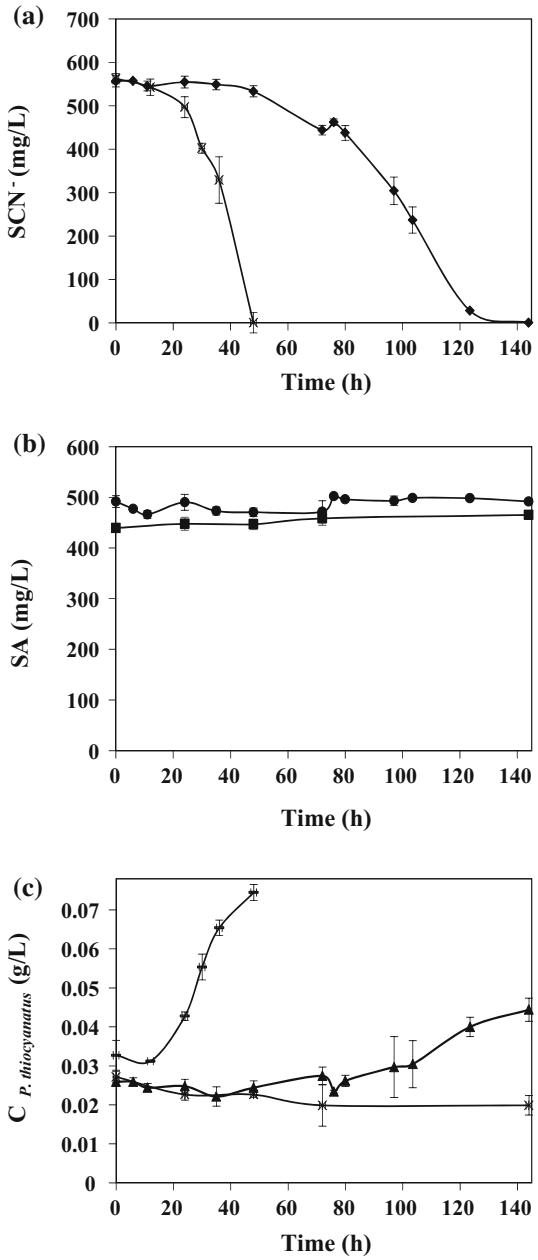

Fig. 2 Evolution of thiocyanate or salicylic acid concentrations and growth curves of *Paracoccus thiocyanatus* in PtMM. **a** Evolution of SCN^- concentration in absence (*cross*) or presence (*diamond*) of SA. **b** Evolution of SA concentration in absence (*square*) or presence of SCN^- (*circle*). **c** Growth curves for *Paracoccus thiocyanatus* in PtMM with SA (*asterisk*), SCN^- (*line*) or both (*triangle*). In all cases: initial SCN^- concentration: 500 mg L^{-1}, initial SA concentration: 500 mg L^{-1}, 250 rpm, 28 °C, 100 mL in 500-mL Erlenmeyer flasks

(Fig. 2c) was observed, obtaining a μ value of 0.0093 h^{-1}. It can be also noted that the bacterial growth and the pollutant degradation started at the same time. Comparing these results, it can be confirmed that SA presence increased the acclimation period of the *P. thiocyanatus,* adversely affecting SCN^- removal.

Kwon et al. (Kwon et al. 2002) also studied the removal of thiocyanate by *Acremonium strictum* and the inhibition by secondary toxicants in shake-flask cultures. In that research, 1200 mg L^{-1} of SCN^- was completely degraded in presence of 312 mg L^{-1} of phenol although the complete degradation of thiocyanate was delayed from 23 h without the addition of phenol to 60 h. For a phenol concentration of 625 mg L^{-1}, thiocyanate degradation was seriously inhibited and only 33 % of thiocyanate was removed after 60 h. Shivaraman et al. (Shivaraman et al. 1985) showed that phenol and cyanide had a negative influence on thiocyanate degradation.

As seen in Fig. 2b, the removal capacity of SA by *P. thiocyanatus* was checked too. The SA removal by *P. thiocyanatus* was negligible in either absence or presence of SCN^-. So, after 150 h, the SA did not change in both cases. A progressive decrease in biomass was observed when only SA was present in mineral medium. However, the biomass slightly increased at the end of the process when SA and SCN^- were simultaneously present in mineral. In view of the results, it can be stated that during the simultaneous SA and SCN^- biodegradation by a co-culture of *P. thiocyanatus* and *P. putida*, each bacterial strain degrades only SCN^- or SA, respectively.

Effect of the culture conditions on P. putida degradation

The effects of biodegradation conditions and medium composition were tested. An inoculum of *P. putida* was introduced into PpMM or CCMM, containing 500 mg L^{-1} of both contaminants and maintaining the biodegradation conditions selected for *P. putida* or co-culture shown in *Materials and methods* section. Figure 3 shows the effect of the biodegradation conditions or culture medium on SA (Fig. 3a) and SCN^- (Fig. 3b) removal and cell growth of *P. putida* (Fig. 3c).

In SA and SCN^- biodegradation by *P. putida* in PpMM using the co-culture conditions, the results show a clear improvement in the biodegradation rate, (S1) when compared with those obtained selecting the pure culture conditions. However, *P. putida* was unable to metabolize SCN^- from the medium. It must be mentioned that the only difference between both experiments is the stirring speed, 200 rpm or 250 rpm for the initial or the co-culture conditions, respectively. The modification of the stirring speed supposed doubling of the degradation rate of *P. putida* [6.25–13.6 mg SA $(L\ h)^{-1}$]. This change was mainly due to a significant increase in the biomass growth (0.0007–0.2338 h^{-1}) since the specific degradation rate remained constant. This fact suggests that higher concentration of dissolved oxygen in the medium improves the SA removal capacity of *P. putida* reducing correspondingly the convection resistance (Díaz et al. 1996). Hadibarata and

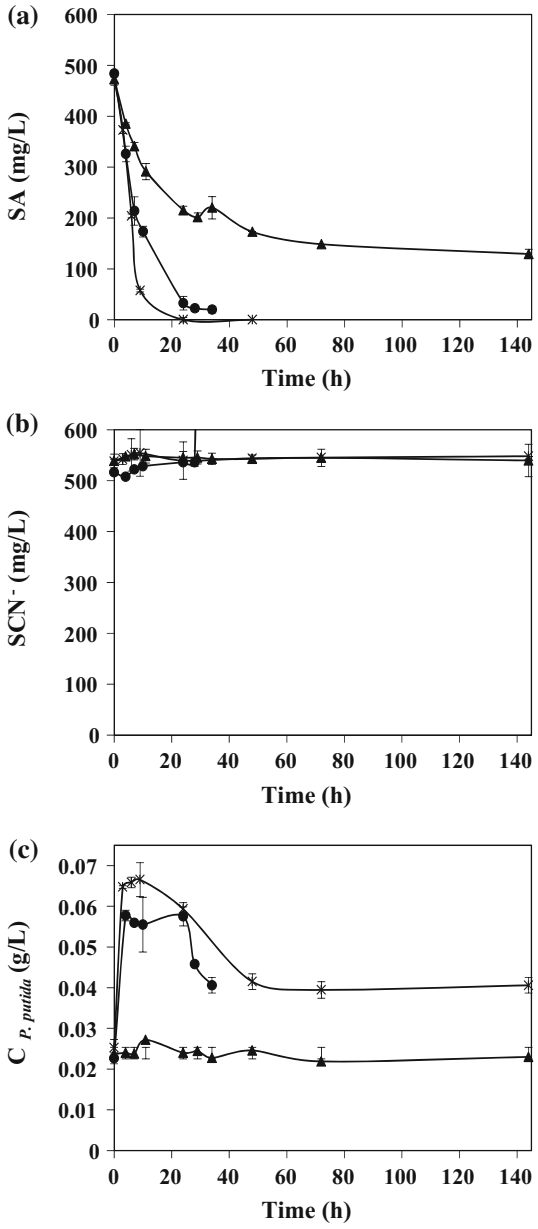

Fig. 3 Evolution of salicylic acid (**a**) or thiocyanate (**b**) concentrations and growth curves (**c**) of *Pseudomonas putida* under different biodegradation conditions: recommended conditions and medium for pure culture (*triangle*), recommended medium for pure culture but co-culture conditions (*circle*) or co-culture medium and conditions (*asterisk*). In all cases: initial SA concentration: 500 mg L^{-1}, initial SCN^- concentration: 500 mg L^{-1}, 30 °C

Teh (Hadibarata and Teh 2014) show that agitation ensures the supply of nutrients and oxygen in the system.

The SA biodegradation can even be more improved using also the CCMM instead of PpMM (see data in S1). Nevertheless, either the new conditions or the new medium did not allow removing SCN^-. In this regard, there was a more marked increase in cell growth (μ value of 0.3137 h^{-1}), with the consequent increase in the degradation rate [0.86 (mg SA (h mg cell)$^{-1}$] when the recommended medium was replaced by the co-culture one. This fact is probably due to the presence of the trace elements solution in the composition of the co-culture medium. In this sense, Qiao and Wang (2010) also observ similar behavior; they proved that trace mineral elen were the essential substrates for pyridine degraded effectively by *Paracocccus* sp strain KT-5.

Effect of the culture conditions on P. thiocyanatus

As in the case of *P. putida*, the effects of biodegradation conditions and medium composition on *P. thiocyanatus* were also evaluated. In this case, an inoculum of *P. thiocyanatus* was introduced into PtMM or CCMM, containing 500 mg L^{-1} of both contaminants and maintaining the biodegradation conditions recommended for *P. thiocyanatus* or selected for co-culture. Figure 4 shows the evolution of the SCN^- (Fig. 4a) and SA (Fig. 4b) concentrations and the *P. thiocyanatus* growth curves (Fig. 4c) obtained using the aforementioned conditions and media.

Summarizing the results of the effect of experimental conditions in PtMM, the change in two degrees in the incubation temperature is barely noticeable for either the specific degradation rate of SCN^- or cellular growth values (see the result in S1). The increase in the temperature either had effect on the SCN^- removal; its concentration remained constant either at 28 or at 30 °C. Cai et al. (Cai et al. 2013) show that the optimal temperature range for *Paracoccus* sp. is between 30 and 35 °C, range in which a small change in temperature marks a very slight shift in cell growth.

Regarding the effect of the medium composition, a decrease in the lag phase (30 h) and an increase in cell growth (0.0186 h^{-1}) were obtained by adding tryptone as additional source of N. The results in this case were similar to the values obtained in individual SCN^- biodegradation by *P. thiocyanatus*. However, SA was again not removed from the mineral medium. This suggests that the additional nitrogen sources were utilized for biomass production. Similar behavior was observed by Chaudhari and Kodam (2010) with co-culture of *Klebsiella pneumoniae* and *Ralstonia* sp. and by Combarros et al. (2015) with *P. thiocyanatus*.

Simultaneous biodegradation of thiocyanate and salicylic acid by co-culture

Once the effect of the pollutants on each bacterium has been evaluated and the best operating conditions for co-culture have been selected, the simultaneous biodegradation of SA and SCN^- in CCMM by *P. putida* and *P. thiocyanatus* co-culture was tested. The biodegradation conditions were 30 °C, 250 rpm and 100 mL of CCMM in

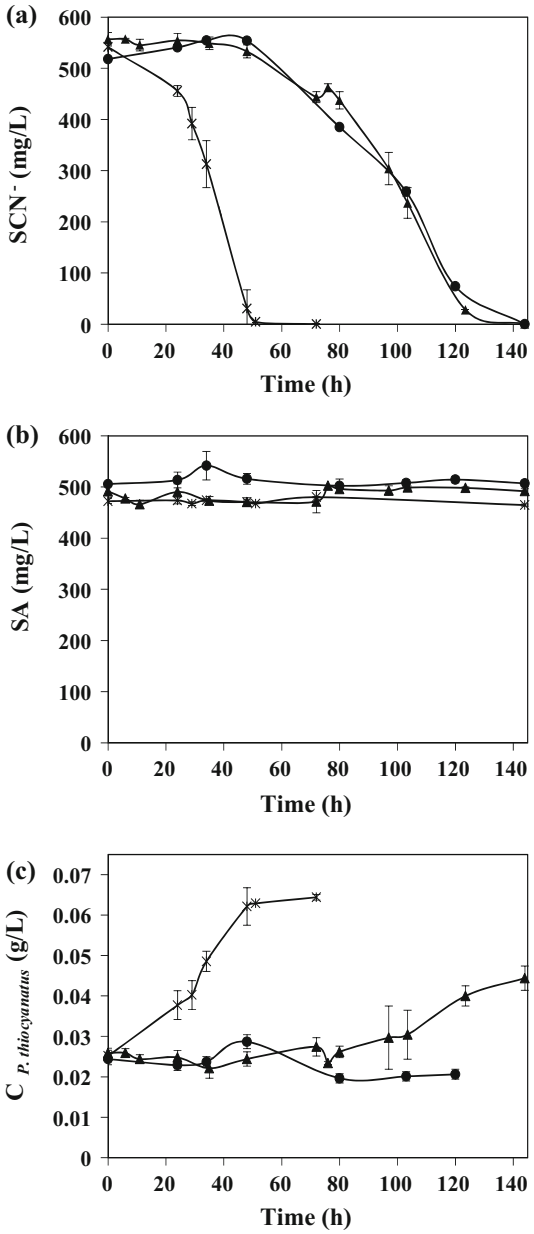

Fig. 4 Evolution of thiocyanate (**a**) or salicylic acid (**b**) concentrations and growth curves (**c**) of *Paracoccus thiocyanatus* under different biodegradation conditions: recommended conditions and medium for pure culture (*triangle*), recommended medium for pure culture but co-culture conditions (*circle*) or co-culture medium and conditions (*asterisk*). In all cases: initial SCN^- concentration: 500 mg L^{-1}, initial SA concentration: 500 mg L^{-1}, 250 rpm, 100 mL in 500-mL Erlenmeyer flasks

500-mL Erlenmeyer flasks. Initial cells concentrations of 10^7 cfu mL^{-1} were inoculated into de CCMM for each bacterium.

First, the behavior of the co-culture in a medium containing only SA or SCN^- was studied (see graph S2 in supplementary data). For the co-culture in presence of only SA, the SA removal was not affected by the presence of *P. thiocyanatus*. However, for the co-culture containing only SCN^-, the presence of *P. putida* involved a worsening of the SCN^- biodegradation process by *P. thiocyanatus* since the time required for SCN^- depletion was increased in 10 h. This effect was particularly marked during the acclimation period, increased from 11 to 17 h by the presence of *P. putida*.

Afterward, the effect of the initial concentrations of both contaminants (between 250 and 4000 mg L^{-1}) on the co-culture was evaluated. Figure 5 shows the biodegradation of both contaminants (thiocyanate and salicylic acid) and the cell growth for six different initial concentrations. In all cases, the medium pH was between 6.70 and 7.20.

The first thing to be pointed out is the complete removal of either SA or SCN^- for initial concentrations of both pollutants up to 2000 mg L^{-1}. However, each pollutant showed a different behavior during the biodegradation. SA removal occurred at the beginning of the process following a constant degradation rate, whereas thiocyanate needed an acclimation period to begin decreasing. This behavior was also observed for pure culture of *P. thiocyanatus*.

Obviously, the higher the initial concentration of the pollutant, the higher the time required for its complete removal. So, complete thiocyanate degradation was achieved after 25, 29 and 46 and 170 h with initial concentrations of 250, 500, 1000 and 2000 mg L^{-1}, respectively. In a similar way, 9, 12, 34 and 110 h were necessary for the complete depletion of 250, 500, 1000 and 2000 mg L^{-1} of SA, respectively. As can be seen, the SA disappeared rather faster than the SCN^-. In fact, Fig. 5a–d suggest that the biodegradation of SCN^- only starts when the SA is exhaust in the medium. Moreover, an induction period in thiocyanate removal was also observed, this lasting until the SA was completely removed from the mineral medium. This sequential removal probably is due to the double inhibitory effect of SA on the SCN^- biodegradation and on the lag phase of the *P. thiocyanatus*. Therefore, when the SA is removed by *P. putida*, its inhibitory effect on *P. thiocyanatus* also disappears and the bacterium recovers its activity. Banerjee (1996) observed a similar behavior during the biodegradation of a synthetic wastewater by activated sludge in a four-stage across-the-flow RBC reactor. According to these authors, phenol was mostly removed in the first two stages, whereas thiocyanate removal was greater in the last two stages, where inhibition due to the presence of phenol was much less. In the work of Li et al. (2011), in which a coke-oven wastewater containing phenolic compounds and thiocyanate was treated with activated sludge in a MBBR reactor, it was also observed that thiocyanate degradation rate had two different values, being smaller when the concentration of phenolic compounds in the medium was higher, while this rate increased as the phenolic compounds concentration decreased.

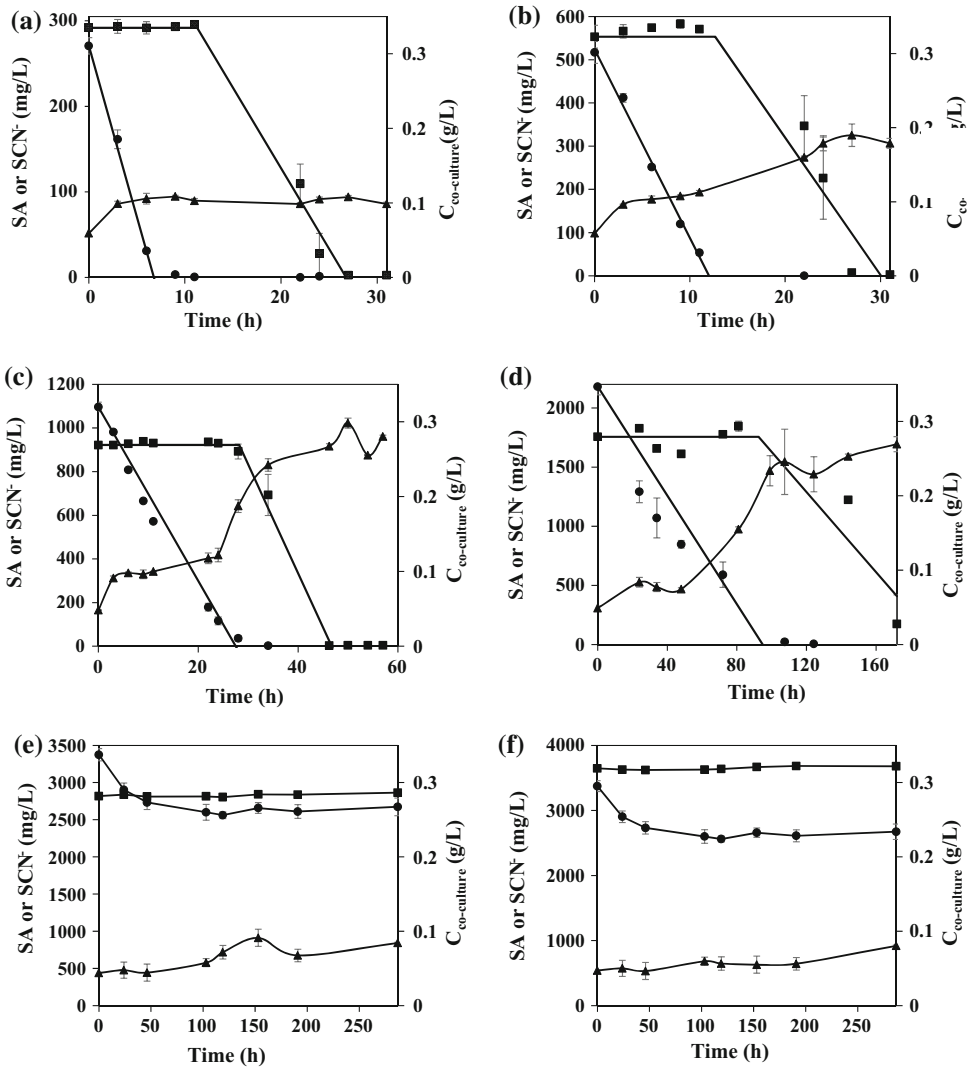

Fig. 5 Evolution of salicylic acid (*circle*) or thiocyanate (*square*) concentrations and growth curves (*triangle*) during the simultaneous biodegradation of both contaminants by a co-culture of *Paracoccus thiocyanatus* and *Pseudomonas putida* using different initial SCN^- and SA concentrations **a** 250 mg L^{-1}, **b** 500 mg L^{-1}, **c** 1000 mg L^{-1}, **d** 2000 mg L^{-1}, **e** 3000 mg L^{-1}, **f** 4000 mg L^{-1}. In all cases: CCMM, 30 °C, 250 rpm, and inoculum size of (1×10^7 cfu mL^{-1} of both bacteria). *Solid lines* in figures denote fitting of thiocyanate and salicylic acid biodegradation to a pseudo-zero-order kinetics model

When the initial concentrations were 3000 or 4000 mg L^{-1}, no removal of thiocyanate was observed. At the same time, salicylic acid concentration decreased slowly during the first 50 h and then it maintained a constant value until the end of the experiment. Thus, only 23 and 11.5 % of the initial SA amount was eliminated when the initial concentrations were 3000 and 4000 mg L^{-1}, respectively.

Figure 5 also reveals that the SA removal by *P. putida* is faster when *P. thiocyanatus* is also present in the medium. This behavior was attributed to the formation of one or several intermediates during the degradation of SA, which can be easily assimilated by both species. In this respect, the presence of *P. thiocyanatus* establishes a competence with *P. putida* for these intermediates. The lower bioavailability of these compounds, in turn, causes that *P. putida* focused its activity on the biodegradation of the parent compound, forming more intermediates and increasing also the removal rate of SA. Additionally as result of consumption of these intermediates, *P. thiocyanatus* is metabolically more active, decreasing Lag time and increasing the specific degradation rate of SCN^-. (See S1, row 10 and 15).

To validate this theory, *P. putida* was initially inoculated in CCMM containing 500 mg L^{-1} of SA and, after periods of time of 4.5, 10 or 22 h, the media were centrifuged and filtered through 0.22-μm filters in order to remove *P. putida*. Afterward, *P. thiocyanatus* was inoculated in these media. As can be seen in figure S3, *P. thiocyanatus* grew in the three media, corroborating the formation of intermediates during SA biodegradation, which can be easily assimilated by *P. thiocyanatus*. The growth was more marked with the medium obtained after 10 h of biodegradation. This can be explained if the concentration of intermediates is maximum in this case. It is logical to think that for 4.5 h, the concentration was lower

due to a lower degree of degradation of SA. For 22 h, the concentration of intermediates is lower because SA was completely removed and the intermediate is the only available carbon source, this being assimilated by *P. putida*. This theory also was validated by measuring the TOC of the samples of the SA–SCN^- biodegradation by co-culture; the results show that the intermediates TOC ($TOC_{Intermediates} = TOC_{Total} - 7 \times C_{SA} - C_{SCN}^{-}$) increase until 11 h of around 204 mg CL^{-1}; after that the TOC concentration declines gradually with time. The TOC measurements also reveals that, although the SCN^- and SA were completely eliminated from the medium, there is always a remnant of about 10 % of the TOC at the end of the experiments (final inert products, non-biodegradable by *P. putida* and *P. thiocyanatus*).

Figure 5 also shows the evolution of cell concentration in mg L^{-1} for each of the initial SCN^- and SA concentrations. An increase in biomass concentration was observed for all initial contaminants concentrations. This increase was more marked for initial concentrations of 500, 1000 and 2000 mg L^{-1}. It is also noticeable that the growth curves showed two phases. The first one, with a faster cell growth, coincides with the degradation of SA, and it is probably due to the growth of *P. putida*. In turn, the second phase of growth and the SCN^- biodegradation occurred at the same time, suggesting the growth of *P. thiocyanatus*. It can be noted that specific growth rates for *P. putida* are higher than for *P. thiocyanatus*.

As can be observed in Fig. 5, the evolution of the concentrations of either SA or SCN^- was successfully fitted to a zero-reaction-order model including term for the induction time (t_i):

$$C_i = C_{i,0} - k(t - t_i) \quad (1)$$

where i is the pollutant (SA or SCN^-) and k is the pseudo-zero-order kinetic constant, which is the same as the volumetric degradation rate. The obtained values of t_i and k during the fitting are summarized in Table 1. In view of the results for the SCN^-, the higher the initial concentration, the longer the period of induction, as might be expected. With SA, the kinetic constant initially increased with the initial concentration, and then it showed a maximum at an initial concentration of around 500 mg L^{-1} (43.6 mg $(L\ h)^{-1}$) and finally decreased, reaching a value of zero for initial concentrations higher than 2000 mg L^{-1}. The SCN^- kinetic constant also showed this behavior except that the maximum was obtained for an initial concentration of 1000 mg L^{-1} (49.8 mg $(L\ h)^{-1}$), indicating that *P. thiocyanatus* has higher tolerance for SCN^- than *P. putida* for SA. Degradation rates between 1 and 87 mg $(L\ h)^{-1}$ were reported for the biodegradation of thiocyanate by other microorganisms (Chaudhari and Kodam 2010; Kim and Katayama 2000; Kwon et al. 2002; Sorokin et al. 2004) similar to the degradation rates obtained in this work. Furthermore, Kwon et al. (Kwon et al. 2002) confirmed that the presence of phenol reduced the thiocyanate degradation rate from 52 mg $(L\ h)^{-1}$ to 6.6 mg $(L\ h)^{-1}$ when phenol concentration increased from 0 to 625 mg L^{-1}. Degradation rates between 3 and 23 mg $(L\ h)^{-1}$ were reported for the biodegradation of salicylic acid by other microorganisms (Juang and Tsai 2006; Loh and Yu 2000), the values lower than those obtained in this work. Sharma et al. (Sharma et al. 2012) studied the effect of the presence of cyanides on the biodegradation of phenolic compounds by a mixed culture: 800 mg L^{-1} of phenol was eliminated at a rate of 32 mg $(Lh)^{-1}$, but when CN^- was added to the medium, the degradation rate decreased to 10.4 mg $(Lh)^{-1}$.

Comparing these results from Figs. 3 and 4, it can be concluded that the presence of *P. thiocyanatus* has no effect on the SA bioremoval rate by *P. putida*. Concerning SCN^-, the time required for its complete depletion by *P. thiocyanatus* when *P. putida* was present or not in the medium was 29 h or 51 h, respectively. As explained earlier, this increase in removal rate of SCN^- is due to the reduction in the inhibitory effect of the SA, which is progressively assimilated by *P. putida*. In the case of co-culture, the value of μ was 0.0295 h^{-1}, considering the total optical density, a value that lies between (0.3137–0.0186) h^{-1} for the pure cultures of *P. putida* and *P. thiocyanatus*.

Regarding the specific degradation rates in the co-culture, it was observed for all the initial concentrations that it increased during the first minutes, achieving a maximum, and then decreased due to the depletion of the substrates. With respect to the effect of the initial concentrations of the pollutants, the specific degradation rate in the case of SA had a maximum value of 0.61 (mg SA(mg cell h) $^{-1}$) when initial SA and SCN^- concentrations were 1000 mg L^{-1},

Table 1 Induction periods and pseudo-zero-order kinetic constants obtained at different initial concentrations of thiocyanate and salicylic acid by a co-culture of *Paracoccus thiocyanatus* and *Pseudomonas putida*

SA_0 (mg L^{-1})	SCN_0^- (mg L^{-1})	SA		SCN^-	
		t_i (h)	k [mg/(L h^{-1})]	t_i (h)	k [mg/(L h^{-1})]
270.7	291.9	0	39.9	11.3	18.8
516.9	553.1	0	43.6	12.7	31.8
1096.4	921.7	0	39.8	28.2	49.8
2180.9	1756.2	0	14.0	92.4	16.9

whereas the maximum specific degradation rate for SCN^- was 0.40 (mg SCN^-(mg cell h)$^{-1}$), being achieved when the initial concentrations were 500 mg L^{-1}. In all cases, the specific degradation rate obtained during simultaneous SA and SCN^- biodegradation by the co-culture is an order of magnitude higher than that obtained by Banerjee (Banerjee 1996). Phenol-specific degradation rate value obtained was 0.021 mg SA(mg VSS h)$^{-1}$ in RBC (rotating biological contactor reactor) first stage, while SCN^--specific degradation rate was 0.026 mg SCN^- (mg VSS h)$^{-1}$ in the final stage of RBC reactor.

As it was previously explained, the growth curves showed two faster increments. The first one was due to the growth of *P. putida* during the biodegradation of the SA, whereas the second one coincided with the biodegradation of SCN^-, so it was attributed to the growth of *P. thiocyanatus*. In order to corroborate this assumption, *P. putida* growth using the co-culture medium and conditions was compared in presence and absence of *P. thiocyanatus* (S4). As can be seen, the growth of a pure culture of *P. putida* coincided exactly with the initial growth observed in the co-culture, so this fact suggests the sequential growth of the bacteria. In the same way, *P. thiocyanatus* growth using the co-culture medium and conditions in presence and absence of *P. putida* were compared (S4). The bacterial growth in co-culture is greater than in the pure culture of *P. thiocyanatus*, probably due to the fact that SA had been previously removed from the medium by *P. putida*. A summary of the different tests and results obtained is given in Table S1 in the supplemental data.

So, assuming a separated growth, the growth curves for each of bacteria during the co-culture experiments can be estimated. Using these data, the specific growth rates can be calculated for both bacteria: μ_{Pp} and μ_{Pt}. The specific growth rates (μ_i) versus salicylic acid or thiocyanate initial concentrations obtained from co-culture experiments are shown in S5. At this point, it is important to note that *P. putida* grows in presence of SA and SCN^-, whereas only SCN^- was present in the medium when *P. thiocyanatus* started to grow rapidly. For this reason, a substrate and toxic inhibition model (Eq. 2) was proposed for the fitting of the specific growth rate of *P. putida* in the co-culture. This model consists of a modification of Tessier model, in which a term defining the toxic inhibition by SCN was added (S5):

$$\mu = \left(\mu_{max} \cdot e^{-S/K_i} - e^{-S/K_s}\right) \cdot \left(1 - \frac{P}{P^*}\right)^n \quad (2)$$

where P is the concentration of toxic (SCN^-), P^* is the concentration of the toxic that slows the reaction absolutely and n is the reaction order. In our case, P^* has a value of 4000 mg SCN^- L^{-1}, as can be observed in Fig. 5.

The next fitting parameters were obtained for the growth of *P. putida* in co-culture with *P. thiocyanatus*: $\mu_{Pp\text{-}max} = 0.052\ h^{-1}$, $K_s = 552.3$ mg L^{-1}, $K_i = 2570.13$ - mg L^{-1}, $n = 0.54$; $r^2 = 0.99$. In a previous work (Combarros et al. 2014), the specific growth rates obtained for a pure *P. putida* culture with Haldane equa for SA concentrations between 0 and 530 mg L^{-1}. The values obtained were μ_{max} of 0.25 h^{-1}, K_s of 61.25 mg L^{-1} and K_i of 704.93 mg L^{-1}. Comparing these results, the value of μ_{Ppmax} in the co-culture is an order of magnitude lower than for the pure culture, while both K_s and K_i are higher, indicating that *P. putida* cells show a higher affinity and tolerance to SA in co-culture form.

In the case of the growth of *P. thiocyanatus*, where the SA was not present in the medium, the experimental data were successfully fitted to a Tessier model (S5). The next fitting parameters were obtained $\mu_{Ptmax} = 0.08\ h^{-1}$, $K_s = 329.2$ mg L^{-1}, $K_i = 755.5$ mg L^{-1} with a $r^2 = 0.97$. In a previous work, Combarros et al. (2015) reported the next parameters for Tessier model using a pure *P. thiocyanatus* culture and SCN^- as only substrate: $\mu_{max} = 0.334\ h^{-1}$, $K_s = 1150$ mg L^{-1} and K_i of 1730 mg L^{-1}. These results suggest that the substrate inhibitory effect on the *P. thiocyanatus* is more marked in the co-culture than in the pure culture.

Physiological status of co-culture of *P. thiocyanatus* and *P. putida* during shake-flask biodegradation

Figure S6 in supplementary data shows the changes in the physiological status of co-culture in terms of metabolic activity and membrane integrity during shake-flask biodegradation. The different panels of S6 illustrate the dual flow cytometric assessment of green fluorescence versus red fluorescence (cFDA/PI). The cFDA is cleaved by the esterase activity inside the living cells, thus releasing a polar fluorescent portion which is unable to pass through the intact membrane. The PI can only cross the plasmatic membrane if it is permeabilized, corresponding to those cells whose membranes are compromised. Taking this into account, the upper left gate (viable and active) of dot plots in S6 shows cells with esterase activity and membrane integrity (cFDA(+), PI(−)). Damaged cells (cFDA(+)/PI(+)) are shown in the upper right gate (damage), being bacteria active but no viable. Likewise, dead cells (cFDA(−), PI(+)) are shown in the lower gate.

Results based on esterase activity and membrane integrity suggest that the loss of metabolic activity was progressive, leading first to an intermediate "damaged" cell state and then irreversibly to cell death. Cytograms show that in the case of the lower SA and SCN^- concentrations, there was a cellular growth and these cells remained within the viable cells gate (Fig. S6A, S6B and

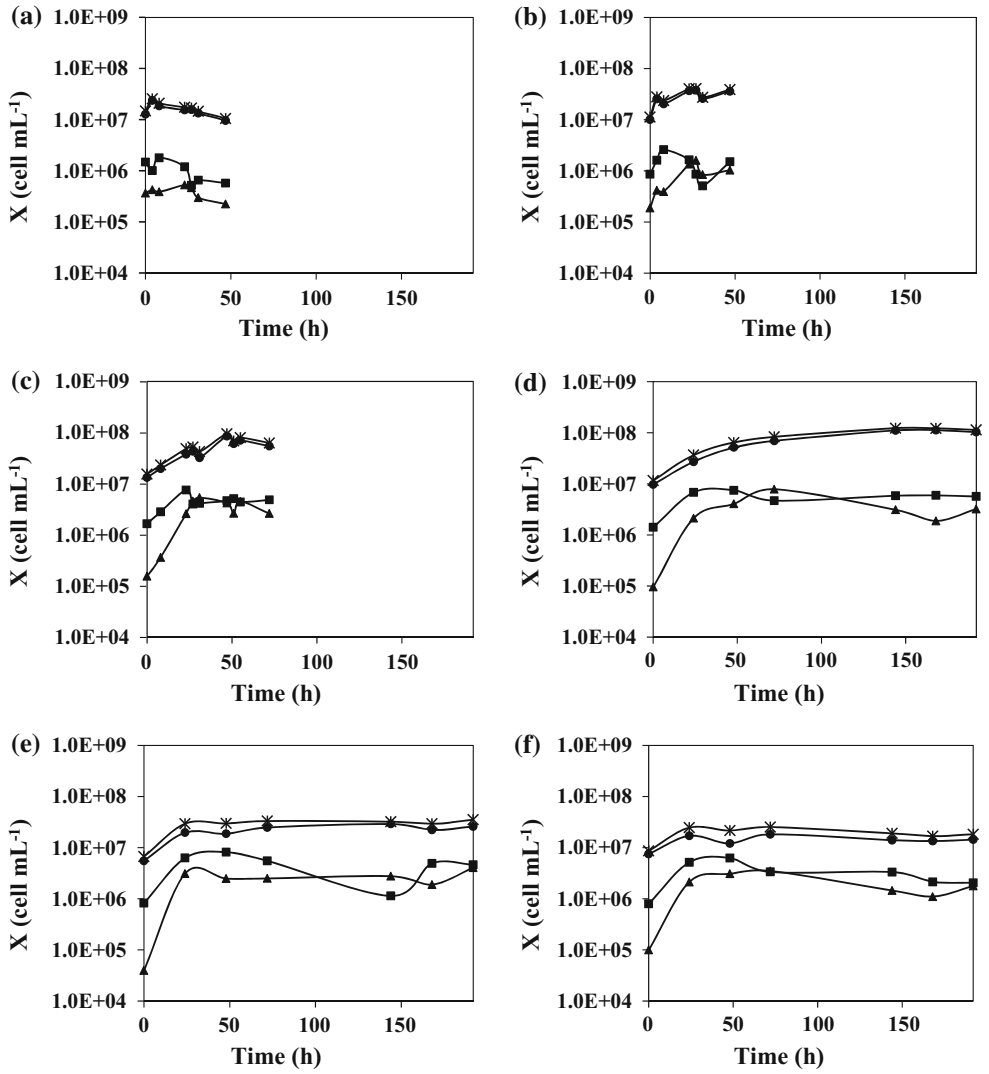

Fig. 6 Cell subpopulations concentration of *Paracoccus thiocyanatus* and *Pseudomonas putida* co-culture throughout the shake-flask of thiocyanate and salicylic acid biodegradation under different initial SCN^- and SA concentrations. **a** 250 mg L^{-1}, **b** 500 mg L^{-1}, **c** 1000 mg L^{-1}, **d** 2000 mg L^{-1}, **e** 3000 mg L^{-1}, **f** 4000 mg L^{-1} (*circle* viable cells, *triangle* damage cells, *square* dead cells, *asterisk* total cells). In all cases: CCMM, 30 °C, 250 rpm, and inoculum size of 1×10^7 cfu mL^{-1} of both bacteria

S6C). The increase in SA and SCN^- initial concentrations caused an increase in total cell concentration but, at the same time, provoked an increase in the percentages of dead and damaged subpopulations (Fig. S6D, S6E and S6F). Finally, for 3000 mg L^{-1} the growth decreased, whereas no cell growth was observed for the concentration of 4000 mg L^{-1} and cells were moved into dead and damaged gate, these results corroborating the no biodegradation of the pollutants.

In supplementary data, Fig. S7 shows representative dot plot diagrams of side scatter (SSC) versus forward side scatter (FSC) signal obtained during simultaneous biodegradation of 3000 mg L^{-1} of both salicylic acid and thiocyanate. As can be seen in these cytograms, an increase in the intensity of the FSC was evidenced in the flow cytometric dot plots during the experiment. Cells of co-culture exhibited both higher relative cell size (forward scatter, FSC) and cell complexity signals (sid scatter, 90°-angle scatter of blue laser light, SSC) with age for all the initial concentrations used. Therefore, examination of these cytograms (Figs. S6 and S7) reveals that shake-flask cultivation displayed marked physiological heterogeneity in terms of metabolic status, membrane integrity and cellular size. A similar behavior was observed in the work of Alonso et al. (Alonso et al. 2012) during the production of lactobionic acid by *P. teatrolens.*

In Fig. 6, the subpopulation concentrations are shown depending on initial SCN^- and SA concentration. Comparing total and viable cells concentrations, it can be noted that both subpopulations had a similar behavior; the

bacterial concentrations (cells mL^{-1}) increased in the early stages of SA and SCN^- biodegradation, reaching a maximum value, and then this maximum value was kept constant until the end of the experiment (Fig. 6a–c). This finding demonstrates that low concentrations of SA and/or thiocyanate in the co-culture medium do not involved a loss in the viability of the mixed population. Up to concentrations of 2000 mg L^{-1} (Fig. 6e, f), the higher the SA and SCN^- initial concentration, the higher the population of viable cells. However, for initial concentrations above 2000 mg L^{-1} (Fig. 6d), this trend was reversed and an increase in the initial concentration caused a reduction in the total bacteria and, at a time, in the proportion of the viable subpopulation. It is remarkable that ups and downs in the viable cells concentration were observed. These changes in viable cells tendency coincide with the moment in which the SA was completely assimilated and SCN^- began to be removed, that is, when *P. putida* stopped growing and *P. thiocyanatus* growth began. Regarding the damaged subpopulation, its concentration (Fig. 6a) remained constant at the beginning and decreased at the end of the process when the initial concentration was 250 mg L^{-1}, probably due to cellular lysis phenomena. However, with higher SA and SCN^- concentrations, a significant increase in damage cells concentration was observed during the first 24 h, this value remaining constant during the rest of the process. The higher the initial concentrations, the more marked the increase in the proportion of damaged bacteria. Concerning the dead bacteria, its concentration in the experiments with 250 and 500 mg L^{-1} of SA and SCN^- (Fig. 6a, b) firstly increased and then slightly decreased, probably also due to the cellular lysis. For concentrations higher than 1000 mg L^{-1} (Fig. 6c) the cellular death makes more significant; in fact, the dead subpopulation when initial concentrations were 3000 or 4000 mg L^{-1} (Fig. 6e, f) was around the 15 and 17 % of the total bacteria. In all cases discussed so far, the increase in dead cells occurred mainly during the removal of SA, when both pollutants are present at high concentrations.

To obtain a deeper knowledge about the effect of high concentration of pollutant on the viability and activity, the next test was conducted: A co-culture was initially exposed during 120 h to a medium that contained 4000 mg L^{-1} of both pollutants, afterward, the biomass was recovered by centrifugation and subsequently inoculated into a new CCMM containing 500 mg L^{-1} of both SA and SCN^-, and the evolutions of both pollutants were followed over time (S8). The thiocyanate was not degraded during the first 50 h, whereas in the case of SA, an induction time was observed. In addition, the previous exposure of the co-culture to high concentrations involved a decreased in the specific degradation rate from 0.53 (mg SA(mg cell h)$^{-1}$ to 0.35 (mg SA(mg cell h)$^{-1}$). These findings corroborate that the exposure to high concentrations of both pollutants had a significant effect on the physiological status of *P. putida*.

In addition, cytometry samples were analyzed by confocal laser microscope to corroborate the results obtained. The observation of stained samples under fluoresc microscopy also confirmed that *P. putida* and *P. cyanatus* co-culture cells were predominantly metabolically active at the initial time of biodegradation, whereas cells were transformed into damage and dead cells at the end of the process. Moreover, aggregates of dead cells were detected during the later stages of cultivation. Interestingly, the observed increase in light scattering properties during flow cytometry analysis (S7) could be ascribed to this phenomenon, as was previously reported by Alonso et al. (2012) for *Pseudomonas taetrolens* cultures.

Conclusion

A complete removal of either SA or SCN^- by co-culture was observed for initial concentrations up to 2000 mg L^{-1} showing a behavior defined as commensalism. The growth of *P. thiocyanatus* was successfully fitted to a Tessier model ($r^2 = 0.97$). To modelize the growth of *P. putida*, a SCN^- inhibition term had to be included ($r^2 = 0.99$). The initial concentrations of phenolic and/or cyanide compounds had a marked effect on the physiological heterogeneity of the co-culture, in terms of metabolic status, membrane integrity and cellular size.

Acknowledgments R. G. Combarros wishes to express gratitude for a research grant from the Government of the Principality of Asturias (Severo Ochoa Programme).

References

Agarry SE, Solomon BO (2008) Kinetics of batch microbial degradation of phenols by indigenous *Pseudomonas fluorescence*. Int J Environ Sci Technol 5:223–232. doi:10.1007/BF03326016

Agarry SE, Audu TOK, Solomon BO (2009) Substrate inhibition kinetics of phenol degradation by *Pseudomonas fluorescence* from steady state and wash-out data. Int J Environ Sci Technol 6:443–450. doi:10.1007/BF03326083

Alonso S, Rendueles M, Díaz M (2012) Physiological heterogeneity of *Pseudomonas taetrolens* during lactobionic acid production. Appl Microbiol Biotechnol 96:1465–1477. doi:10.1007/s00253-012-4254-2

Arutchelvan V, Kanakasabai V, Nagarajan S, Muralikrishnan V (2005) Isolation and identification of novel high strength phenol degrading bacterial strains from phenol-formaldehyde resin manufacturing industrial wastewater. J Hazard Mater 127:238–243. doi:10.1016/j.jhazmat.2005.04.043

Banerjee G (1996) Phenol- and thiocyanate-based wastewater treatment in RBC reactor. J Environ Eng 122:941–948

Cai S, Li X, Cai T, He J (2013) Degradation of piperazine by *Paracoccus* sp. TOH isolated from activated sludge. Bioresour Technol 130:536–542. doi:10.1016/j.biortech.2012.12.095

Chaudhari A, Kodam K (2010) Biodegradation of thiocyanate using co-culture of *Klebsiella pneumoniae* and *Ralstonia* sp. Appl Microbiol Biotechnol 85:1167–1174. doi:10.1007/s00253-009-2299-7

Collado S, Laca A, Díaz M (2009) Wet oxidation of thiocyanate under different pH conditions: kinetics and mechanistic analysis, vol 22. American Chemical Society, Washington

Collado S, Garrido L, Laca A, Díaz M (2010) Wet oxidation of salicylic acid solutions. Environ Sci Technol 44:8629–8635

Combarros RG, Rosas I, Lavín AG, Rendueles M, Díaz M (2014) Influence of biofilm on activated carbon on the adsorption and biodegradation of salicylic acid in wastewater. Water Air Soil Pollut 225:1–12. doi:10.1007/s11270-013-1858-9

Combarros RG, Collado S, Laca A, Díaz M (2015) Conditions and mechanisms in thiocyanate biodegradation. J Residuals Sci Technol 12(3):113–124

Díaz M, García AI, García LA (1996) Mixing power, external convection, and effectiveness in bioreactors. Biotechnol Bioeng 51:131–140. doi:10.1002/(SICI)1097-0290(19960720)51:2<131::AID-BIT1>3.0.CO;2-K

Fall C, Millán-Lagunas E, Bâ KM, Gallego-Alarcón I, García-Pulido D, Díaz-Delgado C, Solís-Morelos C (2012) COD fractionation and biological treatability of mixed industrial wastewaters. J Environ Manag 113:71–77. doi:10.1016/j.jenvman.2012.08.032

Foladori P, Bruni L, Tamburini S, Ziglio G (2010) Direct quantification of bacterial biomass in influent, effluent and activated sludge of wastewater treatment plants by using flow cytometry. Water Res 44:3807–3818. doi:10.1016/j.watres.2010.04.027

Fuentes MS, Alvarez A, Saez JM, Benimeli CS, Amoroso MJ (2014) Methoxychlor bioremediation by defined consortium of environmental Streptomyces strains. Int J Environ Sci Technol 11:1147–1156. doi:10.1007/s13762-013-0314-0

Hadibarata T, Teh Z (2014) Optimization of pyrene degradation by white-rot fungus *Pleurotus pulmonarius* F043 and characterization of its metabolites. Bioprocess Biosyst Eng 37:1679–1684. doi:10.1007/s00449-014-1140-6

Herrero M, Stuckey DC (2014) Bioaugmentation and its application in wastewater treatment: a review. Chemosphere. doi:10.1016/j.chemosphere.2014.10.033

Hewitt CJ, Nebe-von-Caron G (2004) The application of multi-parameter flow cytometry to monitor individual microbial cell physiological state. Adv Biochem Eng Biot 89:197–223

Hsu Y-C, Yang H-C, Chen J-H (2004) The enhancement of the biodegradability of phenolic solution using preozonation based on high ozone utilization. Chemosphere 56:149–158. doi:10.1016/j.chemosphere.2004.02.011

Huang H, Feng C, Pan X, Wu H, Ren Y, Wu C, Wei C (2013) Thiocyanate oxidation by coculture from a coke wastewater treatment plant. J Biomater Nanobiotechnol 4:37–46

Ibáñez SG, Merini LJ, Barros GG, Medina MI, Agostini E (2014) *Vicia sativa*–rhizospheric bacteria interactions to improve phenol remediation. Int J Environ Sci Technol 11:1679–1690. doi:10.1007/s13762-013-0357-2

Juang R-S, Tsai S-Y (2006) Growth kinetics of *Pseudomonas putida* in the biodegradation of single and mixed phenol and sodium salicylate. Biochem Eng J 31:133–140. doi:10.1016/j.bej.2006.05.025

Kim S-J, Katayama Y (2000) Effect of growth conditions on thiocyanate degradation and emission of carbonyl sulfide by *Thiobacillus thioparus* THI115. Water Res 34:2887–2894. doi:10.1016/S0043-1354(00)00046-4

Kim YM, Park D, Jeon CO, Lee DS, Park JM (2008) Effect of HRT on the biological pre-denitrification process for the simultaneous removal of toxic pollutants from cokes wastewater. Bioresour Technol 99:8824–8832. doi:10.1016/j.biortech.2008.04.050

Kwon H, Woo S, Park J (2002) Thiocyanate degradation by *Acremonium strictum* and inhibition by secondary toxicants. Biotechnol Lett 24:1347–1351. doi:10.1023/A:1019825404825

Lei G, Ren H, Ding L, Wang F, Zhang X (2010) A full-scale biological treatment system application in the treated wastewater of pharmaceutical industrial park. Bioresour Technol 101:5852–5861. doi:10.1016/j.biortech.2010.03.025

Li H-q, Han H-j, Du M-a, Wang W (2011) Removal of phenols, thiocyanate and ammonium from coal gasification wastewater using moving bed biofilm reactor. Bioresour Technol 102:4667–4673. doi:10.1016/j.biortech.2011.01.029

Loh K-C, Yu Y-G (2000) Kinetics of carbazole degradation by *Pseudomonas putida* in presence of sodium salicylate. Water Res 34:4131–4138. doi:10.1016/S0043-1354(00)00174-3

Marañón E, Vázquez I, Rodríguez J, Castrillón L, Fernández Y, López H (2008) Treatment of coke wastewater in a sequential batch reactor (SBR) at pilot plant scale. Bioresour Technol 99:4192–4198. doi:10.1016/j.biortech.2007.08.081

McGenity TJ, Folwell BD, McKew BA, Sanni GO (2012) Marine crude-oil biodegradation: a central role for interspecies interactions. Aquat Biosyst 8:10. doi:10.1186/2046-9063-8-10

McLaughlin H, Farrell A, Quilty B (2006) Bioaugmentation of activated sludge with two *Pseudomonas putida* strains for the degradation of 4-chlorophenol. J Environ Sci Health Part A 41:763–777. doi:10.1080/10934520600614348

Mikesková H, Novotný Č, Svobodová K (2012) Interspecific interactions in mixed microbial cultures in a biodegradation perspective. Appl Microbiol Biotechnol 95:861–870. doi:10.1007/s00253-012-4234-6

Nielsen TH, Sjøholm OR, Sørensen J (2009) Multiple physiological states of a *Pseudomonas fluorescens* DR54 biocontrol inoculant monitored by a new flow cytometry protocol. FEMS Microbiol Ecol 67:479–490

Qiao L, Wang J-l (2010) Microbial degradation of pyridine by* *Paracoccus* sp. isolated from contaminated soil. J Hazard Mater 176:220–225. doi:10.1016/j.jhazmat.2009.11.016

Quirós C, Herrero M, García LA, Díaz M (2007) Application of flow cytometry to segregated kinetic modeling based on the physiological states of microorganisms. Appl Environ Microbiol 73:3993–4000. doi:10.1128/AEM.00171-07

Sharma NK, Philip L, Murty Bhallamudi s (2012) Aerobic degradation of phenolics and aromatic hydrocarbons in presence of cyanide. Bioresour Technol 121:263–273. doi:10.1016/j.biortech.2012.06.039

Shivaraman N, Kumaran P, Pandey RA, Chatterjee SK, Chowdhary KR, Parhad NM (1985) Microbial degradation of thiocyanate, phenol and cyanide in a completely mixed aeration system. Environ Pollut Ser A Ecol Biol 39:141–150. doi:10.1016/0143-1471(85)90012-1

Sorokin DY, Tourova TP, Antipov AN, Muyzer G, Kuenen JG (2004) Anaerobic growth of the haloalkaliphilic denitrifying sulfur-oxidizing bacterium Thialkalivibrio thiocyanodenitrificans sp. nov. with thiocyanate. Microbiology 150:2435–2442

Staib C, Lant P (2007) Thiocyanate degradation during activated sludge treatment of coke-ovens wastewater. Biochem Eng J 34:122–130. doi:10.1016/j.bej.2006.11.029

Supplementary material to

'Understanding the Simultaneous Biodegradation of Thiocyanate and Salicylic Acid by *Paracoccus thiocyanatus* and *Pseudomonas putida* '

Combarros, R.G., Collado, S., Laca, A., Díaz, M*

Department of Chemical Engineering and Environmental Technology,

University of Oviedo, C/Julián Clavería s/n, E-33071, Oviedo, Spain

(10 Pages, 7 Figures, 1 Table)

Table of contents

7. **Dot plots representing side scatter light (SSC) versus forward scatter light (FSC) signals of co-culture cells during shake-flask simultaneous biodegradation. (Figure S14).**

8. **Evolution of salicylic acid or thiocyanate concentrations and growth curves during the simultaneous biodegradation of both contaminants by a co-culture of *Paracoccus thiocyanatus* and *Pseudomonas putida*. (Figure S15).**

Corresponding author's e-mail: mariodiaz@uniovi.es
Phone: +34 985 10 34 39; Fax: +34 985 10 34 34

Table S 3: Summary of biodegradation conditions and results of interaction effects between *P. putida-P. thiocyanatus* - SA- SCN^- system

Row	Mineral medium	Culture conditions *	Bacteria	Substrate	ti (h)	Specific degradation rate (mg substrate (h mg cells)$^{-1}$)	μ (h^{-1})	Conversion (reaction time) (%- h)	Volumetric degradation rate (mg substrate (Lh)$^{-1}$)
1	PpMM	Pp conditions	*P. putida*	500 mg SA L^{-1}	0	2.5	0.2459	100% in 22	31
2	PpMM	Pp conditions	*P. putida*	500 mg SA L^{-1}	0	0.92	0.0007	73% in 140	6.25
				500 mg SCN^- L^{-1}	-----	0		0% in 140	0
3	PpMM	Pp conditions	*P. putida*	500 mg SCN^- L^{-1}	0	0	0	0% in 140	0
4	PtMM	Pt conditions	*P. thiocyanatus*	500 mg SCN^- L^{-1}	20	0.32	0.0314	100% in 48	20.7
5	PtMM	Pt conditions	*P. thiocyanatus*	500 mg SCN^- L^{-1}	48	0.35	0.0093	100% in 144	6.7
				500 mg SA L^{-1}	-----	0		0% in 144	0
6	PtMM	Pt conditions	*P. thiocyanatus*	500 mg SA L^{-1}	0	0	0	0% in 144	0
7	PpMM	CC conditions	*P. putida*	500 mg SA L^{-1}	0	0.99	0.2338	96% in 34	13.6
				500 mg SCN^- L^{-1}	-----	0		0% in 144	0
8	CCMM	CC conditions	*P. putida*	500 mg SA L^{-1}	0	0.86	0.3137	100% in 11	46.1
				500 mg SCN^- L^{-1}	-----	0		0% in 144	0
9	PtMM	CC conditions	*P. thiocyanatus*	500 mg SCN^- L^{-1}	60	0.53	0.0097	100% in 135	6.67
				500 mg SA L^{-1}	-----	0		0% in 144	0
10	CCMM	CC conditions	*P. thiocyanatus*	500 mg SCN^- L^{-1}	30	0.36	0.0186	100% in 51	16.7
				500 mg SA L^{-1}	-----	0		0% in 144	0
11	CCMM	CC conditions	*P. putida*	500 mg SA L^{-1}	0	0.89	0.23	100% in 12	39.3
12	CCMM	CC conditions	*P. thiocyanatus*	500 mg SCN^- L^{-1}	11	0.68	0.052	100% in 25	32.2
13	CCMM	CC conditions	*P. thiocyanatus* *P. putida*	500 mg SCN^- L^{-1}	17	0.58	0.027	100% in 40	36.9
14	CCMM	CC conditions	*P. thiocyanatus* *P. putida*	500 mg SA L^{-1}	0	0.64	0.091	100% in 14	40
15	CCMM	CC conditions	*P. thiocyanatus*	500 mg SCN^- L^{-1}	12	0.53	0.0186	100% in 29	35.2
			P. putida	500 mg SA L^{-1}	0	0.39	0.3137	100% in 12	42.1

* Pp conditions: 200 rpm, 30ºC and 100 mL of mineral medium in 250 mL Erlenmeyer flasks; Pt conditions: 250 rpm, 28ºC and 100 mL of mineral medium in 500 mL Erlenmeyer flaks; CC conditions: 30°C, 250 rpm and 100 mL of mineral médium in 500 mL Erlenmeyer flasks

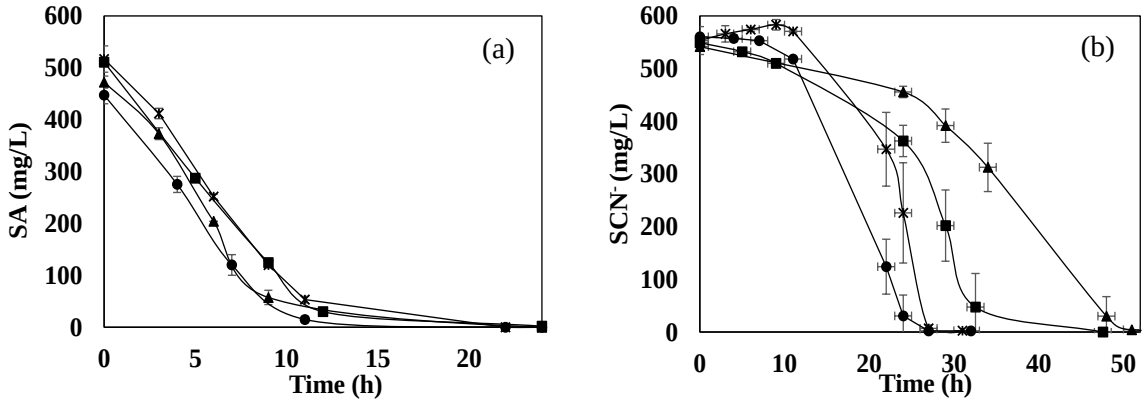

Figure S 9: Evolution of salicylic acid or thiocyanate concentrations under different culture conditions. a) Evolution of SA concentration by *P. putida* (●), by *P. putida* in presence of *P. thiocyanatus* (■), by *P. putida* in presence of SCN^- (▲) and by *P. putida* in presence of P. thiocyanatus and SCN^- (✳). b) Evolution of SCN^- concentration by *P. thiocyanatus* (●), by *P. thiocyanatus* in presence of *P. putida* (■), by *P. thiocyanatus* in presence of SA (▲) and by *P. thiocyanatus* in presence of *P. putida* and SA (✳). In all cases: CCMM, initial SCN^- or SA concentration: 500 mg L^{-1}, 250 rpm, 30 ºC, 100mL in 500 mL Erlenmeyer flasks.

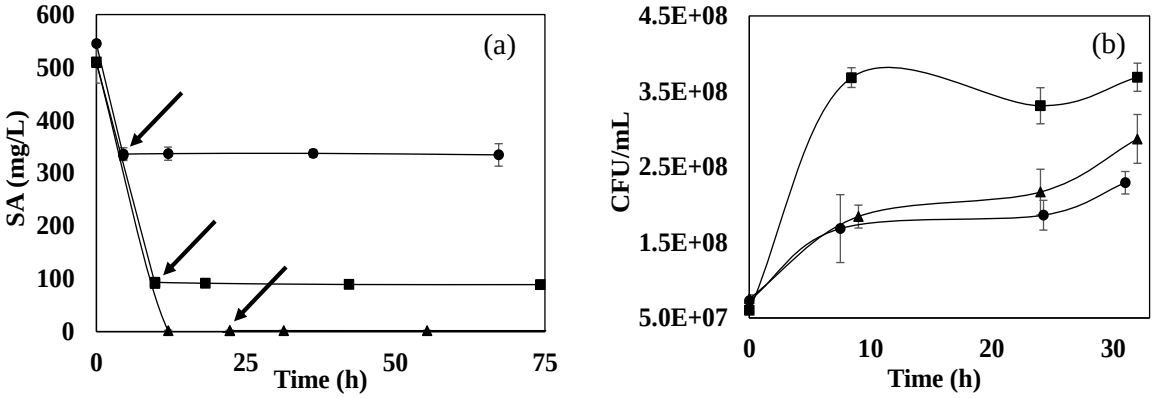

Figure S 10: (a) Evolution of salicylic acid in presence of a pure culture of *P. putida*. Arrows denote the times at which the bacteria was removed: 4.5 h (●), 9.8 h (■) and 22 h (▲). These media were subsequently inoculated with *P thiocyanatus*, following its bacterial growth as $CFUmL^{-1}$ (b). In all cases: CCMM, initial SA concentration: 500 mg L^{-1}, 250 rpm, 30 ºC, 100mL in 500 mL Erlenmeyer flasks. The arrows indicate the time when *P. putida* were removed from the medium and *P. thiocyanatus* were inoculated in that medium.

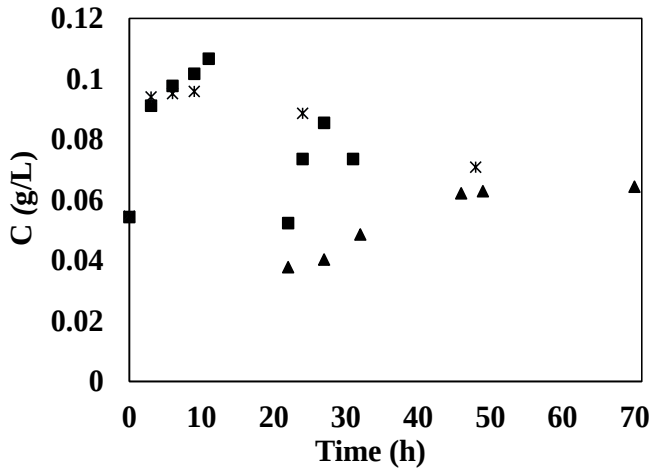

Figure S 11: Evolution of growth curves during the simultaneous biodegradation of both contaminants by a co-culture of *Paracoccus thiocyanatus* and *Pseudomonas putida* (■) and by pure culture of *P. putida* (✳) or *P. thiocyanatus* (▲). In all cases: CCMM, 30ºC, 250 rpm, inoculum size of 1·107 $CFUmL^{-1}$ of both

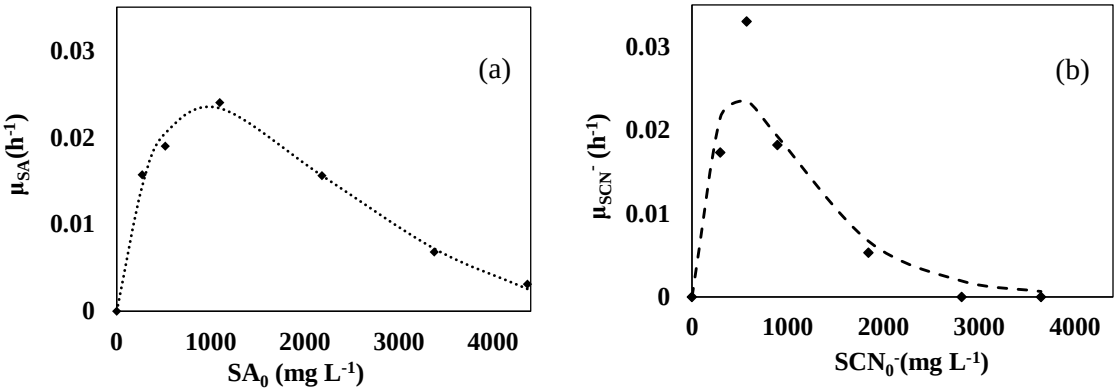

Figure S 12: Specific growth rate of suspended biomass in a thiocyanate and salicylic acid solution using a co-culture of *P. putida* and *P. thiocyanatus* (250-4000 mg L-1). a) *P. putida* specific growth rate b) *P. thiocyanatus* (◆ Experimental data, …… substrate and toxic inhibition model, - - - Teisser model). In all cases: 30ºC, 250 rpm, and inoculum size of 10^7 $CFUmL^{-1}$ of each bacteria.

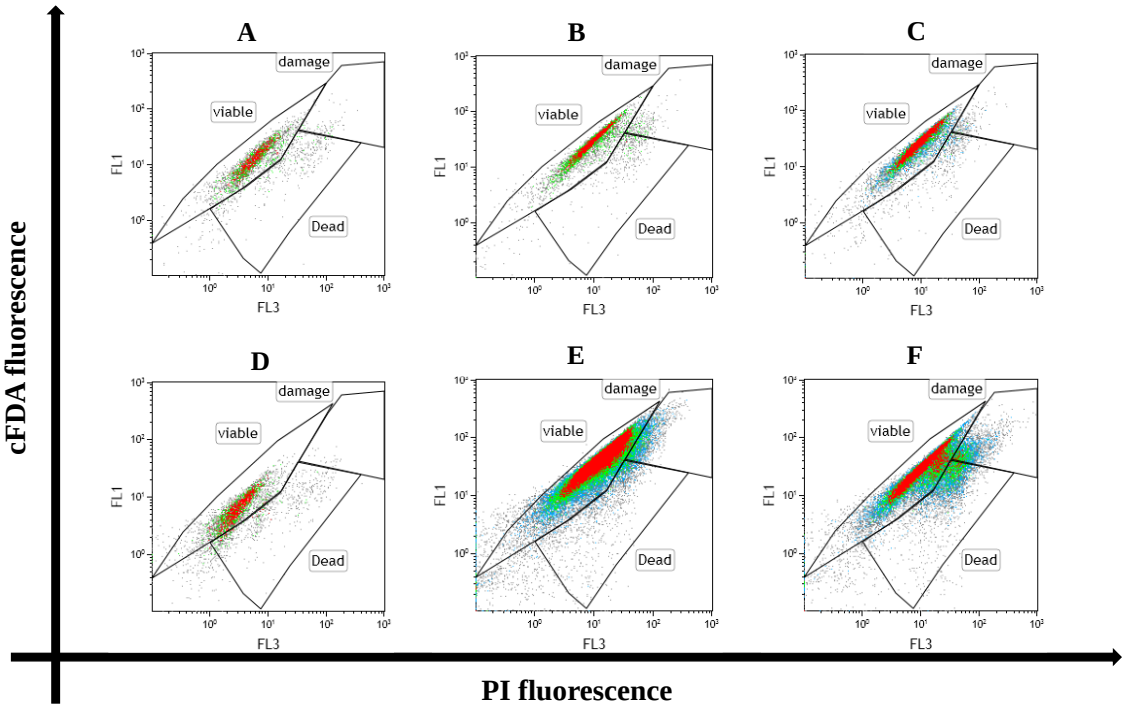

Figure S 13: Dot plots representing cFDA fluorescence versus PI fluorescence of co-culture of *Paracoccus thiocyanatus* and *Pseudomonas putida* cells during shake-flask fermentation. A, B and C plots correspond to an initial SA and SCN^- concentration of 250 mg L^{-1} at 0, 24 and 31 hours respectively. D, E and F plots correspond to an initial SA and SCN^- concentration of 2000 mg L^{-1} at 0, 48 and 144 hours respectively.

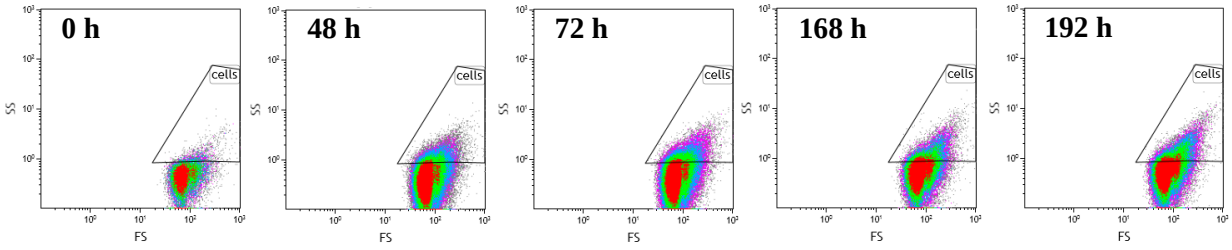

Figure S 14: Dot plots representing side scatter light (SSC) versus forward scatter light (FSC) signals of co-culture cells during shake-flask simultaneous biodegradation to an initial SA and SCN^- concentration of 3000 mg L^{-1} at 0, 48, 72, 168 and 192 hours respectively

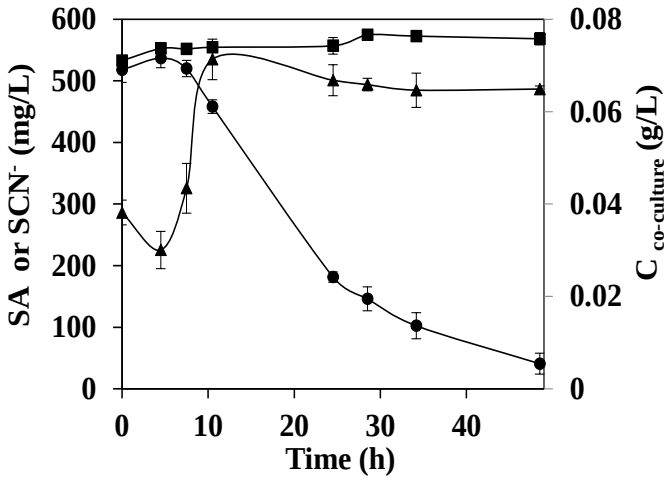

Figure S 15*:* Evolution of salicylic acid (●) or thiocyanate (■) concentrations and growth curves (▲) during the simultaneous biodegradation of both contaminants by a co-culture of *Paracoccus thiocyanatus* and *Pseudomonas putida*. Previously to inoculation, the co-culture was acclimated with 4000 mg L^{-1} of both SCN^- and SA during 120 hours. The culture conditions: CCMM, 30ºC, 250 rpm, initial SCN^- and SA concentrations of 500 mg L^{-1}, and inoculum size of ($1 \cdot 10^7$ CFUmL^{-1} of both bacteria).

6. Conclusiones

- La conclusión general que se puede extraer del presente trabajo es que el tratamiento biológico con un cultivo puro de *Pseudomonas putida* ha resultado ser una técnica de gran versatilidad para el tratamiento de efluentes altamente contaminados por compuestos fenólicos.

- En el tratamiento biológico de ácido salicílico por *Pseudomonas putida* se han obtenido elevadas eficacias de eliminación del contaminante.

- La presencia de agentes externos, como sólidos particulados, otros sustratos o microorganismos, afecta negativamente al estado fisiológico y/o a la actividad metabólica de la bacteria *Pseudomonas putida*.

- La técnica de citometría de flujo se presenta como una técnica con un gran atractivo para determinar el efecto producido de la presencia de material nanoparticulado sobre cultivos puros.

Conclusiones sobre el efecto de la presencia del carbón activo

- La biodegradación por *Pseudomonas putida* ha sido una técnica eficaz para el tratamiento de aguas farmacéuticas sintéticas contaminadas por ácido salicílico.Así, cuando un efluente de aguas farmacéuticas sintéticas con 100 y 500 mgL^{-1} de ácido salicílico fue tratado por biodegradación con *P. putida,* se obtuvieron eliminaciones del 85.7 a las 6 y del 94.7% a las 24 h, respectivamente.

- La biodegradación de ácido salicílico por *P. putida* puede describirse mediante cinéticas de orden cero con respecto a la concentración de ácido salicílico.

- El modelo de inhibición por sustrato definido por la ecuación de Haldane ha sido ajustado a los datos experimentales de biodegradación de ácido salicílico por *P. putida,* con coeficiente de correlación de 0.991, obteniendo los siguientes parámetros de ajuste: μ_{max}=0.25 h^{-1}, K_s=61 mgSA L^{-1} y K_i=705 mgSA L^{-1}.

- Se comprobó que el mecanismo metabólico utilizado por *P. putida* para degradar el ácido salicílico sigue la ruta meta, puesto que se encontró el 2-hidroximuconico semialdehido como intermedios de reacción.

- El carbón Filtrasorb 400 presentaba un mejor comportamiento de adsorción de SA que el GAC 830, con una constante de equilibrio y una capacidad máxima igual a 46.99 y 26.6 gL^{-1} (30.74 mgg^{-1}).

- La cinética del proceso de adsorción de ácido salicílico por carbón activo Filtrasorb 400 presentó valores entre $(8.6\text{-}2.4)\cdot10^{-11}$ (m^2s^{-1}) y $(5.1\text{-}8.8)\cdot10^{-5}$ (ms^{-1}) para el modelo de difusión a través de los poros y el modelo de transferencia de materia en la película líquida. Eficacias de eliminación de ácido salicílico de 55 y 20 % fueron obtenidas para una disolución que contenía 100 y 500 mgL^{-1} a pH 7.

- Las condiciones óptimas de formación de biofilm de *P. putida* sobre carbón activo son 50 rpm y un tamaño de inoculo de 0.05 unidades de densidad óptica. En estas condiciones, $2.9\cdot10^5$ $CFUcm^{-2}$ se adhieren al carbón.

- En el caso de la bioadsorción con biofilm muerto, sólo se elimina del medio el 12 y 6% de la concentración inicial de ácido salicílico (para 100 y 500 mgL^{-1}, respectivamente), lo que demuestra que la presencia de biofilm muerto en el proceso tiene un efecto negativo respecto a la eficacia de eliminación.

- La presencia de carbón activo en el proceso de biodegradación de ácido salicílico por *P. putida* supone una mejora del proceso para altas concentraciones del contaminante, debido a que el sistema biológico con esta configuración está más protegido frente a las condiciones adversas del medio.

Conclusiones sobre el efecto de la presencia de óxidos de grafeno

- La presencia de óxido de grafeno en el sistema de biodegradación de ácido salicílico por *P. putida* tiene un efecto negativo en el crecimiento y viabilidad bacteriana.

- La relación entre el crecimiento celular y la concentración de óxidos de grafeno en el medio viene representada por la ecuación $\mu(h^{-1}) = 0.058 \cdot GO^{-0.62}(mgmL^{-1})$; r^2=0.92; en el caso de aguas residuales urbanas simuladas, mientras que el crecimiento celular se reduce a la mitad incluso con la concentración más baja de óxido de grafeno ensayada, 0.05 $mgmL^{-1}$, para las aguas residuales industriales simuladas.

- La pérdida de viabilidad celular comienza a ser importante a partir de concentraciones de GO mayores de 0.5 y 0.1 $mgmL^{-1}$ para aguas residuales urbanas e industriales simuladas, respectivamente. En ambos casos se observa una disminución del porcentaje de células viables en torno al 20 %, que viene acompañada por un aumento en el porcentaje de células dañadas. El porcentaje de células muertas tuvo un leve incremento, con el aumento de la concentración de óxidos de grafeno, menor del 5%. Estos resultados sugieren que el impacto de los óxidos de grafeno sobre la *P. putida* supone principalmente la pérdida de la integridad de la membrana por el contacto de los bordes de las nanopartículas con la membrana bacteriana, manteniendo la actividad metabólica de las mismas.

- Los óxidos de grafeno tienen un ligero efecto negativo sobre la capacidad de eliminación del ácido salicílico de *P. putida*, excepto para las concentraciones más altas de óxido de grafeno ensayadas (1 $mgmL^{-1}$).

- El proceso de eliminación de ácido salicílico por *P. putida* en presencia de óxido de grafeno se define por una cinética de orden cero. La relación hallada entre la constante cinética calculada por este modelo y la concentración de óxido de grafeno se representa mediante la siguiente ecuación: $k(mg(Lh)^{-1} = 35.5 \cdot GO^{-0.086}(mgmL^{-1})\ ;\ r^2 = 0.99$.

- Los cambios en el tamaño y la complejidad de las células como consecuencia de su interacción con los óxidos de grafeno son insignificantes respecto al tiempo y a la concentración de óxidos de grafeno.

Conclusiones sobre el efecto de la presencia de nanopartículas de dióxido de titanio

- Se observan cambios fisiológicos de *P. putida* de células viables a células viables pero no cultivables en presencia de TiO_2-NPs. Las células dañadas y muertas se mantuvieron en todo momento por debajo del 5 %.

- La nanopartículas de TiO_2-NPs son absorbidas por *P. putida*, por lo que el tamaño y la complejidad de la bacteria aumenta.

- Concentraciones de TiO2-NPs iguales o superiores a 0.5 $mgmL^{-1}$ tienen un claro efecto negativo en el crecimiento de *P. putida* en medios con disponibilidad de fuentes de carbono y nitrógeno fácilmente asimilables. Este efecto negativo sobre el crecimiento celular en aguas residuales industriales simuladas se da a partir de concentraciones de 0.1 $mgmL^{-1}$ de TiO2-NPs, inhibiéndolo completamente para concentraciones superiores a 0.5 $mgmL^{-1}$.

- La capacidad global de eliminación del ácido salicílico por *P. putida* se ve afectada de forma negativa por la presencia de TiO_2-NPs en el medio, lo que supone una disminución de la eficacia de eliminación.

- La evolución de la concentración de ácido salicílico se puede obtener mediante un modelo cinético de pseudo-primer orden. La ecuación que expresa la relación entre la constante cinética del modelo y la concentración de nanopartículas de dióxido de titanio en el medio es $k(h^{-1}) = 0.20 + 0.040 \cdot {TiO_2}^{-0.49}(mgmL^{-1}); r^2 = 0.95$.

- El comportamiento (crecimiento y biodegradación de ácido salicílico) de las diferentes subpoblaciones bacterianas de *P. putida* en presencia de diferentes concentraciones de TiO_2-NPs se puede definir mediante el empleo de un modelo cinético segregado.

Conclusiones sobre la biodegradación de tiocianato por *Paracoccus thiocyanatus*

- *Paracoccus thiocyanatus* es un microorganismo eficaz para el tratamiento de aguas sintéticas contaminadas por tiocianato. Las condiciones óptimas de degradación de tiocianato por *P. thiocyanatus*: inóculo de $5 \cdot 10^7$ $CFUmL^{-1}$ y en fase exponencial temprana, 250 rpm y medio salino sin presencia de fuentes adicionales de carbono, nitrógeno y azufre.

- El tratamiento biológico con el cultivo puro de *P. thiocyanatus* permite eliminar concentraciones de tiocianato de hasta 5000 mgL^{-1}, con velocidades de degradación máximas de 1.20 mg SCN^-(mg células h)$^{-1}$ en ausencia de fuentes adicionales de carbono, nitrógeno y azufre al sistema diferentes a las aportados por el tiocianato. La presencia de fuentes de carbono, nitrógeno o azufre fácilmente asimilables supone la reducción de la concentración máxima de tratamiento hasta 3500 mgL^{-1} y velocidades máximas de degradación de hasta 0.70 mg SCN^-(mg células h)$^{-1}$.

- La biodegradación de tiocianato por *P. thiocyanatus* sigue un modelo de crecimiento celular con inhibición por sustrato definido (ecuación de Teissier) con coeficiente de correlación de 0.99 y parámetros de ajuste μ_{max}=0.059 h^{-1}, K_s=790 mg SCN^-L^{-1} y K_i=6520 mg SCN^-L^{-1} en ausencia fuentes adicionales de carbono, nitrógeno y azufre y μ_{max}=0.344 h^{-1}, K_s=1150 mg SCN^-L^{-1} y K_i=1730 mg SCN^-L^{-1} en presencia de estas fuentes.

- La biodegradación del tiocianato por *P. thiocyanatus* se describe mediante cinéticas de orden cero con tiempos de inducción cuya duración depende de la concentración de tiocianato tanto en presencia como ausencia de moléculas fácilmente asimilables de carbono, nitrógeno y azufre. Los tiempos de inducción obtenidos son menores en medios libres de fuentes adicionales de C, N y S.

Conclusiones sobre el efecto de la presencia de otros microorganismos y sustratos

- La presencia de tiocianato en la biodegradación del ácido salicílico por *P. putida*, tiene un efecto negativo en el proceso, ya que inhibe completamente el crecimiento de la bacteria y reduce en más de la mitad la velocidad específica de degradación del ácido salicílico (de 2.5 mg SA·(h mg células)$^{-1}$ a 0.92 mg SA·(h mg células)$^{-1}$)

- La presencia de ácido salicílico en la biodegradación de tiocianato por *P. thiocyanatus* tiene un impacto negativo en la aclimatación inicial de la bacteria pero no en la asimilación final del tiocianato, puesto que las velocidades de degradación del tiocianato en presencia y ausencia de ácido salicílico son de 0.35 mg SCN^-·(h mg células)$^{-1}$. El ácido salicílico no es asimilado por *P. thiocyanatus*.

- Un aumento en 100 rpm la velocidad de agitación y en la composición del medio supuso, en el caso de la biodegradación simultánea del ácido salicílico y el tiocianato por *P. putida,* un aumento del crecimiento celular (μ=0.314 h^{-1}) y en consecuencia una mejora del tiempo de eliminación del ácido salicílico. En el caso de la biodegradación simultánea de ambos contaminantes por *P. thiocyanatus*, un aumento de 2 ºC de la temperatura de operación y el cambio en la composición del medio supuso un aumento en el crecimiento celular (μ=0.0186 h^{-1}) y una disminución del tiempo de inducción (ti=30 h).

- La presencia de *P. thiocyanatus* en el proceso de biodegradación del ácido salicílico por *P. putida* implica un descenso en el crecimiento celular de *P. putida* pasando de valores de μ=0.23 h^{-1} a μ=0.09 h^{-1}.

- La presencia de *P. putida* en la biodegradación de tiocianato por *P. thiocyanatus* aumenta el tiempo de inducción y reduce el crecimiento celular.

- El empleo de un co-cultivo formado por *P. putida* y *P. thiocyanatus* para la biodegradación simultánea de SA y SCN^- permite alcanzar una eliminación completa de ambos contaminantes, partiendo de concentraciones iniciales de hasta 2000 mgL^{-1} de cada uno de ellos.

- Se observa un comportamiento de comensalismo por parte del co-cultivo, lo que provoca una mejora del proceso de biodegradación de ambos contaminantes respecto a los sistemas con presencia de un solo contaminantes (SA ó SCN^-) y dos bacterias (co-cultivo) o dos contaminantes y una bacteria (*P. putida* ó *P. thiocyanatus*).

- *P. thiocyanatus* en el co-cultivo sigue un modelo de crecimiento bacteriano por inhibición por sustrato (Teissier) con los siguientes parámetros: μ_{max}=0.08 h^{-1}, K_s=329 mg SCN^-L^{-1} y K_i=755.5 mg SCN^-L^{-1} con una correlación de 0.97. Estos resultados sugieren que el efecto de inhibición por sustrato es mucho más marcado cuando la bacteria forma parte de un co-cultivo que cuando está como cultivo puro.

- El crecimiento de *P. putida* en el co-cultivo se modeliza según la ecuación de Teissier con un término de inhibición por la presencia de tiocianato. En este caso, los parámetros de ajuste obtenidos son: μ_{max}=0.052 h^{-1}, K_s=552 mgL^{-1} y K_i=2570 mgL^{-1} y n=0.54, con una correlación del 0.99, lo que indican una mayor afinidad y tolerancia de *P. putida* al ácido salicílico cuando forma parte de un co-cultivo.

- En el tratamiento simultáneo de ácido salicílico y tiocianato por el co-cultivo, la concentración inicial de ambos contaminantes tiene un marcado efecto negativo en el estado fisiológico del co-cultivo, en términos de actividad metabólica, integridad de la membrana, tamaño y complejidad celular

7. Conclusions

- The main conclusion of this work is that biological treatment with the bacteria *Pseudomonas putida* has proven to be a technique of great versatility for the treatment of highly polluted aqueous effluents by phenolic compounds.

- For the biological treatment of salicylic acid by *Pseudomonas putida* high removal efficiencies have been obtained.

- Presence of external agents, such as particulate solids, other substrates or microorganisms, adversely affects the physiological status and/or metabolic activity of *Pseudomonas putida* bacteria.

- The flow cytometry technique is presented as an interesting technique with a high attractive to determine the effect of the presence of nanoparticulate material on pure cultures.

Conclusions concerning the effect of the presence of active carbon

- Biodegradation by *Pseudomonas putida* has been an effective technique for treating of synthetic pharmaceutical wastewater contaminated by salicylic acid. Thus, when a pharmaceutical synthetic wastewater containing 100 and 500 mgL^{-1} of salicylic acid was treated by biodegradation with *P. putida*, removal efficiencies of 85.7% at 6 and 94.7% at 24 h, respectively, were obtained.

- The salicylic acid biodegradation by *P.putida* can be described by zero-order kinetics with respect to the concentration of salicylic acid.

- The substrate inhibition model defined by the Haldane equation has been fitted to the experimental data for salicylic acid biodegradation by *P. putida*, with correlation coefficient of 0.991, obtaining μ_{max}=0.25 h^{-1}, K_s=61 mgSA L^{-1} y K_i=705 mgSA L^{-1}.

- It was proved that the metabolic mechanism used by *P. putida* to biodegrade salicylic acid follows the Meta pathway, since hidroximuconic 2-semialdehyde was found as a reaction intermediates.

- The Filtrasorb 400 activated carbon showed better SA adsorption capacity than GAC SA 830, with an equilibrium constant and maximum capacity equal to 46.99 y 26.6 gL^{-1} (30.74 mgg^{-1}).

- The kinetic model for the salicylic acid adsorption process by Filtrasorb 400 activated carbon presented values between $(8.6\text{-}2.4)\cdot10^{-11}$ (m^2s^{-1}) and $(5.1\text{-}8.8)\cdot10^{-5}$ (ms^{-1}) for the pores diffusion and film mass transfer models, respectively. Removal efficiencies

of salicylic acid of 55 and 20% were obtained for a solution containing 100 and 500 mgL^{-1} at pH 7.

- The optimal conditions for *P. putida* biofilm formation on activated carbon are 50 rpm and an inoculum size of 0.05 optical density units. Under these conditions, $2.9 \cdot 10^5$ $CFUcm^{-2}$ are attached to activated carbon.

- In case of dead biofilm adsorption, only 12 and 6% of initial salicylic acid was removed from the medium (for 100 y 500 mgL^{-1}, respectively), demonstrating that the presence of dead biofilm in the process has a negative effect on the removal efficiency.

- The presence of activated carbon in salicylic acid biodegradation by *P. putida* improves the process for high pollutant concentrations, because of the biological system with this configuration is more protected against the adverse medium conditions.

Conclusions concerning the effect of the presence of graphene oxide

- The presence of graphene oxide in the salicylic acid biodegradation by *P. putida* has a negative effect on the growth and bacterial viability.

- The relationship between cell growth and graphene oxide concentration is represented by the equation $\mu(h^{-1}) = 0.058 \cdot GO^{-0.62}(mgmL^{-1})$; r^2=0.92, in the case of simulated urban wastewaters, whereas cell growth is halved even with the lowest graphene oxide concentration tested, 0.05 $mgmL^{-1}$, for simulated industrial wastewaters.

- The loss of cell viability becomes important from GO concentrations higher than 0.5 y 0.1 $mgmL^{-1}$ for simulated urban and industrial wastewaters, respectively. In both cases, a decrease in viable cells percentage of around 20% is observed, which is accompanied by an increase in the damaged cells percentage. The dead cells percentage showed a slight increase for higher graphene oxide concentration, less than 5%. These results suggest that the impact of graphene oxide on *P. putida* mainly involves the loss of membrane integrity by contact of nanoparticles edges with the bacterial membrane, maintaining their metabolic activity.

- The graphene oxides have a slight negative effect on the salicylic acid removal capacity of *P. putida*, except for the highest graphene oxide concentrations tested (1 $mgmL^{-1}$).

- The salicylic acid removal by *P. putida* in presence of graphene oxide is fitted to a zero order kinetic model. The relationship found between the kinetic constant calculated using this model and the graphene oxide concentration is showed by the following equation: $k(mg(Lh)^{-1} = 35.5 \cdot GO^{-0.086}(mgmL^{-1})\ ;\ r^2 = 0.99$.

- The changes in cell size and complexity of cells as a result of its interaction with graphene oxides are negligible with respect to time and graphene oxide concentration.

Conclusions concerning the effect of the presence of titanium dioxide

- Physiological changes in *P. putida* cells are observed in presence of TiO_2-NPs, from viable to viable but nonculturable cells. The damaged and dead cells were always lower than 5%.

- The TiO_2 nanoparticles are uptake by *P. putida*, so the bacteria size and complexity increases.

- TiO_2-NPs concentrations equal to or higher than 0.5 $mgmL^{-1}$ have a clear negative effect on *P. putida* growth in media with easily assimilated sources of carbon and nitrogen available. This negative effect on cell growth in simulated industrial wastewater is significant for TiO_2-NPs concentrations of 0.1 $mgmL^{-1}$, being completely inhibited for concentrations higher than 0.5 $mgmL^{-1}$.

- The global salicylic acid removal capacity by *P. putida* is negatively affected by the presence of TiO_2-NPs in the medium, causing a decline in removal efficiency.

- The evolution of salicylic acid concentration can be obtained by means of a pseudo-first order kinetic model. The relationship between the kinetic constant of this model and the TiO_2.NPs concentration in the medium is: $k(h^{-1}) = 0.20 + 0.040 \cdot {TiO_2}^{-0.49}(mgmL^{-1})$; $r^2 = 0.95$.

- The behaviour (bacterial growth and salicylic acid biodegradation) of the different *P. putida* bacterial subpopulations in presence of different of TiO_2-NPs concentrations can be defined by using a segregated kinetic model.

Conclusions on thiocyanate biodegradation by *Paracoccus thiocyanatus*

- *Paracoccus thiocyanatus* has been an effective microorganism for the treatment of synthetic wastewaters contaminated by thiocyanate. Optimal conditions for thiocyanate biodegradation by *P. thiocyanatus* are: inoculum of $5 \cdot 10^7$ $CFUmL^{-1}$ in early exponential phase, 250 rpm and minimal medium without additional sources of carbon, nitrogen and sulphur.

- Biological treatment by *P. thiocyanatus* can remove thiocyanate concentrations up to 5000 mgL^{-1}, with maximum degradation rates of 1.20 mg SCN^{-}(mg cells h)$^{-1}$ without additional sources of carbon, nitrogen and sulphur than those provided by thiocyanate. The presence of carbon, nitrogen or sulphur sources easily assimilated, involves, the reduction of the maximum concentration of treatment up to 3500 mgL^{-1} and maximum degradation rates of 0.70 mg SCN^{-}(mg cells h)$^{-1}$.

- The substrate inhibition model defined by the Teissier equation is fitted to the experimental data of thiocyanate biodegradation by *P. thiocyanatus*, with correlation coefficient of 0.99, and fitting parameters of μ_{max}=0.059 h^{-1}, K_s=790 mg $SCN^{-}L^{-1}$ and K_i=6520 mg $SCN^{-}L^{-1}$ in absence carbon, nitrogen and sulphur additional sources and μ_{max}=0.344 h^{-1}, K_s=1150 mg $SCN^{-}L^{-1}$ y K_i=1730 mg $SCN^{-}L^{-1}$ in presence of these sources.

- Thiocyanate biodegradation by *P. thiocyanatus* is described by zero-order kinetic models with induction times whose length depends on thiocyanate concentration, either in presence or absence of carbon, nitrogen or sulphur sources easily assimilated. The induction times are lesser in media without additional sources of C, N and S.

Conclusions concerning the effect of the presence of other microorganisms and substrates

- The presence of thiocyanate in salicylic acid biodegradation by *P. putida*, has a negative effect on the process, since bacterial growth is completely inhibited and the specific degradation rate of salicylic acid is reduced by more than half (from 2.5 mg SA·(h mg cells)$^{-1}$ to 0.92 mg SA·(h mg cells)$^{-1}$).

- The presence of salicylic acid in thiocyanate biodegradation by *P. thiocyanatus* has a negative impact on the initial bacterial acclimation but not in the final thiocyanate assimilation, since specific thiocyanate degradation rates in the presence and absence of salicylic acid are 0.35 mg SCN^{-}·(h mg cells)$^{-1}$. Salicylic acid is not assimilated by *P. thiocyanatus.*

- An increase in stirring speed of 100 rpm and a change in medium composition suppose, in the case of the simultaneous biodegradation of salicylic acid and thiocyanate by *P. putida*, an increase of cell growth(μ=0.314 h^{-1}) and, accordingly the improvement in elimination time of salicylic acid. In the case of the simultaneous biodegradation of both pollutants by *P. thiocyanatus*, an increase of 2 ° C of the operating temperature and the change in medium composition suppose an increase in cell growth (μ=0.0186 h^{-1}) and a decrease in the induction time (ti=30 h).

- The presence of *P. thiocyanatus* in salicylic acid biodegradation by *P. putida* involves a decrease in *P. putida* growth from μ=0.23 h^{-1} to μ=0.09 h^{-1}.

- The presence of *P. putida* in thiocyanate biodegradation by *P. thiocyanatus* increases the induction time and reduces the bacterial growth.

- The use of a co-culture of *P. putida* and *P. thiocyanatus* for simultaneous SA and SCN^- biodegradation allows to achieve the complete removal of both pollutants up to 2000 mgL^{-1}.

- A commensalism behaviour is observed by the co-culture, which causes an improvement of the biodegradation process of both pollutants compared to systems with a single contaminants (SA or SCN^-) and two bacteria (co-culture) or two pollutants and one bacteria (*P. putida* or *P. thiocyanatus*).

- The substrate inhibition model defined by Teissier equation is fitted to the experimental data of thiocyanate biodegradation by the co-culture obtaining μ_{max}=0.08 h^{-1}, K_s=329 mg SCN^-L^{-1} y K_i=755.5 mg SCN^-L^{-1} with a correlation coefficient of 0.97. These results suggest that substrate inhibition effect is more marked when the bacterium is part of a co-culture than when they are as pure cultures.

- The substrate inhibition model defined by Teissier equation, with a term defining the inhibition by the presence of thiocyanate, is fitted to the experimental data of salicylic acid biodegradation by the co-culture. In this case, the adjustment parameters obtained are μ_{max}=0.052 h^{-1}, K_s=552 mgL^{-1} y K_i=2570 mgL^{-1} and n=0.54, with a correlation coefficient of 0.99, which indicates a higher affinity and tolerance of *P. putida* to salicylic acid when it is part of a co-culture.

- In the simultaneous salicylic acid and thiocyanate biodegradation by co-culture, the initial concentration of both pollutants has a marked negative effect on the physiological state of co-culture, in terms of metabolic activity, membrane integrity and bacterial size and complexity.

8. Bibliografía

[1] C. Orozco, A. Pérez, M.N. González, F.J. Rodrígez, J.M. Alfayate, Contaminación ambiental: Una visión desde la química, Thomson Editores Spain, (2003).

[2] T.G. Spiro, W.M. Stigliani, Química medioambiental, 2ª Edición, Pearson Educación S.A., Madrid, (2003).

[3] Metcalf, Eddy, Ingeniería de aguas residuales. Tratamiento, vertido y reutilización., McGraw-Hill, 3ª Edición. Madrid, (2000).

[4] G. Lei, H. Ren, L. Ding, F. Wang, X. Zhang, A full-scale biological treatment system application in the treated wastewater of pharmaceutical industrial park, Bioresource Technology, 101 (2010) 5852-5861.

[5] G. Banerjee, Phenol- and thiocyanate-based wastewater treatment in RBC reactor, Journal of Environmental Engineering, 122 (1996) 941-948.

[6] A. Chaudhari, K. Kodam, Biodegradation of thiocyanate using co-culture of Klebsiella pneumoniae and Ralstonia sp, Appl Microbiol Biotechnol, 85 (2010) 1167-1174.

[7] H. Huang, C. Feng, X. Pan, H. Wu, Y. Ren, C. Wu, C. Wei, Thiocyanate Oxidation by Coculture from a Coke Wastewater Treatment Plant, Journal of Biomaterials and Nanobiotechnology, 4 (2013) 37-46.

[8] C. Fall, E. Millán-Lagunas, K.M. Bâ, I. Gallego-Alarcón, D. García-Pulido, C. Díaz-Delgado, C. Solís-Morelos, COD fractionation and biological treatability of mixed industrial wastewaters, Journal of Environmental Management, 113 (2012) 71-77.

[9] H. Mikesková, Č. Novotný, K. Svobodová, Interspecific interactions in mixed microbial cultures in a biodegradation perspective, Appl Microbiol Biotechnol, 95 (2012) 861-870.

[10] M. Díaz, Ingeniería de Bioprocesos, Ediciones Paraninfo, Madrid, (2012).

[11] M. García-Rivero, M.R. Peralta-Pérez, Cometabolismo en la biodegradación de hidrocarburos, Revista mexicana de ingeniería química, 7 (2008) 1-12.

[12] M. Herrero, D.C. Stuckey, Bioaugmentation and its application in wastewater treatment: A review, Chemosphere, 140 (2015) 119-128.

[13] T.J. McGenity, B.D. Folwell, B.A. McKew, G.O. Sanni, Marine crude-oil biodegradation: a central role for interspecies interactions, Aquatic Biosystems, 8 (2012) 10-10.

[14] H. McLaughlin, A. Farrell, B. Quilty, Bioaugmentation of Activated Sludge with Two Pseudomonas putida Strains for the Degradation of 4-Chlorophenol, Journal of Environmental Science and Health, Part A, 41 (2006) 763-777.

[15] H. Duan, L.C.C. Koe, R. Yan, X. Chen, Biological treatment of H2S using pellet activated carbon as a carrier of microorganisms in a biofilter, Water Research, 40 (2006) 2629-2636.

[16] H.M. Ehrhardt, H.J. Rehm, Phenol degradation by microorganisms adsorbed on activated carbon, Appl Microbiol Biotechnol, 21 (1985) 32-36.

[17] G.M. Walker, L.R. Weatherley, Biological activated carbon treatment of industrial wastewater in stirred tank reactors, Chemical Engineering Journal, 75 (1999) 201-206.

[18] W. Xing, H.H. Ngo, S.H. Kim, W.S. Guo, P. Hagare, Adsorption and bioadsorption of granular activated carbon (GAC) for dissolved organic carbon (DOC) removal in wastewater, Bioresource Technology, 99 (2008) 8674-8678.

[19] S.-A. Ong, E. Toorisaka, M. Hirata, T. Hano, Granular activated carbon-biofilm configured sequencing batch reactor treatment of C.I. Acid Orange 7, Dyes and Pigments, 76 (2008) 142-146.

[20] T.C. Voice, D. Pak, X. Zhao, J. Shi, R.F. Hickey, Biological activated carbon in fluidized bed reactors for the treatment of groundwater contaminated with volatile aromatic hydrocarbons, Water Research, 26 (1992) 1389-1401.

[21] R.G. Rice, C.M. Robson, Biological Activated Carbon Enhanced Aerobic Biological Activity in GAC System, Ann Arbor Science Publishers, Michigan., (1982).

[22] J. Pengkang, J. Xin, W. Xianbao, F. Yongning, C.W. Xiaochang, Biological Activated Carbon Treatment Process for Advanced Water and Wastewater Treatment, in: M.D. Matovic (Ed.) Biomas Now: Cultivation and Utilization

InTech2013.

[23] F. Orshansky, N. Narkis, Characteristics of organics removal by PACT simultaneous adsorption and biodegradation, Water Research, 31 (1997) 391-398.

[24] B. Nowack, T.D. Bucheli, Occurrence, behavior and effects of nanoparticles in the environment, Environmental Pollution, 150 (2007) 5-22.

[25] S. Liu, M. Hu, T.H. Zeng, R. Wu, R. Jiang, J. Wei, L. Wang, J. Kong, Y. Chen, Lateral Dimension-Dependent Antibacterial Activity of Graphene Oxide Sheets, Langmuir, 28 (2012) 12364-12372.

[26] O. Akhavan, E. Ghaderi, Escherichia coli bacteria reduce graphene oxide to bactericidal graphene in a self-limiting manner, Carbon, 50 (2012) 1853-1860.

[27] W. Ghosh, P. Roy, Chemolithoautotrophic oxidation of thiosulfate, tetrathionate and thiocyanate by a novel rhizobacterium belonging to the genus Paracoccus, FEMS Microbiology Letters, 270 (2007) 124-131.

[28] A. Kumar, A.K. Pandey, S.S. Singh, R. Shanker, A. Dhawan, A flow cytometric method to assess nanoparticle uptake in bacteria, Cytometry Part A, 79A (2011) 707-712.

[29] A. Bour, F. Mouchet, J. Silvestre, L. Gauthier, E. Pinelli, Environmentally relevant approaches to assess nanoparticles ecotoxicity: A review, Journal of Hazardous Materials, 283 (2015) 764-777.

[30] H. Kušić, N. Koprivanac, A.L. Božić, I. Selanec, Photo-assisted Fenton type processes for the degradation of phenol: A kinetic study, Journal of Hazardous Materials, 136 (2006) 632-644.

[31] F. Tisa, M. Davoody, A.A. Abdul Raman, W.M.A.W. Daud, Degradation and Mineralization of Phenol Compounds with Goethite Catalyst and Mineralization Prediction Using Artificial Intelligence, PLoS ONE, 10 (2015) e0119933.

[32] A. Bódalo, M. Gómez, E. Gómez, A.M. Hidalgo, M.D. Murcia, J.L. Gómez, Eliminación de compuestos fenólicos en aguas residuales (I) Tratamientos químico, Ingeniería química, ISSN 0210-2064, 431 (2006) 141-146.

[33] A. Bódalo, J.L. Gómez, E. Gómez, A.M. Hidalgo, M.D. Murcia, M. Gómez, Eliminación de compuestos fenólicos en aguas residuales (II): Tratamientos físicos y biológicos, Ingeniería química, ISSN 0210-2064, 432 (2006) 136-146.

[34] G. Busca, S. Berardinelli, C. Resini, L. Arrighi, Technologies for the removal of phenol from fluid streams: A short review of recent developments, Journal of Hazardous Materials, 160 (2008) 265-288.

[35] S.G. Poulopoulos, F. Arvanitakis, C.J. Philippopoulos, Photochemical treatment of phenol aqueous solutions using ultraviolet radiation and hydrogen peroxide, Journal of Hazardous Materials, 129 (2006) 64-68.

[36] S.J. Kulkarni, J.P. Kaware, Review on Research for Removal of Phenol from Wastewater International Journal of Scientific and Research Publications, 3 (2013).

[37] www, http://prtr.ec.europa.eu. Consultado en 2015.

[38] T. Al-Khalid, M.H. El-Naas, Aerobic Biodegradation of Phenols: A Comprehensive Review, Critical Reviews in Environmental Science and Technology, 42 (2012) 1631–1690.

[39] W. Zhong, D. Wang, X. Xu, Phenol removal efficiencies of sewage treatment processes and ecological risks associated with phenols in effluents, Journal of Hazardous Materials, 217–218 (2012) 286-292.

[40] A.K. De, B. Chaudhuri, S. Bhattacharjee, B.K. Dutta, Estimation of ·OH radical reaction rate constants for phenol and chlorinated phenols using UV/H2O2 photo-oxidation, Journal of Hazardous Materials, 64 (1999) 91-104.

[41] L.K. Wang, Y.-T. Hung, H.H. Lo, C. Yapijakis, Handbook of Industrial al Hazardous Wastes Treatment, Marcel Dekker, Inc. New York, 2nd Edition (2006).

[42] T. Heberer, Occurrence, fate, and removal of pharmaceutical residues in the aquatic environment: a review of recent research data, Toxicology Letters, 131 (2002) 5-17.

[43] L. Khenniche, F. Aissani, Preparation and Characterization of Carbons from Coffee Residue: Adsorption of Salicylic Acid on the Prepared Carbons, Journal of Chemical & Engineering Data, 55 (2010) 728-734.

[44] S. Collado, L. Garrido, A. Laca, M. Díaz, Wet oxidation of salicylic acid solutions, Environ. Sci. Technol., 44 (2010) 8629-8635.

[45] www, http://www.insht.es/. Consultado en 2015.

[46] A. Goi, Y. Veressinina, M. Trapido, Degradation of salicylic acid by Fenton and modified Fenton treatment, Chemical Engineering Journal, 143 (2008) 1-9.

[47] M. Otero, C.A. Grande, A.E. Rodrigues, Adsorption of salicylic acid onto polymeric adsorbents and activated charcoal, Reactive and Functional Polymers, 60 (2004) 203-213.

[48] K. Fent, A.A. Weston, D. Caminada, Ecotoxicology of human pharmaceuticals, Aquatic Toxicology, 76 (2006) 122-159.

[49] X. Wang, R. Deng, X. Jin, J. Huang, Gallic acid modified hyper-cross-linked resin and its adsorption equilibria and kinetics toward salicylic acid from aqueous solution, Chemical Engineering Journal, 191 (2012) 195-201.

[50] X. Wang, Y. Wang, L. Feng, P. Liu, X. Zhang, A novel adsorbent based on functionalized three-dimensionally ordered macroporous cross-linked polystyrene for removal of salicylic acid from aqueous solution, Chemical Engineering Journal, 203 (2012) 251-258.

[51] M.V.V.C. Lakshmi , V. Sridevi, A review on biodegradation of phenol from industrial effluents, Jr. of Industrial Pollution Control, 25 (2009) 13-27.

[52] S.R. Ramalho, J.D. Beltrán, F. De Lora, Tratamiento de aguas residuales, Ed Reverté, S.A., (2003).

[53] J.D. Seader, E.J. Henley, Separation process Principles, 2ª Edición, John Wiley & Sons, Inc, (2006).

[54] B. Özkaya, Adsorption and desorption of phenol on activated carbon and a comparison of isotherm models, Journal of Hazardous Materials, 129 (2006) 158-163.

[55] R. Qadeer, A.H. Rehan, Study of the adsorption of phenol by activated carbon from aqueous solutions, Turkish Journal of Chemistry, 26 (2002) 357-361.

[56] V. Fierro, V. Torné-Fernández, D. Montané, A. Celzard, Adsorption of phenol onto activated carbons having different textural and surface properties, Microporous and Mesoporous Materials, 111 (2008) 276-284.

[57] M. Ahmaruzzaman, D.K. Sharma, Adsorption of phenols from wastewater, Journal of Colloid and Interface Science, 287 (2005) 14-24.

[58] I. Vázquez, J. Rodríguez-Iglesias, E. Marañón, L. Castrillón, M. Álvarez, Removal of residual phenols from coke wastewater by adsorption, Journal of Hazardous Materials, 147 (2007) 395-400.

[59] O. Hamdaoui, E. Naffrechoux, Modeling of adsorption isotherms of phenol and chlorophenols onto granular activated carbon: Part I. Two-parameter models and equations allowing determination of thermodynamic parameters, Journal of Hazardous Materials, 147 (2007) 381-394.

[60] S.K. Dhidan, Removal of phenolic compunds from aqueous solutions by adsoption onto activted carbons prepared from date stones by chemical activation with FeCl3, Journal of Engineering, 18 (1); 63-77 (2012).

[61] M.A. Atieh, Removal of Phenol from Water Different Types of Carbon – A Comparative Analysis, APCBEE Procedia, 10 (2014) 136-141.

[62] L. Levén, A. Schnürer, Effects of temperature on biological degradation of phenols, benzoates and phthalates under methanogenic conditions, International Biodeterioration & Biodegradation, 55 (2005) 153-160.

[63] I. Vázquez, J. Rodríguez, E. Marañón, L. Castrillón, Y. Fernández, Study of the aerobic biodegradation of coke wastewater in a two and three-step activated sludge process, Journal of Hazardous Materials, 137 (2006) 1681-1688.

[64] E. Marañón, I. Vázquez, J. Rodríguez, L. Castrillón, Y. Fernández, H. López, Treatment of coke wastewater in a sequential batch reactor (SBR) at pilot plant scale, Bioresource Technology, 99 (2008) 4192-4198.

[65] H.-q. Li, H.-j. Han, M.-a. Du, W. Wang, Removal of phenols, thiocyanate and ammonium from coal gasification wastewater using moving bed biofilm reactor, Bioresource Technology, 102 (2011) 4667-4673.

[66] G. Tziotzios, M. Teliou, V. Kaltsouni, G. Lyberatos, D.V. Vayenas, Biological phenol removal using suspended growth and packed bed reactors, Biochemical Engineering Journal, 26 (2005) 65-71.

[67] E.T. Yoong, P.A. Lant, P.F. Greenfield, In situ respirometry in an SBR treating wastewater with high phenol concentrations, Water Research, 34 (2000) 239-245.

[68] J. Desloover, S.E. Vlaeminck, P. Clauwaert, W. Verstraete, N. Boon, Strategies to mitigate N2O emissions from biological nitrogen removal systems, Current Opinion in Biotechnology, 23 (2012) 474-482.

[69] C. Domingo-Félez, A.G. Mutlu, M.M. Jensen, B.F. Smets, Aeration Strategies To Mitigate Nitrous Oxide Emissions from Single-Stage Nitritation/Anammox Reactors, Environmental Science & Technology, 48 (2014) 8679-8687.

[70] W. Jia, S. Liang, J. Zhang, H.H. Ngo, W. Guo, Y. Yan, Y. Zou, Nitrous oxide emission in low-oxygen simultaneous nitrification and denitrification process: Sources and mechanisms, Bioresource Technology, 136 (2013) 444-451.

[71] M.J. Kampschreur, H. Temmink, R. Kleerebezem, M.S.M. Jetten, M.C.M. van Loosdrecht, Nitrous oxide emission during wastewater treatment, Water Research, 43 (2009) 4093-4103.

[72] I. Oller, S. Malato, J.A. Sánchez-Pérez, Combination of Advanced Oxidation Processes and biological treatments for wastewater decontamination—A review, Science of The Total Environment, 409 (2011) 4141-4166.

[73] G. Moussavi, A. khavanin, R. Alizadeh, The integration of ozonation catalyzed with MgO nanocrystals and the biodegradation for the removal of phenol from saline wastewater, Applied Catalysis B: Environmental, 97 (2010) 160-167.

[74] M.H. Entezari, C. Pétrier, A combination of ultrasound and oxidative enzyme: sono-biodegradation of substituted phenols, Ultrasonics Sonochemistry, 10 (2003) 241-246.

[75] W.K. Lafi, B. Shannak, M. Al-Shannag, Z. Al-Anber, M. Al-Hasan, Treatment of olive mill wastewater by combined advanced oxidation and biodegradation, Separation and Purification Technology, 70 (2009) 141-146.

[76] R.M. Miller, G.M. Singer, J.D. Rosen, R. Bartha, Sequential degradation of chlorophenols by photolytic and microbial treatment, Environmental Science & Technology, 22 (1988) 1215-1219.

[77] B. Marrot, A. Barrios-Martinez, P. Moulin, N. Roche, Biodegradation of high phenol concentration by activated sludge in an immersed membrane bioreactor, Biochemical Engineering Journal, 30 (2006) 174-183.

[78] G. González, M.G. Herrera, M.T. García, M.M. Peña, Biodegradation of phenol in a continuous process: comparative study of stirred tank and fluidized-bed bioreactors, Bioresource Technology, 76 (2001) 245-251.

[79] K.-C. Loh, B. Cao, Paradigm in biodegradation using Pseudomonas putida—A review of proteomics studies, Enzyme and Microbial Technology, 43 (2008) 1-12.

[80] S. Collado, I. Rosas, E. González, A. Gutierrez-Lavin, M. Diaz, Pseudomonas putida response in membrane bioreactors under salicylic acid-induced stress conditions, Journal of Hazardous Materials, 267 (2014) 9-16.

[81] N.V. Pradeep, S. Anupama, K. Navya, H.N. Shalini, M. Idris, U.S. Hampannavar, Biological removal of phenol from wastewaters: a mini review, Appl Water Sci, 5 (2015) 105-112.

[82] A.A. Gami, M.Y. Shukor, K.A. Khalil, F.A. Dahalan, A. Khalid, S.A. Ahmad, Phenol and Phenolic Compounds Toxicity, Journal of Environmental Microbiology and Toxicology, 2 (2014) 11-23.

[83] P.E. Cornelis, Pseuddomonas. Genomics and Molecular Biology, Caister Academic Press, (2008).

[84] J.L.E. Ramos, Pseudomonas. Volume 1. Genomis, Life Style and Molecular Architecture, Spinger Science + Business Media. New York, (2004).

[85] D.J. Brenner, N.R. Krieg, J.R. Staley, Bergey's manual of systematic bacteriology. Vol. 2. Part B, 2nd Edition. Springer, (2007).

[86] M.T. Madigan, J.M. Martinko, J. Parker, Brock. Biología de los microorganismos, 10ª edición, Pearson Educación S.A. (2004).

[87] R. Muller, Bacterial Degradation of Xenobiotics, Microbial Control of Pollution, 48 (1992) 52.

[88] P.A. Vandenbergh, A.M. Wright, Plasmid Involvement in Acyclic Isoprenoid Metabolism by Pseudomonas putida, Applied and Environmental Microbiology, 45 (1983) 1953-1955.

[89] M.H. Otenio, M.T. Lopes da Silva, M. Marques, J. Roseiro, E. Bidoia, Benzene, Toluene and Xylene Biodegradation by Pseudomonas putida CCMI 852, Brazilian Journal of Microbiology, 36 (2005) 258-261.

[90] J.L. Ramos, E. Diaz, D. Dowling, V. de Lorenzo, S. Molin, F. O'Gara, C. Ramos, K.N. Timmis, The behavior of bacteria designed for biodegradation, Biotechnology (N Y), 12 (1994) 1349-1356.

[91] D. Regenhardt, H. Heuer, S. Heim, D.U. Fernandez, C. Strömpl, E.R.B. Moore, K.N. Timmis, Pedigree and taxonomic credentials of Pseudomonas putida strain KT2440, Environmental Microbiology, 4 (2002) 912-915.

[92] H. Movahedyan, H. Khorsandi, R. Salehi, M. Nikaeen, Detection of phenol degrading bacteria and pseudomonas putida in activated sludge by polymerase chain reaction, Iran. J. Environ. Health. Sci. Eng, 6 (2009) 115-120.

[93] A. Kumar, S. Kumar, S. Kumar, Biodegradation kinetics of phenol and catechol using Pseudomonas putida MTCC 1194, Biochemical Engineering Journal, 22 (2005) 151-159.

[94] M. Shourian, K.A. Noghabi, H.S. Zahiri, T. Bagheri, G. Karballaei, M. Mollaei, I. Rad, S. Ahadi, J. Raheb, H. Abbasi, Efficient phenol degradation by a newly characterized Pseudomonas sp. SA01 isolated from pharmaceutical wastewaters, Desalination, 246 (2009) 577-594.

[95] A.M. Chakrabarty, Genetic Basis of the Biodegradation of Salicylate in Pseudomonas, Journal of Bacteriology, 112 (1972) 815-823.

[96] J.-H. Ahn, S. Lee, S. Hwang, Growth kinetic parameter estimation of Klebsiella sp. utilizing thiocyanate, Process Biochemistry, 40 (2005) 1363-1366.

[97] F. Bhunia, N.C. Saha, A. Kaviraj, Toxicity of Thiocyanate to Fish, Plankton, Worm, and Aquatic Ecosystem, Bull. Environ. Contam. Toxicol., 64 (2000) 197-204.

[98] S. Ebbs, Biological degradation of cyanide compounds, Current Opinion in Biotechnology, 15 (2004) 231-236.

[99] C.-H. Hung, S.G. Pavlostathis, Aerobic biodegradation of thiocyanate, Water Research, 31 (1997) 2761-2770.

[100] C.-H. Hung, S.G. Pavlostathis, Kinetics and modeling of autotrophic thiocyanate biodegradation, Biotechnology and Bioengineering, 62 (1999) 1-11.

[101] Y. Katayama, A. Hiraishi, H. Kuraishi, Paracoccus thiocyanatus sp. nov., a new species of thiocyanate-utilizing facultative chemolithotroph, and transfer of Thiobacillus versutus to the genus Paracoccus as Paracoccus versutus comb. nov. with emendation of the genus, Microbiology, 141 (1995) 1469-1477.

[102] S.-J. Kim, Y. Katayama, Effect of growth conditions on thiocyanate degradation and emission of carbonyl sulfide by Thiobacillus thioparus THI115, Water Research, 34 (2000) 2887-2894.

[103] Y. Katayama, H. Kuraishi, Characteristics of Thiobacillus thioparus and its thiocyanate assimilation, Can. J. Microbiol., 24 (1978) 804-810.

[104] Y. Katayama, Y. Narahara, Y. Inoue, F. Amano, T. Kanagawa, H. Kuraishi, A thiocyanate hydrolase of Thiobacillus thioparus. A novel enzyme catalyzing the formation of carbonyl sulfide from thiocyanate, Journal of Biological Chemistry, 267 (1992) 9170-9175.

[105] E.Y. Bezsudnova, D.Y. Sorokin, T.V. Tikhonova, V.O. Popov, Thiocyanate hydrolase, the primary enzyme initiating thiocyanate degradation in the novel obligately chemolithoautotrophic halophilic sulfur-oxidizing bacterium Thiohalophilus

thiocyanoxidans, Biochimica et Biophysica Acta (BBA) - Proteins and Proteomics, 1774 (2007) 1563-1570.

[106] S. Zohar, I. Kviatkovski, S. Masaphy, Increasing tolerance to and degradation of high p-nitrophenol concentrations by inoculum size manipulations of Arthrobacter 4Hβ isolated from agricultural soil, International Biodeterioration & Biodegradation, 84 (2013) 80-85.

[107] T.R. Silva, E. Valdman, B. Valdman, S.G.F. Leite, Salicylic acid degradation from aqueous solutions using Pseudomonas fluorescens HK44: parameters studies and application tools, Brazilian Journal of Microbiology, 38 (2007) 39-44.

[108] J. Galíndez-Mayer, J. Ramón-Gallegos, N. Ruiz-Ordaz, C. Juárez-Ramírez, A. Salmerón-Alcocer, H.M. Poggi-Varaldo, Phenol and 4-chlorophenol biodegradation by yeast Candida tropicalis in a fluidized bed reactor, Biochemical Engineering Journal, 38 (2008) 147-157.

[109] H.F. Krug, P. Wick, Nanotoxicology: An Interdisciplinary Challenge, Angewandte Chemie International Edition, 50 (2011) 1260-1278.

[110] M. Ghosh, M. J, S. Sinha, A. Chakraborty, S.K. Mallick, M. Bandyopadhyay, A. Mukherjee, In vitro and in vivo genotoxicity of silver nanoparticles, Mutation Research/Genetic Toxicology and Environmental Mutagenesis, 749 (2012) 60-69.

[111] K.P. Olmstead, W.J. Weber, INTERACTIONS BETWEEN MICROORGANISMS AND ACTIVATED CARBON IN WATER AND WASTE TREATMENT OPERATIONS, Chemical Engineering Communications, 108 (1991) 113-125.

[112] W.G. Characklis, Bioengineering report: Fouling biofilm development: A process analysis, Biotechnology and Bioengineering, 23 (1981) 1923-1960.

[113] W.-c. Ying, W.J. Weber, Jr., Bio-Physicochemical Adsorption Model Systems for Wastewater Treatment, Journal (Water Pollution Control Federation), 51 (1979) 2661-2677.

[114] S.-L. Pai, Y.-L. Hsu, N.-M. Chong, C.-S. Sheu, C.-H. Chen, Continuous degradation of phenol by Rhodococcus sp. immobilized on granular activated carbon and in calcium alginate, Bioresource Technology, 51 (1995) 37-42.

[115] I. Ivancev-Tumbas, B. Dalmacija, Z. Tamas, E. Karlovic, Reuse of biologically regenerated activated carbon for phenol removal, Watter Research 32 (1998) 1085-1094.

[116] F. Piccinno, F. Gottschalk, S. Seeger, B. Nowack, Industrial production quantities and uses of ten engineered nanomaterials in Europe and the world, J Nanopart Res, 14 (2012) 1-11.

[117] Y. Ju-Nam, J.R. Lead, Manufactured nanoparticles: An overview of their chemistry, interactions and potential environmental implications, Science of The Total Environment, 400 (2008) 396-414.

[118] A. Neal, What can be inferred from bacterium–nanoparticle interactions about the potential consequences of environmental exposure to nanoparticles?, Ecotoxicology, 17 (2008) 362-371.

[119] A.M. Jastrzębska, P. Kurtycz, A.R. Olszyna, Recent advances in graphene family materials toxicity investigations, J Nanopart Res, 14 (2012) 1320.

[120] M.R. Das, R.K. Sarma, R. Saikia, V.S. Kale, M.V. Shelke, P. Sengupta, Synthesis of silver nanoparticles in an aqueous suspension of graphene oxide sheets and its antimicrobial activity, Colloids and Surfaces B: Biointerfaces, 83 (2011) 16-22.

[121] F. Ahmed, D.F. Rodrigues, Investigation of acute effects of graphene oxide on wastewater microbial community: A case study, Journal of Hazardous Materials, 256–257 (2013) 33-39.

[122] O. Akhavan, E. Ghaderi, Toxicity of Graphene and Graphene Oxide Nanowalls Against Bacteria, ACS Nano, 4 (2010) 5731-5736.

[123] S. Kang, M. Pinault, L.D. Pfefferle, M. Elimelech, Single-Walled Carbon Nanotubes Exhibit Strong Antimicrobial Activity, Langmuir, 23 (2007) 8670-8673.

[124] O. Akhavan, E. Ghaderi, A. Esfandiar, Wrapping Bacteria by Graphene Nanosheets for Isolation from Environment, Reactivation by Sonication, and Inactivation by Near-Infrared Irradiation, The Journal of Physical Chemistry B, 115 (2011) 6279-6288.

[125] S. Gurunathan, J.W. Han, A.A. Dayem, V. Eppakayala, J.-H. Kim, Oxidative stress-mediated antibacterial activity of graphene oxide and reduced graphene oxide in Pseudomonas aeruginosa, International Journal of Nanomedicine, 7 (2012) 5901-5914.

[126] S. Gurunathan, J.W. Han, V. Eppakayala, J.-H. Kim, Microbial reduction of graphene oxide by Escherichia coli: A green chemistry approach, Colloids and Surfaces B: Biointerfaces, 102 (2013) 772-777.

[127] S.M. Notley, R.J. Crawford, E.P. Ivanova, Bacterial Interaction with Graphene Particles and Surfaces, Advances in Graphene Science, Dr. M. Aliofkhazraei (Ed.) (2013).

[128] O.N. Ruiz, K.A.S. Fernando, B. Wang, N.A. Brown, P.G. Luo, N.D. McNamara, M. Vangsness, Y.-P. Sun, C.E. Bunker, Graphene Oxide: A Nonspecific Enhancer of Cellular Growth, ACS Nano, 5 (2011) 8100-8107.

[129] O. Akhavan, M. Abdolahad, Y. Abdi, S. Mohajerzadeh, Silver nanoparticles within vertically aligned multi-wall carbon nanotubes with open tips for antibacterial purposes, Journal of Materials Chemistry, 21 (2011) 387-393.

[130] W. Hu, C. Peng, W. Luo, M. Lv, X. Li, D. Li, Q. Huang, C. Fan, Graphene-Based Antibacterial Paper, ACS Nano, 4 (2010) 4317-4323.

[131] D. Li, F. Cui, Z. Zhao, D. Liu, Y. Xu, H. Li, X. Yang, The impact of titanium dioxide nanoparticles on biological nitrogen removal from wastewater and bacterial community shifts in activated sludge, Biodegradation, 25 (2014) 167-177.

[132] J. Rawat, S. Rana, R. Srivastava, R.D.K. Misra, Antimicrobial activity of composite nanoparticles consisting of titania photocatalytic shell and nickel ferrite magnetic core, Materials Science and Engineering: C, 27 (2007) 540-545.

[133] B. Erdural, U. Bolukbasi, G. Karakas, Photocatalytic antibacterial activity of TiO2–SiO2 thin films: The effect of composition on cell adhesion and antibacterial activity, Journal of Photochemistry and Photobiology A: Chemistry, 283 (2014) 29-37.

[134] B. Li, W. Huang, C. Zhang, S. Feng, Z. Zhang, Z. Lei, N. Sugiura, Effect of TiO2 nanoparticles on aerobic granulation of algal–bacterial symbiosis system and nutrients removal from synthetic wastewater, Bioresource Technology, 187 (2015) 214-220.

[135] A. Besinis, T. De Peralta, R.D. Handy, The antibacterial effects of silver, titanium dioxide and silica dioxide nanoparticles compared to the dental disinfectant chlorhexidine on Streptococcus mutans using a suite of bioassays, Nanotoxicology, 8 (2014) 1-16.

[136] A. Bonnefond, E. González, J.M. Asua, J.R. Leiza, J. Kiwi, C. Pulgarin, S. Rtimi, New evidence for hybrid acrylic/TiO2 films inducing bacterial inactivation under low intensity simulated sunlight, Colloids and Surfaces B: Biointerfaces, 135 (2015) 1-7.

[137] M. Cho, H. Chung, W. Choi, J. Yoon, Linear correlation between inactivation of E. coli and OH radical concentration in TiO2 photocatalytic disinfection, Water Research, 38 (2004) 1069-1077.

[138] S. Gelover, L.A. Gómez, K. Reyes, M. Teresa Leal, A practical demonstration of water disinfection using TiO2 films and sunlight, Water Research, 40 (2006) 3274-3280.

[139] G. Fu, P.S. Vary, C.-T. Lin, Anatase TiO2 Nanocomposites for Antimicrobial Coatings, The Journal of Physical Chemistry B, 109 (2005) 8889-8898.

[140] L. Zhang, J.C. Yu, H.Y. Yip, Q. Li, K.W. Kwong, A.-W. Xu, P.K. Wong, Ambient Light Reduction Strategy to Synthesize Silver Nanoparticles and Silver-Coated TiO2 with Enhanced Photocatalytic and Bactericidal Activities, Langmuir, 19 (2003) 10372-10380.

[141] A.-G. Rincón, C. Pulgarin, Absence of E. coli regrowth after Fe3+ and TiO2 solar photoassisted disinfection of water in CPC solar photoreactor, Catalysis Today, 124 (2007) 204-214.

[142] N.-Q. Puay, G. Qiu, Y.-P. Ting, Effect of Zinc oxide nanoparticles on biological wastewater treatment in a sequencing batch reactor, Journal of Cleaner Production, 88 (2015) 139-145.

[143] X. Zheng, R. Wu, Y. Chen, Effects of ZnO Nanoparticles on Wastewater Biological Nitrogen and Phosphorus Removal, Environmental Science & Technology, 45 (2011) 2826-2832.

[144] T. Le, K. Murugesan, E.-J. Kim, Y.-S. Chang, Effects of inorganic nanoparticles on viability and catabolic activities of Agrobacterium sp. PH-08 during biodegradation of dibenzofuran, Biodegradation, 25 (2014) 655-668.

[145] K. Anil, M.G.H. Zaidi, Implications of SPION and NBT Nanoparticles upon In Vitro and In Situ Biodegradation of LDPE Film, J. Microbiol. Biotechnol., 20 (2010).

[146] S.M. Cook, W.G. Aker, B.F. Rasulev, H.-M. Hwang, J. Leszczynski, J.J. Jenkins, V. Shockley, Choosing safe dispersing media for C60 fullerenes by using cytotoxicity tests on the bacterium Escherichia coli, Journal of Hazardous Materials, 176 (2010) 367-373.

[147] R.-S. Juang, S.-Y. Tsai, Growth kinetics of Pseudomonas putida in the biodegradation of single and mixed phenol and sodium salicylate, Biochemical Engineering Journal, 31 (2006) 133-140.

[148] H. Kwon, S. Woo, J. Park, Thiocyanate degradation by Acremonium strictum and inhibition by secondary toxicants, Biotechnology Letters, 24 (2002) 1347-1351.

[149] N.K. Sharma, L. Philip, S. Murty Bhallamudi, Aerobic degradation of phenolics and aromatic hydrocarbons in presence of cyanide, Bioresource Technology, 121 (2012) 263-273.

[150] R.R. Dash, A. Gaur, C. Balomajumder, Cyanide in industrial wastewaters and its removal: A review on biotreatment, Journal of Hazardous Materials, 163 (2009) 1-11.

[151] R.D. Neufeld, T. Valiknac, Inhibition of Phenol Biodegradation by Thiocyanate, Journal (Water Pollution Control Federation), 51 (1979) 2283-2291.

[152] M.D. Adjei, Y. Ohta, Factors affecting the biodegradation of cyanide by Burkholderia cepacia strain C-3, Journal of Bioscience and Bioengineering, 89 (2000) 274-277.

[153] X. Pan, Y. Li, H. Huang, Y. Ren, C. Wei, Biodegradation of thiocyanate and inhibitory interaction with phenol, ammonia in coking wastewater, CIESC Journal, 60 (2009) 3089-3096.

[154] L. Ayed, B. Harbi, A. Cheref, A. Bakhrouf, S. Achour, Application of the mixture design to optimise the formulation of active consortia to decolorize azo-dye methyl red, Water Sci Technol, 62 (2010) 2837-2845.

[155] L. Ayed, E. Khelifi, H.B. Jannet, H. Miladi, A. Cheref, S. Achour, A. Bakhrouf, Response surface methodology for decolorization of azo dye Methyl Orange by bacterial

consortium: Produced enzymes and metabolites characterization, Chemical Engineering Journal, 165 (2010) 200-208.

[156] A.A. Kadam, A.A. Telke, S.S. Jagtap, S.P. Govindwar, Decolorization of adsorbed textile dyes by developed consortium of Pseudomonas sp. SUK1 and Aspergillus ochraceus NCIM-1146 under solid state fermentation, Journal of Hazardous Materials, 189 (2011) 486-494.

[157] J.P. Jadhav, D.C. Kalyani, A.A. Telke, S.S. Phugare, S.P. Govindwar, Evaluation of the efficacy of a bacterial consortium for the removal of color, reduction of heavy metals, and toxicity from textile dye effluent, Bioresource Technology, 101 (2010) 165-173.

[158] N.J. Pino, M.C. Dominiquez, G.A. Penuela, Isolation of a selected microbial consortium capable of degrading methyl parathion and p-nitrophenol from a contaminated soil site, J Environ Sci Health B- Pesticides Food Contaminants and Agricultural Wastes, 46 (2011) 173-180.

[159] N. Pino, G. Peñuela, Simultaneous degradation of the pesticides methyl parathion and chlorpyrifos by an isolated bacterial consortium from a contaminated site, International Biodeterioration & Biodegradation, 65 (2011) 827-831.

[160] A. Hamitouche, A. Amrane, Z. Bendjama, F. Kaouah, Phenol biodegardation by mixed culture in batch reactor-optimization of the mineral medium composition, Desal Water Treat, 25 (2011) 20-24.

[161] N.V. Grigor'eva, T.F. Kondrat'eva, E.N. Krasil'nikova, G.I. Karavaiko, Mechanism of cyanide and thiocyanate decomposition by an association of Pseudomonas putida and Pseudomonas stutzeri strains, Microbiology, 75 (2006) 266-273.

[162] M. Goswami, N. Shivaraman, R.P. Singh, Microbial metabolism of 2-chlorophenol, phenol and ρ-cresol by Rhodococcus erythropolis M1 in co-culture with Pseudomonas fluorescens P1, Microbiological Research, 160 (2005) 101-109.

[163] H. Shen, Y.T. Wang, Simultaneous chromium reduction and phenol degradation in a coculture of Escherichia coli ATCC 33456 and Pseudomonas putida DMP-1, Applied and Environmental Microbiology, 61 (1995) 2754-2758.

[164] C. Gruden, S. Skerlos, P. Adriaens, Flow cytometry for microbial sensing in environmental sustainability applications: current status and future prospects, FEMS Microbiology Ecology, 49 (2004) 37-49.

[165] G. Giraffa, Studying the dynamics of microbial populations during food fermentation, FEMS Microbiology Reviews, 28 (2004) 251-260.

[166] H.M. Shapiro, Practical flow citometry 4 th ed. Wiley-Liss, New York, (2003).

[167] G. Nebe-von-Caron, P.J. Stephens, C.J. Hewitt, J.R. Powell, R.A. Badley, Analysis of bacterial function by multi-colour fluorescence flow cytometry and single cell sorting, J Microbiol Methods 42 (2000) 97-114.

[168] P. Foladori, L. Bruni, S. Tamburini, G. Ziglio, Direct quantification of bacterial biomass in influent, effluent and activated sludge of wastewater treatment plants by using flow cytometry, Water Research, 44 (2010) 3807-3818.

[169] M. Díaz, M. Herrero, L.A. García, C. Quirós, Application of flow cytometry to industrial microbial bioprocesses, Biochemical Engineering Journal, 48 (2010) 385-407.

[170] K. De Roy, L. Clement, O. Thas, Y. Wang, N. Boon, Flow cytometry for fast microbial community fingerprinting, Water Research, 46 (2012) 907-919.

[171] Y. Wang, F. Hammes, K. De Roy, W. Verstraete, N. Boon, Past, present and future applications of flow cytometry in aquatic microbiology, Trends in Biotechnology, 28 (2010) 416-424.

[172] M.G. Wilkinson, Flow Cytometry in Microbiology: Technology and Applications, Caister Academic Press2015.

[173] G. Vesey, P. Hutton, A. Champion, N. Ashbolt, K.L. Williams, A. Warton, D. Veal, Application of flow cytometric methods for the routine detection of Cryptosporidium and Giardia in water, Cytometry, 16 (1994) 1-6.

[174] F.X. Abad, R.M. Pintó, A. Bosch, Flow Cytometry Detection of Infectious Rotaviruses in Environmental and Clinical Samples, Applied and Environmental Microbiology, 64 (1998) 2392-2396.

[175] F. Hammes, M. Berney, Y. Wang, M. Vital, O. Köster, T. Egli, Flow-cytometric total bacterial cell counts as a descriptive microbiological parameter for drinking water treatment processes, Water Research, 42 (2008) 269-277.

[176] D. Marie, C.P.D. Brussaard, R. Thyrhaug, G. Bratbak, D. Vaulot, Enumeration of Marine Viruses in Culture and Natural Samples by Flow Cytometry, Applied and Environmental Microbiology, 65 (1999) 45-52.

[177] J. Porter, C. Edwards, J.A. Morgan, R.W. Pickup, Rapid, automated separation of specific bacteria from lake water and sewage by flow cytometry and cell sorting, Applied and Environmental Microbiology, 59 (1993) 3327-3333.

[178] P.A. del Giorgio, Y.T. Prairie, D.F. Bird, Coupling Between Rates of Bacterial Production and the Abundance of Metabolically Active Bacteria in Lakes, Enumerated Using CTC Reduction and Flow Cytometry, Microb Ecol, 34 (1997) 144-154.

[179] S. Riffard, S. Douglass, T. Brooks, S. Springthorpe, L.G. Filion, S.A. Sattar, Occurrence of Legionella in groundwater: an ecological study, Water Sci. Technol., 43 (2001) 99-102.

[180] M.F. DeFlaun, M.E. Fuller, P. Zhang, W.P. Johnson, B.J. Mailloux, W.E. Holben, W.P. Kovacik, D.L. Balkwill, T.C. Onstott, Comparison of methods for monitoring bacterial transport in the subsurface, Journal of Microbiological Methods, 47 (2001) 219-231.

[181] J.B. Rose, Environmental ecology of Cryptosporidium and public health implications, Annual Review of Public Health, 18 (1997) 135-161.

[182] L. Ma, G. Mao, J. Liu, H. Yu, G. Gao, Y. Wang, Rapid quantification of bacteria, viruses in influent, settled water, activated sludge, effluent from a wastewater treatment plant using flow cytometry., Water Sci. Technol., 68 (2013) 1763-1769.

[183] S. Günther, C. Koch, T. Hübschmann, I. Röske, R.A. Müller, T. Bley, H. Harms, S. Müller, Correlation of Community Dynamics and Process Parameters As a Tool for the Prediction of the Stability of Wastewater Treatment, Environmental Science & Technology, 46 (2012) 84-92.

[184] L. Mehlig, M. Petzold, C. Heder, S. Günther, S. Müller, M. Eschenhagen, I. Röske, K. Röske, Biodiversity of Polyphosphate Accumulating Bacteria in Eight WWTPs with Different Modes of Operation, Journal of Environmental Engineering, 139 (2013) 1089-1098.

[185] G. Ziglio, G. Andreottola, S. Barbesti, G. Boschetti, L. Bruni, P. Foladori, R. Villa, Assessment of activated sludge viability with flow cytometry, Water Research, 36 (2002) 460-468.

[186] J. Porter, J. Robinson, R. Pickup, C. Edwards, Recovery of a bacterial sub-population from sewage using immunofluorescent flow cytometry and cell sorting, FEMS Microbiology Letters, 133 (1995) 195-199.

[187] G. Wallner, R. Erhart, R. Amann, Flow cytometric analysis of activated sludge with rRNA-targeted probes, Applied and Environmental Microbiology, 61 (1995) 1859-1866.

[188] H.M. Shapiro, Microbial analysis at the single-cell level: tasks and techniques, Journal of Microbiological Methods, 42 (2000) 3-16.

[189] R.P. Haugland, Handbook of Fluorescent Probes and Research Chemicals, Molecular probes Inc., Eugene, Oregon, USA., (2002) 9th edition.

[190] G. Bogosian, E.V. Bourneuf, A matter of bacterial life and death, EMBO Reports, 2 (2001) 770-774.

[191] C. Quirós, M. Herrero, L.A. García, M. Díaz, Application of Flow Cytometry to Segregated Kinetic Modeling Based on the Physiological States of Microorganisms, Applied and Environmental Microbiology, 73 (2007) 3993-4000.

[192] C. Quirós, M. Herrero, L.A. García, M. Díaz, Quantitative Approach to Determining the Contribution of Viable-but-Nonculturable Subpopulations to Malolactic

Fermentation Processes, Applied and Environmental Microbiology, 75 (2009) 2977-2981.

[193] C.J. Hewitt, G. Nebe-von-Caron, The application of multi-parameter flow cytometry to monitor individual microbial cell physiological state, Adv. Biochem. Eng. Biot., 89 (2004) 197- 223.

[194] D.A. Veal, D. Deere, B. Ferrari, J. Piper, P.V. Attfield, Fluorescence staining and flow cytometry for monitoring microbial cells, Journal of Immunological Methods, 243 (2000) 191-210.

[195] S. Alonso, M. Rendueles, M. Díaz, Selection method of pH conditions to establish Pseudomonas taetrolens physiological states and lactobionic acid production, Appl Microbiol Biotechnol, 97 (2013) 3843-3854.

[196] C. Quirós, Desarrollo de modelos cinéticos segregados para el control de procesos fermentativos, Tesis doctoral. Universidad de Oviedo, (2008).

[197] A.M. Steger, A. Oppedahl, L.R. Etzel, K.R. Harkins, Advanced Analytical Technologies, Inc., Ames, IA., American Society for Microbiology Annual Meeting, Mayo., (2002).

[198] F. Garcia-Ochoa, V.E. Santos, A. Alcon, Structured kinetic model for Xanthomonas campestris growth, Enzyme and Microbial Technology, 34 (2004) 583-594.

[199] M. Cánovas, V. García, V. Bernal, T. Torroglosa, J.L. Iborra, Analysis of Escherichia coli cell state by flow cytometry during whole cell catalyzed biotransformation for l-carnitine production, Process Biochemistry, 42 (2007) 25-33.

[200] M.A. Henson, Dynamic modeling of microbial cell populations, Current Opinion in Biotechnology, 14 (2003) 460-467.

[201] C. Cipollina, M. Vai, D. Porro, C. Hatzis, Towards understanding of the complex structure of growing yeast populations, Journal of Biotechnology, 128 (2007) 393-402.

[202] R.G. Combarros, S. Collado, A. Laca, M. Díaz, Conditions and mechanisms in thiocyanate biodegradation, Journal of Residuals Science and Technology, 12 (2015).

[203] L. Ploux, S. Beckendorff, M. Nardin, S. Neunlist, Quantitative and morphological analysis of biofilm formation on self-assembled monolayers, Colloids and Surfaces B: Biointerfaces, 57 (2007) 174-181.

[204] K.-C. Loh, Y.-G. Yu, Kinetics of carbazole degradation by Pseudomonas putida in presence of sodium salicylate, Water Research, 34 (2000) 4131-4138.

[205] www, http://www.norit.com/ . Consultado en 2015.

[206] www, http://www.chemvironcarbon.com/. Consultado en 2015.

[207] M.C. Jiménez Moleón, M.L. Arias, M. Lucero, Extensión de la adsorción de compuestos fenólicos sobre carbón activado vegetal, Facultad de Ingeniería CIRA, México (2005).

[208] D. van der Kooij, H.R. Veenendaal, C. Baars-Lorist, D.W. van der Klift, Y.C. Drost, Biofilm formation on surfaces of glass and Teflon exposed to treated water, Water Research, 29 (1995) 1655-1662.

[209] S. Saraswat, J.P.N. Rai, Heavy metal adsorption from aqueous solution using Eichhornia crassipes dead biomass, International Journal of Mineral Processing, 94 (2010) 203-206.

[210] F.D. Snell, C.T. Snell, Colorimetric methods of analysis.

Including some turbidimetric and nephelometric methods., New York, D. Van Nostrand Company, Inc., Volume III (1953).

[211] A.P.H.A. APHA, Standard Methods for the Examination of Water and Wastewater, 20 th. Ed. Washington, (1999).

[212] Y.-C. Hsu, H.-C. Yang, J.-H. Chen, The enhancement of the biodegradability of phenolic solution using preozonation based on high ozone utilization, Chemosphere, 56 (2004) 149-158.

[213] T.S. Sreeprasad, M.S. Maliyekkal, K. Deepti, K. Chaudhari, P.L. Xavier, T. Pradeep, Transparent, Luminescent, Antibacterial and Patternable Film Forming Composites of Graphene Oxide/Reduced Graphene Oxide, ACS Applied Materials & Interfaces, 3 (2011) 2643-2654.

[214] M.J. Fernández-Merino, S. Villar-Rodil, J.I. Paredes, P. Solís-Fernández, L. Guardia, R. García, A. Martínez-Alonso, J.M.D. Tascón, Identifying efficient natural bioreductants for the preparation of graphene and graphene-metal nanoparticle hybrids with enhanced catalytic activity from graphite oxide, Carbon, 63 (2013) 30-44.

[215] J.I. Paredes, S. Villar-Rodil, A. Martínez-Alonso, J.M.D. Tascón, Graphene Oxide Dispersions in Organic Solvents, Langmuir, 24 (2008) 10560-10564.

[216] J.I. Paredes, S. Villar-Rodil, M.J. Fernandez-Merino, L. Guardia, A. Martinez-Alonso, J.M.D. Tascon, Environmentally friendly approaches toward the mass production of processable graphene from graphite oxide, Journal of Materials Chemistry, 21 (2011) 298-306.

[217] R.G. Combarros, I. Rosas, A.G. Lavín, M. Rendueles, M. Díaz, Influence of Biofilm on Activated Carbon on the Adsorption and Biodegradation of Salicylic Acid in Wastewater, Water Air Soil Pollut, 225 (2014) 1-12.

[218] M. Paschoalino, N.C. Guedes, W. Jardim, E. Mielczarski, J.A. Mielczarski, P. Bowen, J. Kiwi, Inactivation of E. coli mediated by high surface area CuO accelerated by

light irradiation >360 nm, Journal of Photochemistry and Photobiology A: Chemistry, 199 (2008) 105-111.

[219] K. Krishnamoorthy, M. Veerapandian, L.-H. Zhang, K. Yun, S.J. Kim, Antibacterial Efficiency of Graphene Nanosheets against Pathogenic Bacteria via Lipid Peroxidation, The Journal of Physical Chemistry C, 116 (2012) 17280-17287.

[220] L.A. Luongo, X. Zhang, Toxicity of carbon nanotubes to the activated sludge process, Journal of Hazardous Materials, 178 (2010) 356-362.

[221] J. Bezawada, N.V. Hoang, T.T. More, S. Yan, N. Tyagi, R.D. Tyagi, R.Y. Surampalli, Production of extracellular polymeric substances (EPS) by Serratia sp.1 using wastewater sludge as raw material and flocculation activity of the EPS produced, Journal of Environmental Management, 128 (2013) 83-91.

[222] C.M. Ajila, U.J.S. Prasada Rao, Protection against hydrogen peroxide induced oxidative damage in rat erythrocytes by Mangifera indica L. peel extract, Food and Chemical Toxicology, 46 (2008) 303-309.

[223] S. Liu, T.H. Zeng, M. Hofmann, E. Burcombe, J. Wei, R. Jiang, J. Kong, Y. Chen, Antibacterial Activity of Graphite, Graphite Oxide, Graphene Oxide, and Reduced Graphene Oxide: Membrane and Oxidative Stress, ACS Nano, 5 (2011) 6971-6980.

[224] T. Akasaka, F. Watari, Capture of bacteria by flexible carbon nanotubes, Acta Biomaterialia, 5 (2009) 607-612.

[225] A.M. Pinto, I.C. Gonçalves, F.D. Magalhães, Graphene-based materials biocompatibility: A review, Colloids and Surfaces B: Biointerfaces, 111 (2013) 188-202.

[226] S. Alonso, M. Rendueles, M. Díaz, Physiological heterogeneity of Pseudomonas taetrolens during lactobionic acid production, Appl Microbiol Biotechnol, 96 (2012) 1465-1477.

[227] T.H. Nielsen, O.R. Sjøholm, J. Sørensen, Multiple physiological states of a Pseudomonas fluorescens DR54 biocontrol inoculant monitored by a new flow cytometry protocol, FEMS Microbiology Ecology, 67 (2009) 479-490.

[228] C. Bouchelta, M.S. Medjram, O. Bertrand, J.-P. Bellat, Preparation and characterization of activated carbon from date stones by physical activation with steam, Journal of Analytical and Applied Pyrolysis, 82 (2008) 70-77.

[229] Y. Sudaryanto, S.B. Hartono, W. Irawaty, H. Hindarso, S. Ismadji, High surface area activated carbon prepared from cassava peel by chemical activation, Bioresource Technology, 97 (2006) 734-739.

[230] R.C. Bansal, J.B. Donnet, F. Stoeckli, Active Carbon Marcel Dekker, New York (1998).

[231] www, http://www.lenntech.es/biblioteca/adsorption.htm. Colsultado en 2015.

[232] C.H. Giles, D. Smith, A. Huitson, A general treatment and classification of the solute adsorption isotherm. I. Theoretical, Journal of Colloid and Interface Science, 47 (1974) 755-765.

[233] W. McCabe, J. Smith, P. Harriot, Operaciones unitarias en Ingeniería Química, 4th Ed. McGraw Hill. Madrid, (1998).

[234] F. Helfferich, Ion Exchange. Series in Advanced Chemistry., McGraw-Hill Book Company, Inc. New York., (1962).

[235] M. Rendueles, Intercambio Iónico en altas concentraciones. Fenómenos de transferencia de co-iones, Tesis doctoral. Universidad de Oviedo, (1995).

[236] M. Torre, D. Bachiller, M. Rendueles, C.O. Menéndez, M. Díaz, Cyanide Recovery from Gold Extraction Process Waste Effluents by Ion Exchange I. Equilibrium and Kinetics, Solvent Extraction and Ion Exchange, 24 (2006) 99-117.

[237] A.E. Rodrigues, D. Tondeur, Percolation Processes: Theory and Application, Nato Sciences Series E, (1981).

[238] C. Namasivayam, M.V. Sureshkumar, Modelling Thiocyanate Adsorption onto Surfactant-Modified Coir Pith, an Agricultural Solid 'Waste', Process Safety and Environmental Protection, 85 (2007) 521-525.

[239] C. Namasivayam, D. Sangeetha, Kinetic studies of adsorption of thiocyanate onto ZnCl2 activated carbon from coir pith, an agricultural solid waste, Chemosphere, 60 (2005) 1616-1623.

9. Anexos

Anexo I

9.1. Adsorción con carbón activo

9.1.1. Material adsorbente carbonoso: carbón activo convencional

El carbón activo es un material poroso preparado mediante carbonización y activación de materiales orgánicos, especialmente de origen vegetal, hullas, lignitos y turbas, con el fin de obtener un alto grado de porosidad y una importante superficie intrapartícular. Presenta una forma microcristalina y no grafítica [3, 228, 229].

La preparación del carbón activo consta de dos etapas: una primera de carbonización del material de partida seguida de otra de activación (apertura de poros) del material carbonizado, De forma general, cualquier material carbonoso es susceptible de ser el punto de partida para la preparación del carbón activo. Las propiedades del material de partida y las condiciones del proceso de activación determinarán en gran medida las propiedades del material adsorbente final [3, 228, 229].

Se pueden distinguir dos tipos de carbón activo en función de si el sometido a un proceso de granulación o de pulverización [3]:

- Carbón activado en polvo o PAC (Powdered activated carbón), se presenta como un polvo fino negro.
- Carbón activado granular o GAC (Granular activated carbón) que se presenta en grano de hasta 2 mm.

La gran ventaja del carbón activo como adsorbente descansa en la posibilidad de reactivación (hasta 30 veces o más) sin pérdida apreciable del poder de adsorción. Usualmente, la reactivación se lleva a cabo calentando el carbón agotado hasta 930 °C aproximadamente en una atmósfera aire-vapor (reactivación térmica). Esta operación puede realizarse en hornos de hogar múltiple o en hornos rotativos. Los productos orgánicos adsorbidos se queman y el carbón activo se restaura básicamente hasta su capacidad inicial de adsorción [3, 52].

Por otra parte, el carbón activo tiene una escasa especifidad ante un proceso de retención, es un adsorbente “universal”. No obstante, por su naturaleza apolar y por el tipo de fuerzas implicadas en el proceso da adsorción, retendrá preferentemente moléculas apolares y de alto volumen molecular, mientras que sustancias como el nitrógeno, oxígeno y el agua prácticamente no se retienen en el carbón a temperatura ambiente [230].

Los factores más importantes que influyen en la adsorción de compuestos presentes en el agua son [231]:

- El tipo de compuesto que debe ser eliminado. Los compuestos con elevado peso molecular y baja solubilidad se adsorben más fácilmente.
- La concentración del compuesto que desea ser eliminado. Cuanto mayor sea la concentración del adsorbato, la cantidad de adsorbente deberá ser más elevada.
- Presencia de otros compuestos orgánicos ocurrirá una competencia entre los diferentes compuestos por los lugares de adsorción disponibles.
- El pH del agua. Por ejemplo, los compuestos ácidos se eliminan más fácilmente a valores de pH bajos.
- Area superficial.
- Tamaño y distribución del poro.

En cualquiera que sea la forma de aplicación de la adsorción como operación de separación o almacenamiento, resulta fundamental el conocimiento de las características del adsorbente y del equilibrio de adsorción que se establece entre éste y los compuestos de la corriente que se va a tratar. El conocimiento del equilibrio de adsorción para un determinado sistema adsorbato-adsorbente posibilita el diseño de las condiciones de operación, presión y temperatura de trabajo.

9.1.2. Equilibrio de adsorción

Una de las formas más habituales de representación del equilibrio de adsorción es mediante la relación entre la cantidad adsorbida y la presión, en el caso de gases o vapores, o la concentración en la fase líquida, en el caso de adsorción de líquidos, para una temperatura determinada. Esta relación se conoce como isoterma de adsorción para un determinado sistema adsorbato-adsorbente [3, 53].

En el equilibrio de adsorción existe una proporción definida de soluto repartida entre las dos fases, líquida y sólida. Esta distribución es habitualmente definida mediante el parámetro capacidad de equilibrio (ec. 3), definido como [18]:

$$q_e = \frac{C_0 - C_e}{W} \cdot V \qquad \text{(ec. 3)}$$

donde, q_e es la capacidad de equilibrio, C_0 es la concentración inicial del adsorbato en la fase líquida, C_e es la concentración de adsorbato en la fase líquida en el equilibrio, V es el volumen de disolución y W es la masa de adsorbente.

Brunauer y sus colaboradores en el año 1938 propusieron para la adsorción en fase gas, 6 tipos de isotermas empleando los mecanismos de adsorción en función de la presión relativa a la que ocurren. Sin embargo, Giles (1960) propuso un sistema de clasificación de las isotermas de adsorción en disolución, en el que divide las isotermas en 4 clases en función de la pendiente de la parte inicial de la curva. Las tipo "S" (*S- shape*), son aquellas en las que se produce una adsorción cooperativa, a medida que aumenta la concentración de equilibrio aumenta la capacidad del solido por retener el adsorbato. Las isotermas tipo "L" (*Langmuir*), son las más comunes, se caracterizan porque a medida que aumenta la concentración en equilibrio en la fase fluida el número de centros activos disponibles disminuye, hasta llegar a una meseta que representa que el sólido no puede retener más adsorbato. Las curvas tipo "H" (*High affinity*), son aquellas en las que el adsobente tiene una gran afinidad por el adsorbato lo que ocasiona que aún a muy bajas concentraciones de adsorba cantidades significativas. Finalmente, las curvas tipo "C" (*Constant*) se caracterizan por una proporción de centros activos constantes, mostrando un comportamiento intermedio entre las curvas tipo "S" y "L" y se encuentran en sistemas donde el soluto penetra en el sólido más fácilmente que el disolvente. En la Figura 3 se pueden ver la clasificación de las isotermas de adsorción propuestas por Giles, divididas a su vez en subgrupos que indican la extensión en la que ha tenido lugar la adsorción [232].

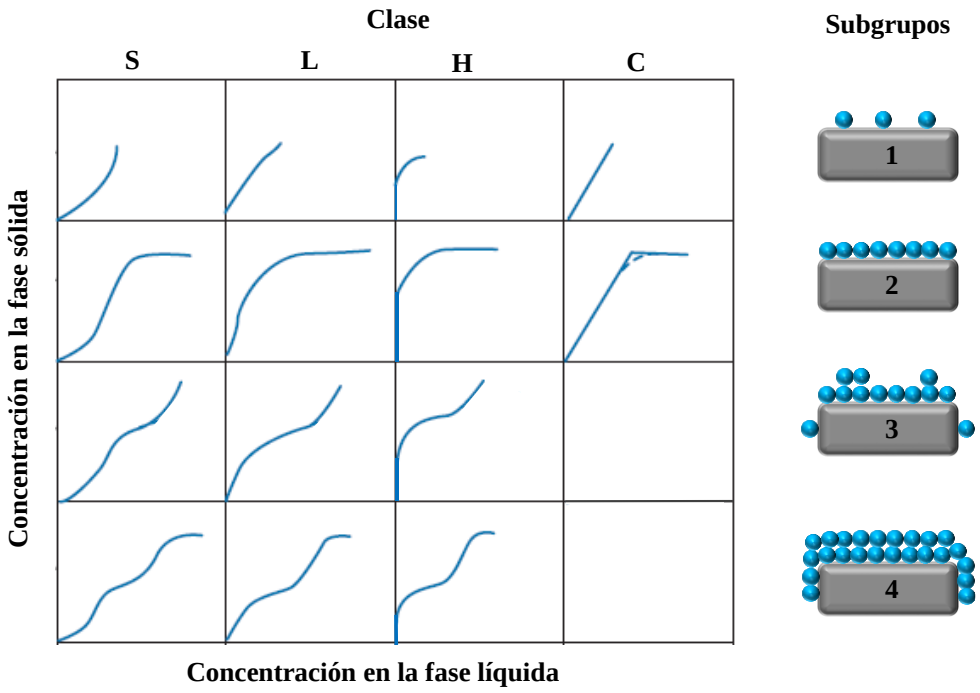

Figura 9.1: Clasificación de Giles de las isotermas de adsorción

La forma más sencilla de representar el equilibrio de adsorción es suponer que para concentraciones muy bajas de adsorbato en la superficie del adsorbente, las moléculas de adsorbato son independientes unas de otras. De esta forma, se puede asumir que la fase

adsorbida, que se presenta diluida, se comporta como un gas ideal bidimensional, pudiéndole ser aplicada la ley de los gases ideales para el caso particular de un sistema no volumétrico. En este caso, se puede establecer la proporcionalidad entre la extensión de la adsorción y la concentración o la presión parcial del adsorbato en el límite de llenado cero, lo que al final se reduce a la ley de Henry (ec. 4) [3, 53].

$$q = K_H\, Ce \qquad (ec.\,4)$$

donde q es la capacidad del sistema, K_H es la constante de Henry y C_e es la concentración de equilibrio.

La ecuación de Langmuir (1916) (ec. 12) representa adecuadamente ciertos casos de quimisorción y ha sido de especial relevancia para el desarrollo de posteriores modelos de fisisorción. Se supone que el adsorbente dispone de un número finito de sitios de adsorción, estando parte de ellos ocupados por moléculas de adsorbato y otra parte libres. La velocidad de adsorción depende de la presión y del número de sitios libres, mientras que la velocidad de desorción es dependiente del número de sitios ocupados. El estado de equilibrio se obtiene cuando ambas velocidades, adsorción y desorción, se igualan, para cierto valor de presión y proporción de sitios libres [3, 53].

$$q = \frac{(Q_0\, k\, C_e)}{(1 + k\, C_e)} \qquad (ec.\,5)$$

donde, k la constante de equilibrio de la isoterma de Langmuir, Q_0, es la capacidad máxima o llenado de la monocapa.

Existen además una serie de ecuaciones empíricas para el ajuste de datos de adsorción. La primera de ellas fue el modelo de Freundlich (1906) (ec. 13), que tiene en cuenta aquellos comportamientos no lineales entre la cantidad adsorbida y la concentración o presión parcial de la fase fluida; por tanto, propone una relación lineal entre las funciones logarítmicas de capacidad de adsorción y concentración de equilibrio. Además, no establece un valor límite de la cantidad adsorbida según aumenta la presión. Este modelo no reproduce correctamente los datos de sistemas confinados a baja temperatura o a presión elevada [3].

$$q = k\, C_e^{\,1/n} \qquad (ec.\,6)$$

donde, k y n son parámetros empíricos de la isoterma de Freundlich.

Para aumentar el grado de ajuste de los datos experimentales que presentan un valor límite de la cantidad adsorbida, se propuso un modelo híbrido entre la isoterma de Langmuir y la de Freundlich, conocido como la isoterma de Sips (1948), o modelo de Freundlich

generalizado (ec. 7). Este modelo, al igual que el modelo de Freundlich, no se reduce a la ley de Henry para el límite de presión cero.

$$q = \frac{Q_0(kC_e)^{\left(\frac{1}{m}\right)}}{1 + (kC_e)^{\left(\frac{1}{m}\right)}} \qquad \text{(ec. 7)}$$

donde, m es un parámetro empírico de la isoterma de Sips, Q_o es la capacidad de adsorción límite.

Otro tipo de isoterma que representa el equilibrio entre la cantidad adsorbida y la concentración es la isoterma del factor de separación constante representada mediante la ecuación 8 [233].

$$q = \frac{(kQ_TC_e)}{(C_T + (k-1)C_e)} \qquad \text{(ec. 8)}$$

donde, k representa a la constante de equilibrio, Q_T es la cantidad máxima de sustancia adsorbida, C_T es la máxima concentración de equilibrio del adsorbato en la fase líquida, C_e es la concentración de equilibrio para las diferentes concentraciones de trabajo.

En la figura 12, se muestran uno de los programas Matlab utilizado para el cálculo de los parámetros de las isotermas en estudio.

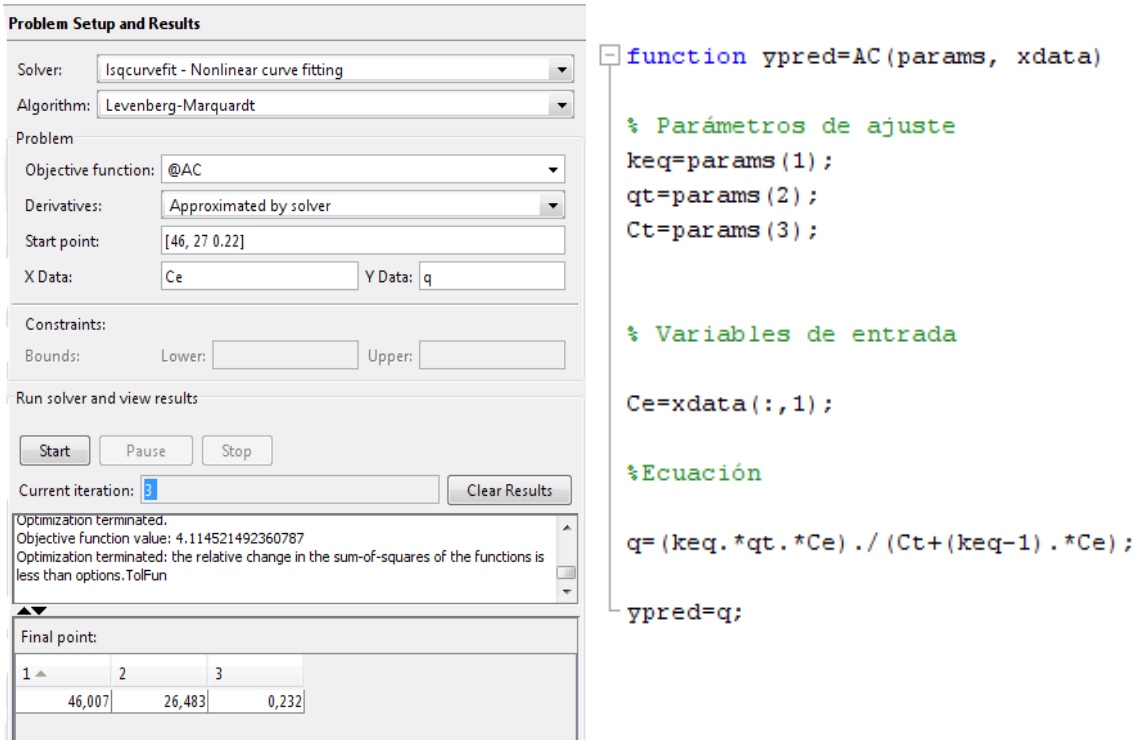

Figura 9.2: Programa Matlab para el cálculo de los parámetros k, C_T y Q_T de la isoterma Factor de separación constante

9.1.3. Cinética de adsorción

En el estudio de la cinética del proceso de adsorción, las etapas presentes en este proceso son:

- Difusión del compuesto a través de la capa del fluido que rodea la partícula (película liquida).
- Difusión del compuesto en el interior de los poros del sólido.
- Adsorción del compuesto en los sitios activos del sólido.

En el proceso de adsorción, tanto la difusión en el interior de la partícula como en la película líquida pueden ser etapas controlantes e incluso en algunos casos las dos intervienen en la velocidad del proceso, en ningún caso se encontrará control por la etapa de adsorción puesto que la etapa de fijación es en general muy rápida [234].

El modelo de película de Nernst (1904) es una herramienta muy útil y que ha demostrado buenos resultados a pesar de sus arriesgados supuestos. Se supone la existencia de una película estancada de líquido bien diferenciada de la masa por un límite.

Los procesos de difusión se describen por la primera ley de Fick (ec. 9):

$$J_i = -D\,\Delta C_i \qquad (ec.\,9)$$

Donde, J_i es el flujo del elemento en estudio, D es el coeficiente de difusión y ΔC_i es el gradiente de concentración del elemento.

Esta ecuación representa el caso más simple de difusión, un sistema ideal donde no hay procesos simultáneos que interfieran lo que no está muy de acuerdo con la realidad, puesto que la difusión está unida a otros procesos lo que implica que su valor no suele ser constante.

En el proceso de adsorción se da una situación especial, la matriz ocupa una fracción sustancial del volumen en el medio lo que supone que obstruye la difusión y, en consecuencia, la predicción de las velocidades de difusión. La teoría cinética del proceso de adsorción resuelve esta dificultad considerando al carbón activo como una fase cuasi-homogénea y no tiene en cuenta las heterogeneidades con respecto a las dimensiones moleculares y en la estructura geométrica de las partículas; la ecuación de Fick también se aplica a la fase sólida. Otro factor que influye en el proceso, es el tamaño y forma de las partículas, en este caso se asume que todas las partículas son esféricas y de tamaño uniforme, ya que un tratamiento riguroso en el que se tendría en cuenta la uniformidad e irregularidad de forma y tamaño de las partículas sería muy compleja [235].

Se han obtenido por diferentes autores soluciones de las ecuaciones diferenciales, tanto para el interior de la partícula como en la película líquida; y los coeficientes de difusión en las dos fases, que serán diferentes. En estos modelos se supone geometría esférica y matriz porosa para la fase sólida y se establecen condiciones iniciales, de contorno y las restricciones oportunas [236, 237].

Modelo de difusión a través de los poros

Las ecuaciones que definen el modelo son las siguientes [236, 237]:

- Balance de materia en el interior de la partícula (ec. 10).

$$\frac{\partial q_i(R,t)}{\partial t} = \frac{\partial q_{ie}(R,t)}{\partial t} + \varepsilon_i \frac{\partial C_{pi}(R,t)}{\partial t} = \frac{1}{R^2}\left[\frac{\partial}{\partial R} R^2 \varepsilon_i D_p \frac{\partial C_{pi}(R,t)}{\partial t}\right] \qquad \text{(ec. 10)}$$

- Balance de materia en la disolución (ec. 11)

$$\varepsilon_i V\big(C_{iT} - C_i(t)\big) = (1-\varepsilon_i)\sqrt{q_{ie} + \varepsilon_i C_i(t)} \qquad \text{(ec. 11)}$$

- Concentración media en la partícula (ec. 12)

$$\sqrt{q_{ie} + \varepsilon_i C_i(t)} = \frac{3}{R_0^3}\int_0^R R^2 \left(q_{ie} + \varepsilon_i\, C_{pi}\right)(R,t)dR \qquad \text{(ec. 12)}$$

Las condiciones iniciales y límite necesarias para resolver el sistema son:

- Condiciones iniciales

$$C_{pi}(R,0) = 0$$

- Condiciones límite

$$\text{En R} = 0 \;\rightarrow\; \left|\frac{\partial C_{pi}(R,t)}{\partial t}\right|_{R=0} = \left|\frac{\partial q_i(R,t)}{\partial R}\right|_{R=0}$$

- En la interfase

$$(\text{R} = \text{R}_0) \rightarrow\; C_{pi}(R_0,t) = C_i(\,t)$$

Este sistema de ecuaciones se resuelve empleando un programa Fortran, que utiliza una subrutina denominada PDECOL (Madsen et al., 1979), en el que se emplea el método de colocación ortogonal en elementos finitos para resolver el sistema no lineal de ecuaciones diferenciales [236].

Modelo de transferencia de materia en la película líquida

Este modelo supone que el intercambio de los iones está limitado por la transferencia de materia a través de la capa límite que rodea a cada partícula del sólido [234].

Las ecuaciones que describen el comportamiento son (ec. 13):

$$\frac{dq_i}{dt} = K_f a_p (C_i - C^*) \qquad \text{(ec. 13)}$$

Para ajustar los datos experimentales a la ecuación, es preferible definir una constante aparente de transferencia de materia (K) como producto del coeficiente de transferencia de materia por la superficie específica. La ecuación de ajuste será (ec. 14):

$$\frac{dq_i}{dt} = K(C_i - C^*) \qquad \text{(ec. 14)}$$

Para realizar el cálculo de K es necesario linealizar la ecuación (ec. 15)

$$q_i = \frac{V_L C_0 - V_L C_i}{V_r}$$

$$\Delta V = \frac{V_L}{V_r}$$

$$q_i = \Delta V (C_0 - C_i)$$

$$\frac{dq_i}{dt} = -\Delta V \frac{dC_i}{dt}$$

$$-\Delta V \frac{dC_i}{dt} = K(C_i - C^*) \rightarrow \frac{dC_i}{dt} = \frac{K}{-\Delta V}(C_i - C^*) \qquad \text{(ec. 15)}$$

Integrando se llega a (ec. 16):

$$\ln \frac{(\mathrm{C_i} - \mathrm{C^*})}{(\mathrm{C_0} - \mathrm{C^*})} = -\frac{\mathrm{K}}{\Delta \mathrm{V}} \mathrm{t} \qquad \text{(ec. 16)}$$

Aplicando un balance de materia al sistema, y las variables adimensionales X y Δv, se obtiene la ecuación 17 que proporciona la evolución en el tiempo de la carga del compuesto en el carbón activo

$$q_i(t) = C_0(\Delta V)\left(1 - \frac{C^*}{C_0}\right)(1 - exp\left(\frac{-Kt}{\Delta V}\right) \qquad (ec. 17)$$

A continuación, se muestra el programa Fortran utilizado en el cálculo de la difusividad en el interior de los poros del carbón activo a partir de los datos de los experimentos en tanque agitado [235].

```
*           MODELO DE DIFUSION NOS POROS (CALCULOS DE DIFUSIVIDAD)
      IMPLICIT REAL*8 (A-H,O-Z)
*            PARAMETER (TAB=9)
      DIMENSION USOL(1,11),XBKPT(11),SCTCH(20)
      DIMENSION WORK(1000),IWORK(80),X(11)
      COMMON/IOUNIT/LOUT
      COMMON/GEAR0/DTUSED,NQ,NSTEPS,NF,NJ
      COMMON/EDINP/XLEFT,XRIGHT
      COMMON/PARAM/DIF,POROP,POROL,DP,CKEQL,CAPT,C0,TP,Q0
     1        CKE,RS,H,Z,CT
      CHARACTER TAB*1
      TAB=CHAR(9)
*           EXTERNAL PDECOL
*           DEFINICAO DOS PARAMETROS
*
      OPEN (UNIT=18,FILE='datdif',STATUS='OLD')
      READ (18,*) POROL,C0,DIF,CKEQL,CAPT,CT,POROP,DP,RS,TFIM
*
*            PARAMETROS CALCULADOS
*
      TP=(DP/2.D0)**2/DIF
      CKE=1.D0+CKEQL*C0
      Q0=(((2*C0*CKEQL*CAPT)+1)-(1+(4*C0*CKEQL*CAPT))**0.5)/
     1       (2*C0*CKEQL)
*           Q0=C0*CKEQL*CAPT/(1+CKEQL*C0)*RS
*           Q0=CKEQL*CAPT*C0/(CT+((CKEQL-1)*C0))
*           WRITE (*,*) "TFIM"
*           READ (*,*) TFIM
      OPEN (UNIT=11,FILE='resdif')
      OPEN (UNIT=10,FILE='R3')
      WRITE (10,*) 'Co=',C0
      WRITE (10,*) 'POROL=',POROL
      WRITE (10,300) TP/60.D0
      EPS=1.D-4
      NPDE=1
      KORD=4
      NINT=10
```

```
      NPTS=11
      NCC=2
      MF=22
      NCPTS=KORD+(NINT-1)*(KORD-NCC)
      T0=0.D0
      DT=1D-6
      TOUT=1D-5
      INDEX=1
      IWORK(1)=1000
      IWORK(2)=80
      DO 16 I=1,IWORK(1)
   16         WORK(I)=0.D0
      DO 19 I=3,IWORK(2)
   19         IWORK(I)=0.D0
      XBKPT(1)=0.D0
               XBKPT(2)=.3D0
               XBKPT(3)=0.6D0
               XBKPT(4)=.7D0
               XBKPT(5)=.75D0
               XBKPT(6)=.8D0
               XBKPT(7)=.85D0
               XBKPT(8)=.92D0
               XBKPT(9)=.96D0
               XBKPT(10)=.99D0
      XBKPT(NINT+1)=1.D0
      XLEFT=XBKPT(1)
      XRIGHT=XBKPT(NINT+1)
      X(1)=0.D0
      DO 22 I=2,NPTS-1
   22       X(I)=X(I-1)+0.1D0
      X(NPTS)=1.D0
   25   CALL PDECOL (T0,TOUT,DT,XBKPT,EPS,NINT,KORD,
      1                 NCC,NPDE,MF,INDEX,WORK,IWORK)
      IF (INDEX.NE.0) GO TO 58
      CALL VALUES (X,USOL,SCTCH,NPDE,NPTS,NPTS,0,WORK)
*
*              escrita de resultados
*
      WRITE (11,100) TOUT*TP/60.D0,TAB,USOL(1,1)*CT,TAB,
     1    USOL(1,NPTS)*CT
```

```
      WRITE (10,200) TOUT*TP/60.D0
      WRITE (10,400) (X(J),TAB,USOL(1,J),J=1,NPTS)
*
      IF (TOUT.LT.TFIM) GO TO 55
      STOP
   55   TOUT=TOUT+TOUT/10D0
      GO TO 25
   58  WRITE (11,800) INDEX
      STOP
  100  FORMAT (E10.4,A1,E10.4,A1,E10.4)
  200  FORMAT (/,'TOUT = ',E10.4,/)
  300  FORMAT ('TP = ',E10.4,' min',/)
  400  FORMAT (E10.4,A1,E10.4)
  800  FORMAT (/,5X,'INDEX=',I3)
      END
*
**********************************************************************
**
*
**********************************************************************
**
*
      SUBROUTINE F(T,X,U,UX,UXX,FVAL,NPDE)
      IMPLICIT REAL*8(A-H,O-Z)
      DIMENSION U(NPDE),UX(NPDE),UXX(NPDE),FVAL(NPDE)
      COMMON/PARAM/DIF,POROP,POROL,DP,CKEQL,CAPT,C0,TP,Q0
     1        CKE,RS,H,Z,CT
      COMMON/EDINP/XLEFT,XRIGHT
*
      IF (X.EQ.XRIGHT) GO TO 21
      DEN=1.D0+(CKEQL-1.D0)*U(1)
      ALFA=POROP/(POROP+((CKEQL*CAPT/CT)/(DEN**2)))
      IF (X.EQ.0) GO TO 5
      FVAL(1)=ALFA*((2.D0/X)*UX(1)+UXX(1))
      RETURN
    5   FVAL(1)=ALFA*4.D0*UXX(1)
      RETURN
   21     FVAL(1)=-3.D0*((1.D0-POROL)/POROL)*POROP*UX(1)
      RETURN
      END
```

```
*
**********************************************************************
***
*
**********************************************************************
***
*
      SUBROUTINE BNDRY (T,X,U,UX,DBDU,DBDUX,DZDT,NPDE)
      IMPLICIT REAL*8 (A-H,O-Z)
      DIMENSION U(NPDE),UX(NPDE),DZDT(NPDE)
      DIMENSION DBDU(NPDE,NPDE),DBDUX(NPDE,NPDE)
      COMMON /EDINP/ XLEFT,XRIGHT
*
      IF (X.NE.XLEFT) GO TO 1
      DZDT(1)=0.D0
      DBDU(1,1)=0.D0
      DBDUX(1,1)=1.D0
      RETURN
 0001      DZDT(1)=0.D0
      DBDU(1,1)=0.D0
      DBDUX(1,1)=0.D0
      RETURN
      END
*
**********************************************************************
***
*
**********************************************************************
***
*
      SUBROUTINE UINIT (X,U,NPDE)
      IMPLICIT REAL*8(A-H,O-Z)
      DIMENSION U(NPDE)
      COMMON /EDINP/ XLEFT,XRIGHT
*
      IF (X.NE.XRIGHT) GO TO 1
      U(1)=1.0D0
      RETURN
0001      U(1)=0.0D0
      RETURN
```

```
      END
*
**********************************************************************
***
*
**********************************************************************
***
*
      SUBROUTINE DERIVF (T,X,U,UX,UXX,DFDU,DFDUX,DFDUXX,NPDE)
      IMPLICIT REAL*8 (A-H,O-Z)
      DIMENSION U(NPDE),UX(NPDE),UXX(NPDE)
      DIMENSION
DFDU(NPDE,NPDE),DFDUX(NPDE,NPDE),DFDUXX(NPDE,NPDE)
      CONTINUE
      RETURN
      END
      SUBROUTINE
PDECOL(T0,TOUT,DT,XBKPT,EPS,NINT,KORD,NCC,NPDE,MF,INDEX 000010
*,WORK,IWORK)
```

Anexo II

9.2. Adsorción y bioadsorción del tiocianato

9.2.1. Adsorción con carbón activo

9.2.1.1. Relación líquido-sólido óptima: Influencia del pH

El proceso de adsorción de tiocianato con el carbón activo Filtrasorb F400 (Chemviron) se llevó a cabo por lotes. Para ello, y tras el pretratamiento previo del carbón activo, se calculó la relación L/S óptima del sistema a distintos pH de la disolución acuosa (2, 3, 4 y 5.8). Se utilizó, en este caso, 250 mL de disolución acuosa que contenía una concentración de 100 mgL^{-1} de tiocianato en un vaso de 500 mL sometido a una velocidad de agitación de 250 rpm durante 90 min. La cantidad de carbón activo granulado añadido en cada ensayo varió entre 0.12 y 2.5 g.

La capacidad de adsorción del carbón a cada uno de las relaciones líquido-sólidas analizadas y con cada valor de pH se muestra en la figura 8.3.

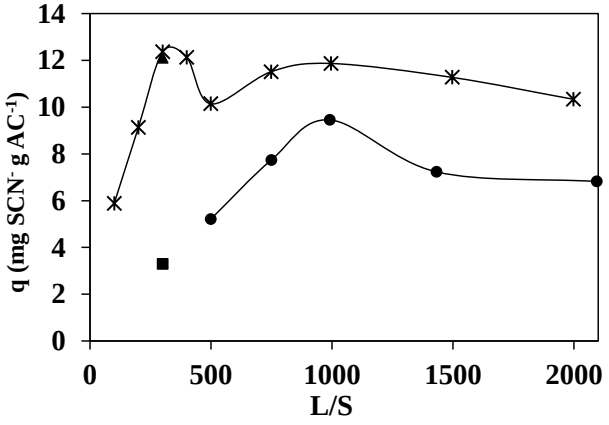

Figura 9.3: Capacidad de adsorción del tiocianato con el carbón activo Filtrasorb F400 a distintas relaciones líquido-sólido y valores de pH igual a 2 (▲), 3 (✳), 4 (■) y 5.8 (•). En todos los casos 250 mL de disolución con concentración inicial de tiocianato de 100 mgL^{-1}, 250 rpm y 90 minutos de tiempo de contacto.

En vista de los resultados se puede afirmar que el pH de la disolución influye de forma notable en el proceso de adsorción con carbón activo [238, 239], obteniéndose valores de capacidad de adsorción entre 1.5 y 2 veces mayores en el caso de pH 3 que en con pH 5.8. Por lo tanto, se seleccionó la relación líquido –sólido óptima del proceso, 300 mLg^{-1}, valor que concuerda con los obtenidos por Namasivayam y Sangeetha [239] y Namasivayam y Sureshkumar [238].

La capacidad de adsorción del carbón con la relación líquido-sólido óptima se estudió con disoluciones de tiocianato (100 mgL^{-1}) con valores iniciales de pH ajustados a 2 y 4, tal y como se muestra en la figura 8.3. Se comprobó que la capacidad de adsorción del tiocianato en la disolución con pH 2 es similar al obtenido con la disolución con pH 3, mientras que la capacidad de adsorción a pH 4 disminuye considerablemente. Estas diferencias en la capacidad de adsorción del carbón activo en función del valor de pH se hacen más notables con concentraciones de tiocianato inferiores, tal y como le ocurre a Namasivayam y Sangeetha [239] y Namasivayam y Sureshkumar[238].

9.2.1.2. Equilibrio de adsorción

Se realizaron estudios de adsorción del tiocianato con una relación líquido-sólido de 300 mLg^{-1} en un medio salino (PtMM) en el que el rango de concentración de tiocianato varió entre 10 y 90 mgL^{-1}. En este caso, el pH de la disolución se dejó libre, tal y como se hizo en el proceso de biodegradación del tiocianato (pH 8.4), permitiendo de este modo que ambos procesos fueran comparables. En la figura 8.4. se muestra la capacidad de adsorción del carbón Filtrasorb F400 para cada una de las concentraciones iniciales de tiocianato en la disolución, así como el ajuste de la isoterma de adsorción de Langmuir a los datos experimentales.

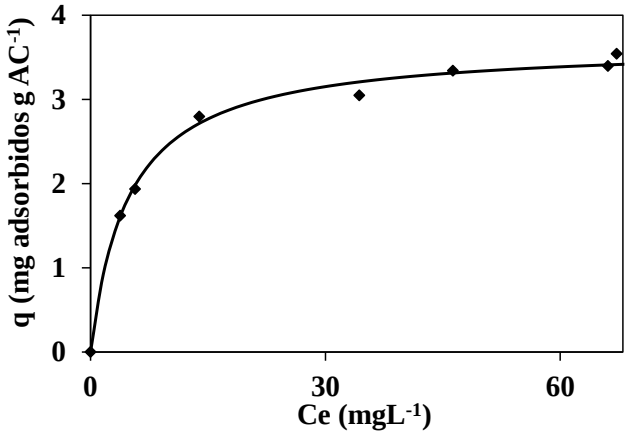

Figura 9.4: Ajuste de la isoterma de adsorción de Langmuir a los datos experimentales empleando una disolución sintética de tiocianato (10-90 mgL^{-1}), 20 ºC, 250 rpm, relación líquido-sólido 300 mLg^{-1} y pH 8.4

Los parámetros obtenidos en el ajuste de la isoterma de Langmuir a los datos experimentales fueron q_t= 3.66 mg (SCN^{-}·g $carbon^{-1}$) y K_{eq}= 0.2070 (L·mg $carbon^{-1}$). Estos resultados son inferiores a los encontrados en la bibliografía, debido al elevado valor de pH utilizado en el presente ensayo. Por ejemplo valores de q_t= 8.6 mg (SCN^{-}·g $carbon^{-1}$) y K_{eq}= 0.1702 (L·mg $carbon^{-1}$) fueron obtenidos en un proceso de adsorción a pH 2, relación líquido-sólido 250 mLg^{-1} y con un rango de concentraciones de tiocianato comprendido entre 10 y 50 mgL^{-1} por Namasivayam y Sureshkumar [238]. Namasivayam

y Sangeetha [239] calcularon valores de q_t= 16.2 mg (SCN^-·g $carbon^{-1}$) y K_{eq}= 0.471 (L·mg $carbon^{-1}$) con una relación líquido-sólido 250 mLg^{-1} y un rango de concentraciones de tiocianato comprendido entre 20 y 80 mgL^{-1} a 35 ºC. Ambos trabajos emplearon un carbón activo con superficie modificada obtenido a partir de la cascara del coco.

En este caso, la capacidad de adsorción de tiocianato del carbón Filtrasorb F400 es baja lo que supone que la efectividad de eliminación del tiocianato de la corriente acuosa por este método físico no sea adecuada en comparación con la eliminación biológica del contaminante por *Paracoccus thiocyanatus.*

9.2.2. Adsorción y biodegradación combinada

Se llevó a cabo a continuación el análisis del proceso de bioadsorción del tiocianato con un carbón activo biológico que presentaba un biofilm de *Paracoccus thiocyanatus.*

En primer lugar, se estudiaron las condiciones óptimas de formación del biofilm de *P. thiocyanatus* sobre el carbón activo Para ello, se inoculó la bacteria es su fase de crecimiento exponencial en 100 mL de medio de crecimiento de *P. thiocyanatus* al que se le había añadido 0.333 g de carbón activo, incubándose el sistema durante 24, 48, 96, 120, 144, 168 y 192 horas con una agitación de 75 rpm. Transcurrido esos tiempos, el carbón activo biológico se inoculó en un medio salino (PtMM) que contenía una concentración de 3000 mgL^{-1} de tiocianato, manteniéndose el sistema a 28 ºC y 250 rpm.

Lo resultados del proceso de bioadsorción del tiocianato por el carbón activo biológico se muestran en la figura 8.5. El proceso de bioadsorción no consiguió en ningún caso mejorar la eficacia obtenida con la biodegradación de tiocianato por un cultivo de *P. thiocyanatus* en suspensión.

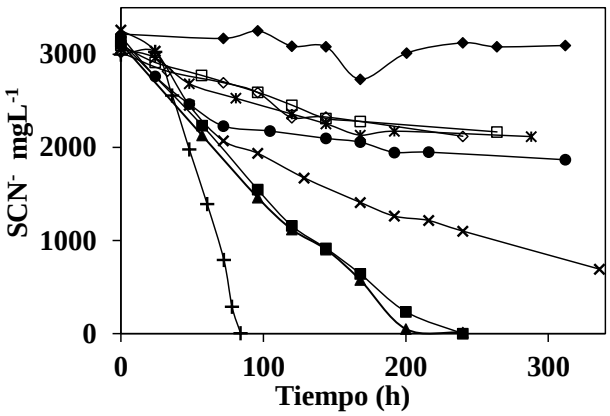

Figura 9.5: Evolución de la concentración del tiocianato en un proceso de biodegradación por *P. thiocyanatus* (+) y en un proceso de bioadsorción con biofilm de *P. thiocyanatus* sobre el carbón activo formado durante 24 h (◆), 48 h (■), 72 h (▲), 96 h (×), 120 h (●),

144 h (✳), 168 h (□), 192 h (◊). En todos los casos 28 ºC, 250 rpm, 3000 mgL^{-1} de tiocianato

A partir de las 48 horas de formación del biofilm sobre la superficie del carbón activo, se observó la formación de un agregado celular, que alcanzó su mayor tamaño a las 72 h. Sin embargo, a partir de las 96 horas de formación del biofilm, este agregado celular se desprendió de la superficie del carbón y no se volvió a adherir sobre él durante el resto de los tiempos estudiados.

Puesto que en Combarros *et al.* [217], el carbón activo biológico fue más eficaz que el proceso de biodegradación del ácido salicílico sólo a altas concentraciones, en este caso, los biofilm formados tras 48 y 72 h se añadieron a un medio salino que contenía 7000 mgL^{-1} de tiocianato, no obteniendo, en ambos casos, eliminación alguna del tiocianato del medio acuoso.

Anexo III

9.3. Divulgación científica de los datos obtenidos en Technical University of Denmark

ICON 4 – 4th International Conference on Nitrification, June 28th – July 1st 2015, Edmonton (Canada)

Challenges encountered calibrating N_2O dynamics from mixed cultures

Carlos Domingo-Félez[1], Carles Pellicer-Nàcher[1], Morten S. Petersen[1], Rosana González-Combarros[1], Marlene Mark Jensen[1], Gürkan Sin[2], Barth F. Smets[1]

[1]*Department of Environmental Engineering. Technical University of Denmark. Miljøvej 113, 2800 Kgs Lyngby, Denmark*
[2]*Department of Chemical Engineering. Technical University of Denmark. Miljøvej 113, 2800 Kgs Lyngby, Denmark*

Nitrous oxide (N_2O) is a by-product of biological nitrogen removal with a strong environmental impact as a greenhouse gas. Research has focused on conceptualizing our understanding of the complex interrelationships within these systems to lastly develop mitigation strategies. However, the development of accurate process models has been proven difficult as several proposed model structures have failed to describe observations. The present study used a pseudo-mechanistic model distinguishing N_2O production from autotrophic and heterotrophic bacteria to successfully describe experimental data collected during controlled batch tests with activated sludge biomass. Interestingly, under conditions of no carbon addition experimental and modelling results indicated a strong influence of heterotrophic bacteria on N_2O production, further confirmed on a different activated sludge biomass. Further, mapping the uncertainty of the model parameters showed a higher uncertainty in the N_2O predictions compared to other better described nitrogenous species such as ammonium, nitrite or nitrate. Even though the total N_2O production was not sensitive to certain parameters the contribution of individual pathways was. Unfortunately, an in-depth literature review revealed a high degree of uncertainty in these parameter values and a lack of quality data to accurately assess whether autotrophic or heterotrophic microbial processes contributed more to the total N_2O pool. Therefore elucidating knowledge gaps encountered during model calibration combined with optimal experimental design will facilitate the development of strategies to minimize the carbon footprint of wastewater treatment plants. This work represents a step further in understanding the N_2O production and emissions associated to conventional wastewater treatment.

Figura 9.6: Póster presentado en ICON 4 – 4th International Conference on Nitrification

DTU Environment
Department of Environmental Engineering

Technical University of Denmark

Challenges encountered calibrating N_2O dynamics from mixed cultures

Carlos Domingo-Félez[1]*, Carles Pellicer-Nàcher[1], Morten S. Petersen[1], Rosana González-Combarros[1], Marlene Mark Jensen[1], Gürkan Sin[2], Barth F. Smets[1]

[1]Department of Environmental Engineering, Technical University of Denmark, Kongens Lyngby, Denmark.
[2]Department of Chemical Engineering, Technical University of Denmark, Kongens Lyngby, Denmark.

Introduction and Objectives

- Nitrous oxide (N_2O) is a by-product of biological nitrogen removal with a high greenhouse gas potential emitted during wastewater treatment which negatively impacts the carbon footprint of the process.
- None of the proposed process models describing N_2O production can predict all the available data.
- Assumptions during model calibrations from systems with mixed cultures are usually not contrasted, which will impact the model prediction capabilities.
- This study critically assesses challenges encountered during calibration of nitrogen-removing mixed biomasses.

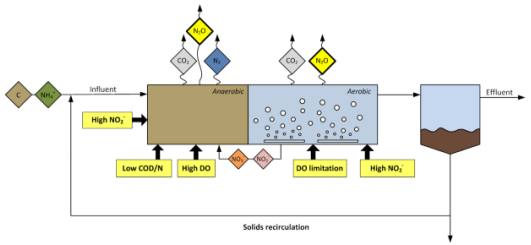

Material and Methods

Experimental Setup

Activated sludge biomass from 2 WWTPs. Batch tests under controlled substrate conditions. Online monitoring of relevant nitrogenous species. Mass transfer characterization of the systems.

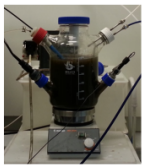

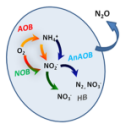

Results

Model calibration

Model predictions followed products of [NH_4^+], [NH_4^+ + NO_3^-] and [NH_4^+ + NO_2^-] spikes and aerobic/anoxic hydrolytic processes.

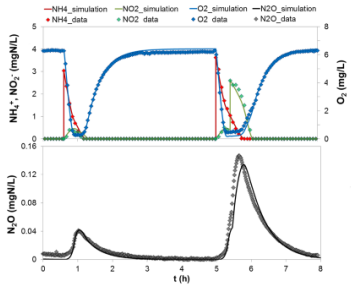

Heterotrophic interference on autotrophic conditions

Decay products affect N_2O production even under no addition of carbon sources.

Anoxic N_2O consumption (mgN/gVSS.h)		
Washed & Aerated (1 day)	Washed & Aerated (2 days)	Washed & Aerated (2 days) & NO_2^-
3.52 ± 1.48	0.54 ± 0.16	0.13 ± 0.09

Modelling N_2O dynamics

ASM-based model structure including the nitrifier and heterotrophic denitrification N_2O-producing pathways. Parameter subset obtained during model calibration used during uncertainty analysis. Parameter uncertainty ranked based on literature values (5-25-50%); randomly sampled (LHS = 250 samples). Monte Carlo simulations (n = 1000) to map parameter uncertainty into outputs. MATLAB and AQUASIM were used for model simulations.

Mapping parameter uncertainty into model outputs

Error propagation in the nitrification/dentirification model revealed a higher uncertainty for intermediates (NO, N_2O) than for other nitrogenous species (NH_4^+, NO_2^-, NO_3^-).

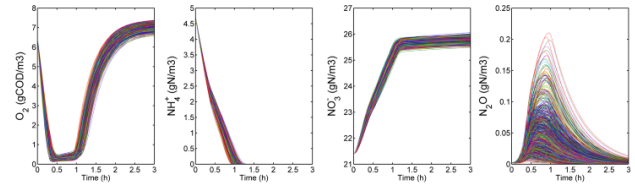

If the uncertainty of model parameters is carried during parameter estimation the confidence regions of the new parameter estimates increase significantly.

Sensitivity of N_xO to literature uncertainty

Uncertainty of certain model parameters does not impact total N_2O produced. However it significantly affects which microbial community is responsible for its production and the total NO production.

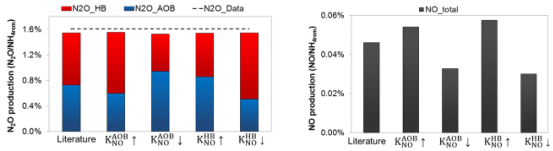

Conclusions

- Heterotrophic activity interferes with autotrophic N_2O production in activated sludge under no carbon fed conditions.
- Scarce N_2O literature revealed large prediction uncertainties.
- Individual N_2O production pathways (autotrophs/heterotrophs) are sensitive to certain parameters while the total N_2O produced is not.
- Developing new mitigation strategies to reduce the carbon footprint of wastewater treatment still lacks understanding of biological processes.

cadf@env.dtu.dk
@Metlab_DTU

Research supported by:
LaGas, a grant from the Danish Council for Strategic Research

Anexo IV

9.4. Lista de Figuras

Anexo V

9.5. Lista de Tablas

Anexo VI

9.6. Divulgación de la Tesis

9.6.1. Artículos científicos

Combarros, R.G., Rosas, I., Lavín, A.G., Rendueles, M. Díaz, M. 2014. Influence of biofilm on activated carbon on the adsorption and biodegradation of salicylic acid in wastewater. Water Air and Soil Pollution, 225 (2), 1-12.

Combarros, R.G., Collado, S., Laca, A., Díaz, M. 2015. Conditions and mechanisms in thiocyanate biodegradation. Journal of Residuals Science and Technology, 12(3), 113-124.

Combarros, R.G, Collado, S., Laca, A., Díaz, M. Understanding the Simultaneous Biodegradation of Thiocyanate and Salicylic Acid by *Paracoccus thiocyanatus* and *Pseudomonas putida*. International Journal of Environmental Science and Technology, DOI 10.1007/s13762-015-0906-y.

Combarros, R.G, Collado, S., Díaz, M. Toxicity of graphene oxide on growth and metabolism of *Pseudomonas putida* (under review).

Combarros, R.G, Collado, S., Díaz, M. Toxicity of titanium dioxide nanoparticles on *Pseudomonas putida* (under review).

9.6.2. Contribuciones a congresos

Combarros, R.G., Rosas, I., Lavín, A.G., Rendueles, M. Díaz, M. "Biological activated carbon treatment of salicylic acid contained in an industrial wastewater". 22-099-P. ISBN: 97884-615-4777-7. 12th Mediterranean Congress of Chemical Engineering. Barcelona. 15th-18th November 2011.

Combarros, R.G., Rendueles, M., Laca, A., Lavín, A.G., Díaz, M. "Biodegradation and adsorption of phenolics in carbon biofilms". Oral Communication (T7-042). International Congress of Chemical Engineering 2012. Sevilla. 24th-27th June 2012.

Combarros, R.G., Laca, A., Rendueles, M., Díaz, M. "Biodegradación de tiocianato. Características de la operación con *Paracoccus thiocyanatus*". M-MAMB-P-37. XXXIV Reunión Bienal de la Real Sociedad Española de Química. Santander. 15-18 septiembre 2013.

Combarros, R.G., Collado, S., Laca, A., Díaz, M "Impact of TiO_2 nanoparticles on biodegradation of salicylic acid by *Pseudomonas putida*". II International Congress of Chemical Engineering ANQUE. Madrid. 1st-4th July 2014.

Combarros, R.G., Collado, S., Laca, A., Díaz, M. "Use of co-cultures for the simultaneous biodegradation of cyanide and phenolic compounds". 13th Mediterranean Congress of Chemical Engineering. Barcelona. 30th September-3rd October 2014.

Domingo-Félez, C., Pellicer-Nàcher, C., Petersen, M. S., Combarros, R.G., Jensen, M. M., Sin, G., Smets, B. F. "Challenges encountered calibrating N2O dynamics from mixed cultures". ICON 4 – 4th International Conference on Nitrification, June 28th – July 1st 2015, Edmonton (Canada).

Combarros, R.G., Collado, S., Oulego, P., Díaz, M. "Effect of engineered nanomaterials on wastewater biotreatment". XXXV Congreso Bienal de la Real Sociedad Española de Química (RSEQ) 19-23 de Julio 2015.